HIGH MOISTURE EXTRUSION OF SOY PROTEIN AND MILLET FLOUR BLENDS FOR DEVELOPMENT OF TEXTURIZED PROTEIN RICH FOODS

A THESIS TO BE SUBMITTED TO

THE UNIVERSITY OF TRANS-DISCIPLINARY HEALTH SCIENCES AND TECHNOLOGY

FOR THE AWARD OF THE DEGREE OF
DOCTOR OF PHILOSOPHY

BY

ABDUL MATEEN

UNDER THE GUIDANCE OF

PROF. GURMEET SINGH

THE UNIVERSITY OF TRANS-DISCIPLINARY HEALTH SCIENCES AND TECHNOLOGY

SEPTEMBER 2024

THE UNIVERSITY OF TRANS-DISCIPLINARY HEALTH SCIENCES AND TECHNOLOGY

Private University Established in Karnataka by ACT 35 of 2013

BENGALURU - 560064

DECLARATION BY THE CANDIDATE

I declare that this thesis entitled **"High moisture extrusion of soy protein and millet flour blends for development of texturized protein rich foods"** submitted for the award of Doctor of Philosophy to THE UNIVERSITY OF TRANS-DISCIPLINARY HEALTH SCIENCES AND TECHNOLOGY, Bengaluru, is my original work, conducted under the supervision of my guide **Prof. Gurmeet Singh**. I also wish to inform that no part of the research has been submitted for a degree or examination at any university. References, help and material obtained from other sources have been duly acknowledged.

I hereby confirm the originality of the work and that there is no plagiarism in any part of the dissertation.

Place: Bengaluru **Signature of the Candidate**
Date:

Name of candidate: Abdul Mateen
Reg. No.: 10518010222
(September 2018)

THE UNIVERSITY OF TRANS-DISCIPLINARY HEALTH SCIENCES AND TECHNOLOGY

Private University Established in Karnataka by ACT 35 of 2013

BENGALURU - 560064

CERTIFICATE

This is to certify that the work incorporated in this thesis **"High moisture extrusion of soy protein and millet flour blends for development of texturized protein rich foods"** submitted by Abdul Mateen was carried out under my supervision. No part of this thesis has been submitted for a degree or examination at any university. References, help and material obtained from other sources have been duly acknowledged. I hereby confirm the originality of the work and that there is no plagiarism in any part of the dissertation.

Research Supervisor

Prof. Gurmeet Singh
Date:
Dean (Research & Extension)
The University of Trans-Disciplinary Health Sciences and Technology

Acknowledgement

The present work was carried out in the Centre of Ayurveda Biology and Holistic Nutrition at the University of Trans-Disciplinary Health Sciences and Technology (TDU).

I would like to express my gratitude to those who have contributed considerably to the successful completion of this thesis. In particular, I would like to extend my sincere gratitude to the following:

First and foremost, I would like to thank my advisor Prof. Gurmeet Singh for assigning the topic and providing continuous support throughout the research work and thesis writing process. Over the past 5 years, I have not only gained valuable knowledge but also imbibed qualities of professionalism under his mentorship. Prof. Singh's kindness and encouragement have played a pivotal role in shaping my academic and professional endeavours. Furthermore, I extend my thanks to my doctoral advisory committee members, Dr Madhuresh, Dr Shovan, Dr Subramanya, and Dr Venkat for their valuable advices during my research work.

I would also like to acknowledge Rural India Supporting Trust for their financial support to carry out this research.

Many thanks go to my friends Mr. Manoj, Mr. Kumarswamy and others who assisted me during the extrusion trials and analytical work. I would also like to express my gratitude to my friend, Mr. Aishwarya Dubey for our insightful discussions that spanned long hours.

Finally, I’d like to thank my family and my wife Aiman for their love and unwavering support.

Table of Contents

List of Tables

List of Figures

List of Abbreviations

Abbreviation	Definition
AAS	Amino Acid Score
AI	Anisotropic Index
ANOVA	Analysis of Variance
CPP	Chickpea Protein Isolate
db	dry basis
DSF	Defatted Soy Flour
EAA	Essential Amino Acids
FRF	Fiber Rich Fraction
HME	High Moisture Extrusion
HMMA	High Moisture Meat Analogue
HZ	Heating Zone
L/D	Length to Diameter Ratio
LVER	Linear Viscoelastic Region
MP	Melt Pressure
MT	Melt Temperature
PCA	Principal Component Analysis
PPI	Pea Protein Isolate
RPI	Rice Protein Isolate
SME	Specific Mechanical Energy
SPI	Soy Protein Isolate
SRF	Starch Rich Fraction
TPA	Texture Profile Analysis
wb	wet basis
WG	Wheat Gluten
WHC	Water Holding Capacity
WMF	Whole Millet Flour
WS	Water Solubility

List of Symbols

Symbols	Name	Units
ω	Angular frequency	$rads^{-1}$ (radian per second) or Hz (hertz)
$\dot{\gamma}_a$	Apparent shear rate	s^{-1} (per second)
η	Apparent viscosity	Pa·s
A	Area	m^2 (square meter)
n'	Behaviour index	-
G^*	Complex modulus	Pa (Pascal)
η^*	Complex viscosity	Pa·s
K'	Consistency index	-
ΔP	Differential pressure	bar
F	Force	N (Newton)
H	Height	cm (centimetre)
L	Length	cm (centimetre)
L*	Lightness	-
G´´	Loss modulus	Pa (Pascal)
MFR	Mass flow rate	$gmin^{-1}$ (gram per minute)
a*	Redness	-
n	Screw speed	rpm (rotation per minute)
τ_w	Shear stress	Pa (Pascal)
SME	Specific mechanical energy	$kJkg^{-1}$ (kilojoule per kilogram)
G´	Storage modulus	Pa (Pascal)
T	Torque	Nm (Newton meter) or BU (Brabender Units)
ΔE	Total colour difference	-
Q	Volumetric flow rate	cm^3s^{-1} (cubic centimetre per second)
W	Width	cm (centimetre)
b*	Yellowness	-

Synopsis

Protein deficiency, a deficit in the quantity and quality of protein in diet, is a major public nutritional and health problem in many developing countries especially in India. Beside low intake of proteins, a significant factor contributing to widespread protein deficiency in India is that a large portion of India's dietary protein comes from plant based foods which have low amino acid scores in general. Thus, quality of protein is intertwined. Additionally, the plant proteins coming primarily from cereals and pulses in the diet, bring along a high carbohydrate and phytate load at intakes required to achieve protein sufficiency. This potentially leads to susceptibility to metabolic syndrome and mineral nutrient deficiency. Transitioning to a diet predominant in diary and meat is culturally unlikely, but also environmentally a poor choice. Going forward the world population is expected to reach 10 billion people by 2050 with India accounting for nearly 2 billion. Since meat and dairy proteins have a much higher environmental footprint, it is desirable that the growing protein needs of humanity are met through plant proteins. A potential option that meets both nutritional and environmental challenges is the use of blends of plant protein isolates that combine legumes and cereals to obtain high amino acid scores and digestibility. Further, extrusion of these protein rich blends creates novel textures.

Expanded 'non-anisotropic' structured proteins made through low moisture extrusion have been available in the market for few decades. However, their consumer uptake has been low. A major reason is texture. The products are expanded during extrusion and lead to light, spongy, non-anisotropic texture. Developing products that can extend the textural range by increasing density, fibrousity and anisotropy may help product developers craft new consumer opportunities. In this thesis plant protein based products have been developed and characterized that have dense and anisotropic textures with a good amino acid profile using blends of soy protein isolate and minimally processed millet flour and the fractions in a high moisture extrusion process using a twin screw extruder. These can be used for many applications such as soy chap and meat analogues.

The physicochemical and nutritional characteristics of plant protein isolates of soy, pea, chickpea, rice and wheat, were analyzed in the laboratory as these isolates are commonly used for making texturized plant protein rich foods. The results are presented in **Chapter 3** and show significant differences from each other. Together, water

absorption capacity and water solubility of a protein are key determinants of the textural quality of their extrudates. The fibrous textures are a result of the difference in values of these properties between the key components of the blends used for extrusion. Generally, the greater the difference the more the fiber density. Soy isolate used in this study had a water absorption capacity of more than 5 g/g protein, while wheat gluten could absorb around 2 g/g. PPI, CPP and RPI had water absorption capacities in between SPI and WG. When it came to water solubility, chickpea isolate had the highest WS whereas, WG and RPI the lowest. SPI and PPI had intermediate solubilities. Thus, SPI provides the best physicochemical characteristics for high moisture extrusion. It has a high water absorption capacity and moderate solubility. It is suitable for blending with other materials with properties very different from itself, such as millet flours which have been used in this work) to give good fibrous textures.

Another important consideration for high moisture extrusion is the least gelling concentration. Gelling plays a key role in the cooling die. SPI gelled at 12% while the gelling concentration was 14% for PPI, 16% for CPP and 20% for RPI. While WG also gelled at 12% concentration, due to its low water absorption capacity its gels released a lot of free water.

A few researchers suggest the use of oil in the blends during extrusion. While this was outside the scope of experiments in this work, if oil has to be included in the blends during extrusion, then having some emulsion capacity is important. SPI, PPI and CPP had higher emulsion capacities and would be more suitable for this compared to RPI and WG which have poor emulsion capacities.

Pasting properties of the protein powders give an indication of the melt viscosities. SPI had the highest final viscosity and RPI the least with the descending order being SPI > PPI > CPP > WG > RPI. Rheological characteristics of the powders give even a better idea of how the melts behave under extrusion conditions. Interestingly the descending order of complex viscosity for the powders is SPI > CPP > RPI > WG > PPI, which is different from the order based on the pasting curves.

There are a number of parameters that effect the textural quality of protein extrudates as described in **Chapter 4**. In this thesis we divide them into raw material parameters, system parameters, process parameters and product properties. The main raw material parameter is the protein concentration of the feed. The process parameters include feed

moisture content, barrel temperature, screw speed and feed rate. The system parameters include the specific mechanical energy, melt temperature and melt pressure. The effect of protein concentration and the process parameters on the textural quality was studied for soy proteins. Protein concentration of the blend (dry basis) and moisture were found to be the most important parameter. Barrel temperature profile also had a significant impact on the texture of the extrudates. The other parameters, namely screw speed and feed rate, had smaller effects and could be used for finer modulation of texture.

Textural parameters such as hardness correlated linearly with protein concentration of wet basis. By changing protein concentration and process parameters, a wide range of hardness (11X) and chewiness (9.6X) was created. The range in values of resilience (2.2X), cohesiveness (1.4X) and springiness (1.2X) was much smaller than hardness and chewiness. Hardness and chewiness of real meat were in the range of HMMA obtained by levering process parameters. Other parameters (resilience, cohesiveness & springiness) of HMMA were out of the range obtained (higher values than real meat). A part of this gap was bridged using millet flours as blend components.

In **Chapter 5**, three types of millet - sorghum, pearl millet and finger millet flours were used as secondary components, each blended separately with soy protein isolate. The addition of millets reduced the hardness and chewiness of millets while at the same time showing improved visual fibers. This was shown from incorporation levels of millet flours up to 30%. Each millet had a slightly different effect on the texture and colour of the extrudates. Sorghum and pearl millet blends had thicker fibers and whiter in colour while finger millet blends had finer fibers and reddish brown in colour. Comparative texture profile analysis between extrudates and real meat (chicken breast) revealed that all millet blends brought the textural values closer to those of real meat. Notably, finger millet significantly shifted the texture band towards the real meat profile. Besides providing positive changes in texture and providing a natural colour pallet, incorporation of millets also improved the amino acid profiles of the extrudates. SPI is low on sulphur containing amino acids (SAA) while millets lack lysine. Blends of SPI and millet flours at 30% showed balanced amino acid profile, good amino acid score and equivalent protein content compared to real meat, though it reduces the overall protein content marginally.

Compared to SPI and wheat gluten blends, which are the most common blends used in industry, the SPI and millet flour blends have a better amino acid score. This is because

wheat gluten is low on lysine and incorporation of wheat gluten at high levels of 30% negatively impacts the amino acid scores of the extrudates significantly. Additionally, millets are gluten free and therefore the SPI and millet flour blends are suitable for a population that is gluten intolerant.

In **Chapter 6**, one of the millets, finger millet, was fractionated by separating the hull. The flour obtained from the hull and the dehulled grains were characterized. The hull flour was found to be rich in fiber and the dehulled flour was found to be low in fiber. Its starch content was much higher than the hull fraction. Therefore, the hull fraction was called fiber rich flour or FRF and the dehulled fraction was named starch rich flour or SRF. FRF had 9.4 times the fiber compared to SRF while SRF contained 1.7 times the amylopectin compared to FRF.

SPI was blended with SRF and FRF and extruded. All extrudates displayed visual fibration. However, they differed in the fiber density, that is, the number of fibers per unit cross section length. SPI100% showed the least fiber density while SRF and FRF blends showed a high density of fibers. Among the blends, SRF had the thicker and longer fibers and FRF had the thinner and shorter fibers. However visual anisotropy did not translate into cutting strength anisotropy. Cutting strength anisotropy was maximum for SRF blends and minimum for SPI100%. Extrudates from blends had a textural profile closer to real meat compared to SPI100% extrudates. SRF was closest among different blends. Extrudates from FRF blends were more resilient than those from SPI100%; SRF blends were less resilient.

A mechanistic approach was used to understand the structure from a protein interaction in different solvents. Protein solubility in phosphate buffer showed least solubility and all extrudates showed comparatively lower protein solubility than non-extruded materials, suggesting native proteins were aggregated during the high moisture extrusion. The presence of higher hydrogen and disulfide bonds in SRF blend extrudates probably die to the higher starch/amylopectin content and resulting in a higher anisotropic index. Higher hydrophobic interactions in FRF blend extrudates was mostly due to the insoluble dietary fiber which contains hydrophobic units. Other factors for the harder structure of FRF blend extrudates could be due to the presence of Ca^{2+}in FRF.

An image analysis method was developed to quantify the features of the fibers in the extrudates. This straightforward tool assists researchers and manufacturers in quantitatively characterizing visual fibrations.

The key takeaway from the study is the significance of aligning the properties of the protein and minimally processed flours/fractions for successful structure formation to create desired textures for masses with good nutritional profile. The integration of millets into blends, represents a paradigm shift in the development of protein rich texturized products. As the demand for sustainable and affordable texturized plant based foods continues to grow, millets stand as an ingredient and the way of minimally processed fractions as an innovative approach, offering a path to meet the expectations of texture and environmental impact.

List of Publications

This Thesis

Mateen, A., & Singh, G. (2024). Evaluating millet flour fractions as blend components with soy protein isolate for creating high moisture meat analogues using a twin screw extruder. *Food Hydrocolloids*. *[submitted for publication]*

Mateen, A., & Singh, G. (2023). Evaluating the potential of millets as blend components with soy protein isolate in a high moisture extrusion system for improved texture, structure, and colour properties of meat analogues. *Food Research International*, 173. https://doi.org/10.1016/J.FOODRES.2023.113395

Mateen, A., Mathpati, M., & Singh, G. (2023). A study on high moisture extrusion for making whole cut meat analogue: Characterization of system, process and product parameters. *Innovative Food Science & Emerging Technologies*, 85. https://doi.org/10.1016/J.IFSET.2023.103315

Patents

Singh, G., Mateen, A., & Mathpati, M. (2023). Proteinaceous food product and process of preparation thereof. IP India. [Patent Appl. No. 202441054624]

Other publications

Dey, D., Singh, G., Ishwarya, P., & Mateen, A. (2024). Functionality and extrusion processing of millets - A Review. *Food Reviews International*. 1-29. https://doi.org/10.1080/87559129.2024.2367643

Dubey, A., Mateen, A. & Singh, N. (2024). Exploring textural, solubility and rheological characteristics of high-moisture extruded meat analogues: effects of wheat gluten and rice protein incorporation in pea protein isolate and feed moisture levels. *International Journal of Food Science and Technology*. https://doi.org/10.1111/ijfs.17279

Singh, G., Vinayagan, N., & Mateen, A. (2022). Scientific Approach to the Role of Turmeric in Ayurvedic Formulations and Their Phytochemistry. In Chemistry, Biological Activities and Therapeutic Applications of Medicinal Plants in Ayurveda (pp. 22–44). *The Royal Society of Chemistry*. https://doi.org/10.1039/9781839166211-00022

Oral presentations

Singh, G. & Mateen, A. (2023) Extending the Food Applications Landscape of Millets - Opportunities & Challenges, *International Conference on Innovations to Transform Drylands*, ICRISAT, Hyderabad, India.

Mateen, A. & Singh, G. (2022). A Study on High Moisture Extrusion for Making Meat Analogues: Characterization and Research Gap. *International Conference on Sustainable Approaches in Food Engineering and Technology*. Tezpur, India. *[Best Presentation Award]*

Poster presentations

Mateen, A., & Singh, G. (2024). A new approach for using millets in texturized plant-based foods. *Symposium on Technological Advancements in Staple Food Fortification (FortiSF2024)*, Indian Institute of Technology, Kharagpur, India. *[Best Poster Award]*

Mateen, A., Mathpati, M., & Singh, G. (2023). Unveiling rheological transformations in high moisture extrusion: Bridging insights from raw material to extruded meat analogues. *Complex Fluids International Conference (CompFlu 2023)*, Indian Institute of Madras, Chennai, India.

Mathpati, M., Mateen, A., & Singh, G. (2023). Low Moisture Extrusion for Textured Vegetable Protein (TVP) Production from Soy and Pea Protein Isolates: System Response, Expansion Ratio and Rehydration Properties. *Complex Fluids International Conference (CompFlu 2023)*, Indian Institute of Madras, Chennai, India.

Mateen, A., & Singh, G. (2023). Utilizing millets in plant-based meat analogue applications: Effect of incorporation of millets at different levels in a high moisture extrusion. International Conference on Innovations to Transform Drylands, ICRISAT, Hyderabad, India. *[Best Poster Award]*

Devi K. L., Gothe, S., Mateen, A., Mathpati, M. & Singh, G. (2023). A compositional physico-chemical property comparison of millets with cereals and legumes identifying innovation opportunities for new product development, *International Conference on Innovations to Transform Drylands*, ICRISAT, Hyderabad, India.

Chapter 1

Introduction

1.1 Protein deficiency and future protein demand

Proteins are an important constituent of human diet. They contribute to various functions such as muscle building, tissues repair and maintenance, facilitating biochemical reactions as enzymes, hormone production, immune system support, nutrient transport and storage (Wu, 2016). Proteins are macromolecules consists of amino acid building blocks. There are 20 different amino acids, nine of which are not produced by the human body and must be obtained from food. These are referred as essential amino acids (Emery, 2013). The quality of protein sources depends on their essential amino acid composition and digestibility.

Protein deficiency, which is defined as a deficit in the quantity and quality of protein in diet, is a major public nutritional and health problem in many developing countries especially in India (Bhutia, 2014) and is a contributing factor to stunting, wasting, increased susceptibility to infections and impaired cognitive development in children (Rampal, 2018). A survey conducted in 2017 indicates that 73% of the Indian population suffers from protein deficiency which is the highest percentage in the world (Suri, 2020). In a 2015 study, India recorded the lowest average protein intake, standing at around 50 g/capita/day, compared to other Asian regions and developed countries (Ranganathan et al., 2016).

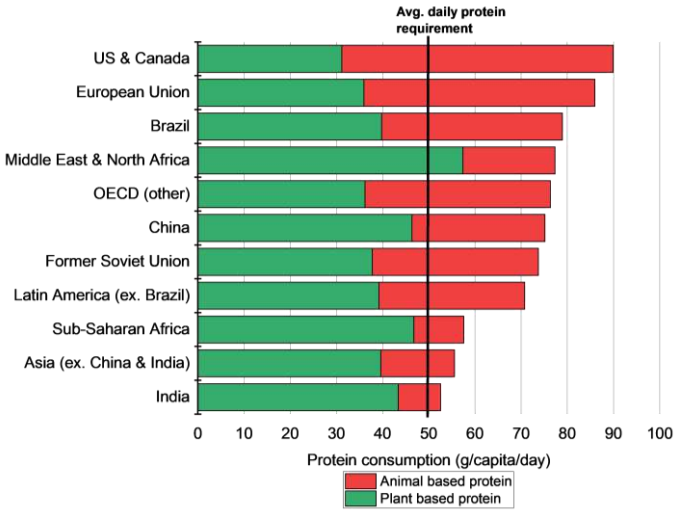

Figure 1.1 Protein consumption (g/capita/day) in different regions of the world. Source: Ranganathan et al. (2016) with source data from FAO (2015).

A significant factor contributing to widespread protein deficiency in India is that a large portion of India's dietary protein comes from plant based foods, primarily cereals and

pulses. Both these have lower amino acid scores, i.e. lower levels of one or more essential amino acids, compared to dairy and animal proteins. This implies that the dietary intake of proteins needs to be much more than the 0.8g/kg body weight recommendation, which is based on a high quality protein, to make up for sufficient amounts of all the essential amino acids. Thus, quality and quantity of protein are intertwined.

The large dependence on plant sources for proteins leads to other nutritional problems. One problem is a diet that is carbohydrate loaded. Every gram of protein is accompanied by carbohydrate of around 10 grams in rice, 7 grams in wheat, and 3 grams in pulses. This results in a carbohydrate excess in our diet when compared to the 55% carbohydrate and 15% protein guidance given by National Institute of Nutrition (NIN, 2011) even at the 0.8 kg protein/kg body weight level, which as stated above is already insufficient from a quality (essential amino acid profile) perspective. Getting adequate requirements of essential amino acids from a cereal-rich diet implies even a greater excess in carbohydrate intake. The other nutritional problem is the phytate load that accompanies a cereal and legume-based protein diet. An analysis of the Lancet diet which is a largely vegetarian diet with some meat (EAT-Lancet, 2019) and NIN diet (NIN, 2011) showed that these diets have >2000 mg of phytates, which was much higher than the recommended 1000 mg and would adversely affect mineral uptake, especially iron, zinc, and calcium (Schlemmer et al., 2009).

Table 1.1 Protein sources in Indian diet and the composition of protein, carbohydrate and phytate content. Source: Longvah et al. (2017).

Protein food sources	Protein (%)	Carbohydrate (%)	Phytate (mg/100g)
Rice	7.8	77.1	266
Wheat	10.5	64	632
Red gram (Toor)	21.7	55.2	277
Bengal gram (Chana)	21.5	46.7	450
Green gram (Mung)	23.8	52.5	170
Milk	3.2	4.9	-
Meat	18-22	-	-
Fish	15 - 22	-	-
Egg	13.2	-	-

Table 1.2 Recommended diet charts of Lancet and NIN providing quantity (g) of protein, carbohydrate and phytate per day. Source: EAT-Lancet (2019) *and NIN (2011).*

Lancet diet chart					NIN diet chart				
Food	Quantity (g)	Protein (g)	Carbohydrate (g)	Phytate (mg)	Food	Quantity (g)	Protein (g)	Carbohydrate (g)	Phytate (mg)
Whole grains	232	23.2	150.8	1160	Cereal & millets	450	40.5	315	2250
Tubers or starchy vegetables	50	0.75	7	10	Roots & tubers	200	3	28	40
Other vegetables	300	6	12	105	Green leafy & other vegetables	300	6	12	105
Fruits	200	2.4	28	50	Fruits	100	1.2	14	25
Dairy foods	250	25	26	-	Dairy foods	300	30	31	-
Beef, lamb and pork	14	2.9	-	-					
Poultry	29	5.8	-	-					
Egg	13	1.7	-	-	Pulses	90	20	45	270
Fish	28	5.6	-	-					
Legumes	75	16	37	225					
Nuts	50	9	10	500					
Added fats	51.8	-	-	-	Fat	30	-	-	-
Added sugar	31	-	31	-	Sugar	30	-	30	-
Total	1323	98.35	302	2050	Total	1300	100	475	2690

Dairy proteins have low carbohydrate load and meat proteins none (Longvah et al., 2017). They have no phytates. Their amino acid scores are also high (Schaafsma, 2000). However, compared to plant proteins, animal and dairy proteins have a much higher environmental footprint (Smetana et al., 2023). Sabaté et al. (2015) studied the environmental implications of generating 1 kg of protein from various plant and animal based sources. Their findings revealed that producing 1 kg of protein from beef required 18X more land, 10 X more water, 12 X more fertilizer, 10 X more pesticides and 9 X more fuel compared to an equivalent amount of protein derived from kidney beans. The environmental impact of other protein sources of food is given in Fig. 1.2.

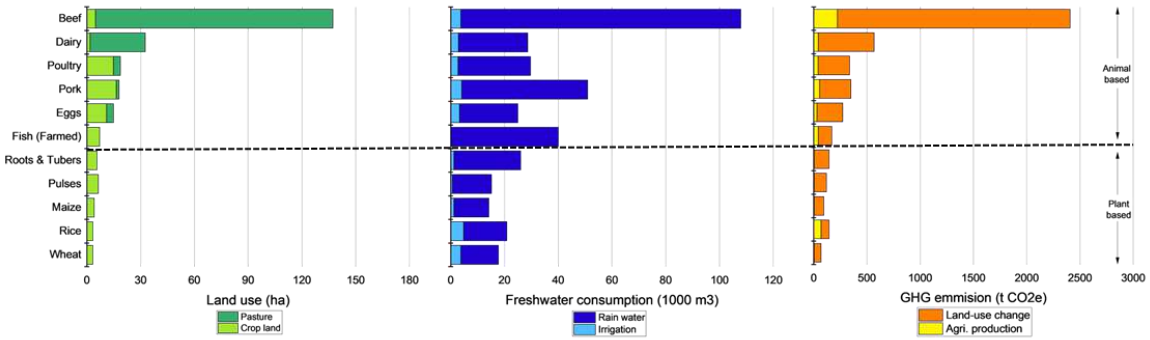

Figure 1.2 Environmental impact of per ton proteins consumed from animal based and plant based food sources. Source: Ranganathan et al. (2016).

A high preference and consumption of animal-based proteins over plant-based proteins in the developed world has led to very high environmental footprint of global food systems. Approximately 34% of GHGs are attributed to food system (Crippa et al., 2021), with livestock industry contributing up to 18% (Allen & Hof, 2019; Gomez-Zavaglia et al., 2020; Vermeulen et al., 2012). 50% of the habitable land is devoted to agriculture and half of that is for crops and pastures for animal produce. Thus, even though proteins contribute to 15% of daily calories, their environmental footprint is nearly 50%, due largely to the preferred consumption of animal-based proteins over plant based proteins.

Going forward the environmental impact is expected to get worse as global population is projected to reach approximately 10 billion people by 2050, up from 8 billion in 2024. Projections show that the higher population and an expected higher living standard in the future, will require a 51% increase in food production to meet the demand in 2050. The protein requirement is expected to be disproportionately higher than the percentage increase in food requirement and further, current trends indicate a growing consumer

demand for animal-source proteins. This will impact the environmental footprint negatively, though the nutritional quality of proteins is expected to improve.

Scientists, environmentalists and policy makers have taken cognisance of this and food choices are reflected in the second goal of the United Nations' 2030 sustainable development agenda (United Nations, 2022; van Dijk et al., 2021). There is a realization that plant-based proteins and other alternative proteins must become our major dietary protein sources in the future. Such plant-based diets have a potential to reduce GHG emissions (González-García et al. 2018, Sabaté et al. 2015, Scarborough et al. 2014). Scarborough et al. (2014) demonstrated that a high meat diet emitted 7.19 $kgCO_2e$/day, whereas a plant based diet emitted 3.81 $kgCO_2e$/day, nearly half of the GHG emissions. Furthermore, following a vegan diet reduced emissions to 2.89 $kgCO_2e$/day. Thus, transitioning from animal based to plant based protein can help tackle climate change (Farchi et al., 2017; Nijdam et al., 2012).

However, these plant-based proteins and alternative proteins need to have a high quality amino acid profile and should not have a high carbohydrate or phytate load. This requires designer plant protein blends made that have high amino acid score. Further, the protein blends need to be made from protein rich fractions of cereals, proteins, fungi or other sources that have carbohydrate, phytate and other accompanying loads reduced so that high consumption of these proteins do not result in macronutrient or micronutrient imbalances.

Protein dense food ingredients from plant-sources have been available for a few decades. Tofu is one such example, which is made by curdling of soy proteins. Expanded ‘non-anisotropic’ structured proteins made from defatted soy are also available in the market. However, their consumer uptake has been low. A major reason is taste and texture. The current products are made by a low moisture extrusion process using a single or low L/D (length to diameter ratio) twin screw extruder. The products are expanded during extrusion and lead to light, spongy, non-anisotropic texture upon hydration and cooking (Guy, 2001).

Developing products that can extend the textural range of available products can help product developers craft new consumer opportunities. In this thesis plant protein based products have been developed that have dense and anisotropic textures. These complement the low density, expanded nugget-type, non-directional texture products.

This extended range will open up new consumer food opportunities. One application of such products are meat analogues. We have used meats as a comparison for the types of textures that can be produced. However, it should be born in mind that in the Indian context, meat analogues are not the only products that can be made using high density, anisotropically structured plant proteins. Products such as 'chaaps' (a high density product made from a steaming a shaped mince of soybeans or soy nuggets and wheat flour) and other paneer equivalents are equally likely to be adopted by consumers.

1.2 High moisture extrusion and protein blends

High moisture extrusion technology using long L/D twins crew extruders in combination with cooling dies have the ability to create dense, anisotropic, fibrous structures from protein-rich powders. The mechanisms that shape the fiber structure are still unclear. The multiple process variables, system parameters and product characteristics that interact with each other make mechanistic understanding a challenge. The interactions between process variables, system parameters, and product characteristics make it hard to isolate the impact of a single process variable or parameter and the lack of knowledge about how ingredients, processing and structure formation are related hinders the development of products with specific targets.

Studies on high moisture extrusion of plant proteins have focused on soy and pea isolates or concentrates as the primary ingredient. These have good amino acid profile compared to most other plant proteins. Secondary and tertiary ingredients commonly studied have been wheat gluten, various starches and fibers. These have been added to improve the textural properties and reduce the hardness and rubbery texture. Most of these secondary ingredients are highly processed and add to consumer unfamiliar terms on the food labels. In this study, we explore the potential of minimally processed secondary ingredients such as whole millet flours and dry fractions as secondary ingredients to improve both the texture and nutritional profile of textured proteins.

The world grew 91.45 billion kg in year 2021 of millets and around 87 billion kg was accounted for by the three major millets - sorghum (Sorghum bicolor), pearl millet (Pennisetum glaucum), and finger millet (Eleusine coracana). India is the largest producer of millets with 41% share in the world (FAOSTAT, 2021; Garí, 2002). While their production and consumption have traditionally been confined to specific regions (Asia and Africa), there is a growing global interest in millets due to their climate

friendly and sustainability perspective. The United Nations has designated 2023 as the International Year of Millets to emphasize their significance and encourage their use beyond traditional regions. This interest stems from the fact that compared to other cereals, millets have a smaller environmental footprint (D. B. Rao et al., 2022; N. D. Rao et al., 2018; J. Wang et al., 2018). Being C4 plants, they are resilient to drought and suitable for arid conditions. This resilience positions them as potential contributors to transforming drylands and providing livelihoods in water stressed areas (Kheya et al., 2023; Rao et al., 2022). New food applications of millets could create the demand needed to support such initiatives. In addition to their environmental benefits, millet flours boast a favourable nutritional profile with low glycemic index carbohydrates, high quality protein, a balanced amino acid profile, elevated mineral content (calcium, iron, zinc), and dietary fibers compared to other cereal flours (Anitha et al., 2020; Hassan et al., 2021; Shobana et al., 2009). Millets are also gluten-free.

1.3 Aim and outline of the thesis

This thesis presents results of the experiments conducted to understand the interplay of system parameters, process parameters and product attributes in texturization of plant proteins using a twin-screw extruder. Further it details the work done in developing textured plant proteins with the following salient features -

- Good nutritional profile: high amino acid score, low carbohydrate and phytate load
- Desirable product textures: high material density, anisotropic, fibrous structure
- Cleaner labels: use of minimally processed secondary ingredients that enhance the sustainability credentials of the product

The novel textured plant proteins developed in this work serve as intermediate ingredients from which chefs and product developers can craft protein-rich consumer offerings.

The objectives of the thesis are given below

1. Physicochemical and nutritional characterization of plant proteins.
2. Full spectrum characterization of whole meat analogues made by high moisture extrusion of soy-based protein over a wide range of process and system parameters and identifying textural gaps with respect to real meat

3. Develop HHMA using soy and millet blends - literature analysis of various blends used in published literature and developing a millet based blend.
4. Protein quality analysis of SPI and whole millet flour blends using amino acid score.
5. Study of starch-rich & fiber rich fractions of one millet as a blend component during high moisture extrusion
6. Mechanistic understanding of the texturization obtained by SPI and millet fraction blends.

Chapter 2 presents the review of literature on high moisture extrusion process, ingredients, and fiber structure formation. It includes the current state of knowledge, the existing gaps and the research questions that motivate this study. This chapter also presents the theoretical framework and the key concepts that guide the analysis.

Chapter 3 covers the physicochemical and nutritional characterization of different plant proteins and other ingredients. This characterization helps in understanding the differences among the ingredients which gives some understanding of their behaviour during the texturization process though extrusion and the extrudates.

Chapter 4 focusses on characterization of extrudates of soy proteins. Soy proteins form the base component for incorporating millet flours and fractions in the subsequent chapters. Understanding their extrusion characteristics are important before moving onto the blends. This is done by studying the interplay of process parameters (feed moisture content, barrel temperature, screw speed, feed rate and protein concentration), system parameters (specific mechanical energy, melt temperature and melt pressure) and product properties (texture profile analysis, cutting strength, anisotropic index and colour values). Blends of soy protein isolates and defatted soy flour were utilized to create blends with varying protein concentration. These were then extruded under various process conditions to create a large product sample set. The samples were characterized for their texture and cutting properties. The data was analysed to understand the effect of process and system parameters on the product properties. A comprehensive textural characterization, referred to as ‘full spectrum texture evaluation’ including parameters such as hardness, chewiness, resilience, cohesiveness,

springiness, cutting strength, anisotropic index, and tensile strength was conducted to facilitate a detailed comparison of extrudates.

Chapter 5 covers the studies on use of millet flours as a secondary ingredient and their effect on textural properties of the extrudates. Three millet flours (sorghum, pearl millet and finger millet) were used at various incorporation levels with soy protein isolates, generating a wide range of textures in the extrudates, spanning from thick to thin fibers in the extrudates. The variety of textures generated can be attributed to the varying starches and dietary fibers present in millet flours. Consequently, there is a need to comprehend the impact of these macromolecular components, leading to the focus of **Chapter 6**. In this chapter, two fractions were derived from finger millet - one from the hull and the other from the dehulled grain. A detailed compositional analysis of the two fractions was done that established that the two fractions were compositionally very distinct from each other. Further, the compositional differences manifested in clear-cut differences in physicochemical characteristics of the two fractions. These fractions were incorporated into soy protein isolate at different levels and at different barrel temperatures during extrusion. To deepen the understanding of fibrations in the extrusion process, a protein-protein interaction study was employed as a mechanistic approach. Additionally, the chapter presents a methodology for quantifying visual fibration in the extrudates through image analysis. Rheological assessments of extrudates were also performed under shear conditions (amplitude and frequency modes) to complement textural properties obtained under normal compressive and tensile forces.

Chapter 7 presents a discussion of all the outcomes presented throughout the thesis and key conclusions. The insights detailed in all chapters are integrated in design rules for the creation of fibrous structures. Finally, scientific challenges to be resolved prior to commercialization of textured proteins through high moisture extrusion technology are outlined.

Chapter 2

Review of literature

2.1 Introduction

This chapter delves into the recent findings regarding the texturization techniques of plant proteins, with a specific focus on extrusion technology and the high moisture extrusion process. Additionally, it provides a review of potential protein sources utilized in high moisture extrusion, giving particular attention to ingredients and blends and their physicochemical and nutritional properties. A comparative analysis of current extruded products such as soy chunks, dry TVP and high moisture extrudates are conducted to comprehend the textual differences and the potential of these products as texturized protein dense foods. Lastly, the characterization methods of high moisture textured fibrous products are reviewed.

2.2 Methods of texturization

Researchers have explored various protein texturizing techniques to create textured products. The concept originated in the 1970s, aiming to develop texturizing methods using different proteins, primarily soy. By adding soy protein isolate to defatted brewer's yeast, they enhanced protein content and improved the texture of meatball, hamburger and wiener formulations (Gibson & Dwivedi, 1970). Over years, a number of technologies have been explored to improve the texturization of proteins.

Stanley et al. (1972) investigated rehydrated soy spun fiber, revealing structural differences between beef and soy. Electrospinning, investigated by Mattice & Marangoni (2020), produced zein fibers with uniform width. While electrospinning yields minute individual fibers, it was noted that this technology has significantly low throughput, leading to challenges in terms of efficiency.

The shear cell, specifically the concentric cylinder and cone–cone (shear cell) and devices has been studied by Krintiras et al. (2015). These are based on a flow driven structure, using a soy protein isolate and wheat gluten to create anisotropic structures for meat replacement. Operating with a rotating bottom cone and stationary upper cone, the sealed cell minimizes water evaporation, treating the sample at high temperatures (95–140 °C) followed by cooling (Krintiras et al., 2014). The resulting fiber formation is well defined due to its simple geometry and fewer parameters (temperature and shear rate), enabling precise control over system and product properties (Dekkers et al., 2018). However, it involves a longer residence time (~ 20 minutes), has a low

processing volume and needs premixing as it operates as a batch process (McClements & Grossmann, 2022).

3D printing technology, a relatively simple concept, involves using a paste like material from protein powder, water and other ingredients for layer by layer structure formation (Dankar et al., 2018). However, this technique has limitations, primarily optimized for thermoplastic materials from few ingredients and struggles with solid like characteristics. Introducing new ingredients necessitates system reoptimization for key parameters like viscosity, rheology, and cooking properties (Dankar et al., 2018; Yang et al., 2017). Despite its fairly slow printing speed, adjustments can be made for speed and flow rate, though this may impact accuracy and appearance. Concerns about microbial growth because of extended printing time and low heat treatment have been raised, affecting food safety (McClements & Grossmann, 2022).

Freeze structuring approach involves freezing a protein emulsion followed by ice crystal removal to create a structure with macro and microscale pores and fibers (Chantanuson et al., 2022). Parameters like temperature of freezing and rate can be adjusted to modify ice crystal and related fibrous and porous structures (Chantanuson et al., 2022; Dekkers et al., 2018). As subsequent process (such as freeze drying, calcium chloride addition) is needed after freezing, impacting process complexity.

Out of all the processing methods, extrusion stands out as the most established and extensively studied technique for creating textured food products. At present it is the most cost effective and scalable method amongst all the texturization techniques. This one step continuous process requires minimal labour and the extruder's energy consumption is comparatively low. Additionally, this continuous process ensures high throughput (Bouvier & Campanella, 2014).

2.3 Extrusion processing

The extrusion process is described as thermomechanical process in which food biopolymer powder such as protein or starch are hydrated, melted, plasticized and discharged from the die in presence of heat, pressure and mechanical shear. The biopolymers employed in extrusion typically exist in an amorphous or partially crystalline solid state (a condition influenced by the microstructure and composition of these biopolymers). The extrusion heating process involves transforming the

biopolymers from a solid to a liquid state described as the glass transition. If the material is partially crystalline polymers, this transition involves melting. The materials converted to a liquid state are then transformed to a solid or rubbery state which is different from the initial solid state of the biopolymers through a process that involves aggregation at a macrostructural level (Bouvier & Campanella, 2014).

Food extrusion has been employed since the mid-20th century. The first process involved cold extrusion – the extruder and die combination allowed for continuous mixing and shaping of pasta products (Harper 1989), thus converting batch process into continuous processes. Later, extrusion cooking was developed, that significant include heat transfer. It is a high temperature short time process where food ingredients undergo continuous cooking and are forced through a die to shape and texture them (Akdogan, 1999; Guy, 2001). The wide ramge of temperature, pressure and shear rate that materials could be exposed to during extrusion made extrusion technology very popular. Its adaptability, high throughput and energy efficiency resulted in development of application across a wide range of products, including breakfast cereals, ready-to-eat snacks, baby food, flavour encapsulation, pet food, fish feed, textured proteins, meat analogues and more (Akdogan & McHugh, 1999).

Food extruders typically consist of a barrel with temperature control, one or more rotating screws, feeding hopper and a die. In a single screw extruder, the screw's rotation moves the feed material through the barrel until it comes out of a shaping die. However, its mixing efficiency is poor. Corotating twin screw extruders offers good mixing (Bouvier & Campanella, 2014; Guy, 2001; Mościcki, 2011). Further, in a corotating twin screw extruder, one screw flight interacts the adjacent screw, aiding in removing material adhered to the screw surface and conveying the extrudate. This not only results in self cleaning, but also provides a sharp control over residence time distribution and process stability (Guy, 2001; Riaz, 2000). These characteristics have made twin screw extruders very popular in food industry.

Beside number of screws, food extruders are characterized by the geometric dimensions of the barrel – length to diameter ratio (L/D ratio). This is determined by dividing the total length of the barrel by the diameter of the bore. Common L/D ratios for food extruders range from 1:1 up to 60:1 (Ganjyal, 2020). Other parameters include screw configuration. In a twin screw extruder it typically incorporates various screw elements,

including conveying, mixing, kneading, or shear elements, depending on the processing needs.

Research on utilizing extrusion for texturizing proteins dates back to late 1980s and early 1990s (Cheftel et al., 2009; Kitabatake et al., 1988; Megard et al., 1985). Two main processing regimes are used producing very different product characteristics – low moisture regime and high moisture regime.

2.3.1 Low moisture extrusion

Low moisture extrusion regime involves moisture levels below 40% to manufacture texturized vegetable proteins (TVP) and are characterized by an expanded structure (McClements & Grossmann, 2022; Ozturk & Hamaker, 2023; Sha & Xiong, 2020). The early technology of low moisture extrusion involved the use of defatted soy flour in single screw extruders with short die attached at the end of an extruder to make expanded products such as soy chunks. These were characterised by spongy textures upon hydration. Attempts to create more meat-like textures have resulted in a shift towards twin screw extruders. These result in denser products and are called TVP's. The process involves a sequence of events triggered by a sudden pressure drop upon exiting the extruder die: rapid water evaporation, simultaneous cooling, increased viscosity, transition to the glassy state, bubble expansion and stabilization of the material structure (Guyony et al., 2023). An in-depth review of the texturization process of plant based proteins through extrusion and its influence on protein conformation and quality has been done by various researchers (Zhang, et al., 2019). The products produced through this technique are further discussed in section 2.4.1 and section 2.5.2.

2.3.2 High moisture extrusion

To achieve protein texturization at higher density, it is crucial to limit the expansion of the protein matrix as it emerges from the die. This implies a lower pressure drop as the product exits the die. This is accomplished by employing a combination of high moisture of the feed and a long cooling die. HME operates at feed moisture level of > 40% and up to 75% where viscosities of the melt will be lower, allows comparatively less mechanical energy input and low pressure build up in the system than low moisture extrusion. The cooling die serves multiple functions during protein texturization and plays a pivotal role in high moisture extrusion cooking. As the name suggests, the cooling die cools the material (Cheftel et al., 2009; Noguchi, 1990). The temperature is

bought to below the boiling point of water, which limits the expansion as the material exits the extruder. Importantly, by using long cooling die, the material is brought below the melt temperature gradually. This cooling over a longer flow regime allows for aggregation of proteins, phase change in layers, stretching of the layers in the direction of the flow due to lamellar shear all of which lead to the development of a fibrous structure (Schmid et al., 2022; Zhang et al., 2022). At the die exit, the solidified extrudate is shaped into the desired product appearance based on the die geometry (Akdogan, 1999).

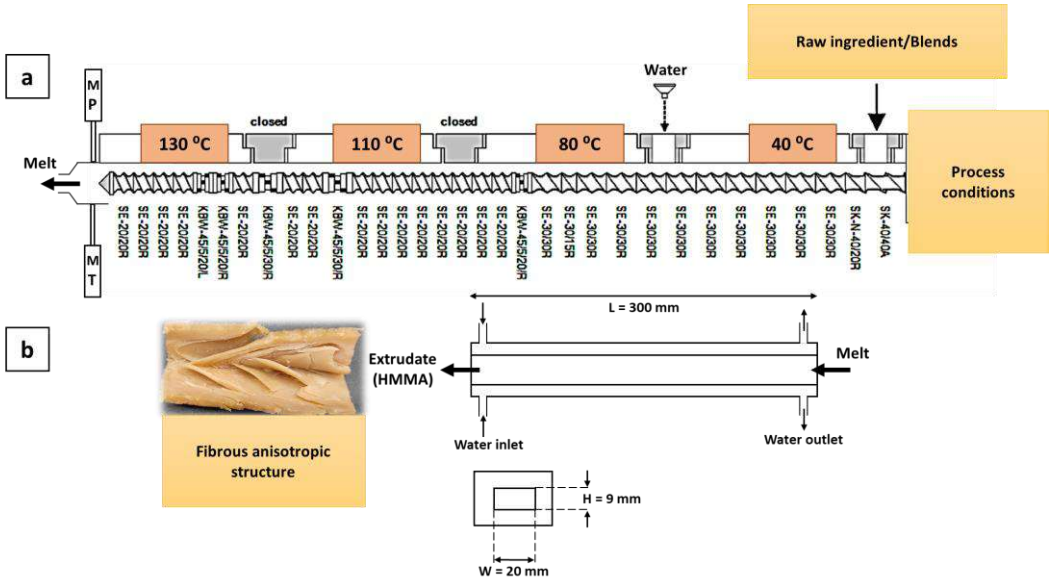

Figure 2.1 Schematic representation of (a) twin screw extruder setup with screw configuration and (b) long cooling die and an extrudate showing fibrous structure as an example MT – Melt temperature, MP – Melt pressure. SK, SK-N, SE – conveying elements, KBW – kneading elements, R – righthand side/forward, L – lefthand side/reverse. First number represent pitch and second number represent length of an element. In kneading elements, first number represents angle, second number represents No, of lobes and last number represents length.

A high L/D (length to diameter of barrel) is used in HME to allow for full wetting and hydration of the protein particles which is essential for a formation of homogenous melt. This also requires good mixing which is achieved by the high shear design of the extruder. The conveying and shearing of the ingredients can be controlled by different screw elements which were configured appropriately. A schematic representation of a twin screw extruder and the screw configuration is shown in Fig. 2.1.

By appropriately adjusting process variables such as feed moisture content and cooking temperature, a variety of fibrous structures can be obtained (Noguchi, 1990; Thiébaud et al., 1996).

2.3.2.1 Effect of processing parameters

High moisture extrusion cooking is a multistep process involving conveying, mixing, kneading, cooking, shearing, compression and flow alignment before being expelled through a shaping die. These operations are influenced by several independent variables related to both the machinery and the raw material, including screw configuration, barrel temperature, feed rate, screw speed and various feed properties (Meuser et al., 1984; Ryu, 2020). These variables impact various other parameters in the barrel, such as melt temperature, melt pressure, shear and product quality. Some of the parameters in each of these groups are summarized in Fig. 2.2 to show the relationship between them.

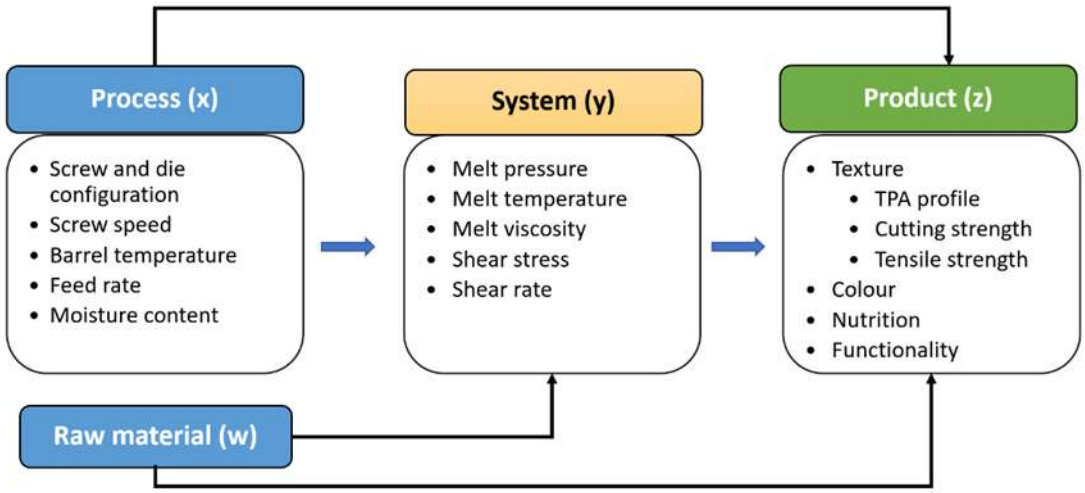

Figure 2.2 Relationship between the process, system and product parameters

The interplay of these parameters leads to molecular transformations and chemical reactions in the feed materials, contributing to the stabilization of the three dimensional network formed during cooling after the extrusion step. Consequently, the characteristics of the extruded products such as size, shape, texture, and moisture level, which directly influence the properties of the final product are determined by the interdependent system parameters. Thus, the careful selection of appropriate extrusion equipment, the characterization of feed materials and the meticulous control of process parameters are essential for achieving the desired product quality (Bouvier & Campanella, 2014; Camire, 1991; Schuchmann, 2008).

Table 2.1 Studies on extrusion parameters during high moisture extrusion.

Sl. No.	Parameters studied	Temperature (°C)	Moisture content (%)	Screw speed (rpm)	System parameters	Product properties studied	Main findings (on textural properties)	Protein source	Reference
1	BT, MC	140, 150, and 160	28, 36, 44, 52, and 60	160	SME, Viscosity, RT	Hardness, chewiness, tensile strength, cutting strength	Decrease in tensile strength, hardness and chewiness; formation of fibrous structure and aggregation	SPI (92.68% protein)	(Chen et al., 2010)
2	BT, SS, FR	130, 150 160, and <170 and >170	42.5	200	-	Cutting strength, AI	Formation of multilayered structures; well oriented, fine, good quality fibers and loss of fibers at high BT	Dehulled soy (20% oil)	(Hayashi et al., 1991)
3	BT	165 and 175	72.46 (in the surimi)	150	-	Microscopic, rheological	2X increase of tensile strength, higher orientation of texturized products, Browing reaction at high temperature	Surimi (16.6% protein), starch (96:4)	(Aoki et al., 1989)
4	BT, MC, SS	135, 155, and 180	40, 55 and 68	400 - 1800	SME, MT, MP	Colour, cutting force, cooking yield, microstructure, IVPD	Improved texture and fiber formation with increasing BT; With increase in MC - Decrease in cooking yield, soft structure due to reduced cross-linking	Lupin protein concentrate and isolate (50:50)	(Palanisamy, Franke, et al., 2019)

Sl. No.	Parameters studied	Temperature (°C)	Moisture content (%)	Screw speed (rpm)	System parameters	Product properties studied	Main findings (on textural properties)	Protein source	Reference
5	BT, SS	100 and 130	60 ± 3	180, 500 and 800	SME, MT, MP	Rheological	Change of isotropic to anisotropic structures, high oriented flow pattren	SPC (67% protein)	(Pietsch et al., 2019)
6	BT, SC	110 and 145	40	300	SME, MP	AI, Visual	Change of isotropic to anisotropic structures, characteristic flow-oriented fracture behaviour	Wheat gluten (83% protein)	(Pietsch et al., 2017a)
7	BT, MC	137.8, 148.9, and 160	60 and 70	150	SME, MP	Hardness, chewiness, gumminess, cohesiveness, elasticity, protein solubility	Decrease of elasticity, hardness, chewiness, cohesiveness, gumminess	SPI, wheat starch (9:1)	(Lin et al., 2000)
8	BT, MC	120, 140 and 180	30 and 40 (increase)	200	-	Chemical interactions	Breaking of disulfide and non-covalent bonds, higher sulfhydryl groups	SPI (83.6% protein)	(Prudêncio-Ferreira & Arêas, 1993)
9	SC	160	50	160	SME	Hardness, Chewiness, Tensile strength, Cutting	Increasing hardness, density of structures Increased chewiness	SPI (92.25% protein)	(Fang et al., 2014)

						strength, Colour			
Sl. No.	**Parameters studied**	**Temperature (°C)**	**Moisture content (%)**	**Screw speed (rpm)**	**System parameters**	**Product properties studied**	**Main findings (on textural properties)**	**Protein source**	**Reference**
10	BT, SS, FR	100, 125 and 155	54 ± 1	180, 400, and 800	-	SDS-EP, AI, hardness, young's modulus	Increase in hardness, young's modulus and improved AI with increase in BT	Wheat gluten	(Pietsch et al., 2019)
11	MC	160	40 and 45 (increase)	400	-	Hardness, Springiness, cohesiveness, AI	Reduction of hardness, cohesive and less springy samples; Loss of firmness	SPC (69% protein), soy fiber, insect-based protein (68% protein)	(Smetana et al., 2019)
12	MC	150	60, 70, and 80 (increase)	-	-	Flavour change	Reduces hardness and retain the flavour with increase in moisture	SPI mixed with 0%–40% wheat gluten	(Guo et al., 2020)
13	SS	<90	63	70–100	-	Tensile strength, colour	Incomplete "melting" led to short, thick fibers that lacked regular alignment	Surimi (15% protein) & SPC (80/20 ratio)	(Thiébaud et al., 1996)
14	BT	100, 120, 140 and 160	55	150	SME	Cutting strength	CS and SME increases with increase in BT	Pea protein isolate	(Osen et al., 2014)

Sl. No.	Parameters studied	Temperature (°C)	Moisture content (%)	Screw speed (rpm)	System parameters	Product properties studied	Main findings (on textural properties)	Protein source	Reference
15	BT, SS, MC	135, 145 and 155	50, 55 and 60	180 and 240	SME, MT, MP	Hardness, Springiness, Tensile strength, Cutting strength, colour	Increases hardness, CS, TS with increase in BT and SS but decreases with increase in MC.	Peanut protein	(Zhang et al., 2020)
16	SS, MC	150	60, 63, 65 and 70	500, 700 and 900	SME	Hardness, Chewiness, Resilience, Springiness, Cutting strength, Colour	Textural properties decrease with increase in MC and decrease in SS	Rapeseed protein and Pea protein	(Zahari et al., 2021)
17	BT, SS, MC, FR	125, 135, 145, and 155	45, 50, 55, and 60	180, 210, 240, and 270	SME, Torque	Hardness, Chewiness, Springiness, Tensile strength, Cutting strength, Colour value	Textural properties increases with increase in BT, SS and decreases with increase in MC and FR	Peanut protein, Soy protein isolate, Wheat gluten	(Zhang et al., 2022)

Literature on the impact of process parameters on system and product parameters have been summarized in Table 2.1, along with their key findings. While process parameters influence product properties by affecting system parameters, the limitations of inline measurement have maintained the extrusion process as a black box. However, it's worth noting that these studies were confined to a few process and system parameters. Furthermore, investigations into the full spectrum of textural characterization were also limited in terms of the studied process parameters. Therefore, there is a need to explore the complete textural properties of the extruded product in relation to all process and system parameters. In Chapter 4, we studied these relationships in detail to gain insights that will facilitate more precise control of the machine and product quality.

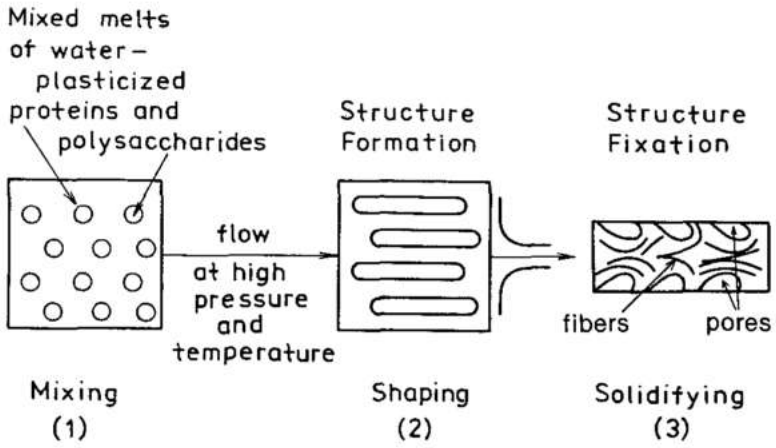

Figure 2.3 Illustrates an early model depicting the mechanism of structure formation during food processing, encompassing thermoplastic extrusion. Adapted from Tolstoguzov (1993).

2.3.3 Structure formation mechanism

High moisture extrusion involves heating and later cooling of the protein and water mixture, promoting the texturization into layered or fibrous structures (Cheftel et al., 2009). (Tolstoguzov et al., 1985) proposed an initial model outlining the mechanism of protein texturization in thermoplastic extrusion, drawing inspiration from the spinneretless spinning process. The model involved the deformation and orientation of emulsion droplets during flow until they adopt a filamentous form. This process is contingent on the phase separation of polymers in the liquid medium, driven by their thermodynamic incompatibility, resulting in the formation of a water-in-water emulsion suitable for spinning. The suggestion that phase separation of macromolecules such as proteins above a certain concentration could occur in the die was put forth as the

mechanism behind the filamentous structure observed in thermoplastic protein extrudates, even in the presence of only one type of protein (Tolstoguzov, 1988, 1993; Tolstoguzov et al., 1985).

Mitchell & Areas (1992) introduced the "suspension model" for the extrusion and texturization of biopolymers. They viewed the extruded material as a two-phase system, proposing that insoluble particulates, whether protein or nonprotein, serve as fillers within a continuous molten mass flowing through the extruder. They explained that soy produced a limited amount of indeterminate insoluble material, determined by protein resolubilization through selective reagents. Since the amount of insoluble material varied with the extrusion temperature, they suggested that an increase in the volume fraction of the insoluble phase would likely decrease extrudate expansion and stability.

Considering these findings, Camire (1991) introduced a model illustrating the crosslinking of protein texturization during extrusion cooking, depicted in Fig. 2.4.

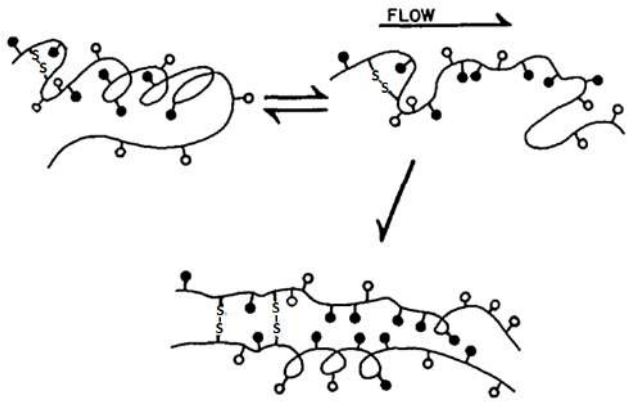

Figure 2.4 Diagram illustrating the unfolding of a protein molecule, alignment with the flow in the extruder barrel, and the creation of new bonds with another molecule. Hydrophilic amino acid residues are denoted by open circles, hydrophobic residues by closed circles, hydrophobic residues by closed circles and S-S disulfide bridges are represented. Adapted from Camire (1991).

Early investigations into the development of fibrous structures in high moisture conditions proposed that protein bodies undergo melting and subsequent fusion, resulting in a larger, elastic protein mass. This mass is then stretched in the direction of extrusion, forming the observed fibers (Noguchi, 1990). Bounie & Van Hecke (1997) modified these models to apply to high moisture extrusion cooking porcess, providing further insight into the texturization and fiber formation mechanism (Fig. 2.5).

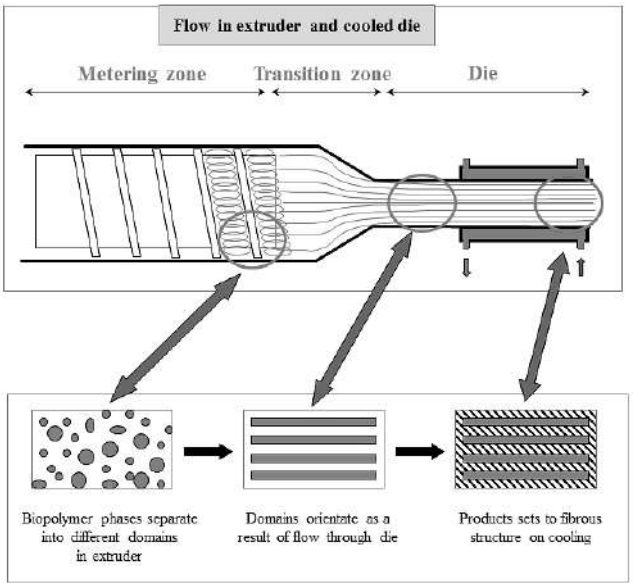

Figure 2.5 Model illustrating the phase separation mechanism during stream alignment in the cooling die. Adapted from Bounie & Van Hecke (1997).

They suggested that in the process of texturization, proteins undergo phase separation from other components like starch and insoluble fiber, creating two phases rich in individual components during stream alignment in the die. The shearing at the die entrance leads to the formation of fibrous structures composed of the separated proteins, interupted with gelatinized starch layers (Bounie & Van Hecke, 1997).

Recent investigations into the development of anisotropic structures utilizing plant proteins have employed a shear-induced structuring technique (Grabowska et al., 2014; Krintiras et al., 2014, 2015, 2016). A shearing device with a couette design was utilized to induce laminar flow of a protein mass between two plates. They noted that the formation of anisotropic structures requires the presence of structural domains that are responsive to shear flow. The alignment of domains, such as particles or micelles, relies on both the interactions between the domains and the magnitude of the shear flow (Grabowska et al., 2016). Furthermore, the fibrous structure in the product was due to the phase separation and the formation of air bubbles in the matrix (Dekkers et al., 2016).

Examinations of polymers with capillary flow rheometers revealed that Newtonian fluids produce a parabolic velocity profile, shear thinning results in a flattened parabolic profile and shear thickening leads to an extended parabolic velocity profile. In an extruder, the predominant polymer flow is shear flow, where molten polymer layers slide against each other (Giles et al., 2005).

The velocity profile across the die channel is influenced by polymer rheology, shear rate, and fluid temperature distribution in the cooling die. Understanding flow properties in a cooling die is complicated by unique material characteristics such as shear thinning behaviour of the proteinaceous material when sheared inside the die channel and viscoelastic behaviour in the sol/gel state as the fluid temperature decreases. Therefore, knowledge of the temperature distribution in the cooling die is crucial for the melt's flow properties and the coherent fiber formation process. Fig. 2.6 illustrates the 2D simulation of temperature distribution of a Newtonian fluid through a cooling die during laminar flow in a high moisture extrusion.

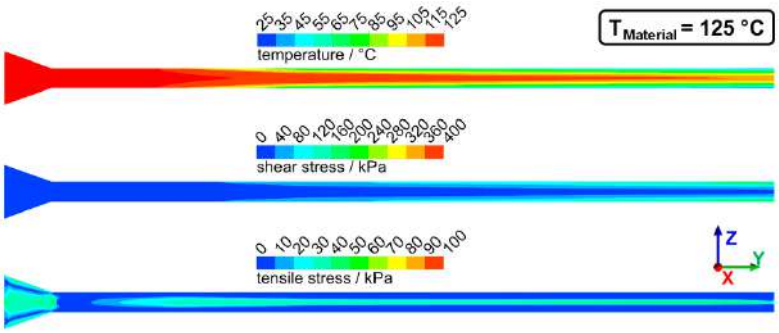

Figure 2.6 Illustrates a 2D simulation of distribution of temperature, shear and tensile stresses in the die section during extrusion trials with material temperature set at 125 °C (Wittek, Ellwanger, et al., 2021).

The temperature distribution in the cooling die channel impacts material viscosity and the flow velocity pattern. Typically, the average velocity of a viscous melt in the die channel falls within the range of 30 to 80 mm/s under laminar flow conditions (Bouvier & Campanella, 2014). In the peripheral zones of the die, velocity gradient and shear forces are generated, facilitating the orientation and alignment of protein molecules in the flow direction (Akdogan, 1999). Cooling of the viscous melt in laminar flow conditions increases viscosity, leading to a phase transition from a liquid to a gel state, ultimately resulting in the formation of fibers in the extrudate (Bouvier & Campanella, 2014).

2.3.4 Protein reactions during texturization

Throughout the extrusion cooking process, the protein matrix experiences both chemical and structural transformations that significantly impact the textural characteristics of the extruded items (Ilo & Berghofer, 2003). The native proteins undergo denaturation and the forces that maintain the tertiary and quaternary proteins

structures are weakened due to the combined effects of temperature and shearing within the extruder.

Individual protein molecules unfold and orient themselves in the direction of material flow toward the die (Camire, 1991). To structurally stabilize the extrudates, existing protein linkages must be cleaved in the heating and shearing zone and new chemical bonds need to be established in the cooling die. Changes in both covalent bonds including peptide bonds and disulfide bonds and non-covalent interactions, including hydrogen bonds, hydrophobic interactions and ionic linkages are anticipated (Liu & Hsieh, 2008; Mitchell & Areas, 1992).

The study of how proteins interact during extrusion and contribute to the structural stabilization of fibrous extrudates has been a subject of extensive research since the introduction of protein extrusion in the 1960s. There is ongoing debate in the literature about the relative significance of non-covalent interactions, intermolecular disulfide bonds and the potential formation of other covalent bonds for the structural stabilization of extrudates. One challenge in understanding protein-protein interactions during extrusion is the complexity of studying these interactions under high temperature and high pressure conditions within the extruder (Liu & Hsieh, 2007, 2008). Monitoring potential chemical interactions between amino acid residues should ideally be conducted before, after and if feasible during extrusion, although this remains a challenging task (Arêas, 1992).

The primary method for investigating protein-protein interactions involves the solubilization of proteins using selective agents that specifically solubilize protein with known mechanism is shown in Table 2.2 (Liu & Hsieh, 2008). Soluble proteins in both extruded and non extruded materials are quantified in buffer systems containing three distinct extraction reagents.

The first type is a salt buffer designed to extract loosely bound proteins not forming a stable network. The insoluble fraction is considered to be the protein linked within the 3D network structure. The second type involves a reagent known for disrupting noncovalent interactions, such as sodium dodecylsulfate (SDS) or urea, while the third type employs a reducing agent capable of cleaving disulfide bonds, such as 2-mercaptoethanol and dithiothreitol (Arêas, 1992). Table 2.1 outlines the types of protein-protein interactions, the involved amino acids and the reagents capable of

disrupting these interactions. A protein solubility profile, employing the mentioned reagents for protein samples before and after extrusion, enables the estimation of the relative contribution of key interactions in protein texturization (Arêas, 1992).

Table 2.2 Categories of interactions, amino acids involved and reagents capable of disrupting these interactions (Liu & Hsieh, 2008).

Type of interaction	Specific interaction	Amino acids involved	Reagents capable of disrupting these interactions
Covalent	Disulfide bonding	Cys/Met	Oxidizing/reducing agents (e.g. 2-mercaptoethanol, DTT, performic acid)
Non-covalent neutral	Hydrogen bonding	Asp, Glu, Thr, Ser, Cys	Strong H-bonding agents (e.g. urea, SDS, thiourea)
Non-covalent neutral	Hydrophobic interactions	Tyr, Try, Phe, Pro, Met, Leu, Ile, Val, Ala, Gly	Ionic and non ionic detergents (e.g. SDS, thiourea)
Non-covalent electrostatic	Acid hydrophilic, basic hydrophilic	Asp, Lys, Arg, His, Glu	Acids, alkali, salt solutions

DTT – dithiothreitol. SDS – sodium dodecylsulfate.

Protein solubility studies date back to 1966 when they were employed to explore the fiber development of spun soy fibers (Kelley & Pressey, 1966). The investigation revealed that spun soybean fibers formation involved contributions from hydrogen bonds, ionic interactions and disulfide bonds. An alternative hypothesis regarding protein texturization suggested that disulfide bonds played a negligible role in the structural stability of soy protein extruded at as high as 180 °C temperatures. Instead, the proposal suggested the occurrence of newly formed intermolecular peptide bonds (Burgess & Stanley, 1976; Simonsky & Stanley, 1982). This proposition was based on three key observations: First, an increase in free sulfhydryl groups after extrusion, indicating the cleavage of disulfide bonds rather than disulfide crosslinking. Second, the enhancement of product characteristics with the addition of reducing reagents to the feed, implying that disulfide bonds were of insignificant during texturization. Third, a reduced texture development after blocking free amino and carboxyl groups, indicating that the structural stability of extrudates was due to peptide bond formation.

However, the proposed mechanism of intramolecular peptide bond formation during protein extrusion faced significant controversy in subsequent studies. This was attributed to the observation that proteins could be resolubilized from extruded products

using extracting solutions containing agents capable of breaking hydrogen bonds and hydrophobic interactions, along with agents capable of breaking disulfide linkages (Arêas, 1992; Hager, 1984; Jeunink & Cheftel, 1979; M. Li & Lee, 1996; Prudêncio-Ferreira & Arêas, 1993). This proposed mechanisms was linked to the high extrusion temperature of 180 °C used by Burgess & Stanley (1976), which may have supplied the necessary energy for peptide bonding (Prudêncio-Ferreira & Arêas, 1993).

While the substantial energy input and shearing likely resulted in significant denaturation and the breakdown of the protein's secondary structure, the process seemed to enable protein interactions that stabilized the three dimensional structure, incorporating antiparallel β sheet conformations (Prudêncio-Ferreira & Arêas, 1993).

2.3.4.1 Interactions among proteins in high moisture extrusion

Since the early investigations by Noguchi (1990) and Cheftel et al. (2009) on high moisture extrusion, there have been endeavours to explore the protein reactions responsible for stabilizing fibrous extrudates in high moisture conditions. In contrast to thermoplastic extrusion, the presence of high amount of water in high moisture extrusion during processing reduces the shear forces in the extruder and protects the proteins (Björck et al., 1983). Moreover, the wet conditions during high moisture extrusion are not conducive to the formation of peptide bonds and there is no indication of newly formed peptide bonds in the extrudates from high moisture extrusion (Noguchi, 1990). This conclusion is drawn from the complete solubility of extrudates from soy protein isolate in extracting solutions that contain agents capable of breaking hydrogen bonds and hydrophobic interactions, along with agents that disrupt disulfide linkages. This suggests the absence of covalent bonds other than disulfide bonds (Chen et al., 2011; Lin et al., 2000; Liu & Hsieh, 2007, 2008).

In contrast to the expanded and sponge-like texture observed in low moisture extrusion, high moisture extrudates exhibit a rubbery gel like consistency. This has led to the hypothesis that the chemical bonds in heat induced soy protein gels and protein extrudates from high moisture extrusion include disulfide bonds, hydrogen bonds and hydrophobic interaction and electrostatic interactions. The key distinction between the two lies in the thermal reversibility and structural rigidity, determined by the relative proportions of each type of bond in their structures (Liu & Hsieh, 2007). Through the method of protein solubilization in selective agents described earlier, it was revealed

that noncovalent bonds played a predominant role over disulfide bonds in the formation of protein gels during heat induced gelation. However, in the creation of the fibrous structure of protein extrudates, both noncovalent and disulfide bonds were found to be significant (Liu & Hsieh, 2007).

Regarding the importance of noncovalent interactions, intermolecular disulfide bonds and potentially other covalent bonds for the structural stabilization of extrudates, Liu & Hsieh (2008) proposed that disulfide bonds play a more significant role than noncovalent interactions in stabilizing the rigid structure. Conversely, Chen et al. (2011) argued that the contribution of noncovalent bonds surpasses that of covalent bonds. Currently, there is still a discrepancy in the literature regarding the relative significance of these various linkages.

More recently, Chen et al. (2023) and Zhang et al. (2020) reported that the use of amylose and amylopectin promoted the crosslinking mechanism of proteins and improved the fibrous structure in the extrudates. Furthermore, Chen et al. (2023) found that the combined presence of amylopectin and stearic acid collaboratively diminished the binding forces among proteins, resulting in the creation of more relaxed and pliable structures within aggregates. These structures were predominantly upheld by hydrophobic interactions and hydrogen bonds. The enhanced flexibility of these structures facilitated the alignment of aggregates in the extrusion direction, contributing to the development of anisotropic fibrous formations in the extrudates.

2.3.4.2 Impact of pressure and shear on protein reactions

Studying the effects of individual system parameters in extrusion technology, such as pressure or shear on protein reactions, is challenging due to the multivariable nature of the process. An approach to investigate the intricate processes within the extruder involves simulating the extrusion process using non continuous experimental setups. In the compression zone of the extruder under high moisture conditions, the maximum pressure is typically below 20 bar. Through the use of a temperature controlled pressure cell to simulate the pressure effect during extrusion, it has been demonstrated that pressures ranging from 20 to 80 bar do not significantly impact protein reactions. Consequently, it can be inferred that the influence of pressure on protein reactions within the extruder is relatively minor (Noguchi, 1990).

In addition to pressure, the degree of shear plays a crucial role in protein reactions during extrusion cooking. Unlike traditional protein extrusion, the presence of high moisture content diminishes shear and this reduction can be indirectly observed through the measurement of mechanical energy within the system (Björck et al., 1983).

Fang et al. (2013) conducted a study to assess the impact of mechanical shear on the molecular characteristics of soy protein extruded with a 50% w.b. moisture content, employing various screw configurations to indirectly introduce different levels of shear. Specifically, they substituted 3 conveying elements with kneading elements (25 mm length, 45° staggering angle) in the cooking zone of the extruder. Varied values of specific mechanical energy ranging from 840 to 1277 kJ/kg were imparted into the product by altering screw configurations. The results indicated that a higher specific mechanical energy led to an increased proportion of low molecular weight fractions approximately 17.43 kDa, suggesting that higher shear can enhance the extent of molecular breakdown in protein aggregates. Moreover, the augmentation of specific mechanical energy reduced the viscosity of the mass at the die exit and yielded extrudates with elevated tensile strength (Fang et al., 2013, 2014). In conclusion, it can be inferred that while pressure during high moisture extrusion cooking has a minor role. The level of shear significantly influences the molecular breakdown of protein aggregates, indicating partial depolymerization of protein due to mechanical shear.

In conclusion, there is an ongoing debate in the literature regarding the relative significance of various types of linkages in high moisture extrusion. Further research efforts are essential to gain deeper insights into the chemical alterations occurring during high moisture extrusion. Such findings hold considerable importance for comprehending and effectively managing the process and ingredients involved in producing high quality extrude food products.

2.4 Ingredients for texturization

This section provides an overview of the ingredients being used in the high moisture extrusion processing for making texturized products. The suitability of a protein source for plant based protein ingredients is influenced by various factors including the economic viability of commercial protein production, nutritional characteristics, the functional properties of the protein and environmental considerations related to crop cultivation and manufacturing. In the context of high moisture extrusion, various plant

proteins have been tested for their ability to achieve texturization including soy, pea, chickpea, lupin, mung, pumpkin seed, wheat gluten, rice protein, and others. We conducted a literature search to retrieve ingredient data.

A detailed list of ingredients used in the research articles to create fibrous texturized food through high moisture extrusion was presented in Table 2.3.

Table 2.3 List of ingredients used in the high moisture extrusion.

Sl. No.	Primary Ingredient	Other blend component(s)	Blend ratio	References
	Single protein			
1	Defatted soy flour	-	100:0	(Maurice & Stanley, 1978)
2	Dehulled soy (20% oil)	-		(Hayashi et al., 1991)
3	Soy protein isolate	-	100:0	(Liu & Hsieh, 2007b)
4	Soy protein isolate	-	100:0	(Liu & Hsieh, 2008)
5	Soy protein isolate	-	100:0	(Chen et al., 2010)
6	Soy protein isolate	-	100:0	(Fang et al., 2014)
7	Soy protein isolate	-	100:0	(Wittek, Zeiler, et al., 2021)
8	Pea protein isolate	-	100:0	(Osen et al., 2014)
9	Pea protein isolate	-	100:0	(Zhang & Ryu, 2023b)
10	Pea protein isolate	-	100:0	(Osen et al., 2015)
11	Lupin protein	-	100:0	(Palanisamy et al., 2019)
12	Soy protein concentrate	-	100:0	(Pietsch et al., 2019)
13	Soy protein conc.	-	100:0	(Zink et al., 2023)
14	Peanut protein	-	100:0	(Zhang et al., 2020)
15	Peanut protein	-	100:0	(Zhang et al., 2019)
16	Peanut protein	-	100:0	(Rehrah et al., 2009)
17	Pea protein isolate	-	100:0	(Ferawati et al., 2021)
18	Faba bean protein conc.	-	100:0	(Ferawati et al., 2021; Nasrollahzadeh et al., 2023)
19	Faba bean protein	-	100:0	(Saldanha do Carmo et al., 2021)

20	Chickpea	-	100:0	(Nasrollahzadeh et al., 2023)
21	Mungbean	-	100:0	(Nasrollahzadeh et al., 2023; Seetapan et al., 2023a)
22	Wheat gluten	-	100:0	(Nasrollahzadeh et al., 2023)
23	Wheat gluten	-	100:0	(Pietsch et al., 2017b)
24	Wheat gluten	-	100:0	(Pietsch, Werner, et al., 2019)
25	Rice	-	100:0	(Nasrollahzadeh et al., 2023)
26	Pumpkin	-	100:0	(Nasrollahzadeh et al., 2023)
27	Hemp protein conc.	-	100:0	(Nasrollahzadeh et al., 2022)
28	**With starch-rich component**			
29	Soy protein isolate	Wheat starch	90:10	(Lin et al., 2000)
30	Soy protein isolate	Rice flour	90:10 80:20 70:30 60:40 50:50	(Han et al., 1989)
31	Soy protein isolate	Corn starch	90:10	(Samard et al., 2019)
32	Pea protein isolate	Amylose/Amylopectin	90:10	(Chen et al., 2022)
33	Pea protein isolate	Amylose/Amylopectin	90:10 (0:1, 1:2, 1:1, 2:1, 1:0)	(Chen et al., 2021)
34	Pea protein isolate	Wheat gluten, corn starch	50:40:10	(Zhang & Ryu, 2023a)
35	Peanut protein	Wheat starch	0 to 8%	(Zhang et al., 2020)
36	Pea protein isolate	Amylopectin:Stearic acid	85:10:5	(Chen et al., 2023)
37	Mungbean protein isolate	Mungbean flour	100:0 90:10 80:20 70:30	(Seetapan et al., 2023b)
38	Soy protein isolate	Sunflower meal	37.5, 50, 62.5	(Singh et al., 2023)
39	Soy protein conc.	konjac glucomannan/ carrageenan/ sodium alginate/ wheat starch	1%/2%/3%/6%	(Zhao et al., 2024)
40	Soy protein conc.	Iota carrageenan	0.75,1.5, 2.25,3%	(Palanisamy et al., 2018)
	With protein-rich component			
41	Soy protein isolate	Wheat gluten	80:20 60:40 40:60	(Park et al., 2017)
42	Soy protein isolate	Wheat gluten	100:0 70:30 50:50	(Zhang et al., 2022)

			30:70 0:100	
43	Soy protein isolate	Wheat gluten	100:0 90:10 80:20 70:30 60:40	(Guo et al., 2020)
44	Soy protein isolate	Wheat gluten	80:20 60:40 40:60	(Wu et al., 2018)
45	Soy protein concentrate	Wheat gluten	90:10 80:20 70:30	(Chiang et al., 2019a)
46	Soy protein isolate	Pea protein isolate	100:0 80:20 60:40 50:50 40:60 20:80 0:100	(Lee et al., 2023)
47	Soy meal	Soy protein isolate, Wheat gluten, wheat starch	43:33:4:8	(Huang et al., 2024)
48	Soy protein isolate	Full fat soy, wheat gluten, corn starch	50:0:40:10 40:10:40:10 30:20:40:10 20:30:40:10 10:40:40:10 0:50:40:10	(Jeon et al., 2023)
49	Soy protein isolate	Whey protein concentrate	85:15 70:30	(Wittek et al., 2021)
50	Pea protein isolate	Rapeseed protein	50%	(Zahari et al., 2021)
51	Soy protein isolate	Wheat gluten, Corn starch	50:40:10	(Samard et al., 2019)
52	Soy protein isolate	Wheat gluten, Corn starch	50:40:10	(Maung et al., 2021)
53	Soy protein isolate	Whey protein	90:10 80:20 70:30	(Adavalli, 2007)
54	Soy protein isolate	Wheat gluten, Starch	6:4:0.5	(Yao et al., 2004)
55	Soy protein isolate	Wheat gluten, Starch	6:4:0.5	(Ranasinghesagara et al., 2005)
56	Soy protein isolate	Oat protein	70:30	(de Angelis et al., 2020)
57	Soy protein concentrate	Microalgae	70:30 50:50	(Caporgno et al., 2020)
58	Soy protein isolate	Wheat gluten, Starches	65:15:20	(Zhang et al., 2016)
59	Soy protein conc.	Wheat gluten	92.11:7.89	(Hua et al., 2023)
60	Chickpea protein	Soy protein conc., wheat gluten	47.76:44.92:7.32	(Hua et al., 2023)

61	Rice protein isolate	Soy protein conc., mungbean protein isolate	51.72:34.7:13.58	(Hua et al., 2023)
62	Pea protein isolate	Soy protein conc., wheat gluten	50.11:39.89:10	(Hua et al., 2023)
63	Soy protein conc.	Pea protein isolate	62.05:37.95	(Hua et al., 2023)
64	Pea protein isolate	Mungbean protein isolate, wheat gluten	66.81:23.19:10	(Hua et al., 2023)
65	Pea protein isolate	Oat protein conc.	100:0 45:55 0:100	(Immonen et al., 2021)
66	Lupin protein isolate	Spirulina	85:15 70:30 50:50	(Palanisamy et al., 2019)
67	Pea protein isolate	Flaxseed protein concentrate	0-8%	(Riazi et al., 2023)
68	Pea protein	Wheat gluten, salt	78:21:1	(Usman et al., 2023)
69	Pea protein isolate	Fungal biomass	100:0 95:5 90:10 85:15	(Zhang et al., 2024)
70	Wheat gluten	Pea protein	100:0 80:20 60:40 40:60 20:80 0:100	(Richter et al., 2024)
71	Germinated pea protein	Wheat gluten, salt	78:21:1	(Guo et al., 2024)
72	Hemp protein conc.	Wheat gluten	90:10 70:30 50:50 0:100	(Zahari, Rinaldi, et al., 2023)
73	Hemp protein conc.	Chcikpea protein conc.	50:50 0:100	(Zahari, Rinaldi, et al., 2023)
74	Soy protein	Hemp	100:0 80:20 60:40 40:60	(Zahari et al., 2020)
75	Hemp protein	Soy/mung protein	70:30	(Nasrollahzadeh et al., 2024)
76	Pumpkin protein	Soy/mung protein	70:30	(Nasrollahzadeh et al., 2024)
77	Faba bean protein isolate	Faba bean protein conc.	30:70 50:50 70:30	(Kantanen et al., 2022)
78	Peanut protein,	Soy protein isolate, Wheat gluten		(Zhang et al., 2022)
	With fiber-rich components			
79	Soy protein isolate	Pectin	1.3 to 4%	(Dekkers et al., 2016)
80	Soy protein isolate	Wheat gluten (70:30), sodium	1 to 5%	(Wang et al., 2023)

		alginate/Xanthun gum, Maltodextrin		
81	Wheat gluten, Starch (9:1)	Phosphates	0, 0.25, 0.5, 1, 2%	(Peng et al., 2021)
82	Pea protein isolate	Oat fiber concentrate	75:25 50:50 25:75	(Ramos Diaz et al., 2022)
83	Soy protein isolate	Pectin/Cellulose	97:3 93:7 91:9	(Schreuders et al., 2022)
84	Pea protein isolate	Pectin/Cellulose	97:3 93:7 91:9	(Schreuders et al., 2022)
85	Pea protein isolate	Konjac glucomannan	99:1	(Xia et al., 2023a)
86	Pea protein isolate	Pea fiber	85:15	(Kaunisto et al., 2024)
87	Peanut protein	Carrageenan/Sodium alginate	99.95:0.05 99.9:0.1 99.5:0.5 99:1	(Zhang et al., 2020)
88	Hemp protein concentrate	Oat fiber	50:50	(Zahari et al., 2023)
89	Yeast protein	Konjac glucomannan	0, 1, 2, 4%	(Xia et al., 2023b)
	With other component			
90	Peanut protein	TGase enzyme	0.1, 0.2, 0.3%	(Faisal et al., 2022)
91	Peanut protein	TGase enzyme	0.1, 0.2, 0.3%	(Zhang et al., 2021)
92	Oat protein conc.	TGase enzyme		(Pöri et al., 2022)
93	Soy protein	Tomato powder	0,5,10,20%	(Lyu et al., 2023)
94	Soy protein	*Haematococcus pluvialis* (microalgae)	0.25-1.25% (for colour)	(Huang et al., 2024)
95	Pea protein	*Haematococcus pluvialis* residue	100:0 90:10 80:20 60:40	(Xia et al., 2022)
96	Soy protein isolate	Mushroom powder	100:0 75:25 50:50 25:75	(Ketnawa et al., 2024)
97	Wheat gluten	Oil	0,2,4,6%	(Kendler et al., 2021)
98	Soy protein conc.	Sacha inchi oil	1-10%	(Prasert et al., 2022)

2.4.1 Ingredients and blend analysis

We have classified the ingredients based on blend proportion: 50% or above refers to the primary ingredient, 50 to 10% refers to the secondary ingredient and less than 10% refers to the tertiary ingredient.

a) Primary ingredients (50 % or above) - Primary ingredients are dominantly a protein rich (isolate or concentrate protein powder). They can be used singly or in the blend with secondary or secondary and tertiary ingredients.
b) Secondary ingredients (10% - 50%) - Secondary ingredients could be protein rich or starch rich or dietary fiber rich component.
c) Tertiary ingredients (less than 10%) - Tertiary ingredients typically consist of starches or hydrocolloids or fibers or enzymes in small quantities to improve the functionality in the product.

Among the primary ingredients, soy protein isolate appeared most frequently and wheat gluten was the highest in the secondary ingredient category (Fig. 2.7). There were more research papers where soy and gluten proteins were used in a blend for better texturization (Chiang et al., 2019b) and most current plant based products on the market are made of soy and gluten (Asgar et al., 2010; GFI, 2021). This presents an opportunity to explore alternative ingredients such as gluten free options.

On the other hand, most of these secondary and tertiary ingredients (such as starches, fiber and hydrocolloids) involve ultra processing and add to unfamiliar names on labels from a consumer perspective. They also add to cost for the manufacturer. One potential solution to these challenges lies in exploring minimally processed, but well characterised natural ingredients so that extrusion and texturization relevant specifications can be set. Another important dimension of blending ingredients is that the blend should contains a balanced amino acid profile as most of the plant based proteins does not contain all the essential amino acids. In general, cereals lack in lysine and legumes lack in sulphur containing amino acids (Temba et al., 2016). Thus, a combination of cereal and legume can help in balancing the amino acid profile and in the following chapter we are looking millets as a secondary ingredient with soy protein isolate.

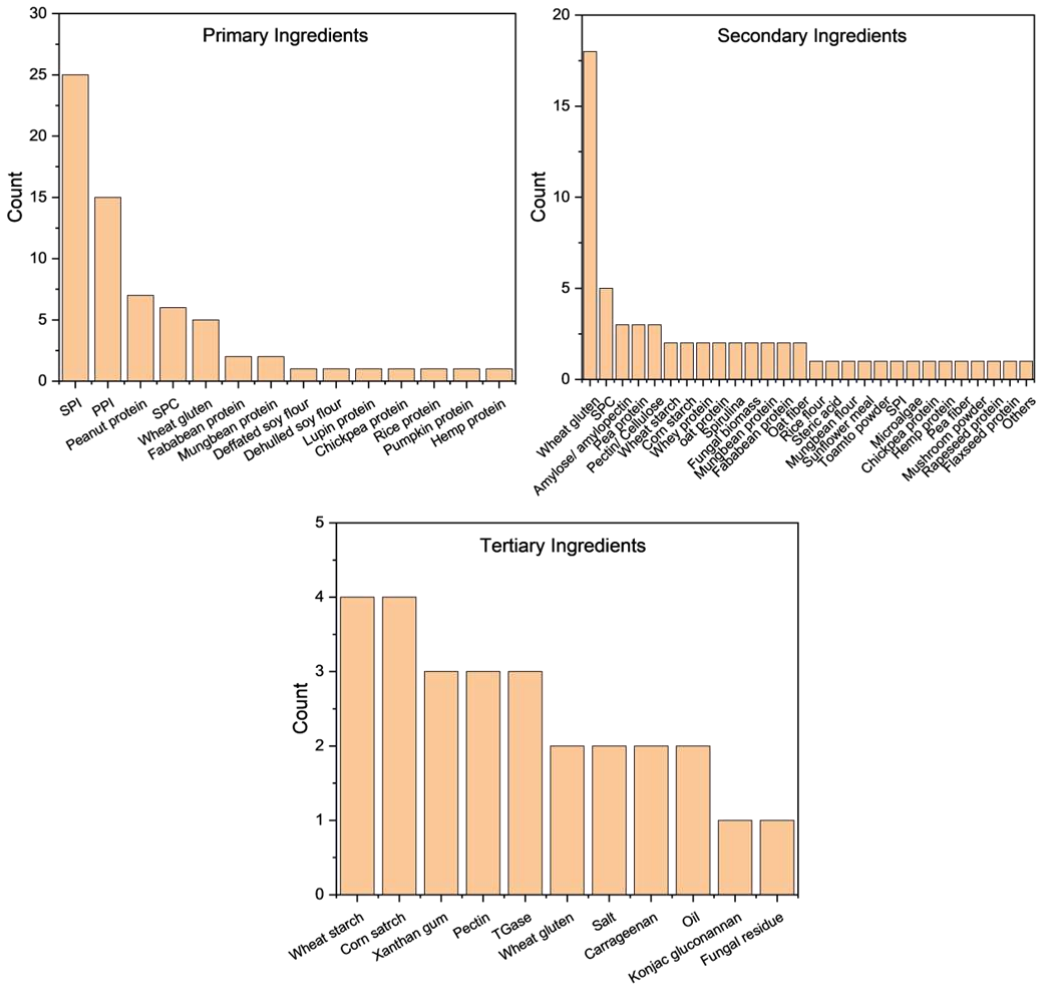

Figure 2.7 Ingredients categorized based on the proportion used in the blend in high moisture extrusion for creating texturized extrudates.

2.4.2 Nutritional aspects

Since the 1970s, nutritional scientists have been addressing the "protein gap" a concern that becomes increasingly significant with the projected population growth. As the demand for plant based proteins rises, it becomes crucial to advance science and technology to preserve the functionality and nutrition of these proteins. Traditionally, protein quality assessments have relied on animal or human studies with measures like net protein utilization (NPU), indicating the fraction of consumed protein retained. NPU considers both digestibility and biological value (BV), combining them into a single value. However, due to its cumbersome nature, current practice favours the use of the protein digestibility corrected amino acid score (PDCAAS) and digestible indispensable amino acid score (DIAAS). These scores assess protein digestibility based on human amino acid requirements, offering a more efficient evaluation.

PDCAAS is determined by multiplying a dietary protein's amino acid score by its fecal nitrogen digestibility, while DIAAS employs ileal digestibility coefficients for estimating true ileal digestibility of essential amino acids (Marinangeli & House, 2017).

Factors contributing to the nutritional quality of animal and plant proteins include essential amino acid content, protein digestibility, net protein consumption, biological value and protein digestibility corrected amino acid score (PDCASS) (FAO/WHO, 2013). Animal proteins are often recommended for meeting dietary protein needs due to their balanced essential and non essential amino acid profile, contrasting with plant sources that may be deficient in certain essential nutrients. The PDCAAS/DIAAS scores reflect this, with animal proteins generally scoring higher (1) compared to plant proteins, which can range from 0.4 to 0.9 (Berrazaga et al., 2019; Hertzler et al., 2020; Phillips, 2017). Several factors contribute to the reduced digestibility of plant proteins, including the presence of antinutrients like phytates and trypsin inhibitors hindering digestion and absorption, structural differences with fewer α helixes and more β sheet structures favouring protein aggregates and the presence of dietary fibers reducing proteolytic digestibility in plants (Sim et al., 2021).

Table 2.4 PDCAAS and DIAAS scores for some of the protein fractions and foods. Adapted from (Hertzler et al., 2020; Sim et al., 2021).

Food	PDCAAS	DIAAS	Limiting amino acids
Whole Milk	1.00	1.14	None
Whey	1.00	0.90	His
Soy protein isolate	0.99	0.92	Met + Cys
Pea protein isolate	0.89	0.66	Met + Cys
Rice protein concentrate	0.57	0.52	Lys
Cooked Rice	0.62	0.59	Lys
Wheat gluten	0.54	0.43	Lys, Thr, Leu
Chickpea protein	0.74	0.83	Met + Cys
Peanut protein concentrate	0.50	0.47	Met + Cys, Lys
Tofu	0.56	0.52	Met + Cys

PDCAAS - Protein Digestibility Corrected Amino Acid Score. DIAAS - Digestible Indispensable Amino Acid Score.

The nutritional value of protein sources, aside from their bioavailability during gastrointestinal digestion is influenced by the kinetics or rate of protein digestion, categorizing proteins into slow and fast proteins (Boirie et al., 1997; Dangin et al., 2003). Whey proteins are known to be digested and absorbed more rapidly in the body compared to native micellar casein, where caseins coagulate with digestive enzymes, leading to slower digestion and subsequent absorption (Boirie et al., 1997). Soy

proteins, on the other hand are absorbed more quickly than casein but at a slower rate than whey proteins. Muscle protein fractional synthetic rates for whey, soy, and casein are reported as 0.091, 0.078, and 0.047% per hour, respectively (J. E. Tang et al., 2009). However, an alternate study found that the postprandial muscle protein synthesis rate for soy proteins did not increase as much as it did after consuming whey proteins (Y. Yang et al., 2012). This difference could be attributed to amino acid composition, particularly the low leucine content in soy, which may enhance protein synthesis while inhibiting protein breakdown (Suryawan et al., 2011).

There are several strategies to enhance the quality of plant based proteins for human consumption. One approach involves removing antinutrients from isolated plant based proteins, such as soy to elevate their nutritional quality to a PDCAAS of 1.00, comparable to animal derived foods. Increasing the quantity of plant based protein consumed per meal is anticipated to effectively compensate for their diminished anabolic response compared to animal protein has also been suggested (Norton et al., 2009). However, it should be noted that employing these strategies may not yield a similar anabolic response to animal sources since removing antinutrients or increasing plant based protein intake might not elevate the essential amino acid content, especially leucine (J. Boye et al., 2010; Gilani et al., 2005). As a result, studies have indicated that consuming wheat protein with an equivalent leucine content to that of whey protein can enhance postprandial muscle protein synthesis rates (Gorissen et al., 2016). Fortifying plant proteins with essential amino acids for protein synthesis is another strategy to improve their nutritional quality. Research has demonstrated that fortifying soy proteins with leucine, isoleucine and valine increases whole body protein synthesis (Engelen et al., 2007). Another suggested approach involves blending the right combination of plant based proteins (Hertzler et al., 2020), thereby enhancing the nutritional quality of plant proteins. According to Day (2013), although the individual PDCASS values of peas and rice are low, combining peas and rice can elevate the PDCASS value to 1.00. Incorporating, fortifying or modifying plant proteins using effective strategies can significantly boost the nutritional quality of plant based proteins, creating new growth opportunities for the food industry.

There are limited but promising investigations indicating that the intake of plant based texturized products may support gut health through the modulation of the microbial profile. Toribio-Mateas et al. (2021) observed favourable alterations in the gut

microbiome of flexitarian consumers incorporating plant based texturized food into their diets, noting an enhanced potential for butyrate metabolism and a reduced population of the *Tenericutes phylum*.

In this thesis, we have looked into the millet flour as secondary ingredients in the blend to enhance the essential amino acid scores and ultimately reaching to PDCAAS value of textured extruded foods to 1.00. Apart from essential amino acids, millets also contain good amount of minerals for example, finger millet has calcium (364 mg/100g) and pearl millet has iron (6.42 mg/100g) (Longvah et al., 2017). They are also rich source of dietary fibers and resistant starches which will improve the gut health. Plant proteins when extruded will have about 20% higher bioavailability of amino acids compared to normal pressure cooked proteins (Devi et al., 2020). Thus, extrusion technology will have an added advantage from the digestibility perspective and simultaneously inactivating the antinutritional factors present in the plant proteins (Nikmaram et al., 2017).

2.4.3 Functional properties of ingredients

Functional properties are those physical and chemical properties of an ingredient that influence their behaviour in food systems during processing, storage, preparation and consumption. These properties arise from the interactions between the protein and other components in food and are influenced by intrinsic physicochemical properties defining the protein structure and conformation, as well as extrinsic environmental factors. Key physicochemical properties include amino acid composition, net charge and hydrophobicity, while external factors encompass temperature, pH, ionic strength, and the presence of other constituents (Kinsella & Whitehead, 1989). Consequently, the application of proteins enables the modification of food properties such as solubility, water holding, fat holding, emulsification, foaming, gelation and thickening. Such properties becomes important and crucial during extrusion processing.

Adequate solubility is viewed as a fundamental requirement for subsequent techno functional properties like gelling, emulsification or foaming. Typically, solubility is assessed through the soluble nitrogen fraction in a standard buffered solution and hinges on the distribution and accessibility of polar and nonpolar groups on the molecule's surface due to its three dimensional folding. The solubility of proteins is significantly

influenced by external factors such as temperature, pH and ionic strength, which dictate the folding of the molecule (Damodaran, 1997; Yada, 2018).

The water holding capacity is influenced by both the macroscopic particle surface, where water is physically held in the cavities and capillaries of the protein particles, and protein-water interactions. Similar principles govern the protein's capability to bind oil and act as a food emulsifier, dictated by its structure and properties at colloidal interfaces. The amphiphilic nature of proteins enables them to be adsorbed at the oil/water interface, forming an interfacial layer that reduces surface tension (Day, 2013).

Among the various functional properties of proteins, the capacity to form gels is particularly significant in the preparation of many food items. Examples of protein gelation applications range from the boiling of an egg to more complex scenarios such as substituting animal protein in dairy and meat products (Clark et al., 2001). The gel structure relies on the protein network, where water along with other minor components like sugars or starch is trapped while contributing to the overall texture. Food protein gels can be categorized into fine stranded cross-linked polymer networks or particle gels, comprising strands or clusters of aggregated protein. The heat induced gelation of globular proteins typically results in turbid gels and involves three successive steps: (1) temperature induced unfolding of the protein with exposure of hydrophobic residues, (2) interaction of these side chains forming aggregates and (3) arrangement of the aggregates into a three-dimensional network (O'Kane et al., 2004).

Apart from the physicochemical properties governing protein-protein interactions and protein-non protein associations, external factors like heating/cooling rate, pH, and ionic strength play a role in influencing network formation (Renkema, 2004). As of now, the gelation characteristics of plant proteins, in general remain incompletely comprehended, prompting substantial endeavours to analyse the chemical forces influencing protein gelation. Renkema & Van Vliet (2002) investigated the heat induced gel formation of soy protein and observed that the rise in elastic modulus during cooling was thermos reversible at neutral pH, suggesting that disulfide bonding and rearrangements do not occur during gelation.

Catsimpolas & Meyer (1970) proposed that the thermal gelation process of soy protein initiates with initial unfolding and dissociation, leading to reversible aggregation and

the formation of an intermediate progel characterized by non-covalent bonding. With further heating, the progel undergoes disruption, followed by irreversible gel formation that involves covalent disulfide bonding. Utsumi & Kinsella (1985) investigated the gelling behaviour of fractions of soy protein, classifying them into two main groups based on their sedimentation coefficient: the 11S size fraction and the 7S size fraction. The study suggested that the gelling of soy protein isolate relies on hydrogen bonding and hydrophobic interactions, with 11S globulins primarily involving electrostatic interactions and disulfide bonds and 7S gels primarily relying on hydrogen bonding. In a study by Sheard et al. (1986), macromolecular changes during the heat treatment of soy protein were examined, proposing that while heat treated soy proteins primarily aggregated through hydrophobic interactions, an increase in protein concentration appeared to enhance the formation of disulfide linkages, stabilizing the protein aggregates.

The current understanding suggests that the principal protein-protein interactions driving the aggregation and gelation of plant proteins are predominantly non-covalent, encompassing hydrogen bonds and hydrophobic interactions, with a minor contribution from covalent disulfide crosslinking. The proportional balance of these bond types in their structure is deemed significant for considerations of thermal reversibility and structural rigidity (Liu & Hsieh, 2007).

2.4.4 Rheological properties of ingredients

The predominant offline rheometers that apply a steady shear rate to the fluid are capillary and rotational rheometers. Typically, rotational measurements are employed to examine the viscosity of flowable liquids. Since most food compositions for extrusion are solid at room temperature and only exhibit flow at elevated temperatures exceeding 100 °C, it is necessary to dilute the food materials for rotational testing. In the context of extrusion, rotational rheometers have been utilized to explore temperature induced alterations in the rheological behaviour of diluted starch or protein suspensions, stemming from phenomena such as starch granule swelling, gelatinization, or protein denaturation during extrusion cooking. This can furnish valuable insights into the techno-functional properties of the raw materials (Bourne, 2002; Sorba & Sopade, 2013; Tabilo-Munizaga & Barbosa-Cánovas, 2005).

Commonly employed empirical tools for routine rheological assessments of extruded foods include the Brabender ViscoAmylograph (now Viscoquick) and the Rapid Visco Analyzer (RVA) (Biliaderis, 2009). These instruments are utilized to characterize the preprocessed state of the hydrated raw material, as well as its postprocessed state (Borwankar, 1992). Changes in viscosity are observed under continuous stirring and following a programmed heating and cooling cycle. Unlike conventional rotational rheometers that use plate, cone or cylinder probes, the rotating paddles in these instruments can prevent the sedimentation of dispersed particles. The pasting properties of extruded products have been documented in various publications (Moisio et al., 2015; Osen et al., 2015; F. Wu et al., 2015; Zahari et al., 2021). Pasting is a phenomenon that follows gelatinization, involving granular swelling, amylose leaching, and the complete disruption of the starch granule.

The RVA curve exhibits a rise in viscosity corresponding to the initiation of starch gelatinization. The peak viscosity signifies the maximum swelling of the hydrated starch granules, followed by disintegration into amylose and amylopectin. Subsequently, upon cooling, the viscosity increases due to gelling until reaching a final viscosity (Saunders et al., 2011). While the viscosity response of diluted fluids aids in determining structural changes in biopolymer structure, evaluating the rheological behaviour of food materials during extrusion necessitates methodologies that can assess rheological properties in both the liquid and solid states.

The physicochemical properties of raw materials (proteins) can vary based on factors such as the source, crop variety and extraction and processing conditions (Sim et al., 2021). Therefore, it is crucial to comprehend the physicochemical properties of proteins used in extrusion. This understanding will enable us to correlate and better understand the behaviour of these proteins during extrusion and its impact on the final product characteristics. Therefore, chapter 3 was dedicated to study the raw material properties of different proteins (derived from soy, pea, chickpea, rice and wheat). Based on this, one protein was selected for further study.

2.5 Texturized food products

2.5.1 First generation products

In Asia, soy has been a staple for centuries, used to create traditional high-protein products like tofu (agglomerated soy protein), tempeh (fermented soy cake), Yuba, and tofu skin, forming an integral part of daily life. The popularity of soy and soy products as a meat substitute in Western markets began in the early 1960s (Davies & Lightowler, 1998; Sadler, 2004). During this period, soy chunks were introduced as an extruded product made from defatted soy flour. These soy chunks also gained popularity in India, coming in various sizes and finding applications from meat extenders to mainstream food in Indian cuisine. Manufactured through the low-moisture extrusion process using a single-screw extruder, these products are expanded in nature and require hydration before use. Soy chunks are spongy and isotropically textured products, with a protein content ranging from 50 to 55%.

2.5.2 Second generation products

Like soy chunks, second-generation products are expanded low-moisture extrusion products. The feed moisture content used in this process varies from 20 to 40%. These products are made from soy protein concentrates or blends of soy and wheat proteins commonly, where the protein content of the products is higher than 60%. They are mostly referred to as low-moisture texturized vegetable protein (LMTVP) or dry TVP. Though they are expanded products, they have an anisotropic structure using single or twin-screw extruders to achieve improved fibrations in the product. They find application in meat substitutes, mostly in the minced product category, such as burger patties, nuggets, sausages, kebabs, etc. (Cornet et al., 2020; Dekkers, Boom, et al., 2018). These TVPs are employed as meat extenders to enhance properties such as viscoelasticity, colour stability, moisture retention, firmness, and juiciness (Vatansever et al., 2020; Yeater et al., 2017). TVP possesses a porous structure and exhibits a prolonged shelf life. Although they are spongy textured, these products have comparatively higher chewiness after hydration due to the higher protein level in the product (Maningat et al., 2022).

2.5.3 Third generation products

Unlike the above products, third-generation products are dense, anisotropic textured products made using twin-screw extruders with higher feed moisture content (above 50%). The technology of high-moisture extrusion (HME) was elaborated in section 2.2.2. These products are commonly referred to as high-moisture texturized vegetable protein (HMTVP) or high-moisture meat analogues (HMMA). The protein content used in the raw material will vary from 70% to 85% on dry weight basis and in the extrudates the protein content will be around 20% to 30%, which are considered as the protein dense texturized foods. These products are characterized by the presence of high moisture content (50-70%), no hydration required, and have similar fibration as that of real meat (Zhang et al., 2021), but this product is not limited to mimicking real meat. It could also be used in many food formats as a new product. The added advantage of this product is that it can be used for both whole cuts as well as minced product applications if the target product category is meat analogue. The HME process will have great control over the texture of the product and can make tailored textures using the process parameters and the formulation, which can be fairly achieved in low moisture extruded products. The visual pictures of soy chunks, LMTVP, and HMTVP are shown in Fig. 2.8.

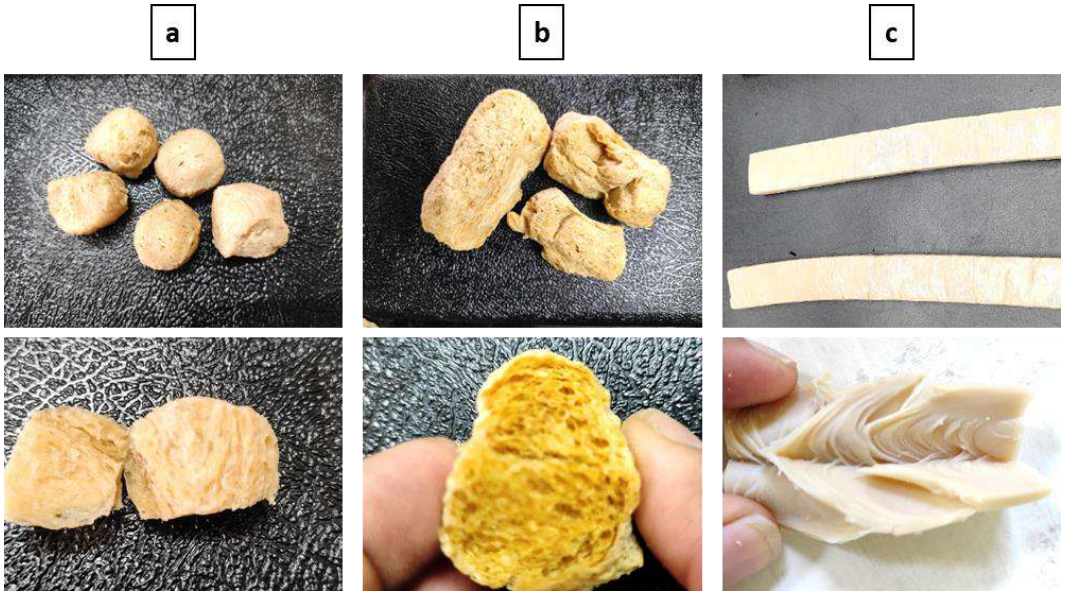

Figure 2.8 (a) Soy chunks, (b) LMTVP (low moisture texturized vegetable protein) and (c) HMTVP (high moisture texturized vegetable protein).

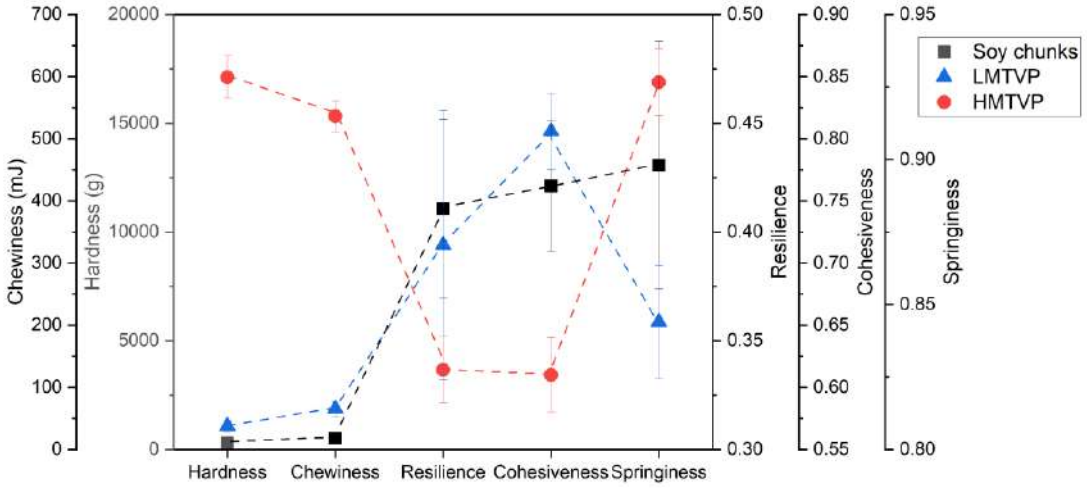

Figure 2.9 Texture profile plot of rehydrated soy chunks, LMTVP and HMTVP.

A textural comparison was conducted among soy chunks, TVP, and high-moisture textured products to analyze the textural differences (Fig. 2.9). Four market soy chunk products, one market sample of soy-gluten TVP (Spramax50, Solae Inc.), and an in-lab made HMMA from SPI-gluten (70:30) were used for the comparison. These chunks and TVP were rehydrated in hot water for 5 minutes and excess water was squeezed out before the textural analysis, whereas the HMTVP was directly used for texture analysis without rehydration. The moisture content for all three samples was between 60% and 65% at the time of texture analysis. The methodology of texture analysis was performed as mentioned in chapter 5 section 2.6. The results show that the low moisture products have lower hardness and chewiness The slight increase in the hardness and chewiness of the LMTVP compared to the soy chunks was mostly due to the higher protein content. However, HMTVP showed the highest hardness and chewiness because of the dense structure whereas, LMTVP product's structure was filled with air and are spongy structured. There was no difference in resilience and chewiness between the soy chunks and LMTVP, whereas the HMTVP had much lower values for resilience and cohesiveness. Springiness showed no significant difference between the soy chunks and LMTVP however, HMTVP was very springy. Overall, the textural properties of the HMTVP were much superior to the low moisture products due to dense structure. The example of HMTVP shown in the plot was at one condition; nevertheless, by manipulating the process parameters, a wide range of textural profiles can be achieved, as discussed in chapter 4.

2.5.4 Structure of meat and meat analogue

It is interesting to compare the fibrous structure created by high moisture extrusion of plant proteins with those in real meat. The texture of real meat is from the hierarchical structural arrangement of muscle comprised of meat fibers (Listrat et al., 2016; Pearson & Young, 1989). These muscle fibers are enveloped and supported by connective tissue, primarily composed of collagen and elastin, varying in length from 10 to 40 mm and diameter from 10 to 100 μm. Muscle fibers are independent structures that are in turn a collection of smaller subunits known as myofibrils. Myofibrils consist of smaller elongated filaments referred to as myofilaments, constructed from sarcomeres. Sarcomeres contain proteins like myosin, forming thick filaments (4 - 16 nm in diameter) and actin forming thin filaments (6 - 8 nm in diameter). The structural elements such as myofibrils and connective tissues significantly influence the quality and sensory characteristics of meat (Damez & Clerjon, 2013; Guo & Greaser, 2022). For instance, the toughness of meat is linked to the distribution of myofibrillar and connective tissues, while meat tenderness is related to the spatial organization of connective tissue within the bundles of meat fibers. Additionally, the water content held between meat fibers contributes to the overall juiciness of the meat (Damez & Clerjon, 2008).

To create fibrous texture through HME process, plant based ingredients undergo intensive heating and mixing within the barrel where the globular plant proteins open and align its polypeptide chains linearly in the long cooling die. This will create an anisotropic structure. At a microstructural level, fibers produced through extrusion from plant proteins lack the well defined nanoscale fibrillar texture and high order structural alignments characteristic (Fig. 2.10). Studies have demonstrated that extrusion is constrained to creating fibrous structures at the microscale, with a fiber diameter of approximately 50 μm (Dekkers et al., 2018). It is important to note that the attempt to replicate a muscle fiber like structure through high temperature extrusion, followed by cooling, inevitably results in tightly associated aggregates stabilized by random hydrophobic interaction and covalent bonds. This contrasts with animal myofibers and myofibrils, where ionic interactions and hydrogen bonds are the primary stabilizing forces and covalent bonds are absent (Xiong, 2017). The relatively moderate cooking temperature (60–80 °C) minimizes fiber aggregation and shrinkage in muscle (Fig. 2.10) but it will have low anisotropy. Consequently, it proves nearly impossible to

recreate the complex hierarchical organization of muscle fibers. Nevertheless, the interconnected sarcomere segments in muscle, comprising longitudinal myosin thick filaments, actin thin filaments and titin filaments, serve as the site where moisture is retained, contributing to the juicy organoleptic properties in cooked meat (Xiong, 2023). Therefore, more research is needed in this area and in this we have discussed some of the ideas to mimic the textural properties for example, using blends in chapter 5 and 6 and use of modified new cooling die.

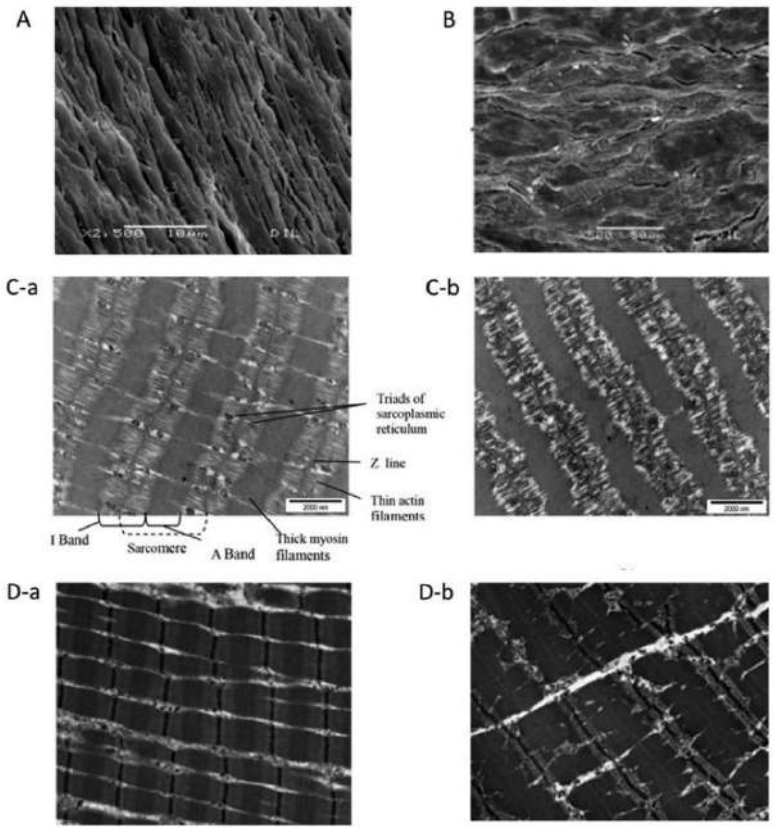

Figure 2.10 Micrographs illustrating high moisture texturized extrudates produced from lupin protein (A) and insect protein (B) are compared with micrographs of raw (C-a) and stewed (C-b; 100 °C for 30 min) beef or raw (D-a) and immersion cooked (D-b; 70 °C for 30 min) beef. Adapted from (Xiong, 2023).

2.6 Characterisation of high moisture texturized foods

In this section, we have reviewed the literature on characterization of the high moisture extrudates or HMMA. The main characteristics of the extrudates is the dense anisotropic structure and fibrousness in the product. To extract information from intricate foods with anisotropic structures, various characterization techniques are employed, including texture analysis, light microscopy or scanning electron microscopy (Krintiras et al., 2014). For example, replicating the texture of real meat

poses a hurdle for extrudates due to the distinct structural differences in proteins derived from non animal sources compared to muscle fibers (Sha & Xiong, 2020). Numerous analytical techniques and methods have been devised by researchers to achieve a meat like texture in extrudates (Schreuders et al., 2019; F. Wang et al., 2023; Zhang et al., 2019). Consequently, this section will delve into the crucial parameters throughout the extrusion processing stages and in the final product. These indicators serve as guiding parameters for the selection of raw materials in extrusion processing, facilitating a more efficient design and development process.

2.6.1 Textural analysis

Texture analysis is a widely used method for quantifying mechanical properties like stress and strain through various measuring procedures. Specific textural parameters are reviewed in this section.

2.6.1.1 Texture profile analysis (TPA)

The texture profile analysis (TPA) test assesses properties such as hardness, chewiness, resilience, cohesiveness and springiness, offering insights into the mouthfeel of extruded products (Schreuders et al., 2021). Achieving partial textural matches does not lead to acceptable products. Hardness is a measure of the peak force to compress the product, and chewiness is a measure of much work is needed to chew the product. Resilience relates to how well a product "fights to regain its original height" post compression, and cohesiveness is how well the product withstands a second deformation relative to its resistance under the first deformation. Springiness is how well a product physically springs back after it has been deformed (Breene, 1975; Friedman et al., 1963). TPA provides a relative value that necessitates comparison with the target product. Factors like meat type and cooking methods contribute to variations in TPA values (Holman & Hopkins, 2021; Zhang et al., 2019). Consequently, it remains challenging to determine whether higher or lower TPA values signify superior product quality without a reference material.

For instance, the hardness of cooked chicken breast and soy based HMMA, which contains 10–20% wheat gluten, exhibits comparability in hardness and chewiness (Chiang et al., 2019a; Schreuders et al., 2019) observed that the TPA properties of pea based HMMA closely resemble those of chicken fillets. HMMA formulated with mung bean protein and peanut protein demonstrates significantly lower elasticity,

cohesiveness, chewiness, and cutting strength compared to SPI, wheat protein and pea protein (Samard & Ryu, 2019). In particular, pea protein based HMMA shows less elasticity, cohesiveness and chewiness than SPI (Kim et al., 2021).

The hardness of extrudates is influenced by extrusion temperature, moisture content, and screw rotation speed in the high moisture extrusion (HME) process (Malav et al., 2015). Earlier studies have demonstrated that extrusion under low feed moisture conditions leads to a harder structure compared to products extruded under higher moisture content (Chen et al., 2011). Furthermore, Maung et al. (2021) reported a sharp decrease in hardness and chewability with an increase in all extrusion process parameters, including moisture content, barrel temperature, and screw speed. The augmentation of intermolecular forces results in tighter binding of protein molecules, leading to a stiffer extrudates. In the context of HME, this enhanced force may be attributed to the adjustment of protein raw materials and extrusion parameters.

TPA tests have demonstrated a positive correlation between the elasticity of a food product and protein concentration. This correlation is attributed to the increased cross-linking among protein molecules at higher protein concentrations (Wee et al., 2018). Chen et al. (2021) observed that the addition of amylopectin rich starch significantly reduced hardness, springiness, chewiness, and tensile strength while increasing fibrations. This effect is explained by the dispersion of spherical branched starch within protein molecules, enhancing protein mobility but hindering elasticity. During the high moisture extrusion (HME) process, higher moisture content in the extrudate leads to reduced springiness. This is primarily because higher moisture content requires less force or energy to disrupt the structure (Grahl et al., 2018). Additionally, it appears that extrusion temperature predominantly influences springiness with lower extrusion temperatures favouring the production of products with higher springiness (Zhang et al., 2020).

Research by Kaleda et al. (2021) indicated that extrudates made from blend of oat and pea protein exhibited higher springiness compared to chicken. However, sensory evaluation results suggested that consumers preferred products with moderate springiness, indicating that excessively springy extrudates may not align with consumer preferences. Wee et al. (2018) findings support this perspective, suggesting that overly springy extrudates may be perceived as rubbery. In summary, within HME, adjusting

the springiness of extrudates to an acceptable range can be achieved by incorporating substances other than protein (such as starch or water) or by fine tuning extruder parameters, including low temperature.

It is to be noted that textural studies on high moisture extrudates have been limited to a few parameters, such as hardness and chewiness. However, it is equally important to explore the entire textural profile. While a few studies have been mentioned above, in this thesis, we have discussed full texture profile of the extrudates, aiming for a comparison with real meat.

2.6.1.2 Cutting strength and anisotropy

Thiébaud et al. (1996) proposed texture determination through shearing, a well established method for evaluating beef tenderness. This approach mimics the sensation experienced when food is cut by front incisors during mastication (Caine et al., 2003; Ruiz De Huidobro et al., 2005). Assessing the quality of fiber formation has been achieved through the determination of cutting strength in longitudinal and transverse directions, considering the flow direction in the cooling die (Fig. 2.12) (F. L. Chen et al., 2010; Fang et al., 2014; Osen et al., 2014).

The cutting and tensile tests serve to elucidate the fibrous nature of TP, particularly its anisotropy. The ratio of vertical to parallel cutting or tensile force serves as an indicator of textured extrudate's fibrous nature (Fig. 2.11). Elevated temperatures contribute to a more pronounced fibrous structure in extrudates containing soybean protein concentrate (SPC) and a similar effect is observed in wheat extrudates (Pietsch et al., 2019; Pietsch, Werner, et al., 2019). Conversely, higher temperatures and feed moisture content can lead to suboptimal texture (Brishti et al., 2021), possibly due to water absorbing input energy, resulting in inadequate protein denaturation. Formulations with SPC and wheat gluten exhibit superior texturization compared to those made with SPI (Chiang et al., 2019a; Fang et al., 2014). The incorporation of amylose and amylopectin in pea protein isolate has decreased the cutting strength values of the extrudates (Chen et al., 2022). The introduction of insect protein and microalgae significantly decreases the shear force of TP in various directions (Caporgno et al., 2020; Smetana et al., 2019), indicating reduced cohesion in both horizontal and vertical directions, potentially enhancing tenderness in applicable products.

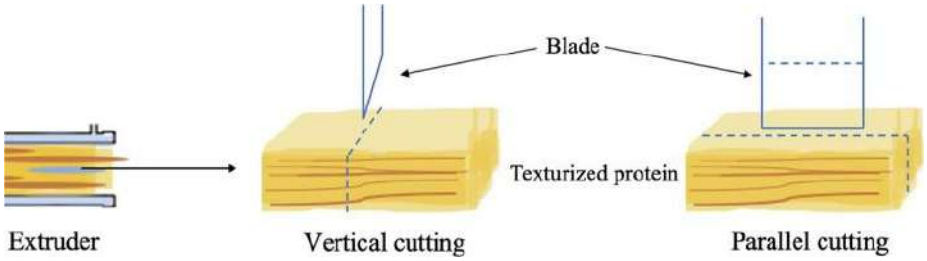

Figure 2.11 Setup for the determination of anisotropy in the texturized products. Adopted from (T. Zhang et al., 2023)

The extent of fibrous formation in extrudates may be linked to protein flow induced by the rotation of the screw within the extruder (Zhang et al., 2021). During cooling, when molten protein fluids commence aggregation, layered and oriented fibrous structures develop when protein aggregation and phase separation rates are nearly equal. If the protein aggregation rate surpasses the phase separation rate, a non oriented gel structure is established. Layered structures manifest when the protein aggregation rate is lower than the phase separation rate (Dekkers et al., 2018; Sandoval Murillo et al., 2019). Previous studies have affirmed that, under appropriate shear rate conditions, a more favourable fiber structure emerges. The fibrous degree of SPC exhibits an initial increase followed by a decrease within the 10–100 rpm range (Grabowska et al., 2016), with mung extrudates displaying the most pronounced fibrous structure at 85 rpm (Brishti et al., 2021).

2.6.1.3 Tensile strength/resistance and anisotropy

Another approach to study anisotropy involves measuring tensile stress or strain, representing the force and deformation at rupture during the stretching of extrudates. Tensile strength, also referred to as tensile resistance or stretching resistance, not only signifies the toughness of the product but also mirrors the strength of the product's network structure. Typically, tensile resistance is assessed using a texture analyser or a food tensile testing machine. Presently, the constituents of extrudates produced through HME primarily consist of composite systems (Sha & Xiong, 2020). However, high moisture extrudates crafted by HME using a single raw material component were found to significantly differ from real meat in terms of tensile strength (Chiang et al., 2019a). Therefore, the raw materials should be composed of a secondary ingredient and the introduction of pectin, carrageenan, starch or plant proteins like wheat gluten can enhance the product's tensile strength.

Analysis of tensile strength in blend of pectin and soy protein isolate (SPI) revealed that elevating pectin concentration heightened the anisotropy of blends (Dekkers et al., 2016). In the composite system involving peanut protein with carrageenan (CA), sodium alginate (SA) and wheat starch (WS), the addition of 0.1% CA or SA significantly improved tensile strength, elasticity, and tensile strength of fiber structures, but it is not helpful to fiber orientation (Zhang et al., 2020). Zhang et al. (2016) demonstrated a significant correlation between starch gelatinization, fiber structure, tensile properties and elasticity of products. Moreover, to enhance sensory properties resembling meat, the incorporation of oil into wheat gluten during processing is anticipated to enhance the sensory quality and texture of extruded products. However, excessive oil addition can impede the formation of anisotropic structures, leading to a reduction in tensile strength. Kendler et al. (2021) illustrated that the tensile strength of extruded products is dependent on raw material temperature, with the tensile strength increasing as the temperature rises. In HME, optimizing the blend system of raw materials and elevating the extrusion temperature effectively boosts the tensile strength of high moisture extrudates, facilitating the formation of the product's fiber network structure.

2.6.1.4 Quantification of fiber formation

Various microscopic techniques have been employed to examine the microstructure of high moisture extrudates, including light microscopy (Lin et al., 2002; Noguchi, 1990) and advanced techniques, including scanning electron microscopy (SEM), atomic force microscopy (AFM), and confocal laser scanning microscopy (CLSM) (Lin et al., 2002; Schreuders et al., 2019; Wang et al., 2017; Zhang et al., 2019), have been employed to offer more intricate insights into microstructural properties across various scales. Researcher commonly use SEM and CFSM techniques to measure the fiber’s morphology and the thickness of the fibers in micro and nano scale. At the production scale, this techniques becomes expensive for analysis.

An alternative non-destructive approach to quantify the fiber formation of extruded meat substitutes was developed using fluorescence polarization spectroscopy (Yao et al., 2004). This method relies on the relationship between fluorescence emission light intensity and the structural orientation of the sample. The degree of polarization is determined from the emitted fluorescence intensities of a sample parallel and

perpendicular to the plane of linearly polarized excitation light. As multiple measurements with different polarization directions are required to quantify the degree of fiber formation, this method cannot be implemented on a production line. To monitor fiber formations in an industrial setting, Ranasinghesagara et al. (2006) proposed another non-destructive method using a real time scanning system based on photon migration to map fiber formations in meat substitutes. The technique involves utilizing light that travels through a turbid medium, experiencing absorption and random scattering. As the light exits the sample surface and is captured as optical reflectance, the scattered photons convey essential information regarding the optical properties of the medium, deducible from reflectance measurements using light transport theories. Employing a laser as the light source, this method facilitates a real time, two dimensional mapping of fiber formation and orientation across the entire sample. This approach can serve as a rapid and non-invasive means for online monitoring of fiber formation in meat analogues (Ranasinghesagara et al., 2009). However, it's important to note that these non-destructive methods are restricted to optically quantifying the fiber formation exclusively on the surface of the extrudates.

A recent advancement in the realm of food structure analysis involves the utilization of micro computed tomography (microCT) also called X-ray tomography (Mathanker et al., 2013). This non-destructive technique provides three dimensional insights into products and processes, offering substantial potential for enhancing our comprehension of the interplay between macro and microstructure. Mathmann et al. (2014) explored the impact of temperature as a process parameter on the resultant texture, demonstrating that image analysis of micro computed tomography measurements can effectively distinguish between extrusion samples. (Dekkers, Hamoen, et al., 2018) used microCT to show the differences in the textured product as impacted by the process temperature and found air as a dispersed phase in the soy protein matrix.

Despite the potential for recording the degree of fiber formation using a high resolution camera, visual inspection remains subjective and lacks a numeric index for accurate product comparison. To enhance the visual assessment of samples, Ranasinghesagara et al. (2005) introduced an image processing technique that characterizes sample fiber formation based on digital images, relying on the detection of linear lines and curves on the sample surface. However, this method necessitates partially destructive preparations of the samples before analysis. The authors propose using this method as

a standard quantitative approach for evaluating other non-destructive methods. However, the method of quantifying the fibers is complex. Therefore, we have developed a simple one click method of image processing which yields quantitative details of fibers in the extrudates using MATLAB software.

2.6.2 Rheological properties

Rheological properties of the extruded samples were done under shear stress to characterize its viscoelastic and flow behaviour. Viscoelastic substances like food gels display characteristics of both an ideal solid and an ideal liquid (Bourne, 2002). Dynamic rheological experiments, known as small strain oscillatory shear, can be employed to assess the viscoelastic properties of foods. Unlike rotational measurement, this test involves subjecting the material to a small strain oscillation around a central point with a sinusoidal velocity while measuring the shear stress referred as amplitude sweep. This sweep test was carried out for assessing the structural strength of the extrudate samples. Each sample exhibits a specific range where both storage and loss modulus (G' and G") remain constant and unaffected by the applied deformation. This region is commonly identified as the Linear Viscoelastic Region (LVR) and its width is contingent on the material's structural strength. Any alteration in storage and loss modulus signifies that the applied deformation surpasses the LVR, leading to a modification in the sample's structure. Beyond a certain deformation point, non linear deformation commences, marked by a non linear increase in loss modulus (G") and subsequent crossover of G' and G". Typically, the crossover point is determined by the equilibrium of G' = G". The loss factor tan δ can serve as a characteristic value to identify the crossover point, calculated as the ratio of G" to G'. At the crossover point, tan δ equals 1 (Lopes da Silva & Rao, 2007). Additionally, it also validates the measured textural properties of extrudates.

Pietsch et al. (2021) investigated high moisture extrudates composed of soy protein concentrate (SPC), wheat gluten (WG), and a 1:1 blend of the two. The amplitude sweep test revealed the highest G' for SPC, the lowest for WG, and the blend falling in between, indicating the hardness or firmness of the product. WG exhibited the highest linear viscoelastic region (LVR) and shear rate for the crossover point, suggesting greater viscoelastic properties compared to SPC. In the frequency test of the same extrudates, similar behaviour for G' and G" explained the hardness or softness. The

substance displayed shear-thinning characteristics and was predominantly elastic, as G' > G". Additionally, the extrudate sample produced from SPC demonstrated the highest viscosity. The complex viscosity continued to rise from the SPC-WG blend to WG. Since these measurements were conducted on bulk samples, they imply that samples with the highest complex viscosity are more resistant to shear stresses. Consequently, samples with higher viscosity are likely to be perceived by consumers as firmer and easier to bite.

Another study conducted by Wang et al. (2022) documented the rheological properties of extrudates derived from soy (SPI) and pea protein isolates (PPI), examining the influence of extrusion temperature. As the temperature increased (from 120 to 140 °C), both G' and G" experienced an increase. However, with a subsequent rise in temperature (140 to 160 °C), no noticeable difference in rheological properties was observed. Additionally, the study noted that extrudates from SPI exhibited higher rheological values compared to those from PPI.

2.6.3 Colour properties

Most of the preceding studies on extruded texturized products have concentrated on aspects such as texture, nutritional content and some flavour (Emin et al., 2017; Z. Guo et al., 2020; L. Yang et al., 2023). However, colour and appearance are also critical factors influencing consumer acceptance and purchase decisions for products (Xia et al., 2023a). Target food products such as real meat exhibits a distinct colour both before and after cooking, primarily attributed to myoglobin, the sarcoplasmic heme protein responsible for meat colour (Suman & Joseph, 2013). While the inherent colour of extrudates is essential, it can be modified by incorporating pigments (Ryu et al., 2023). Achieving a lighter colour is advantageous for adjusting extrudate's colour. For instance, the addition of yeast protein contributes to a lighter colour in extrudates. When yeast protein replaced 50% of soybean protein and pea protein, the lightness values increased from 43.12 and 45.45 to 50.37 and 48.19, respectively (Xia et al., 2023a; Xia et al., 2023b).

The inclusion of spirulina makes the extrudate's hue deeper, leading to an unappealing visual aspect (Grahl et al., 2018; Palanisamy et al., 2019). *Auxenochlorella protothecoides*, a yellow microalga offers the potential to generate extrudates with a more visually pleasing and attractive appearance (Caporgno et al., 2020). The addition

of wheat gluten enhances the shine of soy based extrudates (Chiang et al., 2019a), while the incorporation of hemp protein results in a duller appearance (Zahari et al., 2020). The augmentation of water content has a more pronounced effect on lightening products compared to variations in extrusion temperature and screw speed (Palanisamy, Franke, et al., 2019).

Chapter 3

Physicochemical and nutritional characterization of protein ingredients

Abstract

The presented chapter aims to characterize the functionality of various plant-based protein isolates, including soy protein isolate (SPI), pea protein isolate (PPI), chickpea protein (CPP), rice protein isolate (RPI) and wheat gluten (WG), which are commonly used for texturization. The results indicate that SPI exhibited the highest water absorption capacity, water solubility, emulsifying activity index, emulsion stability index, foaming stability, least gelation concentration and pasting viscosity at neutral pH compared to the other protein isolates. PPI stands next to SPI in performance, suggesting its potential as a substitute, particularly in functions related to hydration. However, RPI overall functionality did not match that of the other proteins and WG's foaming ability could not be replaced by any other protein except for chickpea protein, which showed the highest foaming capacity and stability. These findings provide valuable insights for food scientists, engineers and manufacturers on the appropriate application of different plant proteins in various food products especially texturization. This understanding of physicochemical properties of proteins will help in designing blends and its impact of extrusion process.

Keywords: Plant proteins, Physicochemical, Nutrition, Amino acids, Rheology.

1 Introduction

An comprehensive understanding of ingredient properties is essential for understanding the process and product characteristics involving them. Our focus centres on protein-rich constituents, a pivotal element in food blends. In chapter 2, we have reviewed the various proteins used as primary and secondary ingredients in protein texturization using low and high moisture extrusion processes. These include soy, pea, wheat, lupin, mung, fava bean, etc. An understanding of the compositional and physicochemical properties of these protein rich ingredients is key for understanding their nutritional value and their texturization.

Soy protein isolate (SPI) is the most commonly used protein isolate globally (Asgar et al., 2010; GFI, 2021; Wild et al., 2014). Due to its wide use, low cost and good nutritional value, it has been selected as a base material for the studies reported in this thesis. To ensure that the justification was valid, its nutritional profile and physicochemical properties were compared with four other proteins. These four plant protein isolates were pea protein isolate (PPI), chickpea protein isolate (CPP), rice protein isolate (RPI), and wheat gluten isolate (WG). All these isolates contain protein content exceeding 80%. The experimentatal procedure used to determine the physicochemical properties of the five isolates are given below.

2 Material and methods

2.1 Materials

The procurement details of the five plant proteins are as follows: Soy protein isolate - SPI (Solae SUPRO® 620, DuPont Shineway Luohe Food Co. Ltd., Luohe, China), pea protein isolate - PPI (Yantai Oriental Proteins Tech Co. Ltd., Zhoayuan, China), chickpea protein - CPP (Shughengheng Jiangsu Chemical Co. Ltd., Jiangsu, China), rice protein - RPI (AVT Naturals Products Ltd., Aluva, India) and vital wheat gluten - WG (Guanxian Xinrui Industrial Co. Ltd., China). All the chemicals and reagents were procured from Sigma-Aldrich Chemicals Pvt. Ltd., Bengaluru, India.

2.2 Colour values and visual images of ingredients

The colour values of raw material samples were measured by using a colorimeter (CR-400 chroma meter, Konica Minolta Sensing Inc., Japan). Colour was recorded according to the CIE-lab L*, a*, b* scale. L* represents brightness or lightness from 0

to 100 (black to white), a* represents green to red (positive or negative) and b* represents blue to yellow (negative or positive) (Benković et al., 2015). At least five measurements were taken for each sample at randomly chosen locations. The visual images of the samples were acquired by a high resolution digital camera (Nikon D70, Nikon Co. Ltd., Thailand) in a photo box with black walls and two LED light strips illuminating at the sample.

2.3 Particle size distribution (PSD) and bulk density

The particle size distribution of the different protein powder samples was measured by laser diffraction using a particle size analyzer S3500 (Microtrac Retsch GmbH, Germany) with wet dispersion. The volume fractions at 200, 100, 50 and 10 µm were determined using the instrument software. The measurements were conducted in triplicate.

For bulk density, 50 g of powder sample was placed in a 100 ml measuring cylinder. The cylinder was gently tapped on a laboratory bench multiple times to achieve a consistent volume. The bulk density was determined by dividing the weight of the sample by its corresponding volume and expressed the values in kg/m^3 (Huang et al., 2019). All the samples were analysed in triplicates.

2.4 Proximate composition

Moisture content of samples was determined by using moisture analyser (MA 50.R, Radwag, Radom, Poland) following ISO 712:2009 method (ISO, 2009). The total protein content (nitrogen × 6.25), lipid content and ash content of proteins, millet flours and protein-millet blends were determined by using standard methods and expressed on a dry basis (AOAC, 1990). The ash content was estimated gravimetrically by burning the samples at 550 °C in a muffle furnace. The starch content was analysed by using standard method IS 4706 P(2):1978 (BIS, 1978). The total, soluble and insoluble dietary fibers were analysed by enzymatic-gravimetric method AOAC 991.43 (AOAC, 2005). All the samples were analysed in triplicates.

2.5 Amino acid composition and scores

Amino acid composition was assessed using an Agilent 1260 Series HPLC (Agilent Technologies, Waldbronn, Germany) equipped with a diode array detector, following the Agilent method (Mengerink et al., 2002). The system included an Agilent

AdvanceBio AAA 4.6 × 100 mm column housed in a thermostatic column compartment maintaining a temperature of 40 °C. Sample preparation was carried out according to the procedure outlined by Osen et al. (2015). The samples underwent 24-hour hydrolysis at 110 °C using 6 M HCl, resulting in protein hydrolysates. Separation and quantification of amino acids involved pre-column derivatization with FMOC (Flourenylmethoxycarbonyl) chloride for primary amino acids and OPA (o-phthaldialdehyde) for proline. Calibration was performed using a standard amino acid mix (0.5 μmol/ml for each amino acid). The mobile phase A consisted of 40 mM NaH2PO4 (pH 7.8), while mobile phase B comprised acetonitrile: methanol: water (45:45:10 v/v). A 2.5 μl injection was made and separation occurred at a flow rate of 2 ml/min with a gradient allowing for 1.9 min at 0% B followed by a 16.3 min step that raised eluent B to 53%. Subsequently, washing at 100% B and equilibration at 0% B were conducted in a total analysis time of 26 min. Three repeated measurements were performed for each sample.

The amounts of different amino acids obtained were quantified in mg/g protein and compared with the FAO/WHO (2013) reference pattern of essential amino acids for 'Older Child, Adolescent, Adult' (FAO/WHO, 2013). The essential amino acids' ratio to the total amino acids was denoted as E/T (%). The approach employed for calculating the amino acid score (AAS) was as per the FAO/WHO guidelines, as outlined below (eq. 3.1):

$$AAS = \frac{mg\ of\ AA\ in\ 1\ g\ of\ test\ protein}{mg\ of\ AA\ in\ 1\ g\ of FAO/WHO\ reference\ pattren} \times 100 \qquad (3.1)$$

2.6 Water and oil absorption capacity

Water absorption capacity (WAC) analysis was performed using the method described by Ogunwolu et al. (2009). 1 g of the raw material powder sample was mixed with 10 g of distilled water using a stirrer. The suspension was then centrifuged at 1800 × g for 20 min at 22 °C (C-24plus, Remi Electrotechnik Ltd., Vasai, India). After centrifuge and decanting the supernatant, the wet pellet was weighed to calculate WAC by dividing the wet pellet weight by the sample weight. For analysing oil absorption capacity (OAC), water was replaced by oil (refined sunflower oil) and proceeded further.

2.7 Water solubility

The decanted supernatant from the WAC analysis was dried overnight to calculate the water solubility (WS) by dividing the weight of soluble solids after drying by the sample weight.

2.8 Protein solubility and zeta potential

The protein solubility at different pH values ranging from 2 to 12 was performed according to the method of (Boye et al., 2010). 100 mg of protein sample was mixed with 10 mL of distilled water and the pH was set to the required level using 1 N HCl or 1 N NaOH. The mixtures were stirred constantly for 30 min and then centrifuged at 4000 × g for 30 min. The protein content in the supernatant was measured by the Bradford (1976) method. Solubility was computed as the percentage of protein in the supernatant divided by the total protein in the original sample. The solubility profile was plotted by plotting the average protein solubility of two samples against pH.

The zeta potential of the protein isolates was measured according to the method of (Rani et al., 2023) using a Zetasizer Nano ZS (Malvern Instrument Ltd., UK) with a He-Ne laser (632.8 nm, 4 mW) at a 173° back scattering angle to the incident beam and at 25 °C. Protein suspensions in de-ionized water (2 mg/ml for all samples; pH 2-12) were freshly prepared and filtered using a 0.45 μm membrane (Pall life sciences, USA) before analysis.

2.9 Emulsion activity and stability

Emulsifying activity index (EAI) and stability index (ESI) of proteins was measured following the method of Akasha et al. (2016) as reported by (Zhao et al., 2020). 300 mg of the proteins were blended with 30 ml of distilled water. 10 ml of sunflower oil was added to this suspension and the pH was set to 7.0. The mixture was then homogenised for 1 min at 20000 rpm using digital homogenizer (Ultra-Turrax T 25, IKA Co., Germany). 50 μl of the emulsions were taken from the bottom of the container at 0 and 10 min after homogenisation and mixed with 5 ml of 0.1% SDS solution. The absorbance of this solution was measured at 500 nm using UV/Visible spectrophotometer (Perkin Elmer, Lambda 25, USA). The EAI and ESI of the protein was calculated using eq. (3.2) and eq. (3.3) respectively.

$$EAI\ (m^2/g) = \frac{2 \times T \times A_\circ \times DF}{C \times \varphi \times 10^3} \quad (3.2)$$

$$ESI\ (min) = \frac{A_\circ}{A_\circ - A_{10}} \times 10 \quad (3.3)$$

Where C is the protein weight per volume (g/ml), φ is the fraction of oil by volume, T is 2.303, A_0 is the absorbance right after the homogenization, DF (dilution factor) is 100 in this case, A_{10} is the absorbance of the sample 10 min after the homogenization.

2.10 Foaming capacity and stability

The method of measuring foaming properties was according to Shevkani et al. (2015) as follows: a protein suspension (1% w/v, 50 ml) at pH 7.0 was homogenized in a measuring cylinder (100 ml) using a digital homogenizer (Ultra-Turrax T 25, IKA Co., Germany) at 15,000 rpm for 2 min. The volume of the suspensions increased after mixing and the percent increase was the foaming capacity (FC). The foam stability (FS) was calculated as the percentage of foam left after 30 min.

2.11 Least gelation concentration

Least gelation concentration (LGC) of proteins were measured following the method of Sathe & Salunkhe (1981) as reported by Boye et al. (2010). Protein powders were measured into test tubes with 5 mL of distilled water to create suspensions with concentrations ranging from 2% to 20% (w/v). The samples were vortexed and the tubes were sealed and heated in a water bath at 100 °C for 60 min. The tubes were quickly cooled under tap water and then cooled at 4 °C overnight. The tubes were inverted to check if the suspensions had gelled. A solid gel was considered to have formed when the suspensions did not move on inversion. A soft gel was considered to have formed when a semisolid was formed that moved slightly on inversion. The lowest gelling concentration (LGC) was calculated as the minimum concentration at which a self supporting gel was formed. All analysis was done in at least duplicate.

2.12 Pasting properties

The pasting properties of proteins as a function of temperature was assessed using a Rapid Visco Analyzer (RVA 4500, PerkinElmer Inc., CT, USA) following the AACC Method 76-21 STD 2 (AACC, 1997). Protein slurries with 10% solids concentration

were heated to 50 °C and stirred at 960 rpm for 10 s to ensure thorough dispersion. The slurry was maintained at 50 °C for 50 s, then heated to 95 °C at a rate of 6 °C per 60 s, held at 95 °C for 300 s, and finally cooled to 50 °C. Each sample underwent duplicate measurements.

2.13 Rheology

Rheology of protein dispersions was studied under extrusion like conditions in a rheometer (MCR 302e, Anton Paar GmbH, Graz, Austria) using a pressure cell with a C-PTD temperature module. A protein powder dispersion of 20% (w/w) was prepared in a distilled water and added in the concentric cylinder of pressure cell. The cell was pressured to 15 bar using a compressed nitrogen gas. Temperature sweep was carried out by initially holding at 25 °C for 1 min then increasing to 130 °C at a heating rate of 6 °C/min. temperature of 130 °C was held for 1 min and cooled to 25 °C at the same rate and finally held for 25 °C for 1 min. The change in the storage modulus (G´), loss modulus (G´´) and complex viscosity (η*) as a function of temperature was measured at shear rate of 1% and frequency of 1 Hz using software (RheoCompas^{TM} 1.32, Anton Paar GmbH, Graz, Austria).

2.14 Statistical analysis

All the data were expressed as mean ± standard deviation. One-way ANOVA with Tukey test was used with significance of 0.05 level to identify the significant differences. Principal component analysis (PCA) was carried out using the scores of all the protein samples and the nutritional and physicochemical properties as loadings. These statistical analyses were carried out using OriginPro software version 2023b (OriginLab Corporation, Northampton, MA, USA).

3. Results and discussion

3.1 Visual images, colour values, PSD and bulk density of protein powders

Colour parameters (L*, a*, b*) and visual images of the protein isolates are shown in Table 3.1 and Fig. 3.1 respectively. SPI, RPI and WG are light white powders with L* values greater than 80. PPI and CPP were slightly darker in colour (around 78%) than other proteins, which may be due to the presence of pigments originated from the flour (Shevkani et al., 2015). PPI was comparatively more reddish and yellowish than other

proteins. The difference in the colours of these proteins was mostly due to the source and processing conditions.

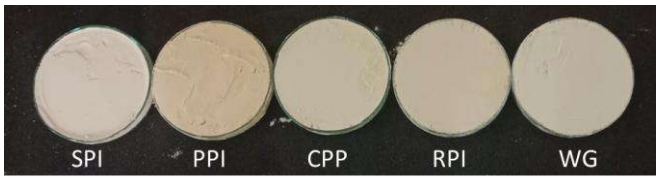

Figure 3.1 Visual images of different protein powders.

Table 3.1 Colour values and bulk density of protein powders.

Samples	Colour value			Bulk density (kg/m^3)
	L*	a*	b*	
SPI	89.08 ± 0.10^{a}	2.19 ± 0.02^{c}	16.84 ± 0.42^{c}	323.75 ± 16.89^{c}
PPI	78.78 ± 0.08^{d}	4.21 ± 0.03^{a}	20.43 ± 0.23^{a}	362.5 ± 14.53^{c}
CPP	77.80 ± 0.70^{e}	3.97 ± 0.05^{b}	18.60 ± 0.64^{b}	475.2 ± 12.4^{b}
RPI	83.54 ± 0.09^{c}	2.13 ± 0.05^{c}	18.65 ± 0.14^{b}	474.2 ± 15.79^{b}
WG	87.59 ± 0.09^{b}	0.49 ± 0.02^{d}	15.01 ± 0.07^{d}	551.48 ± 20.61^{a}

Values followed by different letters within each parameter show statistically significant differences ($p \leq 0.05$).

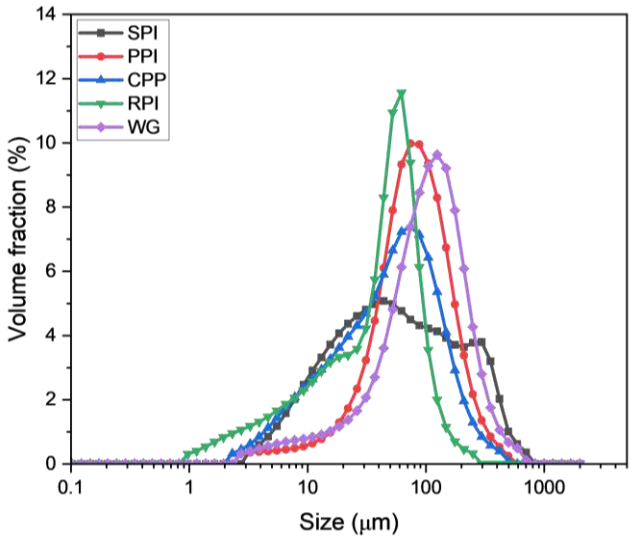

Figure 3.2 Particle size distribution (PSD) curves of protein powders.

The particle size distribution of protein powders is depicted in Fig. 3.2 and detailed in Table 3.2. The analysis revealed that SPI and PPI had over 60% of particles measuring less than 100 μm. CPP exhibited a slightly finer particle profile, with over 75% of particles being under 100 μm. The smallest particles were observed in RPI, where more

than 90% were less than 100 µm. In contrast, Wheat Gluten (WG) displayed a coarser particle distribution, with over 50% of particles exceeding 100 µm in size.

Table 3.2 Particle size distribution (PSD) of protein powders.

Particle size (µm)	Volume fraction (%)				
	SPI	PPI	CPP	RPI	WG
>200	18.44 ± 0.59^{a}	8.54 ± 0.18^{c}	5.18 ± 0.15^{d}	0.79 ± 0.02^{e}	17.25 ± 0.52^{b}
200-100	15.99 ± 0.43^{d}	29.36 ± 1.09^{b}	18.82 ± 0.64^{c}	7.40 ± 0.28^{e}	36.01 ± 0.79^{a}
100-50	18.57 ± 0.76^{c}	37.16 ± 1.49^{a}	28.42 ± 1.19^{b}	38.01 ± 1.63^{a}	26.77 ± 1.18^{b}
50-10	37.87 ± 0.68^{a}	21.55 ± 0.54^{b}	36.56 ± 0.62^{a}	37.18 ± 0.71^{a}	15.36 ± 0.25^{c}
<10	9.13 ± 0.32^{c}	3.39 ± 0.10^{e}	11.02 ± 0.33^{b}	16.62 ± 0.52^{a}	4.61 ± 0.16^{d}

Values followed by different letters within each parameter show statistically significant differences ($p \leq 0.05$).

Bulk density of protein powders was shown in Table 2.1. The bulk density of the samples ranged from 321.6 kg/m3 to 487.6 kg/m3, with WG having the highest value and SPI having the lowest value. This difference was due to the difference in the particle size of protein powders.

3.2 Proximate composition

The results of the proximate analysis of the samples are shown in Table 3.2. The moisture content of the samples ranged from 5.79% to 8.7%. The protein content of the samples varied from 81% to 96.1%, with SPI having the highest value and CPP having the lowest value and all protein samples are considered as protein isolate (contains protein > 80%). The lipid and dietary fiber content of the samples were very low, ranging from 0.16 to 0.82 % and 0.74 – 0.89 % respectively.

Table 3.3 Proximate composition of different proteins.

Parameters	**SPI**	**PPI**	**CPP**	**RPI**	**WG**
Moisture (% wb)	5.79 ± 0.21^{d}	8.20 ± 0.22^{b}	8.70 ± 0.18^{a}	7.60 ± 0.19^{cd}	7.96 ± 0.26^{c}
Protein (% db)	96.1 ± 0.84^{a}	87.5 ± 0.78^{b}	81.00 ± 0.56^{d}	85.20 ± 0.81^{c}	86.54 ± 0.82^{bc}
Lipid (% db)	0.16 ± 0.07^{e}	0.31 ± 0.06^{d}	0.82 ± 0.05^{a}	0.68 ± 0.07^{c}	0.72 ± 0.08^{b}
Starch (% db)	0.17 ± 0.02^{e}	6.98 ± 0.04^{d}	12.50 ± 0.03^{a}	7.96 ± 0.06^{b}	7.50 ± 0.08^{c}
TDF (% db)	0.74 ± 0.04^{d}	0.77 ± 0.05^{c}	0.89 ± 0.04^{a}	0.80 ± 0.04^{bc}	0.86 ± 0.06^{b}
Ash (% db)	2.83 ± 0.07^{d}	3.90 ± 0.06^{c}	4.68 ± 0.07^{a}	4.56 ± 0.10^{ab}	4.27 ± 0.12^{b}

Values followed by different letters within each parameter show statistically significant differences ($p \leq 0.05$).

The starch content of SPI was the lowest (0.17 ± 0.02 %) and CPP had the highest (12.5 ± 0.03 %) and other protein were in the range of 6.98 – 7.96 %. The ash content of the samples ranged from 2.83% to 4.68%, with CPP having the highest value and SPI having the lowest value. The results indicate that the samples have different composition (mainly the protein and starch content) which may affect their functional and processing characteristics.

3.3 Amino acid profiling and scoring

Amino acid composition represents the nature of protein side chain profiles and greatly influences the physicochemical and functional behaviours of the protein (Brishti et al., 2017). As shown in Table 3.3, Lys and Glu are the major hydrophilic amino acid residues, while Leu, Val, Ile, and Gly are the major hydrophobic amino acids in the pulse protein isolates. Legume proteins (SPI, PPI and CPP) had relatively higher amount of hydrophilic amino acids and RPI and WG had the lowest concentration of hydrophilic amino acids. Additionally, the essential amino acids (Lys, Leu, Ile, Met, Phe, Thr, Val and Try) content of SPI, PPI and CPP was greater ($P < 0.05$) than the other proteins in this study. Tang et al. (2021) reported that SPI had the lowest hydrophilic amino acids whereas our study showed higher levels in SPI. Various factors, including the origin of pulse flour, its varieties, and extraction techniques, contribute to the diversity of amino acid profiles. The balance between hydrophilic and hydrophobic amino acids plays a crucial role in determining solubility, water absorption capacity and the surfactant properties of the protein (Nakai & Modler, 1996).

As expected, the legume proteins lack methionine and cereal proteins lack lysine as essential amino acids making them imbalance amino acid profile from health perspective. The amino acid scores as shown in Table 3.4 indicates that the legumes had low scores (<100) in sulphur containing amino acids (SAA) whereas, cereal proteins (RPI and WG) had low scores for lysine. Thus, blending of proteins from legumes and cereals in right proportion will create nutritionally balanced amino acid profile. Another aspect of the nutrition is the digestibility of proteins which is combining referred as PDCAAS (protein digestibility corrected amino acid score). Generally, the plant proteins have low digestibility than animal proteins, thus lower PDCAAS (Berrazaga et al., 2019).

Table 3.4 Amino acid profile of different proteins (mg amino acid/g protein).

Amino acids	SPI	PPI	CPP	WG	RPI	Ref. pattern **
Aspartic acid	115.51 ± 3.26^{a}	106.34 ± 3.74^{b}	101.45 ± 2.32c	40.26 ± 1.38^{d}	88.24 ± 1.73^{c}	
Glutamic Acid	189.78 ± 3.11^{b}	163.79 ± 4.12^{c}	180.32 ± 4.21d	317.34 ± 4.81^{a}	185.63 ± 4.69^{b}	
Serine	51.91 ± 1.92^{a}	51.76 ± 2.56^{a}	48.67 ± 1.52b	39.04 ± 1.61^{b}	49.17 ± 2.05^{a}	
Histidine*	27.93 ± 1.18^{b}	27.48 ± 1.41^{b}	25.89 ± 1.97a	18.13 ± 0.51^{d}	21.89 ± 0.35^{c}	16
Glycine	41.46 ± 1.22^{b}	55.62 ± 1.82^{a}	40.14 ± 0.38c	38.22 ± 1.43^{b}	40.12 ± 1.68^{b}	
Threonine*	37.75 ± 2.68^{a}	38.05 ± 1.79^{a}	40.76 ± 0.42b	26.17 ± 1.13^{b}	38.76 ± 1.82^{a}	25
Arginine	72.81 ± 1.95^{b}	81.29 ± 2.48^{a}	90.21 ± 1.73b	47.33 ± 1.82^{c}	67.34 ± 3.34^{b}	
Alanine	34.94 ± 1.38^{b}	42.13 ± 2.01^{a}	41.58 ± 0.27c	31.92 ± 1.27^{bc}	39.45 ± 1.52^{a}	
Tyrosine	38.43 ± 1.93^{b}	37.87 ± 1.26^{b}	35.43 ± 1.52a	24.51 ± 1.18^{c}	43.58 ± 1.29^{a}	
Valine*	51.33 ± 2.16^{a}	52.44 ± 1.75^{a}	50.12 ± 1.83b	43.97 ± 2.09^{b}	48.23 ± 1.61^{ab}	40
Methionine*	12.75 ± 0.42^{c}	11.68 ± 0.53^{cd}	11.94 ± 0.32d	18.67 ± 0.74^{b}	27.91 ± 0.99^{a}	
Cysteine*	10.07 ± 0.28^{c}	9.62 ± 0.51^{c}	8.61 ± 0.11d	17.39 ± 0.18^{b}	20.87 ± 1.28^{a}	
Tryptophan*	12.63 ± 0.31^{b}	6.23 ± 0.26^{c}	10.37 ± 0.26^{c}	13.81 ± 0.21^{a}	13.67 ± 0.08^{a}	6.6
Phenylalanine*	51.90 ± 1.93^{bc}	55.98 ± 1.72^{a}	50.85 ± 1.38^{c}	44.56 ± 0.88^{d}	52.14 ± 0.58^{b}	
Isoleucine*	48.56 ± 1.38^{b}	57.11 ± 1.39^{a}	41.26 ± 1.01^{6c}	30.76 ± 0.27^{d}	38.85 ± 1.39^{c}	30
Leucine*	83.03 ± 1.38^{a}	82.53 ± 2.83^{a}	79.71 ± 2.49^{bc}	68.49 ± 2.46^{c}	78.29 ± 3.49^{ab}	61
Lysine*	64.15 ± 2.79^{b}	71.39 ± 2.11^{a}	70.18 ± 1.06^{b}	28.39 ± 1.49^{c}	32.18 ± 1.21^{c}	48
Proline	50.45 ± 2.72^{b}	36.06 ± 1.09^{c}	50.09 ± 1.22^{d}	94.82 ± 2.16^{a}	46.06 ± 2.08^{b}	
E/T (%)	40.20	41.61	43.48	32.88	39.98	
SAA (Met+Cys)	22.82	21.30	20.55	36.06	48.78	23
AAA (Phe+Tyr)	90.33	93.85	86.28	69.07	95.72	41
Hydrophilic/ hydrophobic	1.56	1.44	1.58	1.39	1.34	

*Essential amino acids (EAA). ** WHO/FAO suggested reference pattern of essential amino acids for 'Older child, Adolescent, Adult'. SAA – Sulphur containing amino acids. AAA – Aromatic amino acids. E/T – A ratio of essential to total amino acids.

According to Hughes et al. (2011) and Zeng et al. (2022) SPI had highest PDCAAS of 0.98 - 1 followed by PPI (0.73 – 0.89), CPP (0.78), RPI (0.53 – 0.75) and WG (0.25 – 0.54). Therefore, among these proteins SPI has a better nutritional profile and it is justified to use it as a base protein for developing further blends, but it does not mean other proteins cannot be used. Other proteins can be blended at right ratio to get higher PDCAAS values, for example, blending legume proteins with cereal proteins for balancing SAA and lysine profile.

Table 3.5 Amino acid scores of different proteins.

Essential amino acids	SPI	PPI	CPP	RPI	WG
Histidine	212.06	171.75	161.81	136.81	113.31
Isoleucine	168.53	190.37	137.53	129.50	102.53
Leucine	136.11	135.30	130.67	128.34	112.28
Lysine	131.56	148.73	146.21	67.04*	59.15*
SAA	99.21*	94.26*	91.04*	212.08	156.78
AAA	217.88	228.90	210.44	233.46	168.46
Threonine	151.00	152.20	163.04	155.04	104.68
Tryptophan	166.82	94.39	157.12	207.12	209.24
Valine	123.33	131.10	125.30	120.58	109.93

*Limiting essential amino acids.

3.5 Water and oil absorption capacity and water solubility

There was a wide difference in WAC for different samples and SPI has the highest WAC while the WG has lowest WAC (Fig. 3.2). The highest WAC can be attributed to its protein content, protein fraction and the type of amino acids. SPI has the highest level of hydrophilic amino acids resulting in higher WAC. RPI has the highest glutelins (around 80%) protein fraction leading to lower WAC, because of insolubility of glutelin proteins in water at neutral pH (Miedzianka et al., 2023; Wang et al., 2018). Our study also found the lower absorption and solubility. These results are in the similar range as in the literature (Tang et al., 2021; Toews & Wang, 2013; Withana-Gamage et al., 2011). There was not much difference in the OAC which was around 2 g/g. WS follows the same trend as WAC except for the CPP. CPP showed highest WS and WG was lowest in WS. Zhang et al. (2023) reported that the chickpea protein concentrate had significantly higher (1.5 times) water solubility than soy protein concentrate. The probable reason would be the higher level of albumin protein fraction in the chickpea protein which is water soluble.

WAC and WS are important parameter in the high moisture extrusion for texturization. The higher the WAC of a protein, the higher the viscosity generation in the extruder barrel and higher mechanical energy required in the process.

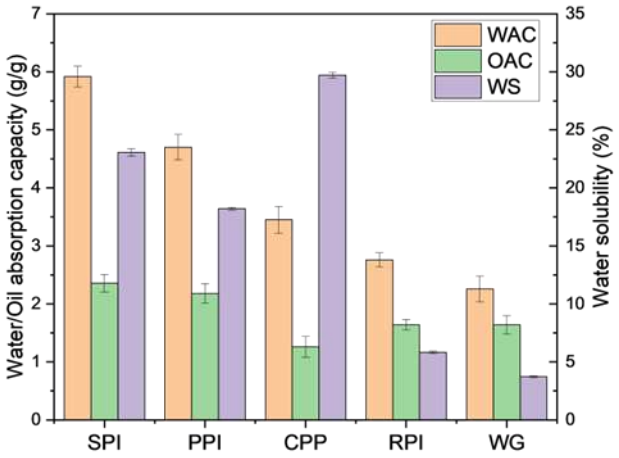

Figure 3.3 Water absorption capacity (WAC), oil absorption capacity (OAC) and water solubility of protein powders.

3.6 Protein solubility (PS) and zeta potential

The solubility of all protein isolates exhibited a nearly U-shaped trend, indicating enhanced dissolution in highly acidic (below pH 3) or highly basic (e.g., above pH 10) solutions, while demonstrating poor solubility near their isoelectric point (pH 4–5, which varies for each protein). This observation is clearly depicted in Fig. a, where the isoelectric points (pI) were approximately pH 4–5 for legume proteins and 6–7 for wheat protein, resulting in minimal solubility. Our findings align with previous reports indicating that pea proteins extracted by ultrafiltration and isoelectric precipitation displayed the lowest solubility between pH 4 and 6 (Boye et al., 2010; Zhao et al., 2020), soybean protein fractions exhibited isoelectric points ranging from 5.1 to 5.6 (Chove et al., 2007) and gluten protein had an isoelectric pH (PI) of 6.4 (Majzoobi & Abedi, 2014). All proteins exhibited higher solubility at basic pH compared to acidic pH. SPI, PPI, and CPP proteins displayed a typical "U shape" in the solubility-pH curve, although not perfectly in the acidic range (Fig. 3.3a). In the acidic range (pH 2–5), wheat protein achieved approximately 60%–70% solubility, significantly higher than other proteins. In contrast to all other proteins, rice protein demonstrated the lowest solubility throughout the entire pH range. Day (2013) also emphasized that rice protein

contains 80% glutelins protein fraction which are insoluble in water due to extensive aggregation, disulfide bond crosslinking and glycosylation except in dilute alkali.

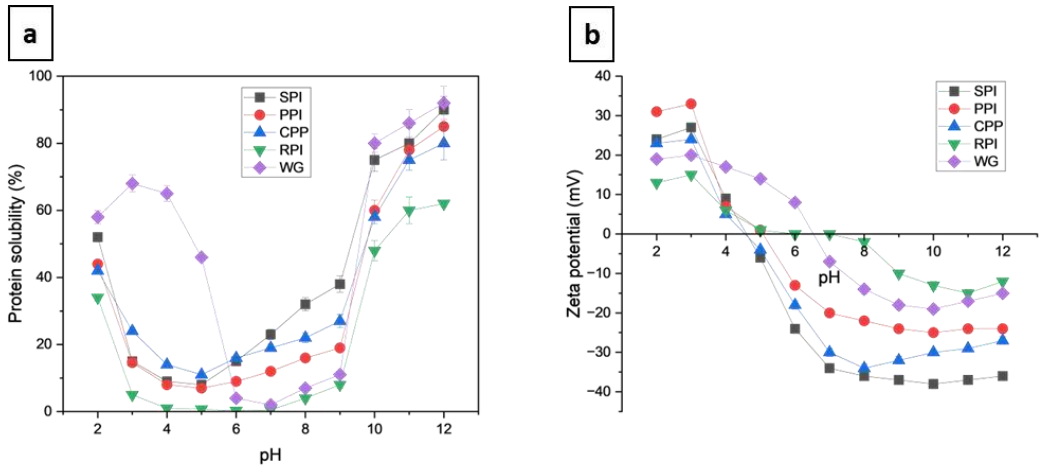

Figure 3.4 (a) Protein solubility and (b) zeta potential of protein powders at different pH (2-12).

Protein solubility and zeta potential are closely related as both are influenced by the electrostatic interactions between the protein and the solvent. This positive correlation was evident as shown in Fig. 3.3b. Generally, protein solubility is higher when the zeta potential is large (positive or negative) as this indicates a strong repulsion between the protein molecules and a lower tendency to aggregate (Malhotra & Coupland, 2004). Conversely, protein solubility is lower when the zeta potential is small (close to zero) as this indicates a weak repulsion or attraction between the protein molecules and a higher tendency to aggregate. Therefore, measuring the zeta potential of proteins can help to optimize their solubility and stability at different pH.

3.7 Emulsion activity and stability

For each protein, there was a positive correlation between EAI and ESI, as shown in Fig. 3.4a. The emulsifying capacity of proteins at pH 7 followed the order SPI > PPI > CPP > WG > RPI, aligning with their solubility rankings. PPI exhibited EAI and ESI values insignificantly different from those of CPP. Previous studies have highlighted that both high surface hydrophobicity and solubility are essential for optimal emulsifying properties, particularly in terms of EAI (Nakai, 1983). (Liu et al., 2014) further emphasized the dominant role of a higher proportion of larger molecular weight (MW) peptides and increased surface hydrophobicity in emulsifying properties when the solubility of the sample reaches a sufficiently high value. Hence, it is reasonable to

observe similar emulsifying properties in SPI, PPI, and CPP, despite variations in their solubility. WG and RPI proteins having extremely low solubility at pH 7, exhibited emulsifying properties that were incomparable to SPI and RPI proteins. However, the results indicated that the emulsifying ability of wheat protein was not considerably lower than that of rice protein, despite both WG and RPI proteins having extremely low solubility at pH 7. This observation could be attributed to the shearing force inducing denaturation in wheat protein, thereby enhancing its surface activity (Zhao et al., 2020).

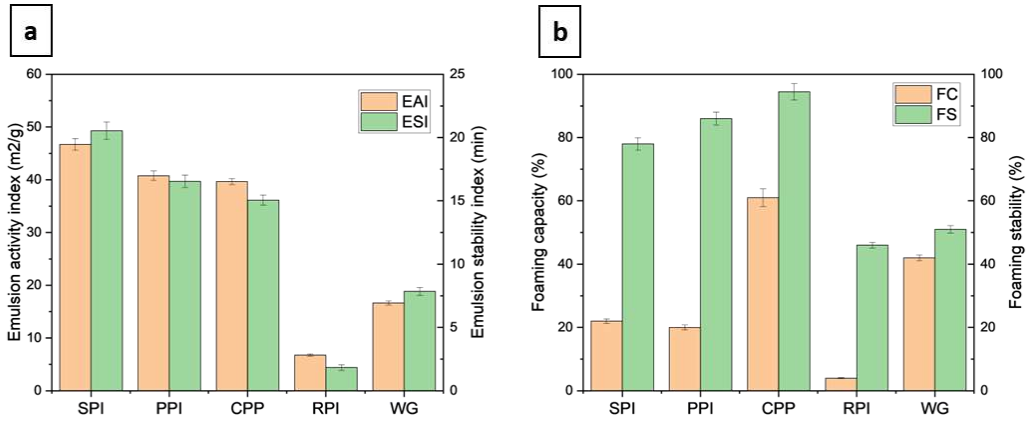

Figure 3.5 (a) Emulsion and (b) foaming properties of protein powders.

3.8 Foaming capacity and stability

CPP protein showed higher foaming properties followed by WG, SPI, PPI and RPI proteins (Fig. 3.4b). The probable reason for the highest foaming properties of chickpea was it contains higher albumin protein fraction (69%) as reported by Soto-Madrid et al. (2022) compared to other proteins like SPI (32%), PPI (15-20%) and WG (2-3%) (Le Gall et al., 2007; Makeri et al., 2017; Žilić et al., 2011). Foaming capacity is associated with the concentration of soluble proteins and soluble proteins aid in reducing the surface tension at the air/water interface, resulting in the formation of air bubbles (Khalid et al., 2003). Despite WG exhibiting low solubility at pH 7, it demonstrated higher foaming capacity than other proteins except CPP, elucidating the rationale behind using wheat flour for bread foam production. However, RPI and WG displayed very poor foaming ability. Although RPI exhibited stability up to 45%, it is insignificant due to its extremely low foam capacity. For optimal foaming ability, a protein should possess high solubility in the water phase, enabling it to reduce interfacial tension and form robust elastic films around dispersed air bubbles (Murray, 2007).

3.9 Least gelation concentration

The minimum gelation concentration (LGC) denotes the minimum quantity of proteins capable of forming a stable gel network without any structural collapse. Hence, a lower LGC value signifies enhanced gelatinization capability. Gel properties of protein isolates are influenced by various factors including but not limited to plant type, cultivars, processing methods, amino acid composition, protein purity, molecular weight, protein structure, and interactions between proteins as well as between proteins and solvents (Moure et al., 2002).

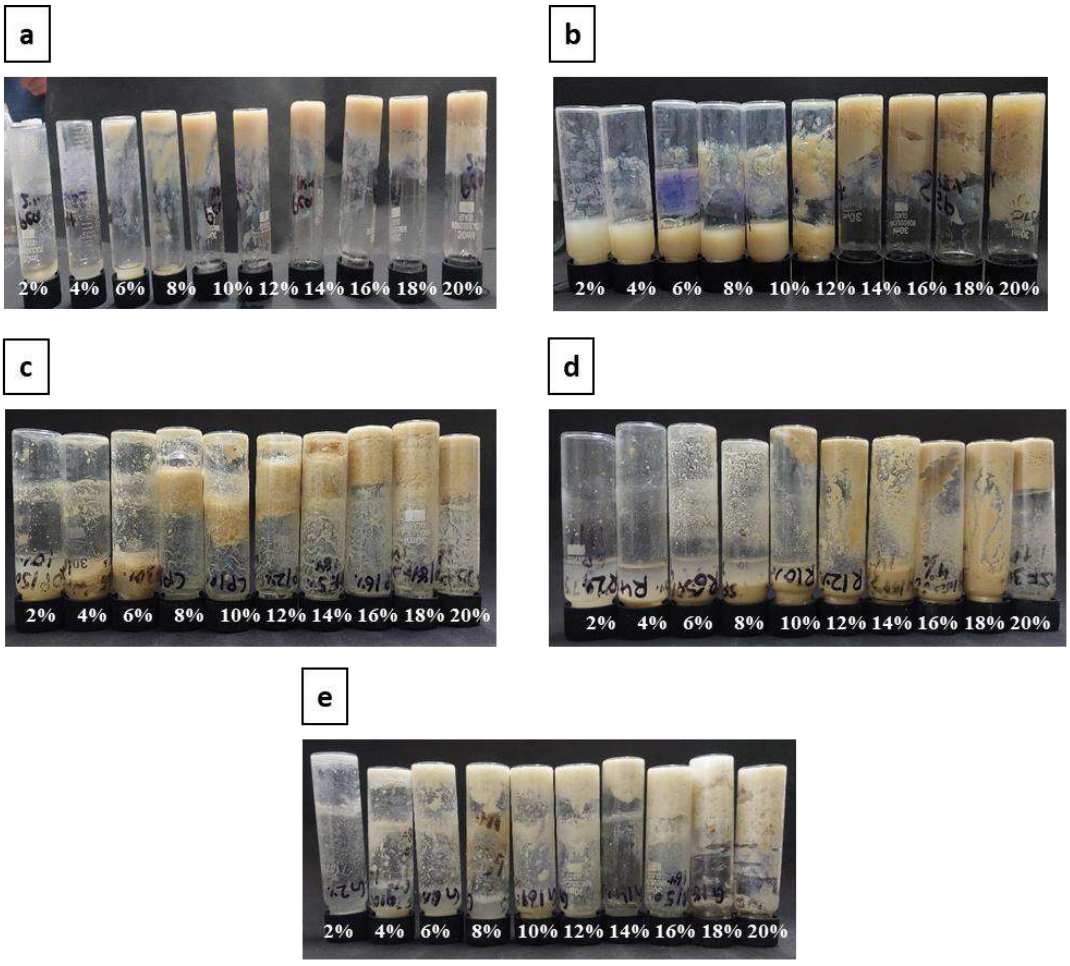

Figure 3.6 Images of samples SPI (a), PPI (b), CPP (c), RPI (d), WG (e) showing the gelling behaviour at different concentrations from 2 to 20% solids.

SPI and WG gelatinized at 12%, PPI at 14% and CPP at 16%. However, the gelatinization of RPI was observed at 20% which was still the soft gel structure as shown in Fig. 3.5. The LGC values observed in this study was in line with the previously reported literature (Ma et al., 2022; Tang et al., 2021; Webb et al., 2023). Hydrophobic interaction emerged as a crucial factor in the creation of protein gel

networks. In contrast, RPI characterized by glutelin with a high molecular weight constituting up to 80% of the total rice protein, displayed limited gelatinization ability due to its insolubility in water at neutral pH (Day, 2013). This suggests that the synergistic effect of a larger amount of unhydrolyzed protein and the presence of very limited exposed hydrophobic polypeptides may hinder the gelatinization ability of rice protein.

3.10 Pasting properties

The pasting properties of various proteins during heating and cooling cycle was illustrated in Fig. 3.6. SPI showed a highest cold swelling followed by CPP and PPI, while RPI and WG does not show any cold swelling property. SPI exhibited rapid viscosity increase with highest peak viscosity compared to other proteins. PPI displayed steady linear growth in viscosity, suggesting controlled thickening properties, while CPP maintained low and stable viscosity throughout the heating and cooling process. RPI and WG were almost flat throughout the process, suggesting no string gelation and structure formation at the given concentration of 10% solids. The final viscosity was highest for the SPI followed by PPI, CPP, WG and RPI. These results are strongly correlated with the properties such as WAC, WS, EAI, PS and LGC of the proteins. Based on these observations, we can expect the similar behaviour these proteins during the extrusion processing.

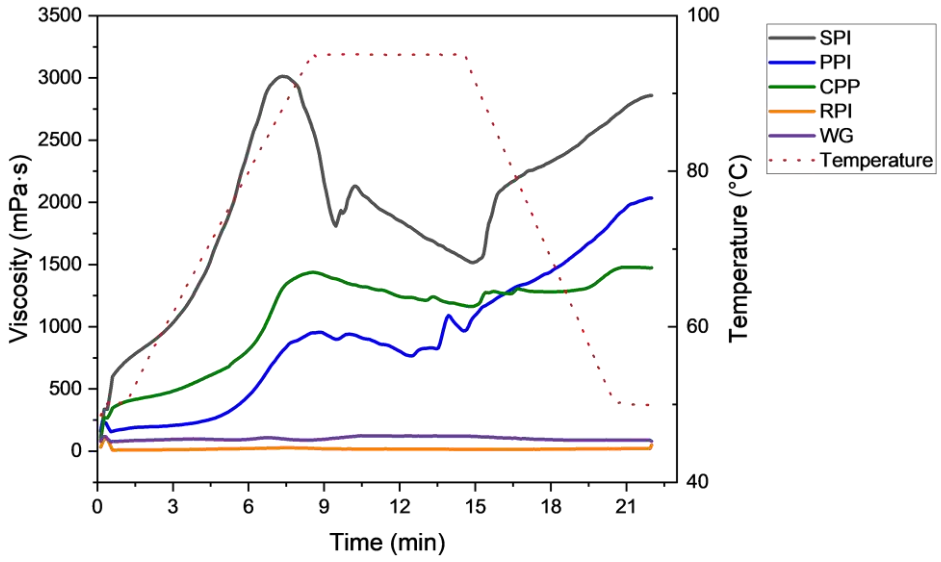

Figure 3.7 Pasting curves of protein powders at 10% solid concentration.

3.11 Rheology

A limitation of pasting property analysis is its inability to exceed 100 °C and the restriction to atmospheric pressure, which may not accurately reflect extrusion conditions. To address this, we simulated extrusion-like conditions by subjecting a protein dispersion initially at 25°C to an oscillation test, heating it to 130°C and then cooling it back to 25°C under pressurized conditions. This approach revealed behaviours in protein dispersions that diverged markedly from those observed in pasting properties. For instance, RPI and WG exhibited a consistent viscosity across the temperature range during the pasting property test. However, under the extrusion like conditions within a pressure cell, these proteins showed a significant increase in complex viscosity, as depicted in Fig. 3.8.

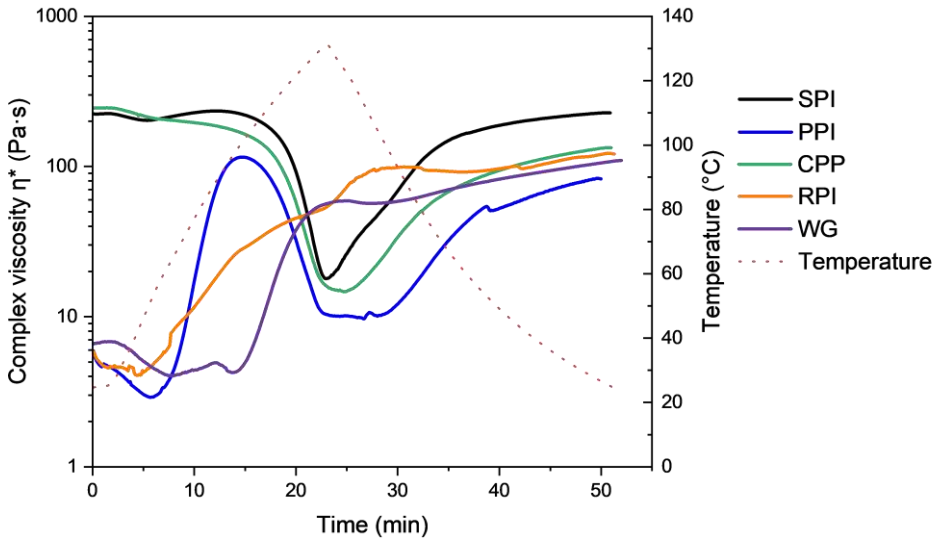

Figure 3.8 Changes in the complex viscosity (η) as a function of temperature (heating and cooling) under high moisture extrusion like conditions.*

SPI and CPP underwent similar transitions, with SPI maintaining a higher viscosity. Pea Protein Isolate (PPI) showed a lower degree of cold swelling. This could be due to the higher WAC or higher WS in SPI and CPP have contributed for the higher cold swelling. The PPI showed increased complex viscosity as temperature reached 100 °C. The onset of melting was evidenced by a decrease in complex viscosity and upon cooling cycle, the viscosity was sharply increased. Ultimately, PPI exhibited the lowest final viscosity among the proteins tested. In contrast to legume proteins, cereal proteins (RPI and WG) showed similar behaviour. Their complex viscosity rose with increasing

temperature, continued to ascend during cooling and stabilized from 100°C onwards during cooling.

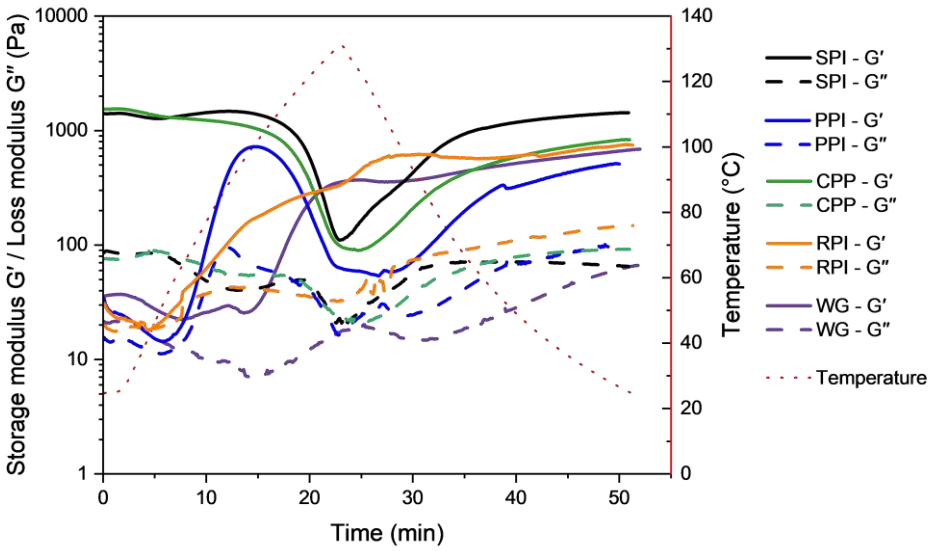

Figure 3.9 Changes in the shear modulus (G´ and G´´) as a function of temperature (heating and cooling) under high moisture extrusion like conditions.

The rheological behaviour of protein dispersions was further explored through viscoelastic property analysis, conducted under the same test conditions previously described. The results illustrated in Fig. 3.9, showed that the storage modulus (G´) of the protein dispersions was similar to the complex viscosity. This correlation is expected since complex viscosity (η*) is calculated as the quotient of maximum stress and shear strain rate amplitude at a given frequency. At the outset, SPI and CPP showed a substantial difference between G´ and the G´´, unlike PPI, which exhibited a smaller difference, suggesting that SPI and CPP formed a highly viscous paste. Conversely, the cereal proteins, RPI and WG, presented as low viscosity dispersions initially. At peak temperatures, the legume proteins melted, reducing the difference between G´ and G´´, resulting in a less viscous melt. On the other hand, cereal proteins showed an increase difference between G´ and G´´. Post heating and cooling cycle, all samples indicated that G’ was greater than G'', signifying the formation of a gel, with SPI exhibiting the strongest gelation properties.

3.12 Principal component analysis

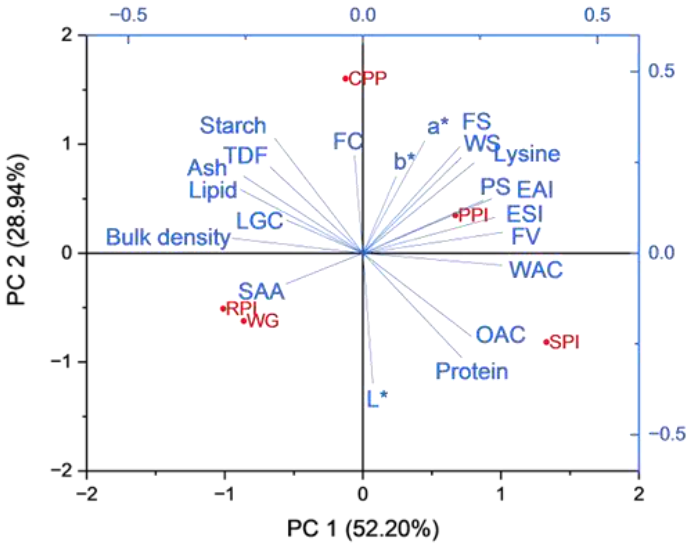

Figure 3.10 Principal component analysis (PCA) biplot showing ingredients as scores and physicochemical and nutritional properties as loadings.

PCA was employed to condense the multidimensional data encompassing physicochemical and nutritional properties of proteins into lower dimensions while retaining the majority of the information. The organization of protein properties data by PCA resulted in distinct clusters, facilitating the identification of similarities and differences based on these characteristics. As shown in the PCA plot in Fig. 3.7, the first and second components collectively explained 81.14% of all variances, revealing clear sample clustering in different quadrants. Cereal proteins (RPI and WG) were situated in the negative PC1/negative PC2 quadrant, SPI and PPI were positioned in the positive PC1 half and CPP was in the positive PC2 half along with PPI. Most physicochemical properties were distributed across SPI, PPI, and CPP scores due to their strong correlation, whereas RPI and WG displayed poor performance in these properties except for the SAA score. Overall, this PCA analysis exhibited a strong correlation with the studied protein properties, offering a straightforward visualization of the entire dataset at once.

4 Conclusion

This study characterized the functionality of different plant proteins which are being used commercially for texturization. Overall compared to other protein isolates, SPI showed highest WAC, WS, EAI, ESI, PS at neutral pH, LCG and pasting viscosity. PPI

closely resembled SPI, suggesting its potential as a substitute for SPI, particularly in functions related to hydration. However, RPI's overall functionality did not match that of the other proteins and WG's foaming ability could not be replaced by any other proteins except for the chickpea protein. Chickpea protein showed highest foaming ability and can be used in various applications where foaming is an important functional requirement for example, bread making. This observation aligned with the outcomes of the PCA analysis on protein functionalities. The properties of the plant proteins investigated in this study would be helpful for the food scientist, engineers and manufacturers in the appropriate application of different plant proteins in food products.

These functionalities play a role in extrusion and texturization become crucial for the texturization and are essentially required for the extrusion process to understand the behaviour of raw materials in the extruder and in the final product. Considering the different proteins and their functionality, SPI stands at the top from both physicochemical and nutritional perspectives. In contrast, RPI and WG cannot be considered as primary protein ingredients due to their poor functionality and will form good textures. The current market volume of SPI is much higher than other proteins and SPI also comes at a comparatively lower cost than PPI and CPP. Hence, in the following chapter, we have used SPI as base primary protein ingredient to study the effect of extrusion process parameters and the blending of millet flours and fraction flours with SPI. The characterization of secondary ingredients used as blend components in the thesis is done in subsequent chapters.

Chapter 4

A study on high moisture extrusion for making whole cut meat analogue: Characterization of system, process and product parameters

This chapter has been published as Mateen, A., Mathpati, M., & Singh, G. (2023). A study on high moisture extrusion for making whole cut meat analogue: Characterization of system, process and product parameters. Innovative Food Science & Emerging Technologies, 85. https://doi.org/10.1016/J.IFSET.2023.103315

Abstract

The study investigated the effect of process parameters on the system and textural properties of soy-based high-moisture meat analogues (HMMA) produced using a twin-screw extruder and compared the resulting properties to those of real meats. The span of values obtained for the various textural properties of the HMMA varied widely, with hardness, chewiness, and cutting strength displaying broad span and resilience, cohesiveness, and springiness showing narrow spans. The data as a whole demonstrates the possibility of creating a diverse range of textures by choosing suitable operating conditions in a twin-screw extruder. In addition, the textural properties of the extruded meat analogues were compared to those of real meat cuts from chicken, lamb, and beef. The hardness, chewiness, and cutting strength of the real meat cuts were within the span obtained for the extruded meat analogues, while resilience, cohesiveness, and springiness were outside the span. The results indicate that it may not be possible to achieve textural equivalence between the extruded meat analogues and real meat cuts on all parameters by only optimizing the operating parameters. Identifying new blend components and creating innovative die designs could be crucial for achieving a full match of textural properties.

Keywords: Extrusion, HMMA, Texture, Real meat

1 Introduction

Sustainable food production for a projected 10 billion people by the end of 2050 will require societal transition and industrial transformation with regard to food choices. Animal-based food products have a disproportionate impact on issues such as biodiversity loss, freshwater depletion, and climate change (Bodirsky et al., 2020; González et al., 2020). This realization has resulted in endeavours to develop plant-protein based food products that can mimic animal-based food products such as dairy, egg, and meat and lead to a shift towards more sustainable food choices without sacrificing taste and delight (Aiking, 2011; Schösler et al., 2012). Energy and land-use calculations suggest that such shifts can contribute significantly to our efforts to save the environment (Nijdam et al., 2012). The success of such endeavours rests on the ability of the plant-based analogues to match the textural, taste, and nutritional properties of real animal-based products (Grunert et al., 2004). Plant-based burgers that mimic meat-based burgers have grown as a market over the last 5-years (Ortega et al., 2022). Meat products range in textural complexity from minced products like ground beef burger patties and chicken nuggets to shreds to more complex whole meat cut products that are recognizable pieces of an animal such as a steak or a filet. Plant-based meat analogues have been very successful in recreating textures for minced meat products, somewhat successful in meat shreds, and much less successful in recognizable cuts (Berke, 2022).

Various technologies are being explored to produce plant-based whole meat analogues. These include twin-screw extruders with cooling dies, (Chiang et al., 2019b), electrospinning (Nieuwland et al., 2014), and shear cell technology (Grabowska et al., 2014). Of these three technologies, the twin-screw extruder with a cooling die offers the potential for scale in the short term. Despite the increased use of extrusion technology in food processing over the past few decades, the extrusion of protein powders using a twin-screw extruder with a cooling die is yet to be understood fully due to its complex multivariate input-output system. A simplified system analysis model has been proposed (Meuser et al., 1984; Ryu, 2020), which categorizes extrusion parameters into three main groups, namely, process, system, and product parameters groups. Some of the parameters in each of these groups are

- Process parameters: raw material/formulation, screw configuration, die dimension, screw speed, moisture content, barrel temperature, etc.
- System parameters: energy input, residence time, melt temperature, melt pressure, melt viscosity, etc.
- Product parameters: texture, colour, nutrition, flavour, digestibility, etc.

The correlations between process, system, and product parameters have been studied extensively. A few of these studies are given in supplementary material.

Though it is clear that operating parameters have effects on the product properties by means of affecting extrusion system parameters, the limitations of in-line detection, have kept the extrusion process as a black box, with researchers focusing on process and product parameters in their studies (Fang et al., 2014; Thiébaud et al., 1996)Maung et al., 2021; Pietsch et al., 2019). In spite of their shortcomings, these studies provide us with valuable relationships between some of the operating parameters and product properties. Generally, it is found that all the process parameters have an influence on system and product properties. These relationships have been sufficient to develop good plant protein-based minced meat products such as burger patties and chicken nuggets.

However, whole meat products have not had the same success yet. In order to mimic real meats using plant-based meat analogues, we need to deliver full-spectrum textural equivalence in the extrudate which includes properties such as hardness, chewiness, springiness, resilience, cohesiveness, and cutting strength. Achieving partial textural matches does not lead to acceptable products. Hardness is a measure of the peak force to compress the product, and chewiness is a measure of much work is needed to chew the product. Resilience relates to how well a product "fights to regain its original height" post compression, and cohesiveness is how well the product withstands a second deformation relative to its resistance under the first deformation. Springiness is how well a product physically springs back after it has been deformed (Breene, 1975; Friedman et al., 1963).

In this chapter, we have studied the full spectrum textural range achievable for twin-screw extruded high-moisture meat analogues using soy-based protein blends over a wide range of process parameters (protein concentration, moisture content, barrel temperature, screw speed, and feed rate). This range was compared to the textural parameters (hardness, chewiness, resilience, cohesiveness, springiness, and cutting

strength) of real meats to understand the gaps between the two and identify the challenges to address through further research for whole-meat analogues to match real meats.

2 Materials and methods

2.1. Material

2.1.1. Preparation of protein blends

Soy protein isolate (SPI) was procured from Shandong Yuxin Biotech Co. Ltd., Shandong, China, and defatted soy flour (DSF) was procured from Gujrat Ambuja Exports, India. According to the manufacturers, the protein content (dry weight basis) of SPI and DSF were 90% and 50% respectively. Two protein powder blends were prepared by mixing SPI and DSF at 25:75 and 50:50 ratios to get 60% and 70% protein levels on a dry weight basis respectively.

2.1.2 Real meat

Three different real meat sources were selected: chicken breast, lamb meat (from leg butt portion), and beef meat (from thick flank/round portion). These meats were locally procured 3 hour post-mortem near the university and kept at 3 ºC during transport. Any excess fat or cartilage was removed from the meats and washed. The chicken breast was split into half measuring around 5.5 – 6.5 inches in length. Lamb and beef meat were cut into steak sizes of similar lengths. The cooking process of meat was performed according to the method described by (Chiang et al., 2019b; Mathevon et al., 1995) with slight modifications. The meats were individually packed in plastic bags and cooked in boiling water. The meats were cooked to an internal temperature of 75 – 80 ºC. The cooked meats were removed and placed on a perforated mesh to cool for 30 min. These meats were cut into 20 x 20 mm cubes and a height of 10 mm for texture analysis.

2.2 Experimental design

Five independent variables were selected for the study – dry blend protein powder, moisture content (MC), barrel temperature (BT) at heating zone 1 – 5 (HZ1 – HZ5), feed rate (FR), and screw speed (SS). Two moisture levels - 60%, and 70%; three heating profiles - low heat (110 ºC), medium heat (130 ºC), and high heat (150 ºC); two

screw speed – low shear (300 rpm) and high shear (900 rpm); two feed rates – low (5 kg/hr) and high (10 kg/hr) as shown in Table 4.1. 48 trials were conducted based on a factorial design 2 x 2 x 3 x 2 x 2.

The protein concentration of the melt is an important parameter affecting the fibration during extrusion. The protein concentration of the melt in the barrel is determined both by the protein concentration of the dry blend and the water added to it. Therefore, we have provided both dry basis and wet basis protein concentrations in the data. The two dry protein blends (60% protein - 25:75 SPI:DSF and 70% protein – 50:50 SPI:DSF) were used at two moisture levels, 60%, and 70%. This gave four different protein concentrations for the melt on a wet basis for our experimentation - 18%, 21%, 24%, and 28%. The 25:75 SPI:DSF dry blend at 70% and 60% moisture results in protein concentrations of 18% and 24% respectively. The 50:50 SPI:DSF dry blend at 70% and 60% moisture results in 21% and 28% protein concentrations respectively.

Table 4.1 Experimental design for raw material protein concentration and thermomechanical treatment.

Protein blend	Feed moisture content (%)	Protein concentration* (%)	Barrel temperature (ºC) from HZ1 to HZ5	Feed rate (kg/hr)	Screw speed (rpm)
SPI: DSF (50:50)	60	18	40-60-80-110-110	5	300
		21	40-80-110-130-130		
SPI: DSF (25:75)	70	24	40-80-120-150-150	10	900
		28			

* A derived independent variable from protein blend and feed moisture content on wet basis in the barrel.

2.3 High moisture extrusion

Experiments were conducted on a pilot-scale twin-screw extruder (TwinLab F-20/40, Brabender GmbH & Co. KG, Germany) with a 20mm screw diameter and 800mm length, resulting in an L/D ratio of 40:1. The extruder's barrel was a clamp shell type with four heating zones (HZ) powered by electrical heaters and water circulation for temperature control. An additional heating zone (HZ5) was mounted next to the fourth heating zone at the screw tip. The extruder setup and screw configuration used in this study was shown in Fig. 4.1. A single screw vertical volumetric feeder was used to feed the dry powder in the barrel at the 0 D position and water feed was at the 10 D position with a peristaltic pump (Watson-Marlow 120U/DV, Watson-Marlow Ltd., United

Kingdom). A long cooling die of 300 mm in length, 20 mm in width, and 9 mm in height was attached with a cooling water circulator (Corio CD-600F, Julabo GmbH, Germany). Cooling water temperature of 30 ºC and a flow rate of 6.97 liter/min were used.

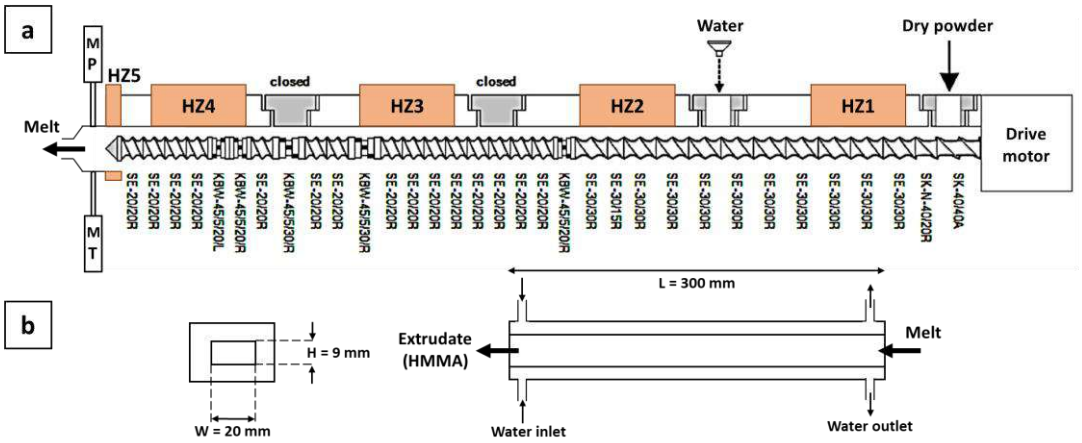

Figure 4.1 a) Extruder setup and screw configuration for high moisture extrusion (SK, SK-N, SE – conveying elements and KBW – kneading elements). b) A long cooling die design.

2.4 Extruder response

The temperature thermocouple and pressure transducer were installed in-line at the end tip of the extruder screw to record the data of melt temperature (MT/ ºC) and melt pressure (MP/ bar). Load on the extruder motor in percentage was recorded and specific mechanical energy (SME) was calculated from eq. (4.1) (Godavarti & Karwe, 1997; Osen et al., 2014; Zhang et al., 2020). Extruder and system parameters were recorded through a user interface computer software MetaBridge (Brabender GmbH & CO. KG, Germany).

$$SME\ \left(\frac{kJ}{kg}\right) = \frac{2\pi\ x\ n\ x\ T}{MFR} \tag{4.1}$$

Where n is screw speed (rpm), T is the motor torque (Nm: the non-load torque was subtracted from the actual torque values) and MFR is the mass flow rate of material (g/min). Once the steady state of the extrusion process was achieved, extrudate samples of approximately 500 g were collected for further analysis.

2.5 Texture profile analysis (TPA)

The textural properties of extruded samples were analyzed by using a Texture Analyser (Ametek Brookfield Inc, USA) as described by Fang et al. (2014) with some modifications. For TPA analysis, extrudate samples were cut into cubes 20 × 20 × 10 mm (L × W × H). Hardness, chewiness, resilience, cohesiveness, and springiness were analyzed using a TA43 probe of 25.4 mm diameter with a 100 kg load cell. Measurement methods were set at 50% deformation of the sample with a compression speed of 0.5 mm/s. At least ten replications of measurements were performed for each sample.

2.6 Cutting strength

The cutting strength was done along and across the flow direction of extrudates from the extruder by using a TA7 knife probe with a TA-CKA craft knife adapter and the setting was at 0.5 mm probe travel speed with 90% cutting of the sample's original size. The cutting strength test was done along and across the flow direction of the extrudate to determine the anisotropic index by eq. (4.2) (Ferawati et al., 2021). In addition to analyzing the HMMA samples, the cutting strength of cooked real meat from chicken breast, lamb, and beef was also determined to compare the fibration. The cutting strength of the real meat was measured by cutting in both directions of fibers i.e., along and across the meat fiber. The measurements for the cutting strength were taken at least five times.

$$Anisotropic\ Index = \frac{cutting\ strength\ along}{cutting\ strength\ across} \tag{4.2}$$

2.7 Colour value

The colour values of the extrudate samples were analyzed using a colorimeter (CR-400 chroma meter, Konica Minolta Sensing Inc., Japan). The colour was recorded in the CIE-lab L*, a*, b* colour space. L* represents the brightness or lightness, ranging from 0 to 100 (black to white), a* represents the red-green axis, ranging from positive to negative (green to red), and b* represents the yellow-blue axis, ranging from positive to negative (yellow to blue) (Benković et al., 2015). The total colour change ΔE was calculated (Fang et al., 2014) using eq. (4.3). All the samples were measured in triplicates.

$$\Delta E = \sqrt{(L^*_{sample} - L^*_{std})^2 + (a^*_{sample} - a^*_{std})^2 + (b^*_{sample} - b^*_{std})^2} \quad (4.3)$$

Where L^*_{sample}, a^*_{sample}, and b^*_{sample} are colour values of extrudates, and L^*_{std}, a^*_{std}, and b^*_{std} are colour values of raw material blends.

2.8 Statistical analysis

All data were expressed as mean ± standard deviation (SD). All the data were analyzed using Pearson correlation coefficient (r) with 2-tailed test of significance between the process parameters and system parameters and product properties of the extrudate were performed using the OriginPro ver 2022 (OriginLab Corporation, Northampton, MA, USA). Statistical significance was set at a 0.05 probability level.

3 Results and discussion

3.1 System parameters

3.1.1 Specific mechanical energy (SME)

The effect of moisture content, protein concentration and process variables on system parameters are shown in Fig. 4.2. Our results show that SME is a strong function of protein concentration, moisture content, screw speed and feed rate ($p < 0.05$). It increases with screw speed and blend protein concentration and decreases as moisture and feed rate is increased. Barrel temperature has minimal effect on SME. The opposite effect of moisture and protein concentration on SME is expected as both increase in moisture and reduction in protein will result in lowering viscosity of melt which will lead to lowering SME at the same screw speed. Other studies have also reported reduction in SME with increase in moisture and reduction in protein concentration and related this with reduction in viscosity (Chen et al., 2010). Our results on effect of screw speed and feed rate also agree with those reported in other studies in the literature (Palanisamy et al., 2019; Pietsch et al., 2019). However, they differ on effect of barrel temperature. Lin et al. (2002) and Osen et al. (2014) reported that SME reduced with increase in barrel temperature while we did not observe a strong relationship between the two parameters.

Further, we observed a tighter band for SME at 70% moisture level (25 to 150 kJ/kg) while the band was much wider at the 60% moisture level (50 to 300 kJ/kg) under the

same range of screw speed and feed rates. This suggests that changes in operating parameters have a bigger impact on SME at lower moisture.

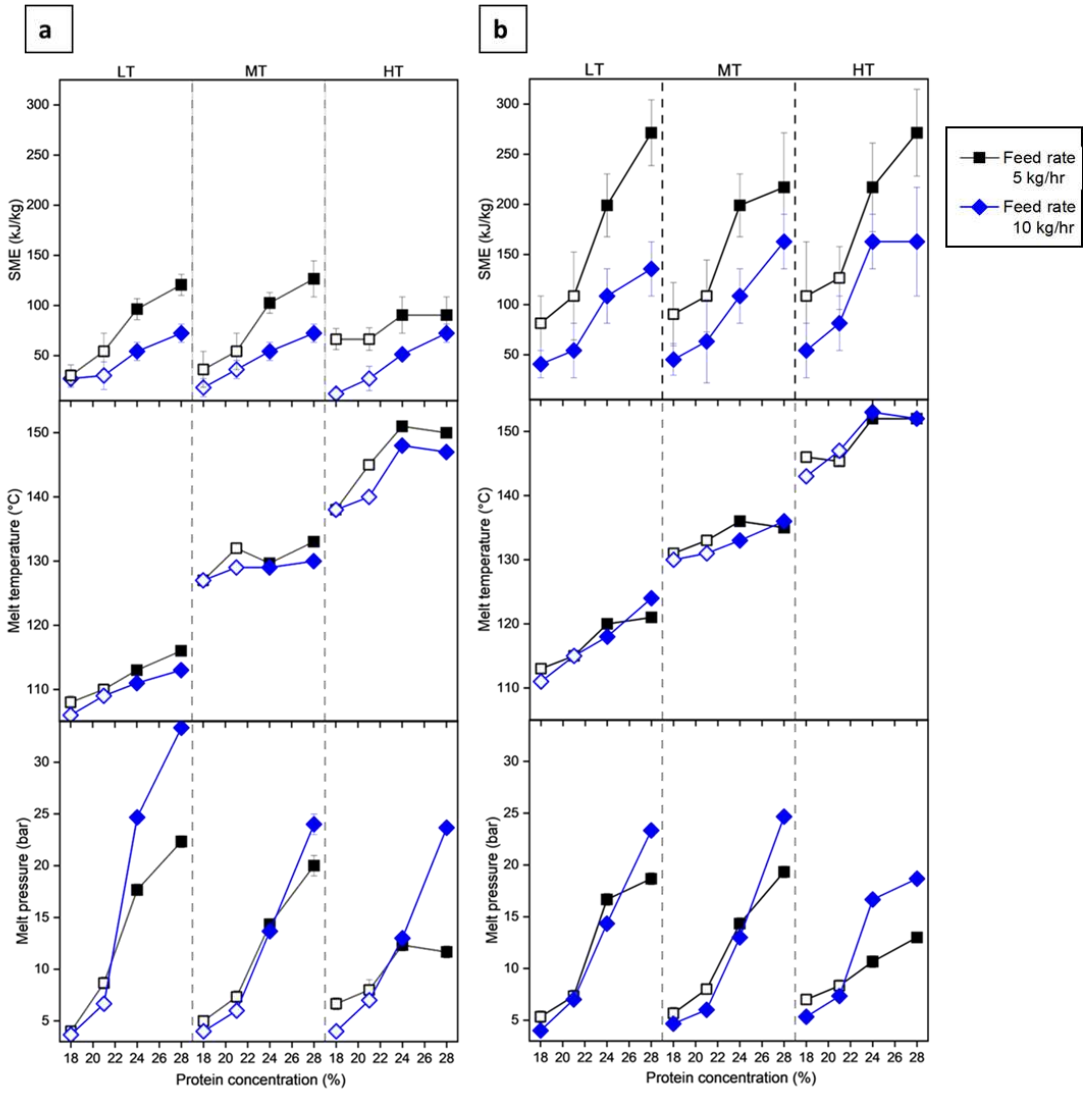

Figure 4.2 Effect of protein concentration and process variables on system response parameters. Unfilled and filled symbols are 70% and 60% moisture content respectively, LT – low barrel temperature, MT – medium barrel temperature, and HT – high barrel temperature

3.1.2 Melt temperature

Melt temperature depends on the heat transferred from the barrel and the heat generated because of shear. It is expected to increase with barrel temperature and screw speed. Our results indeed show a strong positive correlation between melt temperature with barrel temperature. The screw speed also has a positive correlation with melt temperature but is much weaker. The strength of this dependence may vary with scale and the manufacturer's design for heat transfer and may not, therefore, be generalizable.

Additionally, the data does show that the system could deliver a melt temperature in line with the setpoints across the moisture levels at 130 ºC. However, it struggled to do so at 60% moisture levels at 110 ºC where the melt was higher than the setpoint, and at 70% moisture levels at 150 ºC where the melt temperature was lower than the setpoint. This indicates challenges in heat transfer and the need to understand the heating and cooling capabilities of the extruder to obtain the desired melt temperatures.

Lowering moisture content to 60% increases the melt temperature. Melt temperature has a positive correlation with screw speed. Melt temperature increases with an increase in screw speed from 300 rpm to 900 rpm significantly ($p < 0.05$). Our results are in line with literature such as those reported by Pietsch et al. (2019), who found that even though barrel temperature was kept constant the melt temperature increased with screw speed (from 100 ºC to 118 ºC at a barrel temperature of 100 ºC) and attributed this to an increase in viscous energy dissipation. Palanisamy et al. (2019), also found similar results showing screw speed had a positive linear effect on melt temperature during the high moisture extrusion of lupin protein. However, from our results, this increase is marginal compared to the increase with respect to protein concentration and barrel temperature. Melt temperature decreases marginally with an increase in feed rate, this could be due to less residence time at low screw speed (300 rpm) but at higher screw speed (900 rpm), there was an equivalent melt temperature from the feed rates. This could be due to the additional heat generation from the extra shearing effect.

3.1.3 Melt pressure

The melt pressure follows a very similar trend to the SME. With an increase in moisture content from 60% to 70%, melt pressure decreased significantly ($p < 0.05$). A change in melt pressure at the constant flow rate, die geometry, and cooling temperature indicates a change in melt viscosity (Pietsch et al., 2019). The melt pressure bands are broader at 60% moisture compared to 70% moisture showing that the system is much more sensitive to changes in operating parameters at low moisture compared to high moisture. There was a significant increase in melt pressure as protein concentration was increased ($p < 0.05$). The change in melt pressure at 70% moisture, from 18% to 21% protein concentration, was less than at the 60% moisture level, from 24% to 28% protein concentration. The effect of temperature on melt pressure is much less and not significant ($p < 0.05$) as well as less consistent across the various protein concentration

and operating conditions. The melt pressure remains almost constant at 70% moisture levels, whereas at 60% moisture levels, the temperature has a marginally negative impact on the melt pressure. Pietsch et al. (2019), found that there was no significant impact from barrel temperature at 110 ºC on MP at fixed other conditions, and at 140 ºC and 160 ºC, pressure decreased with increased barrel temperature during the high moisture extrusion of soy protein concentrate. This could be due to the change in viscosity of the melt, where higher temperature makes the melt less viscous and thereby, less melt pressure (Bengoechea et al., 2007).

The feed rate has less effect on melt pressure but it does have an interesting interaction with moisture content. At 70% moisture content, the feed rate showed a marginal negative influence, whereas at 60% moisture content, feed rate showed a positive influence. Screw speed also showed a negative influence on melt pressure where it slightly decreases with an increase in screw speed at the lower moisture content (60%) and this could be due to the co-effect from high shear and higher temperature. In the interaction effects of parameters, the protein concentration and moisture content had more influence on melt temperature than other parameters feed rate, barrel temperature, and screw speed. All in all, the highest melt pressure was observed at higher protein concentration, lower moisture content (60%), lower barrel temperature, and lower screw speed.

3.2 Product parameters

3.2.1 Texture properties

High moisture meat analogues created from the 48 runs resulted in a wide range of textures. The hardness ranged from a low of 1197.33 g to a high of 13178.00 g (11.0 X between the lowest and highest) and chewiness ranged from 83.37 mJ to 694.15 mJ (8.3 X). The resilience ranged from 0.23 to 0.46 (2.0 X), cohesiveness ranged from 0.59 to 0.79 (1.3 X) and springiness ranged from 0.80 to 0.95 (1.2 X). The fold changes for resilience, cohesiveness and springiness were much lower, as they are bound values with ranges between 0 and 1. These ranges of the textural parameters were shown in Fig. 4.3.

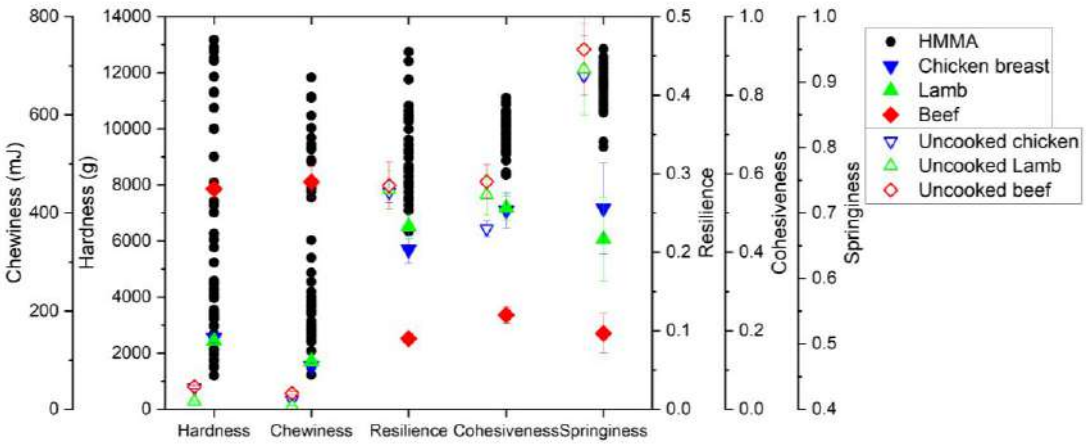

Figure 4.3 Ranges of textural parameters of HMMA obtained from manipulation of process parameters and the texture of real meat.

The textural properties of the meat analogues were compared to that of chicken, lamb, and beef. Chicken and lamb have much lower hardness and chewiness compared to beef. The resilience, cohesiveness, and springiness of beef were way lower than chicken and lamb meat. We found that the hardness and chewiness values of chicken, lamb, and beef fell within the range of hardness and chewiness obtained for the soy protein-based high moisture meat analogues. However, the resilience, springiness, and cohesiveness values of real meat fell outside the range of values obtained for meat analogues as shown in Fig. 4.3. Thus, a full spectrum match of textural properties could not be obtained. The textural values of uncooked and cooked real meat are provided in Fig. 4.3.

The effect of protein concentration and process variables on the textural properties of HMMA were shown in Fig. 4.4.

Generally, it is believed that hardness & chewiness increase significantly with protein concentration and moisture content (Lin et al., 2000; Zahari et al., 2021; J. Zhang, Liu, Jiang, Faisal, et al., 2020). Our results also showed similar interaction with protein concentration and moisture content, on hardness and chewiness. Protein concentration and moisture content are coupled parameters and it is not possible to separate the independent effect of the two. However, the magnitude of the change in hardness obtained over the range of moisture was found to be greater than that obtained over the range of protein concentrations studied. Moisture impacted the absolute values of hardness as well as the spread of the data. As moisture content decreased to 60%, the hardness increased. Barrel temperature and screw speed showed a positive impact on

hardness. As temperature and screw speed increases, hardness also increases and this could be due to the denaturation and agglomeration of protein molecules (Kitabatake et al. 1990), and higher shearing results in surplus heat which results in harder structure. Zahari et al. (2021) showed that lower temperature increases the hardness of pea protein blend HMMA and Lin et al. (2000), showed that at fixed moisture content, a higher cooking temperature resulted in a softer and less chewy soy protein extrudates which contradicts our findings whereas, we observed that with higher temperature the extrudates will be harder and chewier through textural assessment. The feed rate had a marginally negative impact on extrudate hardness.

Chewiness also showed a similar trend because it is a product of hardness, according to the definition of chewiness (Bourne, 2002). The chewiness was significantly ($p < 0.05$) impacted by protein concentration and moisture content with a positive and negative relation respectively. Like hardness, chewiness is also significantly impacted by protein concentration and moisture content. As mentioned above since the two parameters are coupled it is not possible to deconvolute the independent effect of each. Similar to hardness, the magnitude of the change in chewiness obtained over the range of moisture was found to be greater than that obtained over the range of protein concentrations studied. The other parameters such as feed rate, screw speed, and barrel temperature do not show a significant difference.

Resilience relates to how well a product "fights to regain its original height" post compression. Moisture content and screw speed did not influence resilience and were not significant factors ($p < 0.05$). Interestingly, it was found that protein concentration had a positive impact on resilience where the resilience was increased from 18% to 21% and 24% to 28% protein concentration within 70% and 60% moisture content respectively. Barrel temperature and feed rate made a positive significant difference ($p < 0.05$). The effect of barrel temperature and feed rate was majorly impacted at medium and high temperatures and at 60% moisture level.

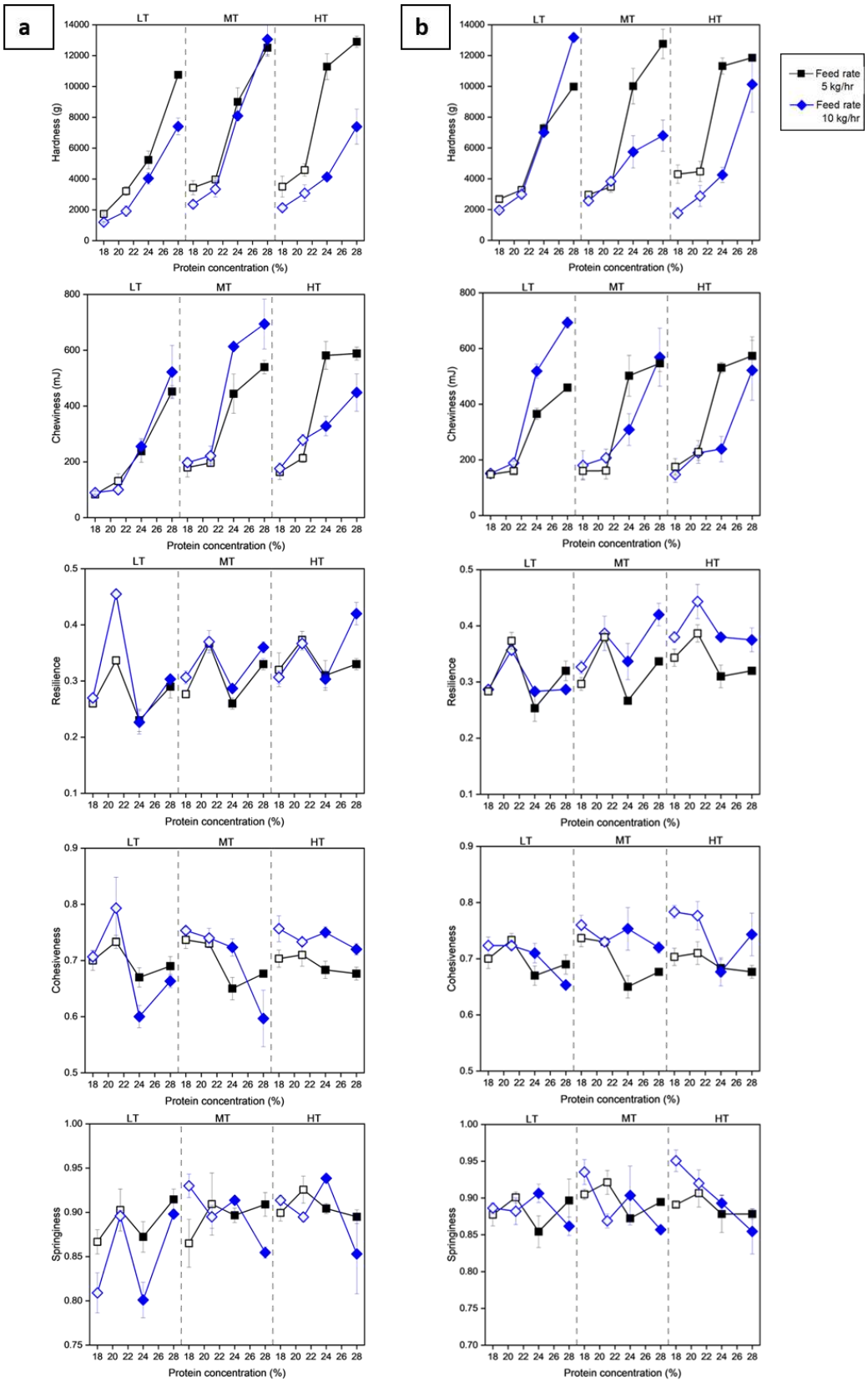

Figure 4.4 Effect of protein concentration and process variables on textural properties of HMMA. Unfilled and filled symbols are 70% and 60% moisture content respectively, LT – low barrel temperature, MT – medium barrel temperature, and HT – high barrel temperature

Yao et al. (2004) found that in high moisture extrusion from a blend of soy protein isolate: gluten: wheat starch (6:4:0.5), hardness, and chewiness showed a negative correlation with the moisture content of feed material, but cohesiveness and springiness has no significant effect from the moisture content. Cohesiveness was positively related to moisture content and feed rate and negatively related to protein concentration within the specific feed moisture level at a significance of $p < 0.05$. Similarly, to resilience, protein concentration showed an interesting interaction with protein concentration where cohesiveness was negatively impacted by protein concentration from 18 to 21% at 70% moisture and from 24 to 28% at 60% moisture levels. Screw speed does not have any impact on cohesiveness and barrel temperature showed a marginally positive impact on cohesiveness.

Springiness was majorly impacted by barrel temperature at a significance of $p < 0.05$. as barrel temperature increases, extrudates become springier. At 18% and 24% protein concentration (from a blend of SPI:DSF 25:75) and with a higher feed rate 10 kg/hr, springiness increases. Whereas, at 21% and 28% protein concentration (from a blend of SPI:DSF 50:50) and with a higher feed rate of 10 kg/hr, springiness decreases. Springiness stood out as a parameter as its trend changed dramatically between the various operating sets. It increased with feed rate at low protein levels but reduced with feed rate at high protein levels for the same moisture levels.

The hardness and chewiness of the extruded proteins were much higher for the 60% moisture extrudates compared to the 70% moisture extrudates. Resilience and springiness had minimal differences between the samples obtained with 70% moisture and 60% moisture extrudates. The cohesiveness appeared to be marginally higher for the 70% moisture levels compared to the 60% moisture levels. Additionally, the bands for all properties were much larger for 60% moisture blends compared to 70% moisture blends. This implies that much finer process control is required for 60% moisture blends for consistent products as they are more sensitive to operating parameters such as screw speed and feed rate. Consequently, it also implies that there is a greater scope to create different textures at 60% low moisture blends compared to 70% high moisture blends by changing operating parameters.

3.2.2 Cutting strength and anisotropy

Cutting strength along and across the flow of extrudates from the die can be used as a tool to analyze the fiber formation in the high moisture meat analogues which intern represents the anisotropic property. The cutting strength of HMMA along the extrudate ranged from 821.67 g to 4766.00 g (5.8 X) and the cutting strength across ranged from 225.00 g to 2429.33 g (10.8 X).

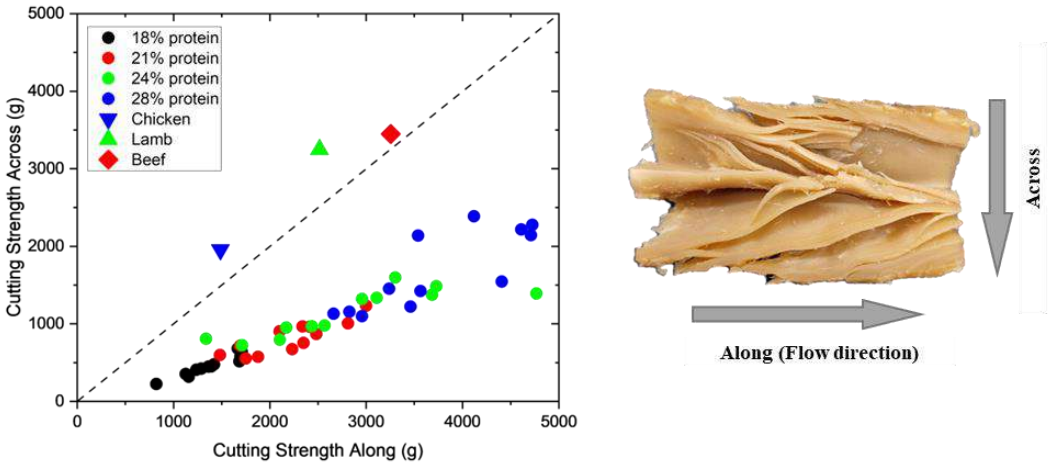

Figure 4.5 Comparison of cutting strength along and across the flow direction of extrudates of HMMA and cutting strength along and across the fibers of real meat.

When we plotted a cutting strength along vs across with the same X and Y axis scale and drew a diagonal line on it, it was found that the relationship was linear as shown in Fig. 4.5. In the same figure, the cutting strength along and across the fibers of real meats was also plotted. The cutting strength of real meats and meat analogues show different trends. It was observed that the real meat data points were marginally above the diagonal line, whereas the HMMA extrudates data points were significantly below the diagonal line. This indicates structurally different fibrations between real meat and extruded meat analogues. Real meats show higher cutting strength across the fibre and lower cutting strength along the muscle fibre. Visually, the fbration in the extruded samples appears along the direction of extrusion. This difference between the visual appearance of fibration and cutting strength may be due to the fact that in real meat fibers are packed in fiber bundles (Listrat et al., 2016), and on the other hand HMMA extrudate fibers are more like an anisotropic structure (Wittek, Zeiler, et al., 2021). Getting meat like textures may involve packing layers of extrudates together in molds.

The effect of protein concentration and process variables on cutting strengths was shown in Fig. 4.6. With respect to the process parameters that impact cutting strength, protein concentration and moisture had the strongest correlation with cutting strengths. The protein concentration showed a positive significant ($p < 0.05$) impact on both cutting strength along and across. Whereas, moisture content had a negative significant ($p < 0.05$) impact on both cutting strength along and across. As protein concentration increase or moisture content decreases to 60%, the force required to cut the extrudate samples either along or across increases. Barrel temperature also has a positive correlation though not as strong as protein concentration. Feed rate and screw speed do not show a significant difference ($p < 0.05$) in cutting strength. However, screw speed showed a marginal increase in cutting strength and this would be due to the surplus heat generation from higher shear which leads to more agglomeration of protein molecules.

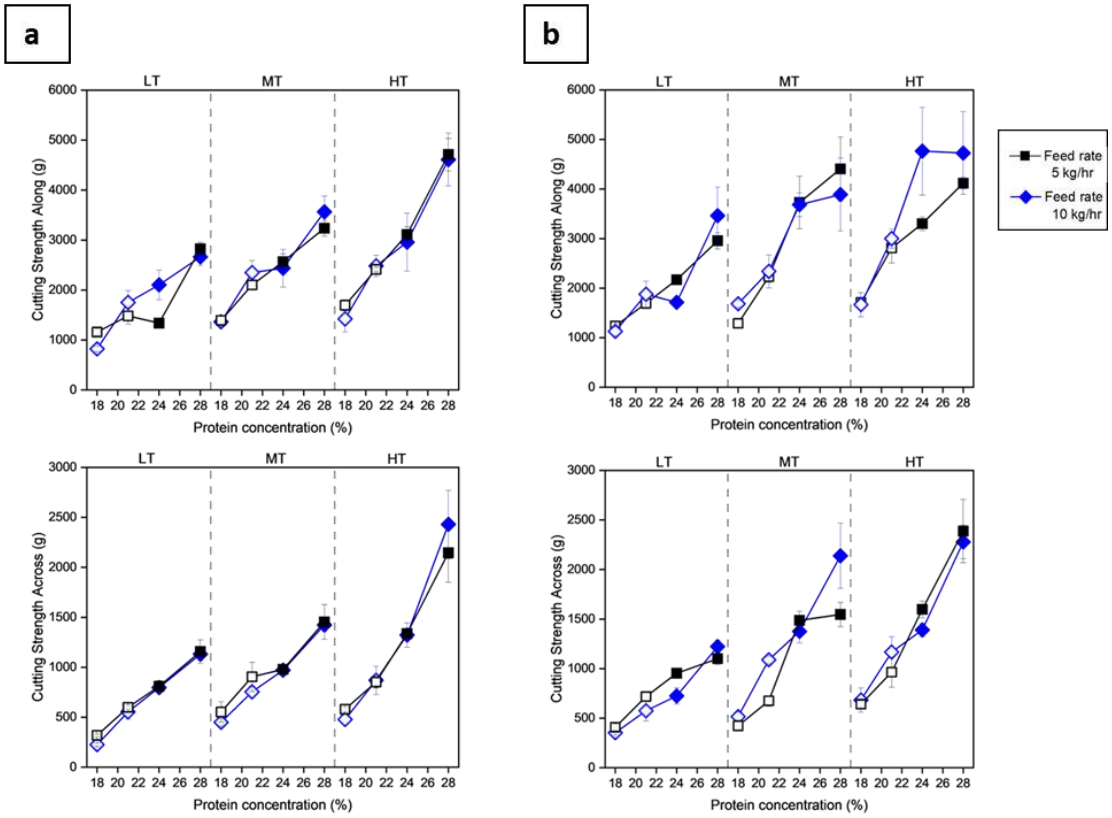

Figure 4.6 Effect of protein concentration and process variables on cutting strength along and across. a) At low shear (300 rpm), and b) At high shear (900 rpm).

It was observed that the low melt temperature extrudates showed a short anisotropic structure. On other hand, as the melt temperature increases, the anisotropic structure also increases, and a similar effect was seen with the decrease in the moisture content of feed material. The anisotropic index was positively impacted by moisture content

and negatively impacted by protein concentration with a significant difference of $p < 0.05$ as shown in Fig. 4.7. Similar type of results was found by Zhang et al. (2020). As barrel temperature increases, the anisotropic index decreases slightly with no significant difference ($p < 0.05$). Whereas, the screw speed and feed rate do not have significant impact on the anisotropic index and the trend was not consistent.

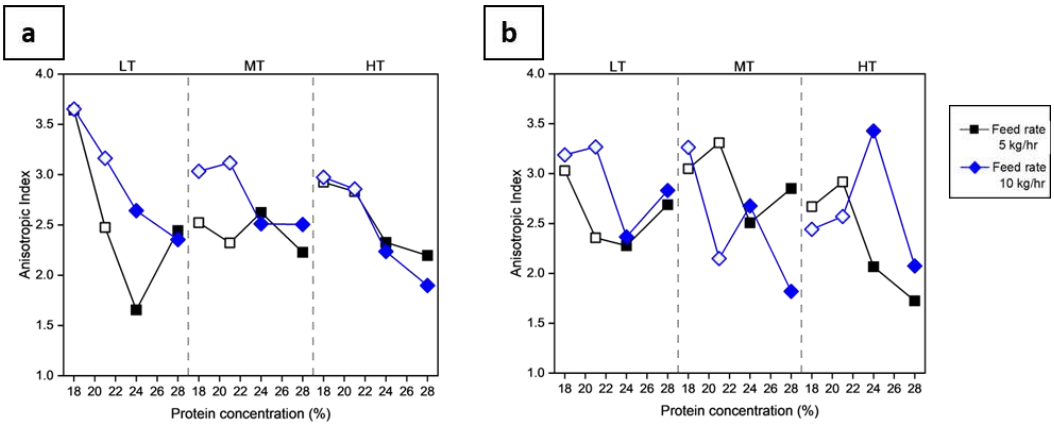

Figure 4.7 Effect of protein concentration and process variables on the anisotropic index. a) At low shear (300 rpm), and b) At high shear (900 rpm).

3.2.3 Colour value

The effect of protein concentration and process variables on colour values of HMMA were shown in Fig. 4.8. L* which represents the lightness/darkness of the sample is expected to correlate strongly with moisture, protein concentration, and barrel temperature. The combination of low moisture, high protein concentration, and high temperature will accelerate the Maillard reaction and caramelization process, which leads to deeper colour (Raigar et al., 2020; Yu et al., 2013). Our results show a positive significant impact ($p < 0.05$) with moisture content and a negative significant impact ($p < 0.05$) with protein concentration as expected, surprisingly barrel temperature had a very weak effect. This is very interesting as barrel temperature has a strong correlation with textural properties. It is therefore possible to change texture while minimally impacting colour. Screw speed and feed rates also have smaller impacts on L* and are other useful colour independent controls of texture. The decrease in L* value due to a higher feed rate is caused by the shorter residence time of the melt in the barrel, which leads to less heat exposure. As the water content in the barrel decreases and leads to higher protein concentration (fresh weight basis) which results in more heat exposure for proteins and makes the darker extrudates.

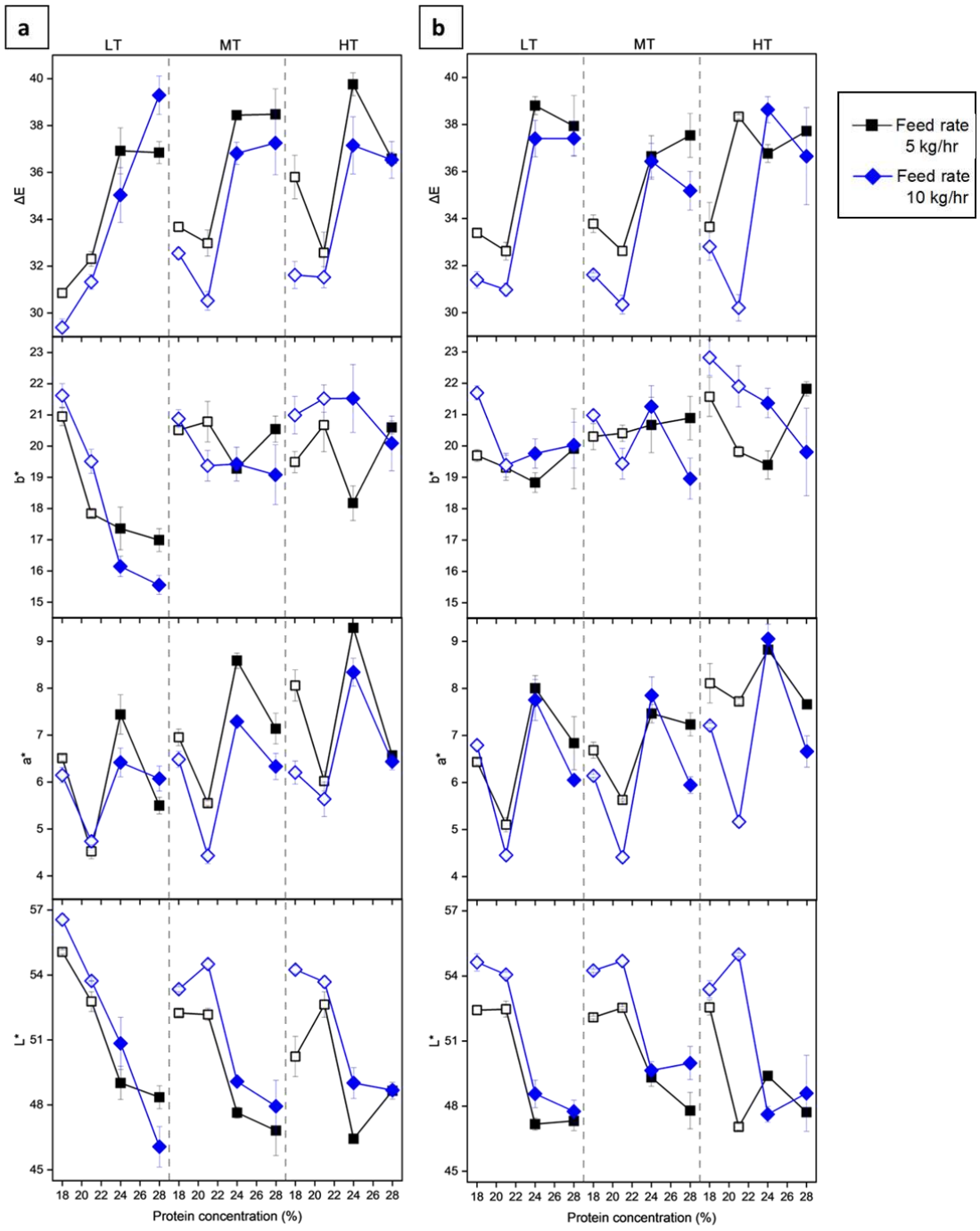

Figure 4.8 Effect of protein concentration and process variables on colour values of HMMA. Unfilled and filled symbols are 70% and 60% moisture content respectively, LT – low barrel temperature, MT – medium barrel temperature, and HT – high barrel temperature, a) At low shear (300 rpm) and b) At high shear (900 rpm).

Barrel temperature and moisture content were significantly ($p < 0.05$) impacted on a* values in positive and negative directions respectively. a* decreases with an increase in protein concentration at specific moisture levels. Screw speed does not show any impact on a* values. The feed rate showed a negative impact but not significantly different ($p < 0.05$). b* values showed a positive significant ($p < 0.05$) impact from moisture

content, barrel temperature and screw speed and negative significant ($p < 0.05$) impact from protein concentration. Feed rate at a protein concentration of 18%, 21%, and 24% made a positive influence on b* values but not a significant ($p < 0.05$) impact.

The total colour change ΔE was influenced significantly ($p < 0.05$) by moisture content and protein concentration. ΔE was decreased by an increase of protein concentration from 18% to 21% at 70% moisture content and 24% to 28% at 60% moisture content. Moisture content found to be the most impactful variable to ΔE.

4 Conclusion

We studied high moisture meat analogues made from soy protein blends for their ability to match the textures of whole meat from chicken, lamb, and beef. The experimental design covered a wide range of operating and system parameters. While all the selected independent parameters such as protein concentration of the blend, moisture content, barrel temperature, screw speed, and feed rate impacted the system and product properties, it was found that the moisture content, protein concentration, and barrel temperature had the most impact on system and product properties. The span of properties is higher at low moisture products than at high moisture. This suggests that greater control is required when extrusion is carried out at low moisture levels. Alternately, the process engineer should aim for the highest moisture products within given constraints as these are likely to be more forgiving from a product variability perspective.

The textures of real meat were mapped onto the textural space of high moisture meat analogues created in the experiments. While the hardness and chewiness parameters of the real meat were in the range of the HMMA's, the resilience, cohesiveness, and springiness values of the real meat fell out of range. These values were found to be lower for the real meats compared to the high moisture meat analogues. This textural gap needs to be addressed for whole meat analogues to mimic real meat cuts. It is unlikely that this gap can be minimised by only processing parameter space. Two areas to explore are die designs and novel raw material blends.

Chapter 5

Evaluating the potential of millets as blend components with soy protein isolate in a high moisture extrusion system for improved texture, structure, and colour properties of meat analogues

This chapter has been published as Mateen, A., & Singh, G. (2023). Evaluating the potential of millets as blend components with soy protein isolate in a high moisture extrusion system for improved texture, structure, and colour properties of meat analogues. Food Research International, 173. https://doi.org/10.1016/J.FOODRES.2023.113395

Abstract

This study explored the use of millets flours as a secondary ingredient with soy protein isolate (SPI) to develop fibrous high moisture meat analogue (HMMA). Three millets (sorghum, pearl millet, and finger millet) with three incorporation levels (10%, 20%, and 30%) were extruded at 60%, 65%, and 70% moisture content. The results showed that millet type, incorporation level, and moisture content significantly influenced the system parameters and textural properties. Good visual texturization was achieved at addition of pearl millet up to 30% incorporation level and sorghum and finger millet up to 20% incorporation level. Furthermore, the textural properties of HMMA made from SPI-millet blends were compared against HMMA made from SPI-gluten blend and real chicken. The HMMA made from SPI-millet flour had lower hardness, chewiness, resilience, springiness, tensile strength, cutting strength than that for SPI and SPI-wheat gluten blend and were much closer to corresponding values for real chicken. The results also showed that each of the three millet types generated distinctly different fibre patterns (thick to thin fibres) and colour (whiter to darker) of HMMA. Thus, HMMA produced from SPI-millet flour blends can offer a wide textural, fibre pattern and colour space for different plant-based meat applications. Since millets do not have gluten, they also offer an opportunity to make gluten-free HMMA's.

Keywords: Millets, High moisture meat analogue, HMMA, Texturization, High moisture extrusion, Gluten-free.

1 Introduction

Research and development efforts to texturize soy and other plant protein concentrates and isolates for obtaining animal meat like textures started in the early 1960's (Zhang et al., 2021). The smaller environmental footprint of soy and other plant proteins compared to animal proteins has given momentum to this research over the last decade and there is growing interest in developing plant-based meat analogues using these ingredients (Tilman & Clark, 2014; Wild et al., 2014). Many structured products made from texturized plant-based proteins have hit the market in recent years. These products deliver textural and sensory equivalency with structured products made from real meat and have developed a market base of environmentally conscious early adopters.

While use of plant-based protein for structured meat product analogues has been a success, creating whole meat analogues using plant proteins has been more challenging. High moisture extrusion using twin screw extruders is currently the most industrially prevalent technology for making plant protein-based whole meat analogues (Zahari et al., 2022). The technology involves extruding plant protein powders using a high L/D (length to diameter ratio) twin screw coupled with a high L/D cooling die to create meat like fibrous texture with a dense structure, strong springiness, and high moisture content (Kumar et al., 2016; Sha & Xiong, 2020). While the extrudates match the texture on some of the textural attributes, full spectrum matches i.e., a match on all parameters that include hardness, chewiness, resilience, cohesiveness, springiness and cutting strength are difficult to achieve. This may require novel blends as feed to the extruder (Mateen et al., 2023).

A review of the various blends studied in published literature over the last four decades was undertaken. Table 2.2 gives a summary of the composition of the blends. We have categorised the blend components as primary, secondary major, secondary minor, and tertiary ingredients based on their weightage in the blend. The primary ingredient in a blend is typically comprises of more than 50% of the blend, the secondary ingredient comprises less than 50% of the blend but greater than 10%, and the tertiary ingredients less than 10% of the blend.

The primary ingredient is the main contributor of protein to the blend. The role of the secondary ingredient is less defined, and it could be a second protein rich powder (e.g., wheat gluten and whey protein powder), a flour (wheat flour), a starch rich powder

(potato starch, corn starch). Tertiary ingredients such as pectin, fibers, enzymes, phosphates, fats, flavourings, salt are used in some cases for additional functionality.

The most commonly used primary ingredient in literature is soy protein isolate followed by pea protein isolate. The most commonly used secondary ingredient is wheat gluten. A number of flours starches and novel ingredients such as wheat flour, rice flour corn starch, oat fiber and algal powders have also been used as secondary blend components.

A few points emerge from these studies. First, not all plant proteins create fibrous structures under high moisture extrusion. Soy & pea proteins are the most amenable to the creation of fibrous structures through high moisture extrusion while other proteins such as rice and algal proteins do not form fibrous structures on their own (Kumar et al., 2022; Lee et al., 2022; Nasrollahzadeh et al., 2023; Palanisamy, Töpfl, et al., 2019). These texturizable protein powders are always the primary ingredient in the blends and comprise of >50% in the blend (Kumar et al., 2022).

Second, there is a minimum protein concentration required for creating good textures. No texture develops at low protein concentrations (typically below 50%) (Dekkers, Boom, et al., 2018; Vatansever et al., 2020). This is probably because the non-protein molecules prevent the protein molecules from aggregating and creating a network. It is likely that the high shear forces generated due to networked proteins during extrusion cooking creates anisotropic extension giving the fibrous appearance to the networks (Ferawati et al., 2021; Vatansever et al., 2020). The minimum concentration requirement for fibration is solved by using protein concentrate & isolate powders (Kumar et al., 2022). Most of the studies use isolates as the primary ingredients as this allows for better control of the blend protein & non-protein content.

On the other extreme, too high a protein concentration results in hardness and density that is beyond animal meat (Hager, 1984; Maurice & Stanley, 1978; McMindes et al., 2014). This requires addition of secondary ingredients that are low in protein and can dilute the protein concentration to bring it within a band where good fibration is achieved while overall the extrudate is not too hard or chewy. This partly explains the reason for addition of secondary ingredients such as starches or flours to the feed blends.

The secondary ingredient may also create a multiphasic melt, especially if the biomolecules it contributes are immiscible with those contributed by the primary ingredient. Tolstoguzov (1993) argued that the multiphasic melt that results from this

immiscibility is responsible for the fibrous structure in the extrudates. Dekkers et al. (2016) also arrive at a similar conclusion. Table 2.2 shows that wheat gluten is a popular choice as a secondary ingredient. It is rich in protein and does not offer any dilution of protein concentration in the blend. The textural contribution of wheat gluten maybe in the formation of a multiphasic melt.

In some studies, ingredients such as plant fiber, pectin and hydrocolloids have also been used (Chiang et al., 2019a; Dekkers et al., 2016; Schreuders et al., 2022; F. Wang et al., 2023)..The reasons for their inclusion are often not clear.. Since their incorporation level is low, they play a minimal role in modulating protein concentration. They may also be playing a role in providing an immiscible phase and contribute to improved fibrous structure. Since most of the tertiary ingredients have high water holding properties, they may also be contributing to juiciness of the extrudate.

Millets have not been studied for their effectiveness as secondary ingredients in high moisture extrusion. The world grew 91.45 billion kg in year 2021 of millets and around 87 billion kg is was accounted for by the three major millets - sorghum (*Sorghum bicolor*), pearl millet (*Pennisetum glaucum*), and finger millet (*Eleusine coracana*) (FAOSTAT, 2021; Garí, 2002). Though much of their production and consumption is restricted to a few geographies, lately there has been a growing interest globally on use of millets as a food from a climate and sustainability perspective. The United Nations has designated 2023 as the International Year of Millets to highlight their importance and promote their use beyond their traditional geographies, The reason for this interest is that compared to other cereals, millets are known to have a smaller environmental footprint (D. B. Rao et al., 2022; N. D. Rao et al., 2018; J. Wang et al., 2018). Being C4 plants, they are resilient to drought and can grow in arid conditions and thus are being actively being looked at for transforming drylands and providing livelihoods in water-stressed geographies (D. B. Rao et al., 2022; J. Wang et al., 2018). New food applications of millets may provide the demand that is needed to support such initiatives. Apart from the environmental benefits, millet flours also have good nutritional profile with carbohydrate of low glycaemic index, high quality protein, balanced amino acid profile, high minerals (calcium, iron, zinc) and dietary fibers compared to other cereal flours (Anitha et al., 2020; Hassan et al., 2021; Shobana et al., 2009). Millets are also gluten free. The rise of gluten sensitivity and gluten intolerance globally has led to many consumers seeking gluten-free food products (Singh et al.,

2018; Tiefenbacher, 2019). Millets offer an opportunity to develop gluten-free meat analogues and cater to this niche but growing consumer segment. Despite the various benefits of millets, there is not much literature reporting new product development using millets in meat analogue applications (Balakrishnan & Schneider, 2022). The use of millets as a blend component for making high moisture meat analogues is one such application. Therefore, this study addresses this gap and explores the potential of 3 major millets – sorghum, pearl millet & finger millet as secondary ingredients in blends used in extrusion for making HMMA.

2 Materials and methods

2.1 Raw materials and protein blend preparation

The raw materials used in this study were soy protein isolate (SPI) Solae SUPRO® 620 (DuPont shineway luohe food co., ltd., China) and wheat gluten (Guanxian xinrui industrial co., ltd., China). Three millets: sorghum (*Sorghum bicolor*) variety Maldandi, pearl millet (*Pennisetum glaucum*) variety Dhanshakti ICTP 8203, and finger millet (*Eleusine coracana*) variety Bharathi VR 762 were procured from the Indian Institute of Millet Research (IIMR), Hyderabad, India. Harvested and sun-dried millet grains with an initial moisture content of approximately 8% were used as the raw material for flour production. Prior to processing, the grains underwent a cleaning procedure to eliminate impurities and foreign matter. This cleaning step involved the use of a millet destoner cum aspirator (DGA S1500, Perfura Technologies Pvt. Ltd., Coimbatore, India), which effectively removed unwanted debris, ensuring grain purity. The cleaned millet grains were then milled to produce flour using a hammer mill equipped with a 500-micron size screen (Thatha Engineering Works, Thrissur, India). The resulting millet flour was packed in polyethylene bags and stored in a cool and dry place until further use. Preparation of protein blends for high moisture extrusion was done by mixing SPI and millet flour using a lab scale ribbon blender (SRM, Shakti Pharmatech Pvt. Ltd., Ahmedabad, India). The three millets were individually blended with SPI at 10%, 20%, and 30% levels. Thus, there were a total of nine blends.

For comparing the texture profile of HMMA with real meat, chicken breast was locally procured 3 hour post-mortem near the university and kept at 0 ºC to 3 ºC during transport. The chicken breast was split into half measuring around 6 – 7 inches in length and 3.5 – 4 inches in width. The average weight of the fillets was 200.94 ± 10.93 g.

The cooking process was performed according to the method described by Zhuang & Savage (2008) with slight modification. The fillets were cooked in a combi oven (CombiMaster Plus CMP 61, Rational AG, Landsberg am Lech, Germany) with 50% humidity at three different internal (70, 75 and 80 °C) and external (80, 100 and 120 °C) temperatures. Therefore, there were a total of nine cooked chicken samples. The cooked meat was cut into 20 x 20 mm cubes and a height of 10 mm (similar to the dimension of HMMA samples). Texture analysis was done as described in section 2.6.

All the chemicals and reagents were procured from Sigma-Aldrich Chemicals Pvt. Ltd., Bengaluru, India.

2.2 Characterisation of raw materials

2.2.1 Particle size distribution and bulk density

Particle size was analyzed using a sieving technique following the standard AACC method 66-20.01 (AACC, 1999). The sieving apparatus consisted of an electromagnetic sieve shaker (EMS-8, Electrolab India Pvt. Ltd., Mumbai, India) with six stacked sieves, each with progressively smaller mesh openings. The mesh sizes of the sieves used were as follows: 600 µm, 425 µm, 212 µm, 106 µm, 75 µm, and 53 µm. A starting sample weight of 150 g was utilized, and the sieves were shaken for a duration of 10 minutes. Subsequently, the various powder fractions were collected and weighed, and the percentage of material retained on each sieve was calculated.

For bulk density, 50 g of powder sample was placed in a 100 ml measuring cylinder. The cylinder was gently tapped on a laboratory bench multiple times to achieve a consistent volume. The bulk density was determined by dividing the weight of the sample by its corresponding volume and expressed the values in kg/m^3 (S. Huang et al., 2019). All the samples were analysed in triplicates.

2.2.2 Proximate composition

Moisture content of samples was determined by using moisture analyser (MA 50.R, Radwag, Radom, Poland) following ISO 712:2009 method (ISO, 2009). The total protein content (nitrogen × 6.25), lipid content and ash content of proteins, millet flours and protein-millet blends were determined by using standard methods and expressed on a dry basis (AOAC, 1990). The ash content was estimated gravimetrically by burning the samples at 550 °C in a muffle furnace. The starch content was analysed by

using standard method IS 4706 P(2):1978 (BIS, 1978). The total, soluble and insoluble dietary fibers were analysed by enzymatic-gravimetric method AOAC 991.43 (AOAC, 2005). All the samples were analysed in triplicates.

2.2.3 Amino acid analysis and evaluation of composition

Amino acid composition was estimated using an Agilent 1260 Series HPLC (Agilent Technologies, Waldbronn, Germany) with a diode array detector, following Agilent method (Mengerink et al., 2002). The system is equipped with Agilent AdvanceBio AAA 4.6 × 100 mm column placed in a thermostatted column compartment and maintained a temperature of 40 °C. The sample preparation was done according to the method described by Osen et al. (2015).The samples were subjected to 24-hour hydrolysis at 110 °C using 6 M HCl, and results in protein hydrolysates. Separation and quantification of amino acids was conducted as pre-column derivatization with FMOC (Flourenylmethoxycarbonyl) chloride for primary amino acids and OPA (o-phthaldialdehyde) for proline. Standard amino acid mix (0.5 µmol/ml for individual amino acid) was used for calibration. Mobile phase A was 40 mM NaH_2PO_4 (pH 7.8) while mobile phase B was acetonitrile: methanol: water (45:45:10 v/v). A 2.5 µl was injected and the separation was obtained at a flow rate of 2 ml/min with a gradient that allowed for 1.9 min at 0% B followed by a 16.3 min step that raised eluent B to 53%. Then washing at 100 % B and equilibration at 0 % B was performed in a total analysis time of 26 min. Three repeat measurements were done for each sample.

The quantities of various amino acids retrieved were expressed in mg/g protein and compared against the FAO/WHO (2013) reference pattern of essential amino acids for Older child, Adolescent, Adult (FAO/WHO, 2013). The ratio of essential amino acids to the total amino acids was presented as E/T (%). The method used to calculate the amino acid score (AAS) followed the guidelines provided by FAO/WHO (eq. 5.1):

$$AAS = \frac{mg\ of\ AA\ in\ 1\ g\ of\ test\ protein}{mg\ of\ AA\ in\ 1\ g\ of FAO/WHO\ reference\ pattren} \times 100 \qquad (5.1)$$

2.2.4 Water absorption capacity (WAC) and water solubility (WS)

This analysis was performed using the method described by Ogunwolu et al. (2009). 1 g of the raw material powder sample was mixed with 10 g of distilled water using a

stirrer. The suspension was then centrifuged at 1800 × g for 20 min at 22 °C (C-24plus, Remi Electrotechnik Ltd., Vasai, India). After centrifuge, the wet pellet was weight to calculate WAC by dividing the wet pellet weight by the sample weight. The supernatant was dried overnight to calculate the WS by dividing the weight of soluble solids after drying by the sample weight.

2.2.5 Pasting properties

The pasting property of proteins, millets and millet blends as a function of temperature was evaluated utilizing a viscosity analyser (ViscoQuick, Brabender GmbH & CO. KG, Germany) following the AACC Method 76-21 STD 2 with slight modification (AACC, 1997; Osen et al., 2014). A homogeneous slurry from the samples was prepared with 8 g solids and 72 g distilled water. The temperature was gradually increased from 30 °C to 93 °C at a heating rate of 7.5 °C per min. It was then maintained at 93 °C for 5 min before being cooled down to 50 °C at a cooling rate of 7.5 °C per min. The final temperature of 50 °C was held for 1 min. The instrument measures the viscosity in torque (BU – Brabender Unit) and logs data every second. To ensure accuracy, duplicate measurements were conducted for each sample and results were expressed as mean values.

2.3 High moisture extrusion

High moisture extrusion processing was done on a pilot-scale twin-screw extruder (TwinLab-F 20/40, Brabender GmbH & CO. KG, Duisburg, Germany) with a screw diameter of 20 mm and length of 800 (L/D ratio of 40:1). The barrel of the extruder was clamp shell type with four heating zone (HZ1 to HZ4) powered by electrical heaters and water circulation in each zone for maintaining the set temperatures through a solenoid valve supported by a water temperature regulating cum circulator system (WTD 6es, Weinreich Industriekühlung GmbH, Lüdenscheid, Germany). The screw configuration consists of broad pitch conveying elements (SK-40/40A, SK-N-40/20R, and SE-30/30R), narrow pitch elements (SE-20/20R), mixing element (Z-8/3/20H-V), and shear or kneading elements (KBW-45/5/30R and KBW-45/5/20R) as shown in Table 5.1. A single screw vertical volumetric feeder was used to feed the dry powder in the barrel at the 0 D position and water feed was at the 10 D position with a peristaltic pump (Watson-Marlow 120U/DV, Watson-Marlow Ltd., United Kingdom). Both the volumetric feeder and peristaltic pump were calibrated for each protein blend before

the extrusion trial. The moisture content was adjusted by altering the motor RPM of the volumetric feeder and peristaltic pump, based on the calibration data. This adjustment results in a variable amount of powder and water feed, while still maintaining a constant throughput. A long cooling die, measuring 300 mm in length, 20 mm in width, and 9 mm in height, was attached to a cooling water circulator (Corio CD-600F, Julabo GmbH, Germany), set to maintain an inlet water temperature of 30 ºC in the cooling die with a water flow rate of 6.9 kg/hr. The schematic representation of the extruder setup and cooling die was shown in Fig. 5.1. The extrusion trials were conducted at a constant barrel temperature profile of 40, 80, 110, and 130 ºC (from HZ1 to HZ4), a screw speed of 600 rpm, and a feed rate of 4 kg/hr. From our previous experimentation and literature, it was found that moisture content is the most influential process parameter than others (Lin et al., 2002; Mateen et al., 2023). Therefore, in this study we have chosen three moistures levels 60%, 65%, and 70% at 130 °C (at HZ4) barrel temperature.

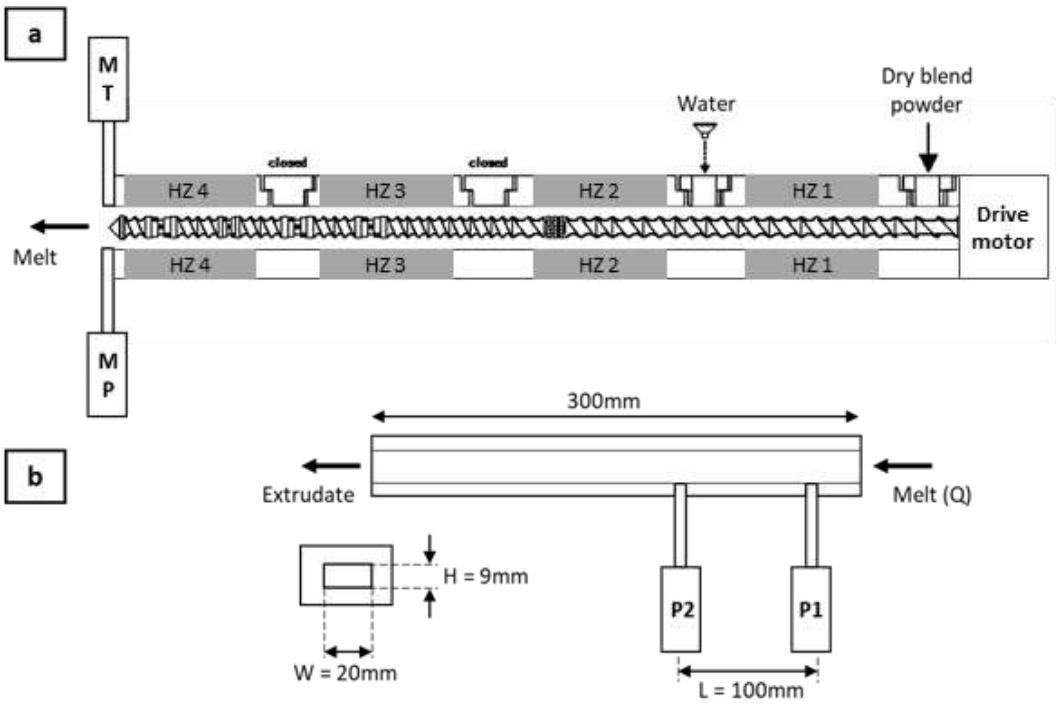

Figure 5.1 a) Extruder setup for feeding, heating zones (HZ1 to HZ4) and measuring sensors for melt temperature (MT) and melt pressure (MP), and b) cooling die (on-line rheometer) for high moisture extrusion.

Table 5.1 Description of screw configuration used in this study with L/D ratios and screw element properties during high moisture extrusion.

Extruder zones	Element name*	No. of elements	L/D of each element	Total L/D of sections	% L/D ratio
Feeding zone	SK-40/40A **(Powder feed)**	1	2	17.25	43.12
	SK-N-40/20R	1	1		
	SE-30/30R	9	1.5		
	SE-30/30R		1.5		
	SE-30/30R		1.5		
	SE-30/30R		1.5		
	SE-30/30R		1.5		
	SE-30/30R		1.5		
	SE-30/30R **(Water feed)**		1.5		
	SE-30/30R		1.5		
	SE-30/30R		1.5		
	SE-30/15R	1	0.75		
Mixing zone	SE-30/30R	1	1.5	4	10
	Z-8/3/20H-V	1	1		
	SE-30/30R	1	1.5		
Melting zone	SE-20/20R	6	1	6	15
	SE-20/20R		1		
	SE-20/20R		1		
	SE-20/20R		1		
	SE-20/20R		1		
	SE-20/20R		1		
Melting and shearing zone	KBW-45/5/30	1	1.5	12.75	31.87
	SE-20/20R	2	1		
	SE-20/20R		1		
	KBW-45/5/30	1	1.5		
	SE-20/20R	2	1		
	SE-20/20R		1		
	KBW-45/5/20	1	1		
	SE-20/20R	2	1		
	SE-20/20R		1		
	KBW-45/5/30	1	1.5		
	SE-20/20R	1	1		
	Screw tip	1	0.25		
	Total	33	40	40	100

*Conveying elements - SK, SK-N and SE. Mixing elements – Z. Shearing elements – KBW.

Colour measurement and macroscopic images of the extrudates were taken after they cooled to room temperature. Then the extrudate samples were kept in the refrigerator (4 ºC) and texture analysis was done on the next day of extrusion.

Table 5.2 Experimental design for 3 millets (as secondary ingredient) with 3 incorporation levels, and 3 feed moisture content.

Run No.	Millet	Incorporation level (%)	Moisture content (%)
1	Sorghum	10	60
2			65
3			70
4		20	60
5			65
6			70
7		30	60
8			65
9			70
10	Pearl millet	10	60
11			65
12			70
13		20	60
14			65
15			70
16		30	60
17			65
18			70
19	Finger millet	10	60
20			65
21			70
22		20	60
23			65
24			70
25		30	60
26			65
27			70

2.4 Experimental design

A 3×3×3 factorial design was used in this study which consists of 3 different millets with 3 different levels of incorporations which were extruded at 3 different feed moisture content as shown in Table 5.2. Therefore, the total number of runs will be 27.

2.5 System parameters

The temperature thermocouple and pressure transducer were installed on-line at the end tip of the extruder screw to record the data of melt temperature (MT/ ºC) and melt pressure (MP/ bar). Load on the extruder motor in percentage was recorded to calculate specific mechanical energy (SME) using eq. (5.2) (Fang et al., 2014; Godavarti & Karwe, 1997; Osen et al., 2014). All the data of extruder response/ system parameters were recorded with a resolution of 0.1 through a user interface computer software MetaBridge (Brabender GmbH & CO. KG, Duisburg, Germany).

$$SME\ \left(\frac{kJ}{kg}\right) = \frac{2\pi\ x\ n\ x\ T}{MFR} \tag{5.2}$$

Where n is screw speed (rpm), T is the actual motor torque (Nm: the non-load torque was subtracted from the recorded torque values) and MFR is the mass flow rate of material (g/min). On attaining the steady state of the extrusion process, the extrudate samples of about 500 g were taken for further analysis.

For measuring the on-line viscosity of the melt, a cooling die which was mounted at the extruder outlet was used as a rheometer (Fig. 5.1b) for measuring the apparent viscosity of melt. It consists of a single rectangular flow channel (dimensions given in section 2.4.) where height H is comparable to the width W, in this case the pressure drop from the edges cannot be neglected. So, we have used a method described by Son (2007) to calculate wall shear stress τ_w (Pa), and the apparent shear rate $\dot{\gamma}_a$ (s^{-1}) using eq. (5.3) and eq. (5.4) respectively.

$$Shear\ stress\ \tau_w = \left(\frac{\Delta P\ H}{2L}\right)\left(\frac{1}{H/W + 1}\right) \tag{5.3}$$

$$Shear\ rate\ \dot{\gamma}_a = \left(\frac{6\ Q}{W\ H^2}\right)\left(1 + \frac{H}{W}\right) f^*\left(\frac{H}{W}\right) \tag{5.4}$$

Where ΔP (Pa) is the pressure difference measured across the length L (cm) in the die rheometer. H and W are the cross sectional dimensions of height and width (cm) respectively as shown in Fig. 5.1b. Q is the volumetric flow rate of melt (cm^3s^{-1}). $f^*(x)$ is a function given as follows

$$f^*(x) = \left[\left(1+\frac{1}{x}\right)^2\left(1-\frac{192}{\pi^5 x}\sum_{i=1,3,5}^{\infty}\frac{tanh\left(\frac{\pi}{2}ix\right)}{i^5}\right)\right]^{-1} \quad (5.5)$$

Therefore, the on-line apparent viscosity η (Pa s) of a rectangular die is

$$Apparent\ viscosity\ \eta = \frac{\tau_w}{\dot{\gamma}_a} \quad (5.6)$$

2.6 Texture profile analysis (TPA)

The textural properties of extruded samples were analyzed by using a CTX Texture Analyser (Ametek Brookfield Inc, USA) as described by Fang et al. (2014); J. Zhang et al. (2020). Extrudate samples were prepared by cutting into 20 x 20 mm cubes. Hardness, chewiness, resilience, cohesiveness, and springiness were measured as described by (Breene, 1975) using a TA3/100 AOAC standard cylindrical probe of 25.4 mm diameter with a 100 kg load cell. Measurement methods were set at 50% sample/target deformation with a 1 mm/s probe travel speed. TPA analysis was done at least ten times per sample.

2.7 Cutting strength

The cutting strength was done along and across the flow direction of extrudates by using a TA7 knife probe with a TA-CKA craft knife adapter and the setting was at 1 mm s^{-1} probe travel speed with 75% cutting of the sample's original size. The cutting strength test was done by cutting samples along and across the flow direction of extrudate to determine the anisotropic index by eq. (5.7) (Chen et al., 2010; Zhang et al., 2020; Mateen et al., 2023). The measurements for cutting strength along and across were taken at least ten times per sample.

$$Anisotropic\ Index\ (AI) = \frac{Cutting\ strength\ along}{Cutting\ strength\ across} \quad (5.7)$$

2.8 Tensile strength

Tensile strength of the extrudates of size 150 mm in length and 20 mm in width was cut and pulled using a TA-DGF001 (dual grip fixture with 25 mm wide grips fitted with rubber inserts to maximize contact adhesion with sample) as described by Noguchi, (1989); Zhang et al. (2016). The measurement procedure was set at a speed of 0.5 mm s^{-1} until the extrudate was broken, and the peak tensile resistant force was recorded. All the samples were measured at least ten times.

2.9 Colour value and macroscopic images

The colour values of raw material, blends, and extrudate samples were measured by using a colorimeter (CR-400 chroma meter, Konica Minolta Sensing Inc., Japan). Colour was recorded according to the CIE-lab L*, a*, b* scale. L* represents brightness or lightness from 0 to 100 (black to white), a* represents green to red (positive or negative) and b* represents blue to yellow (negative or positive) (Benković et al., 2015). The total colour difference (ΔE) of the extrudates was calculated by using the following equation eq. (5.8) (Fang et al., 2014). At least five measurements were taken for each sample at randomly chosen locations. The macroscopic images of the extruded samples were acquired by a high-resolution digital camera (Nikon D70, Nikon Co. Ltd., Thailand) in a photo box with black walls and two LED light strips illuminating at the sample.

$$\Delta E = \sqrt{(L^*_{sample} - L^*_{std})^2 + (a^*_{sample} - a^*_{std})^2 + (b^*_{sample} - b^*_{std})^2} \quad (5.8)$$

Where, L^*_{sample}, a^*_{sample}, b^*_{sample} and L^*_{std}, a^*_{std}, b^*_{std} are colour values of extrudates and raw material/protein blend respectively.

2.10 Statistics

All the data were expressed as mean ± standard deviation (SD). One-way ANOVA and pearson correlation coefficients (r) between the raw material/protein blends, moisture content, system response parameters and extrudate properties were performed with Tukey test and 2-tailed test of significance respectively, using a OringinPro software version 2022 (OriginLab Corporation, Northampton, MA, USA). Statistical significance was set at a 0.05 probability level.

3 Results & Discussion

3.1 Raw material characterization

3.1.1 Particle size distribution and bulk density

The particle size distribution and bulk densities of proteins and millet flours are reported in Table 5.3 and Table 5.4. As expected, the millet flours are coarser than the wheat gluten and soy protein isolate. While more than 80% by weight of the millet flours were >106 µm in size, the SPI and wheat gluten had less than 40% by weight >106 µm in size. Soy protein isolate exhibited the lowest bulk density (323.75 ± 16.89 kg/m^3). Both sorghum and pearl millet flour showed similar densities, measuring 495.49 ± 38.88 kg/m^3 and 491.33 ± 28.95 kg/m^3, respectively. Wheat gluten and finger millet flour had the highest densities, 551.48 ± 20.61 kg/m^3 and 577.40 ± 20.14 kg/m^3, respectively.

Table 5.3 Particle size distribution of proteins powder and millet flours.

Sieve size (µm)	Soy protein isolate		Wheat gluten		Sorghum flour		Pearl millet flour		Finger millet flour	
	g	%	g	%	g	%	g	%	g	%
600 > x > 425	2.25 ± 0.61^b	1.51	1.05 ± 0.10^b	0.70	86.63 ± 9.13^a	58.06	78.77 ± 9.28^a	52.54	4.30 ± 2.46^b	2.88
425 > x > 212	7.50 ± 1.80^c	5.02	1.95 ± 0.26^c	1.30	55.80 ± 3.49^a	37.40	64.43 ± 5.51^a	42.97	39.27 ± 6.28^b	26.29
212 > x > 106	34.20 ± 6.12^c	22.90	57.75 ± 9.23^b	38.63	6.60 ± 5.81^d	4.42	6.53 ± 3.16^d	4.36	81.60 ± 4.08^a	54.62
106 > x > 75	75.30 ± 10.16^a	50.42	72.45 ± 8.19^a	48.46	0.17 ± 0.12^b	0.11	0.20 ± 0.17^b	0.13	22.60 ± 1.22^b	15.13
75 > x > 53	28.20 ± 4.21^a	18.88	15.26 ± 5.02^b	10.21	0.00 ± 0.00^c	0.00	0.00 ± 0.00^c	0.00	1.63 ± 1.33^c	1.09
53 > x > 0	1.90 ± 0.13^a	1.27	1.04 ± 0.11^b	0.70	0.00 ± 0.00^c	0.00	0.00 ± 0.00^c	0.00	0.00 ± 0.00^c	0.00
Amount of sieved powder	149.35 ± 3.80	100	149.50 ± 3.81	100	149.20 ± 0.36	100	149.93 ± 1.21	100	149.40 ± 1.25	100

Values followed by different letters within each parameter show statistically significant differences ($p \leq 0.05$).

3.1.2 Proximate composition

Table 5.4 Proximate composition and physical properties of protein powders and millet flours.

Parameters	Soy protein isolate	Wheat Gluten	Sorghum	Pearl millet	Finger millet
Moisture content (% wb)	6.84 ± 0.22^{d}	7.89 ± 0.18^{c}	7.50 ± 0.09^{c}	8.49 ± 0.38^{b}	9.19 ± 0.07^{a}
Protein concentration (% db)	96.10 ± 0.66^{a}	82.76 ± 0.91^{b}	9.70 ± 0.34^{d}	12.31 ± 0.17^{c}	8.68 ± 0.16^{d}
Lipid (% db)	0.16 ± 0.08^{e}	0.86 ± 0.09^{d}	3.36 ± 0.28^{b}	5.38 ± 0.14^{a}	1.51 ± 0.09^{c}
Starch (% db)	0.17 ± 0.01^{d}	13.47 ± 0.71^{c}	68.03 ± 0.92^{a}	61.47 ± 1.01^{b}	66.30 ± 0.87^{a}
Total dietary fiber (% db)	0.77 ± 0.05^{b}	0.90 ± 0.07^{b}	10.63 ± 0.52^{a}	12.33 ± 0.86^{a}	12.14 ± 1.04^{a}
Soluble dietary fiber (% db)	0.19 ± 0.02^{b}	0.31 ± 0.02^{b}	1.66 ± 0.32^{a}	2.43 ± 0.26^{a}	1.76 ± 0.50^{a}
Insoluble dietary fiber (% db)	0.58 ± 0.04^{b}	0.59 ± 0.05^{b}	8.86 ± 0.65^{a}	9.90 ± 0.70^{a}	10.37 ± 0.83^{a}
Ash (% db)	3.52 ± 0.57^{a}	0.93 ± 0.12^{c}	1.51 ± 0.02^{c}	1.58 ± 0.26^{c}	2.38 ± 0.12^{b}
Bulk density (kg/m^{3})	323.75 ± 16.89^{c}	551.48 ± 20.61^{ab}	495.49 ± 38.88^{b}	491.33 ± 28.95^{b}	577.40 ± 20.14^{a}
Pericarp colour of millets					
L*	-	-	65.89 ± 1.29^{a}	57.74 ± 0.89^{b}	26.91 ± 0.33^{c}
a*	-	-	5.26 ± 0.16^{b}	2.82 ± 0.36^{c}	16.27 ± 0.79^{a}
b*	-	-	24.20 ± 1.05^{a}	19.81 ± 0.18^{b}	10.94 ± 0.49^{c}

wb – wet basis; db – dry basis. Values followed by different letters within each parameter show statistically significant differences ($p \leq 0.05$).

The proximate composition of soy protein isolate, wheat gluten, and millet flours is presented in Table 5.4. While the lipid content of soy and gluten proteins was less than 1%, millet flours contained higher levels. Among the millet flours, pearl millet showed the highest quantity of lipids (5.38 ± 0.14). Similarly, in terms of starch, soy protein isolate contained a negligible amount, while wheat gluten had 13.47 ± 0.71%. Among the millet flours, the starch content was highest in sorghum, followed by finger millet and pearl millet. Pearl millet exhibited the highest total dietary fiber content (12.33 ± 0.86%) among the millet flours. Additionally, pearl millet had the highest levels of

soluble dietary fibers (2.43 ± 0.26%), while finger millet had the highest levels of insoluble dietary fibers (10.37 ± 0.83%). In terms of mineral/ash content, SPI had the highest concentration (3.52 ± 0.57%), while wheat gluten had the lowest (0.93 ± 0.12%). The millet flours contained mineral content in the range of 1.51% to 2.38%.

The total protein content of SPI and wheat gluten was 96.10 ± 0.66 % and 82.76 ± 0.91 % on dry basis respectively. The protein content of the three millet flours (ranged from 8.68 to 12.31 %) were in line with the range of values reported in literature (Hassan et al., 2021; Sheethal et al., 2022). As a result, the soy-millet blends and HMMA exhibited a decrease in protein content as the proportion of millet incorporation increased from 10% to 30% (Table 5.5). The 30% gluten blend had the highest protein content across various moisture levels because gluten contains a higher level of protein (82.76 % db). However, the protein content of the HMMA produced from millet blends in this study fall within the range of real meat protein content (Ahmad et al., 2018; Wood, 2017). Therefore, these blends could be utilized as whole meat cuts or in minced applications to achieve finished products with meat-like protein content as well as higher amino acid scores (Table 5.7).

Table 5.5 Protein concentration of protein-millet blends over different blends and feed moisture content.

	Gluten blend	**Sorghum blends**			**Pearl millet blends**			**Finger millet blends**		
	30%	10%	20%	30%	10%	20%	30%	10%	20%	30%
Raw material blends*	85.26 ± 0.61	81.47 ± 0.27	73.42 ± 0.10	65.36 ± 0.41	81.70 ± 0.13	73.87 ± 0.08	66.05 ± 0.52	81.36 ± 0.63	73.19 ± 0.03	65.03 ± 0.73
Feed moisture in extrusion**										
60%	36.93	32.59	29.37	26.14	32.68	29.55	26.42	32.54	29.28	26.01
65%	32.31	28.51	25.7	22.88	28.6	25.85	23.12	28.48	25.62	22.76
70%	27.70	24.44	22.03	19.61	24.51	22.16	19.82	24.41	21.96	19.51

*Values expressed in dry weight basis. **The protein concentration in the extruder barrel was based on simple mathematical calculation and values expressed in wet weight basis.

3.1.3 Amino acid composition

The amino acid composition of raw materials proteins, millet flours and 30% incorporation in the soy protein isolate were shown in Table 5.6. The amino acid profile

of the individual ingredients (SPI, wheat gluten and millet flours) and the blends were compared by using three methods – FAO/WHO reference pattern, amino acid scores (AAS) and essential to total amino acids ratios.

Soy protein isolate exceeds FAO/WHO reference pattern for all amino acids except methionine (19.10 ± 0.22 mg/g vs 23 mg/g protein in reference pattern). Gluten protein falls short on lysine (28.39 ± 0.82 mg/g) and methionine (18.67 ± 0.51 mg/g protein) as compared to reference pattern. All three millet substantially exceed the FAO/WHO reference pattern for methionine (34.93 to 54.15 mg/g protein as compared to 23 mg/g protein of reference pattern) and match most other essential amino acids except lysine. While all three millets flours fall short on lysine, sorghum and pearl millet also fall short in tryptophan (4.12 and 4.06 mg/g protein respectively, as compared to 6.60 mg/g protein of reference pattern). SPI-gluten blend exceeds all the essential amino acids except for methionine (18.97 mg/g protein). However, SPI-millet blends (30% incorporation), also exceeds all essential amino acids without any short fall compared to reference pattern of FAO/WHO. The methionine content was highest in 30% finger millet blend (29.62 mg/g protein) followed by sorghum (23.89 mg/g) and pearl millet (23.85 mg/g).

From these results, it was found that the millet proteins were compensating for the methionine content in the blend and showed better essential amino acid profile compared to the other protein and bends reported in the literature. For example, yellow pea protein (15.80 mg/g), rapeseed protein (20.00 mg/g) or its 50:50 blend (17.90 mg/g) (Zahari et al., 2021), hempseed protein (13.90 mg/g), flaxseed protein (13.10 mg/g) (Tan et al., 2011). Similar conclusions can also be made from an analysis based on amino acid scores (AAS) (Table 5.7). The millets were also found to have high levels of non-essential amino acids and are in accordance with the literature (Anitha et al., 2020). The essential to total amino acids (E/T) ratios of millets (44.68 % for sorghum, 45.49 % for pearl millet and 50.52 % for finger millet) and SPI-millet blends were higher (44.20 % to 45.95 %) than that of the SPI (43.98 %), gluten (34.27 %) and SPI-gluten blend (41.21 %).

Table 5.6 Amino acid composition of proteins, millet flours and their blends at 30% incorporation level with SPI (mg of amino acid/g protein) and FAO/WHO suggested requirements (Older child, Adolescent, Adult) of essential amino acids.

Amino acids	Soy protein Isolate	Wheat gluten	30% Wheat gluten***	Sorghum flour	30 % Sorghum ***	Pearl Millet Flour	30% Pearl Millet***	Finger Millet flour	30% Finger Millet***	Reference pattern**
Aspartic acid	115.51 ± 1.82^{a}	40.26 ± 0.39^{d}	92.93	79.38 ± 1.62^{b}	104.67	82.05 ± 1.33^{b}	105.47	66.82 ± 0.44^{c}	100.90	
Glutamic Acid	189.78 ± 2.49^{c}	317.34 ± 4.61^{a}	228.04	204.12 ± 3.07^{b}	194.08	182.78 ± 2.89^{c}	187.68	207.37 ± 4.17^{b}	195.05	
Serine	51.91 ± 0.11^{a}	39.04 ± 0.52^{d}	48.05	45.36 ± 0.71^{c}	49.95	44.68 ± 0.64^{c}	49.74	47.24 ± 0.55^{b}	50.51	
Histidine*	33.93 ± 0.39^{d}	18.13 ± 0.82^{e}	29.19	46.39 ± 0.52^{b}	37.67	43.87 ± 0.47^{c}	36.91	80.65 ± 1.35^{a}	47.95	16.00
Glycine	41.46 ± 0.62^{a}	38.22 ± 1.10^{b}	40.49	26.80 ± 0.16^{cd}	37.06	25.18 ± 0.11^{d}	36.58	27.65 ± 0.88^{c}	37.32	
Threonine*	37.75 ± 0.95^{b}	26.17 ± 0.99^{c}	34.28	42.27 ± 0.84^{a}	39.11	43.05 ± 0.21^{a}	39.34	43.78 ± 0.47^{a}	39.56	25.00
Arginine	72.81 ± 1.01^{a}	47.33 ± 0.28^{c}	65.17	53.61 ± 0.93^{b}	67.05	54.43 ± 0.72^{b}	67.29	53.00 ± 0.84^{b}	66.86	
Alanine	34.94 ± 0.74^{d}	31.92 ± 0.35^{e}	34.04	86.60 ± 1.42^{a}	50.44	73.11 ± 0.37^{b}	46.39	57.60 ± 0.43^{c}	41.74	
Tyrosine	38.43 ± 0.89^{a}	24.51 ± 0.75^{d}	34.25	39.18 ± 0.95^{a}	38.65	31.68 ± 0.56^{c}	36.40	35.71 ± 0.27^{b}	37.61	
Valine*	49.33 ± 0.76^{c}	43.97 ± 0.80^{d}	47.72	62.89 ± 1.41^{b}	53.39	62.55 ± 0.85^{b}	53.29	71.43 ± 0.99^{a}	55.96	40.00
Methionine*	19.10 ± 0.22^{c}	18.67 ± 0.51^{c}	18.97	35.05 ± 0.53^{b}	23.89	34.93 ± 0.74^{b}	23.85	54.15 ± 0.42^{a}	29.62	
Tryptophan*	11.01 ± 0.47^{b}	13.81 ± 0.68^{a}	11.85	4.12 ± 0.02^{d}	8.94	4.06 ± 0.09^{d}	8.93	8.06 ± 0.15^{c}	10.13	6.60
Phenylalanine*	50.90 ± 0.66^{a}	44.56 ± 0.38^{c}	49.00	51.55 ± 0.16^{a}	51.09	48.74 ± 0.58^{b}	50.25	50.69 ± 0.98^{a}	50.84	
Isoleucine*	50.56 ± 0.49^{a}	30.76 ± 0.59^{d}	44.62	44.33 ± 0.86^{c}	48.69	43.87 ± 0.37^{c}	48.55	48.39 ± 0.38^{b}	49.91	30.00
Leucine*	83.03 ± 1.20^{c}	68.49 ± 1.35^{d}	78.67	121.65 ± 2.27^{a}	94.62	90.17 ± 1.83^{b}	85.17	91.01 ± 1.74^{b}	85.43	61.00
Lysine*	63.15 ± 0.32^{a}	28.39 ± 0.82^{b}	52.72	24.74 ± 0.53^{c}	51.62	27.62 ± 0.33^{b}	52.49	23.04 ± 0.16^{d}	51.11	48.00
Proline	50.45 ± 0.37^{d}	94.82 ± 1.95^{a}	63.76	88.66 ± 1.38^{b}	61.91	53.61 ± 0.33^{c}	51.40	35.71 ± 0.85^{e}	46.03	
SAA (Met+Cys)	19.10	18.67	18.97	35.05	23.89	34.93	23.85	54.15	29.62	23.00
AAA (Phe+Tyr)	89.33	69.07	83.25	90.72	89.74	80.42	86.65	86.41	88.45	41.00
EAA	437.19	317.46	401.27	472.16	447.68	430.54	435.20	506.91	458.11	290.60
E/T (%)	43.98	34.27	41.21	44.68	44.20	45.49	44.42	50.52	45.97	

*Essential amino acids. **WHO/FAO suggested reference pattern of essential amino acids for 'Older child, Adolescent, Adult'. E/T – A ratio of essential to total amino acids.
***Blends amino acid values by calculation. Values followed by different letters within each parameter show statistically significant differences ($p \leq 0.05$).

Table 5.7 Amino acid score (AAS) of proteins, millet flours and their blends at 30% incorporation level.

Essential amino acid (EAA)	Soy protein Isolate	Wheat gluten	30% Wheat gluten	Sorghum flour	30 % Sorghum	Pearl Millet Flour	30% Pearl Millet	Finger Millet flour	30% Finger Millet
Histidine	212.08	113.31	182.45	289.95	235.44	274.17	230.71	504.03	299.66
Isoleucine	168.54	102.53	148.74	147.77	162.31	146.22	161.84	161.29	166.36
Leucine	136.12	112.28	128.97	199.43	155.11	147.82	139.63	149.20	140.05
Lysine	131.55	59.15*	109.83	51.55*	107.55	57.54*	109.35	48.00*	106.49
SAA	83.05*	81.17*	82.49*	152.40	103.85	151.87	103.70	235.42	128.76
AAA	217.87	168.46	203.05	221.27	218.89	196.15	211.35	210.75	215.73
Threonine	151.01	104.68	137.11	169.07	156.43	172.22	157.37	175.12	158.24
Tryptophan	166.84	209.24	179.56	62.48*	135.53	61.54*	135.25	122.19	153.44
Valine	123.31	109.93	119.30	157.22	133.49	156.38	133.23	178.57	139.89

* Limiting essential amino acids.

3.1.4 Physicochemical properties

Table 5.8 Physicochemical properties of raw materials and their blends.

Samples	WAC (g/g)	WS (%)	Colour value		
			L*	a*	b*
`Raw materials					
SPI	5.92 ± 0.18[a]	23.06 ± 0.32[a]	89.08 ± 0.10[a]	2.19 ± 0.02[b]	16.84 ± 0.42[a]
Wheat gluten	2.26 ± 0.22[b]	3.72 ± 0.08[c]	87.59 ± 0.09[b]	0.49 ± 0.02[e]	15.01 ± 0.07[b]
Sorghum flour	2.40 ± 0.02[b]	4.74 ± 0.07[c]	87.81 ± 0.19[b]	1.03 ± 0.14[c]	13.33 ± 0.27[c]
Pearl millet flour	2.47 ± 0.02[b]	7.30 ± 1.60[b]	78.63 ± 0.54[c]	0.73 ± 0.07[d]	11.73 ± 0.45[d]
Finger millet flour	2.32 ± 0.00[b]	3.66 ± 0.11[c]	73.93 ± 0.84[d]	4.11 ± 0.09[a]	9.79 ± 0.29[e]
Blends					
10% Sorghum	5.72 ± 0.12	21.75 ± 1.06	89.11 ± 0.04	2.07 ± 0.03	16.91 ± 0.09
20% Sorghum	5.44 ± 0.08	19.23 ± 1.89	89.07 ± 0.17	1.91 ± 0.05	16.45 ± 0.34
30% Sorghum	5.41 ± 0.19	14.21 ± 0.38	89.08 ± 0.16	1.80 ± 0.06	15.91 ± 0.38
10% Pearl millet	5.81 ± 0.24	18.29 ± 1.82	88.20 ± 0.20	1.67 ± 0.04	16.05 ± 0.34
20% Pearl millet	5.73 ± 0.08	12.50 ± 0.24	87.27 ± 0.21	1.40 ± 0.03	15.77 ± 0.30
30% Pearl millet	5.32 ± 0.06	9.90 ± 0.03	86.40 ± 0.20	1.18 ± 0.03	15.08 ± 0.27
10% Finger millet	5.29 ± 0.19	22.84 ± 0.64	87.31 ± 0.14	1.98 ± 0.08	15.37 ± 0.47
20% Finger millet	5.12 ± 0.10	19.18 ± 0.09	85.08 ± 0.39	2.36 ± 0.09	14.28 ± 0.30
30% Finger millet	5.02 ± 0.04	11.70 ± 0.17	83.80 ± 0.62	2.54 ± 0.10	13.71 ± 0.27
30% Wheat gluten	5.76 ± 0.28	14.92 ± 0.83	89.16 ± 0.03	0.66 ± 0.02	16.00 ± 0.13

Values followed by different letters within each parameter show statistically significant differences ($p \leq 0.05$).

The three millet flours have much lower water absorption capacity (WAC) and water solubility (WS) compared to SPI. As expected, with increase in incorporation levels from 10% to 30%, WAC and WS of the blends decreased. Blending had a small impact on water absorption. However, the impact of the millet flours on the water solubility of the blends was much higher as shown in Table 5.8. The WAC and WS of wheat gluten and its blend were close to the millets and millet blends of 30% incorporation. Furthermore, it was much closer to the properties of sorghum.

The colorimetric L*a*b* values of all the three whole millet seeds used in this study are given in Table 5.4. Sorghum had the highest L* and b* value amongst the three millets and appeared lighter and whiter in colour compared to the other two millets. The pearl millet had the lowest a* value and visually has a greyish tinge. Finger millet had a very high a* value and the lowest L* and b* values and visually a reddish-brown coloured. These values are reflective of the colour of the pericarp of the millets which forms the outer layer of the millet seed. The colour the pericarp contributes to the colour of the flour (Table 5.8) and as a result the colour directions of the flours are in line with that of the colours of the millet seeds. The L* value of sorghum flour is the highest amongst the three millets and it is the whitest flour amongst the three. The finger millet flour has the highest a* value and the lowest L* and b* values amongst the three and appears the darkest and reddest.

3.1.5 Pasting properties

Pasting properties of proteins and millet flour were illustrated in Fig. 5.2a. Soy protein exhibit cold swelling in the beginning (101.9 ± 1.69 BU) and followed by an increased torque upon heating. Sorghum and finger millet showed the maximum peak viscosity with small difference (344.60 ± 1.32 BU and 354.40 ± 2.97 BU respectively), followed by pearl millet (255.10 ± 2.43 BU), SPI (202.50 ± 3.10 BU) and gluten (30.90 ± 0.87 BU). A similar trend was seen at the end of cooling showing the final viscosities of 448.40 ± 3.66 BU for sorghum, 435.50 ± 2.51 BU for finger millet, 297.30 ± 3.10 BU for pearl millet, followed by SPI (173.40 ± 2.14 BU). These results were in accordance with the general literature showing flours/starch based ingredients with higher viscosity and protein isolates with lower viscosity at the similar temperature profile (Akinwale et al., 2017; J. sheng Chen et al., 2010; Onwulata et al., 2014). The difference in the viscosities of millet flours can be due to the starch content (Table 5.4), indicating the

similar trend in final viscosities. Apart from starch content, the pearl millet had higher levels of lipids, total and soluble dietary fiber which may contribute to the lower viscosity compared to other millet flours. These findings were in line with the literature (FAO, 1995). Gluten remained flat over the test with negligible viscosity change (25.70 – 32.5 BU). This could be because of the insufficient concentration of the protein slurry in water to create gel structure and the low water holding capacity of wheat gluten as shown in Table 5.8. Fig. 5.2b, 5.2c and 5.2d shows the pasting properties of SPI-millet blends. These show less difference between them. In general, for all three sets of blends the viscosity increases as the incorporation of millet flour increases from 10 % to 30%. Akinwale et al. (2017) found similar trend in the pasting property of cassava starch and SPI blends.

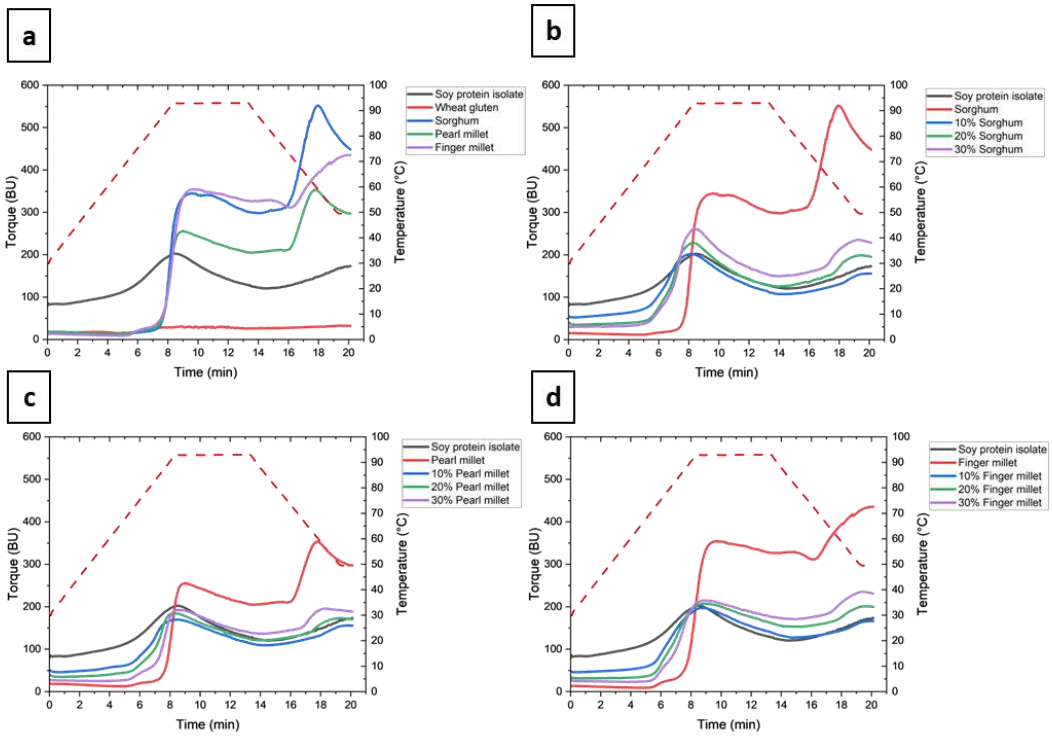

Figure 5.2 Viscosity/pasting properties of (a) protein and millet flours, (b) sorghum blends, (c) pearl millet blends and (d) finger millet blends.

3.2 Colour values of HMMA

The effect of different millets, incorporation levels and moisture content on colour values of HMMA were shown in Fig. 5.3. The millet type and incorporation levels influenced the colour of the blends and the extrudates significantly and in each in its own direction. L* which represents the lightness/darkness of the extrudate was significantly ($p < .05$) correlated with moisture content and type of millet. The

combination of low moisture and high protein concentration will accelerate the Maillard reaction and caramelization process, which leads to deeper colour (Raigar et al., 2020; Yu et al., 2013). Our results also showed similar interaction with respect to moisture content. Sorghum blends showed a lighter extrudates and finger millet blends showed a darker extrudates.

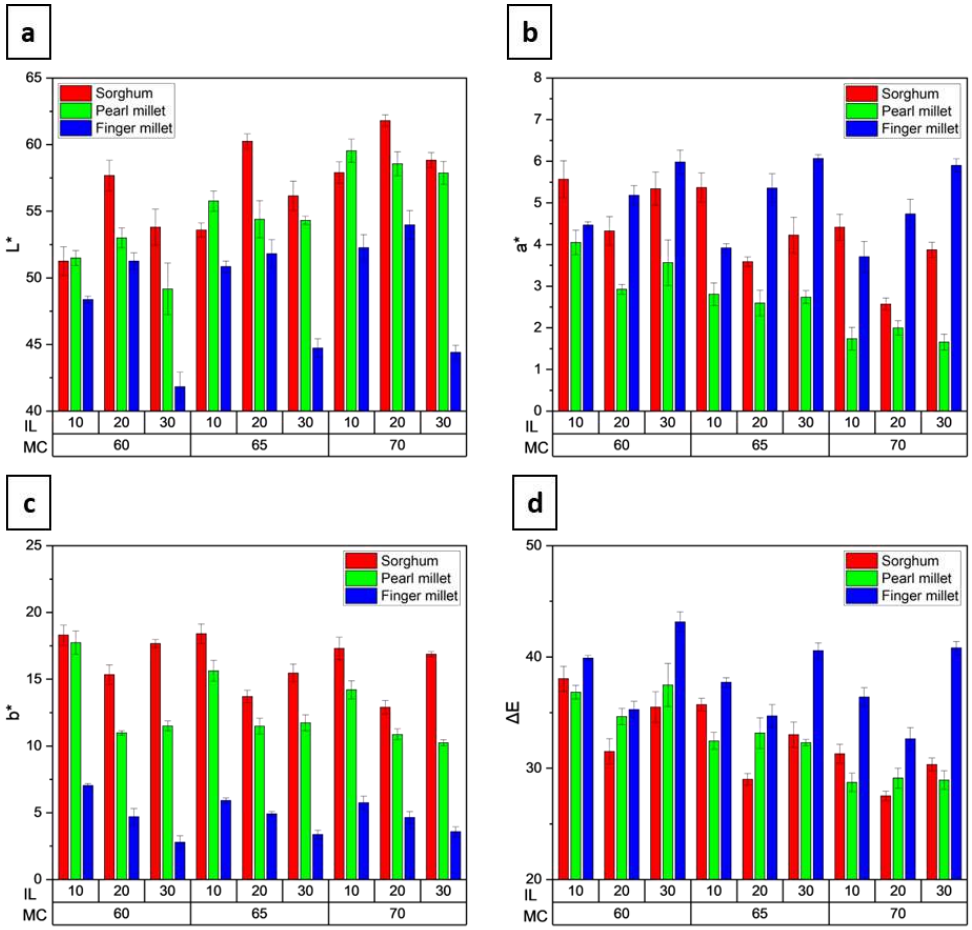

Figure 5.3 Effect of millet incorporation levels (IL) and moisture content (MC) on colour values a) L, b) a*, c) b* and d) total colour difference (ΔE).*

This difference in lightness is not only due to the protein and moisture content relation but also due to the type of secondary ingredient used. In this study, sorghum and finger millet showed distinct colour characteristics because of the polyphenols, flavonoids and tannins (Wang et al., 2022). This colour difference was also seen in the macroscopic images (Fig. 5.5). Incorporation levels from 10% to 30% for pearl millet do not show significant difference ($p < 0.05$) in L* values. On the other hand, sorghum blend extrudates showed an increase in L* value from 10% to 20% and decreases at 30% incorporation level. However, this effect was prominent in the finger millet blends i.e.,

L* slightly increases from 10% to 20% and decreases sharply at 30% incorporation level. This could be due to the inherent colour property of millet which bring in to the extrudates as a result of millets being exposed to heat treatment.

Redness (a*) and yellowness (b*) was significantly impacted ($p < 0.05$) by the type of millet. (J. Zhang, Liu, Jiang, Faisal, et al., 2020) found that at a constant extrusion temperature, increasing the feed moisture content could result in a significant decrease in the redness (a*) and yellowness (b*) values. Whereas, in our result we have found a marginal decrease in redness (a*) and no difference in yellowness (b*) values. Sorghum blend extrudates show a decrease in a* and b* values from 10% to 20% and increases at 30% incorporation level. Pearl millet blend extrudates show no difference in a* and b* values. Whereas, finger millet blend extrudates from 10% to 30% incorporation level resulted in an increase in redness (a*) and decrease in yellowness (b*) values significantly ($p < 0.05$).

The total colour difference ΔE was higher in finger millet blend extrudates in comparison to other millet blends. This large effect in colour may be due to the Maillard reaction and polyphenol oxidation of finger millet during high moisture extrusion cooking (Amadou et al., 2013; Dharmaraj et al., 2014; Kharat et al., 2019). With increase in moisture content, a marginal decrease in ΔE value was observed as shown in Fig. 3.3d. Sorghum and finger millet blend extrudates showed a decrease ΔE values at 20% incorporation levels.

Additionally, the change in colour is strikingly different from protein blends with wheat gluten. In our experiments soy and wheat gluten blends result in whiter meat analogues (Fig. 5.4) indicated by a higher L score and are suitable for white chicken muscle and white fish applications. Soy and pearl millet give very similar whiteness to the soy and gluten blend extrudates.

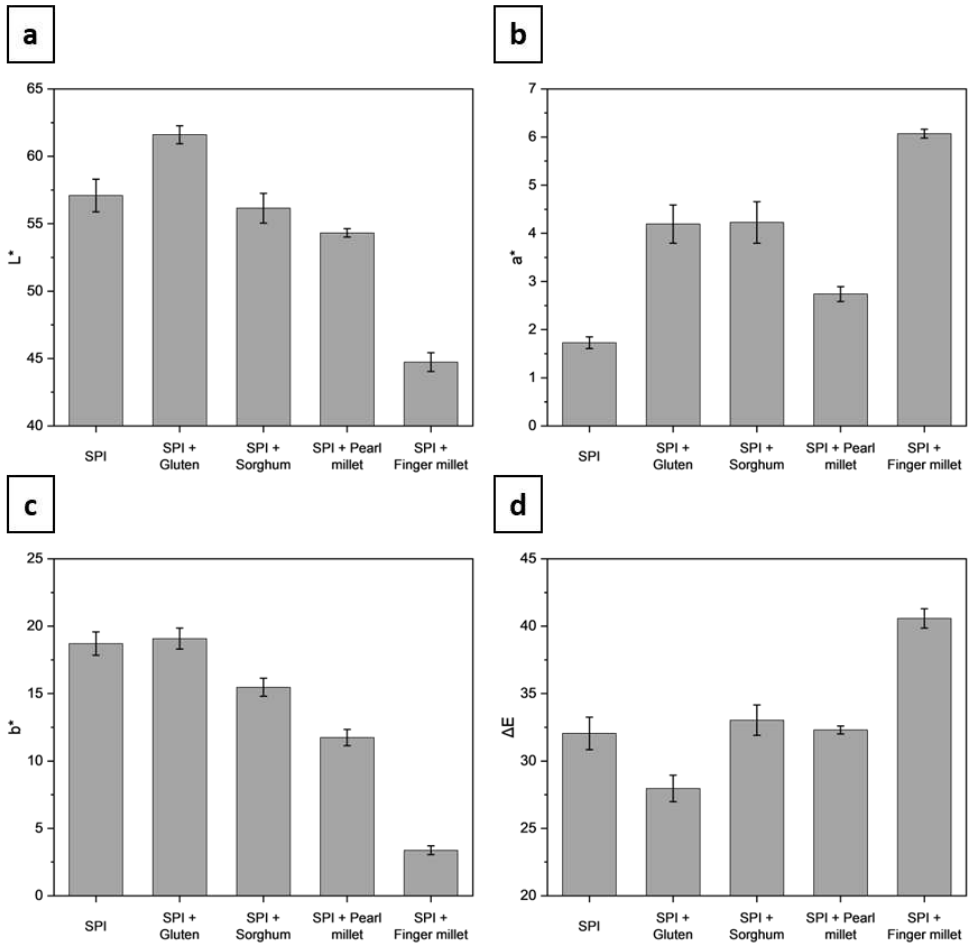

Figure 5.4 Comparison between SPI (100%), SPI + Gluten and SPI + millet blends at 30% incorporation for a) L (lightness), b) a* (redness), c) b* (yellowness) and d) ΔE (total colour difference) of extrudes (HMMA) at 65% feed moisture content.*

High moisture extrudates of sorghum and soy blends, and pearl millet and soy blends have similar L* and b* values to each other and to extrudates of 100% soy. The a* value for sorghum is higher than that for pearl millet and results in browner extrudates while pearl millet gives lighter extrudates. The extrudates from finger millet blends are significantly darker than those of the other millets. They have much lower L* and b* value and a much higher a* value giving them a unique mutton-like brown-pinkish hue.

Thus, the colour range of the soy and millet blends, give the breadth needed to create bases for analogues of meats of different animals – the whiter chicken to the darker mutton analogues. Incorporation levels, moisture level and temperature at which blends are extruded give additional handles for moving around the colour space.

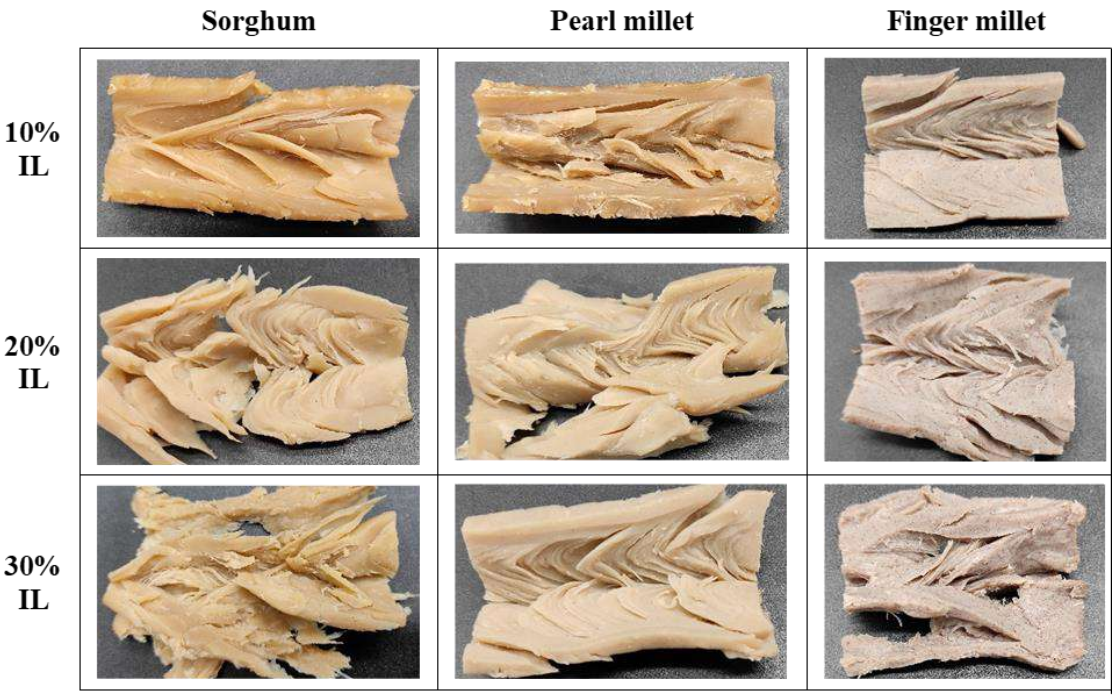

Figure 5.5 Macroscopic images of extrudates (at 65% moisture content) of different millets blends at different incorporation levels (cut-open to show the texture).

3.3 Textural properties

3.3.1 Texture profile analysis (TPA)

Full spectrum textural properties that included hardness, chewiness, resilience, cohesiveness, springiness, cutting strengths and tensile strength were studied for each extrudates.

The textural properties of the SPI-millet flour blends can be modulated by changing the incorporation level of the millet flours and the moisture level used during extrusion. The effect of millet incorporation levels and feed moisture on extrudates was shown in Fig.3.6. The hardness and chewiness increase significantly as we go from 65% to 60% moisture and reduce marginally as moisture is increased from 65% to 70%. The trend is reversed for resilience, cohesiveness and springiness which are highest at 70% moisture and lowest at 60%. Also, going from 65% to 70% has a bigger impact than going from 65% to 60%. The similar trend of effect of moisture content was also seen in the other millet blends as shown in Fig. 5.6b for pearl millet and Fig. 5.6c for finger millet.

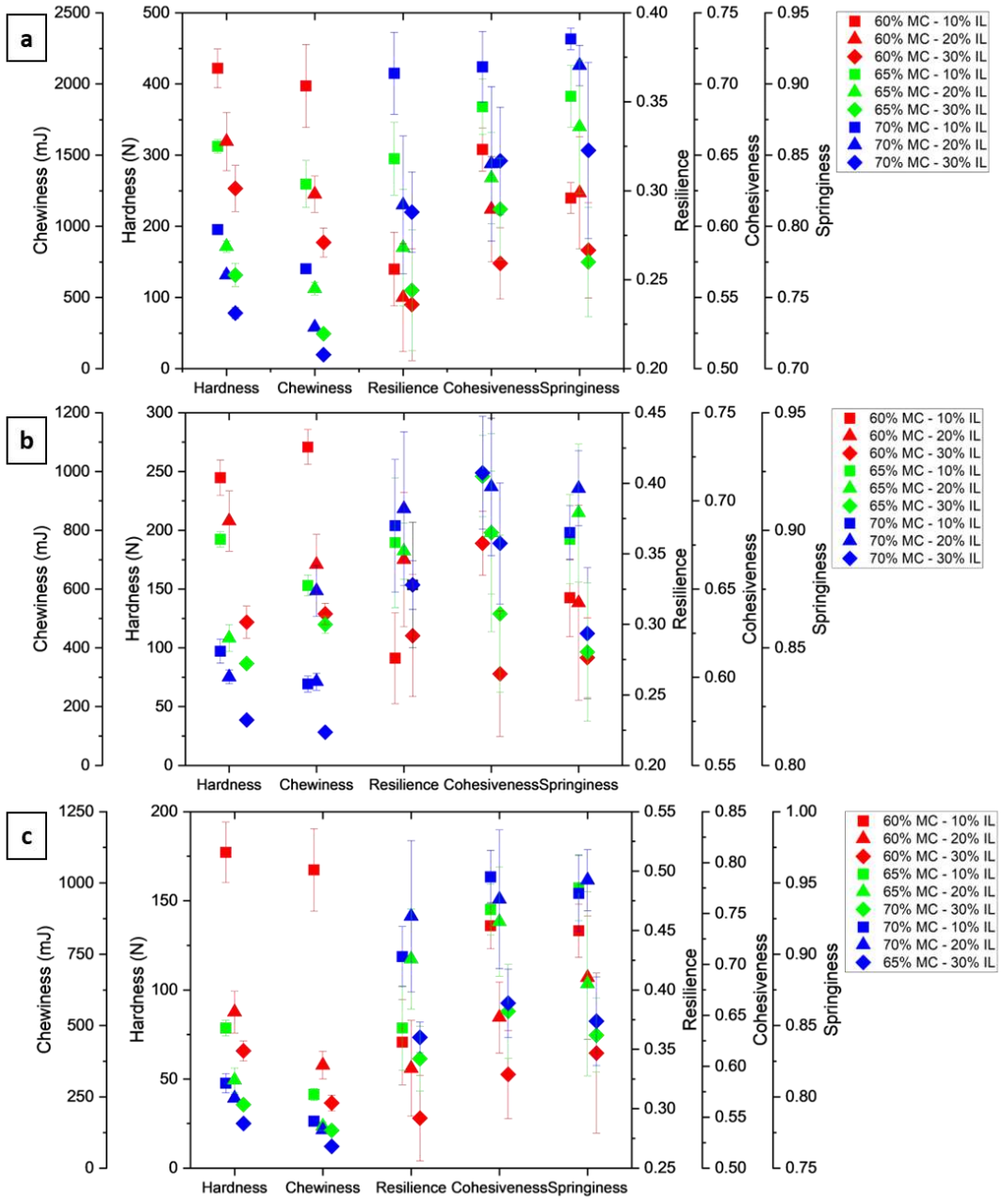

Figure 5.6 Effect of different millets at different incorporation levels (IL) and moisture content (MC) on textural parameters. a) Sorghum, b) Pearl millet and c) Finger millet blends.

The instrumental texture properties at 3 incorporation levels of sorghum into SPI, 10%, 20%, 30% are plotted in Fig. 5.6a. The textural parameter values are highest at 10% incorporation and lowest at 30% incorporation. This is expected as protein concentration of the blend increases at lower incorporation levels of sorghum and other millet blends and the texture is very strongly influence by protein concentration and aggregation during extrusion (Mateen et al., 2023; Lin et al., 2000; Petruccelli & Añón, 1995). Sorghum blend showed a hardness range of78.21 N to 422.06 N (5.4 X) and

chewiness ranged from 98.32 mJ to 1986.56 mJ (20.20 X). Pearl millet showed hardness and chewiness ranges of 38.71 N to 244.77 N (6.3 X) and 113.08 mJ to 1083.44 mJ (9.5 X) respectively. Whereas the finger millet blend showed hardness and chewiness ranges of 25.08 N to 177.18 N (7.0 X) and 76.50 mJ to 1046.03 mJ (13.6 X) respectively. From these ranges of hardness and chewiness, it was found that sorghum had harder and chewier extrudates, whereas finger millet had softer and less chewy extrudates. As expected from hardness and chewiness trends, it was found that they are positively correlated parameters because chewiness is a product of hardness, according to the definition given by Bourne (2002). Pasting properties and macromolecular composition does not have clear differences among the three millet flours to explain the difference in hardness and chewiness, but amylose content could help in explaining the reason. The higher amylose content was seen in sorghum (20 - 30 %) followed by pearl millet (18.3 to 24.6 %) and finger millet (16 %) (Deatherage et al., 1955; R. Singh & Popli, 1973; Wankhede et al., 1979). Chen et al. (2022) found that with addition of 10 % amylose in pea protein isolate showed higher levels of hardness and chewiness compared to 10% addition of amylopectin in high moisture extrusion. This could be due to more rigid and denser structure formed from amylose gel that filled in the protein matrix resulted in steric hindrance for protein rearrangement and cross linking, which therefore leads to a layered rough gel structure.

Sorghum blends showed the least resilient and cohesive extrudates with a range of 0.24 to 0.37 (1.54 X) and 0.57 to 0.71 (1.25 X) respectively. Whereas finger millet blends showed high resilience and cohesive values with a range of 0.29 to 0.46 (1.58 X) and 0.59 to 0.79 (1.34 X) respectively, over a wide span of millet incorporation levels and moisture contents. The resilience and cohesiveness values of pearl millet were in between those of the sorghum and finger millet blends. The millet incorporation levels do not show a significant difference ($p < 0.05$) for resilience values. It seems that at 65% and 70% moisture content, resilience values increased from 10% to 20% and decreased at 30% millet incorporation levels. However, because of the higher standard deviation, the effect was not clear. In general, higher millet incorporation levels in the blend reduce resilience and cohesiveness values. Yao et al. (2004) found that cohesiveness has no significant effect from feed moisture content during the high moisture extrusion of SPI: gluten: wheat starch (6:4:0.5). Whereas our study found that moisture content had a significant positive impact ($p < 0.05$) on cohesiveness.

The springiness of extrudates was significantly ($p < 0.05$) impacted by different blends, incorporation levels, and moisture content. Finger millet blend extrudates showed higher springiness values ranging from 0.83 to 0.95 (1.14 X) and sorghum millet blend extrudates showed a lower springiness values ranging from 0.77 to 0.93 (1.21 X). On the other hand, springiness values of pearl millet blend extrudates were in between the other two millet blends. Increasing the incorporation levels of millet from 10% to 30%, the springiness values were decreasing significantly for different millet at every moisture levels. Moisture content showed a positive relationship with springiness. As moisture content increased from 60% to 70%, springiness also increased. Our findings related to moisture content and springiness were in accordance with the literature (Chen et al., 2010; J. Zhang et al., 2020).

As was the case in instrumental textural parameters, the visual characteristics of the fibrous structures for the three millets were also different. Visually, sorghum and pearl millet containing blends had thicker fibrous bands while the finger millet blend had thinner bands. These visual difference can help in designing meat analogues for different cuts. For example, cuts from shanks & shoulders have coarser fibers (Klont et al., 1998) which may be matched with soy protein blends with sorghum and pearl millet, while the cuts from back have finer fibres and finger millet blends may help in creating a good match for these. The improvement of texturization by the addition of millet flour may be due to the protein-flour interactions. Han et al. (1989) found that addition of up to 30% rice flour to SPI, improves the texturization because of the gelatinized surface structure of rice starch and increased air cell size with in the extrudates. Further this interaction of protein-polysaccharide was explained through multiphasic system (Dekkers, Boom, et al., 2018; Tolstoguzov, 1993).

We were able to obtain good visual fibrous structures for all the three millet blends at incorporation levels of 20% and for pearl millet up to an incorporation level of 30% (Fig. 5.5). The reason for the differences in fibrous structure of the three millets or for the good fibrous structure achieved with pearl millet even at the higher incorporation levels are not well understood. Pearl millet flour is distinct from other two millets in that it has higher protein, total fibers, soluble fibers and lipid content compared to the other two millets. Its viscosity is also lower as indicated by its pasting curve. While these compositional differences may play a role in the observed textural differences,

they alone do not provide a fundamental explanation which may require further work such as that described in papers by Nasrollahzadeh et al. (2023) and Liu & Hsieh (2008).

Instrumental textural parameters were compared between the SPI (100%) Wheat gluten (30%), millet blends (30%) and chicken breast (raw and cooked) as shown in Fig. 5.7. The data points connected with lines is to guide the eye. The behaviour of millets was similar to that of gluten in the soy protein blends in some respects i.e., it reduces hardness, chewiness and cohesiveness. While wheat gluten does not alter the springiness of soy analogues, millet flours allow. Thus, incorporation of millet flours to soy protein provides a textural space to play outside of the space that soy and wheat gluten blends play in. HMMA made from 100% SPI are texturally far off from raw and cooked real chicken (Fig. 5.7). They have higher hardness, chewiness, resilience, cohesiveness and springiness than real chicken. Blending of SPI with wheat gluten shifts the texture profile of the HMMA towards real chicken but a gap persists. The hardness and chewiness shift in the direction of real chicken's but not far enough, and there is little impact on resilience, cohesiveness and springiness. The textural shifts achieved by blending SPI with millets, while still not fully aligning with the profile of real chicken, do a better job of bridging the gap between HMMA and real chicken across the full spectrum of textural properties.

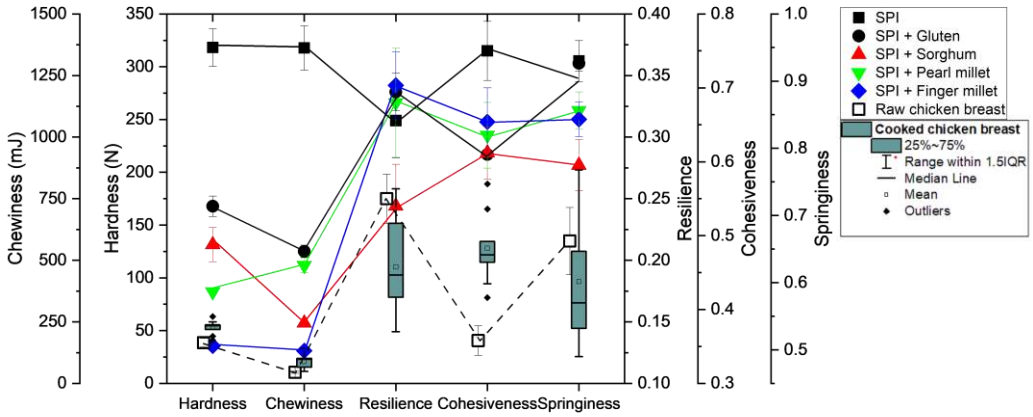

Figure 5.7 Comparison of the textural parameters of HMMA extrudates made with SPI 100%, SPI + Gluten and SPI + millet blends with 30% incorporation at 65% feed moisture content. These HMMA were compared against real chicken breast meat.

Within the textural space of the soy and millet flour blends, each blend is distinctive as shown in Fig. 5.7. Sorghum gave the highest instrumental hardness followed by that obtained for pearl millet. The hardness of sorghum was nearly 4-times that of finger

millet. Pearl millet hardness was in between the two. High moisture meat analogues with soy and pearl millet flour blend had the highest chewiness – nearly 4 time that of the blend with finger millet flour. Resilience, cohesiveness and springiness values were lowest for sorghum and highest for finger millet with pearl millet showing intermediate values.

3.3.2 Cutting strength and Tensile Properties

For completeness, we also studied the effect of the incorporating millet flours in soy protein-millet blends on cutting strength and tensile strength. Cutting strength along and across the flow of the extrudates from the die can be used as a tool to analyze the fiber formation in the high moisture meat analogues which intern represents the anisotropic property. Cutting strength is also referred as shear force to cut the sample and anisotropic index is also referred as fibrous degree where other literature has referred to (Noguchi, 1989; X. Zhang et al., 2022). Cutting strength showed even greater difference than the textural properties between the three millets.

Cutting strength along and across the flow direction of extrudates was significantly impacted ($p < 0.05$) by all the independent parameters millet blends, incorporation levels and moisture content as shown in Fig. 5.8a. Higher cutting strengths were observed in sorghum blends ranging from 4.14 N to 31.70 N (7.6 X) and 3.86 N to 20.28 N (5.2 X) and lower cutting strengths were observed in finger millet blends ranging from 2.24 N to 7.90 N (3.5 X) and 1.91 N to 7.86 N (4.1 X) for along and across the extrudate flow direction respectively. The pearl millet blend extrudates showed in between CS values.

Incorporation levels of millet into SPI and moisture content showed a negative correlation with cutting strength. Zhang et al. (2020) found that the increase in moisture content of extrudates results in a decrease in cutting strength. Our results are in line with the literature. The change in the CS values in sorghum blends as a function of moisture content was way higher than pearl millet and finger millet blends.

Sorghum showed the greatest anisotropy amongst the three millets with cutting strength along the direction of extrusion being higher than cutting strength across the direction of extrusion. Anisotropic index was significantly impacted ($p < 0.05$) by incorporation levels of millets. As incorporation levels of sorghum increases, anisotropic index was decreased but for other millet blends the difference was not consistent.

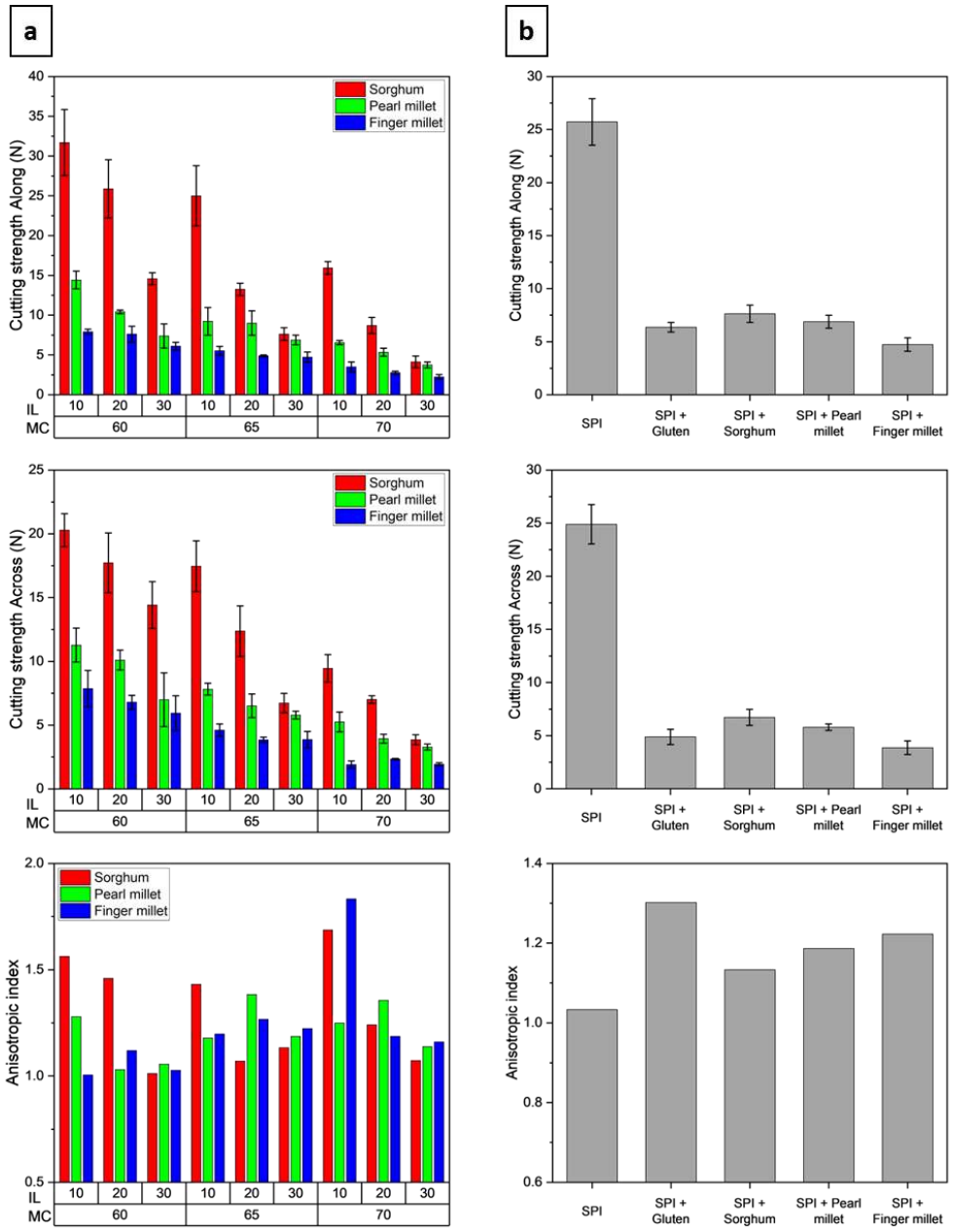

Figure 5.8 a) Effect of different millets at different incorporation levels (IL) and moisture content (MC) on the cutting strength along and cutting strength across the flow direction of extrudates and anisotropic index of high moisture extrudates. b) Comparison between SPI 100%, SPI + Gluten and SPI + millet blends with 30% incorporation at 65% feed moisture content.

Pearl millet and finger millet blends showed anisotropic index increases at 20% and decreases at 30% incorporation level. Zhang et al. (2020) found that the increase in moisture content of extrudates results in a decrease in anisotropy. Anisotropic structures cannot be produced using SPI alone; a second component, such as wheat gluten, is required, according to an early study on high moisture extrusion of plant proteins (Cheftel et al., 2009). We have shown that millet (which are carbohydrate rich) can be

a potential secondary ingredient for creating higher anisotropy even at higher levels of moisture (70%).

A comparative plot of cutting strength and anisotropic index of extrudates made from SPI, SPI+gluten and millet blends (70:30) was shown in Fig. 5.8b. The only SPI extrudates showed higher cutting strength along and across the flow direction with low anisotropic index (1.03). This is because of the high level of protein aggregation in all the special direction of extrudate making the anisotropic value closer to 1. The cutting strengths of gluten blend was in the range of millet blends and anisotropy of finger millet extrudate was much closer.

As the millet incorporation levels and moisture content increases, tensile strength decreased significantly. The most probable reason is the concentration of proteins at higher levels of incorporation and moisture content which makes less protein agglomeration and less cross linking of proteins. The literature also showed the similar results (Chen et al., 2010; Fang et al., 2014; Zhang et al., 2020).

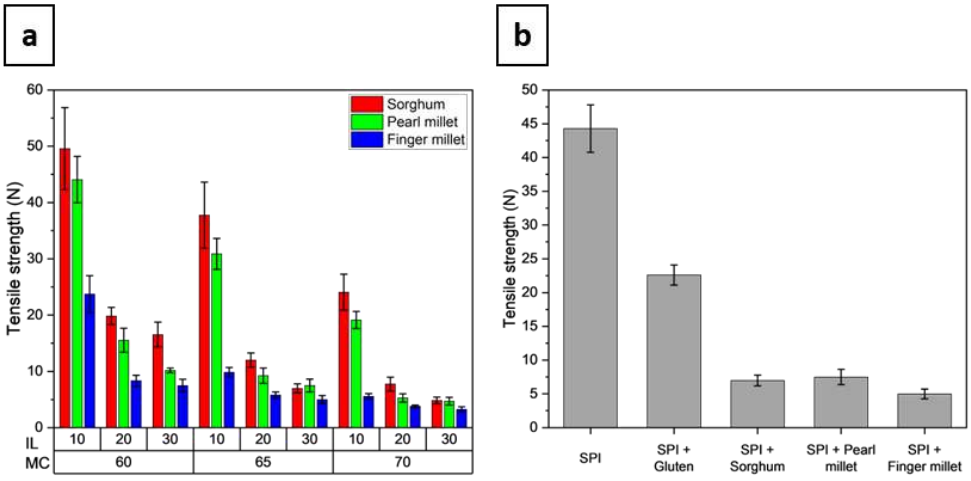

Figure 5.9 a) Effect of different millets at different incorporation levels (IL) and moisture content (MC) on the tensile strength (g) of high moisture extrudates. b) Comparison of the tensile strength (g) of extrudates made with SPI 100%, SPI + Gluten and SPI + millet blends with 30% incorporation at 65% feed moisture content.

A comparative plot of tensile strength of extrudates made from SPI, SPI+gluten and millet blends was shown in Fig. 5.9b. Only SPI extrudate has shown higher resistance to the tensile force (44.28 ± 3.52 N) compared to the blends. Here the gluten blends showed a 2.5X greater tensile strength compared to millet blends. Furthermore, the

millet blends showed a similar tensile strength being finger millet on the slightly lower side.

3.4 System parameters

3.4.1 Specific mechanical energy (SME) and melt viscosity

Specific mechanical energy is the work that the drive motor puts into the material being extruded and thus becomes a good way to characterize the extrusion process(Godavarti & Karwe, 1997). The effects of millet blends, incorporation levels, and moisture content on SME and on-line/melt viscosity were shown in Fig. 5.10a and Fig. 5.10b. Sorghum blends had the highest SME and highest melt viscosity, finger millet blends had the least SME and least viscosity, and pearl millet blends were in between the other two millet blends at every extrusion moisture level.

Similarly, the same trend was also seen at different millet incorporation levels. The SME and viscosity were significantly decreased ($p < 0.05$) as the incorporation level was increased from 10% to 30%. The decrease in SME and melt viscosity from 10% to 30% was most likely due to the protein concentration dilution as millet incorporation increased. As expected, moisture content showed a negative linear relationship with SME with significant impact ($p < 0.05$). The reason for this is because as the moisture content increased, the amount of force needed to drive wet mass through the die decreased, which in turn lowered the amount of friction between the raw material and the screw shaft and extruder barrel (F. L. Chen et al., 2010; Lin et al., 2000). The viscosity of dough/melt in the extruder and at the die was decreased as a result of the water acting as a lubricant (Hayashi et al., 1992) and the lower concentration of protein with a higher moisture content (Akdogan, 1996). The findings of our study were consistent with these earlier reports.

Overall, the use of millet flours as secondary ingredients offers an opportunity to reduce the SME of extrusion while still obtaining good fibrous structures as seen in visual images and instrumental texture analysis. This can have an impact on the life of the motor, the screws and the liners and extend the life of critical parts thus improving the overall economics of the process. The lower SME operation will have longer life of an extruder with less wear and tear (Hou et al., 2020).

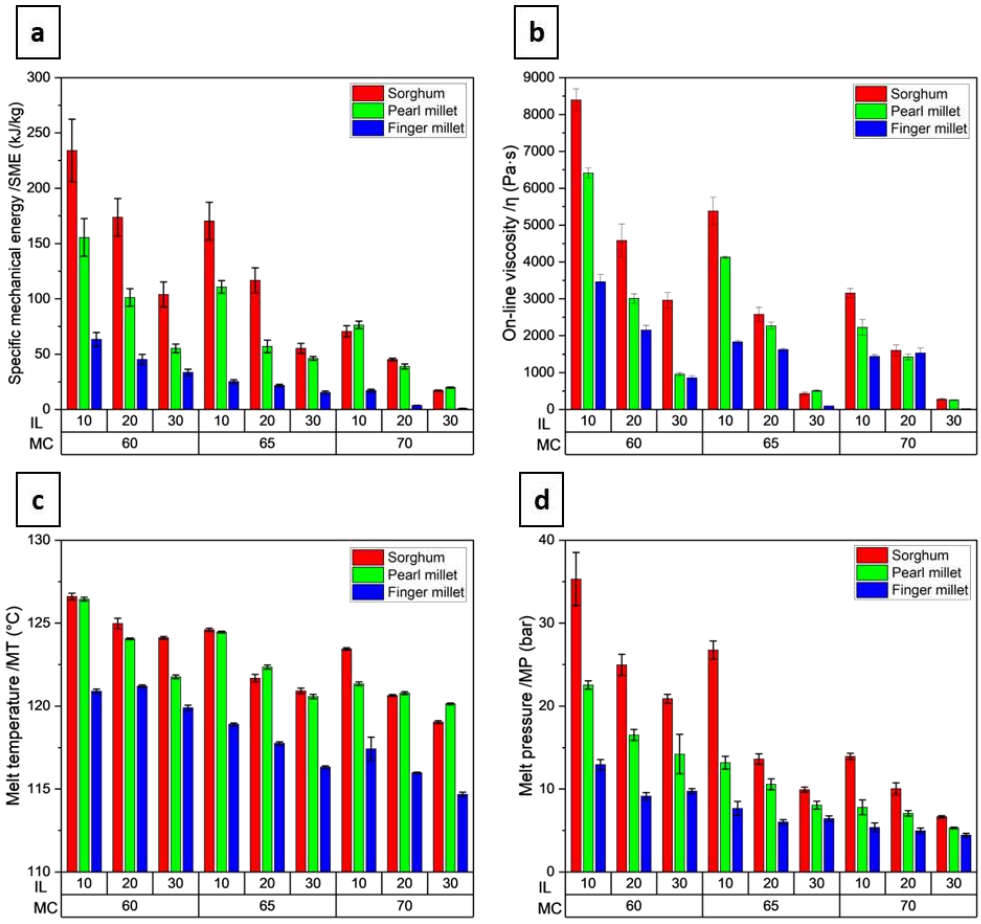

Figure 5.10 Effect of millet blends, their incorporation levels /IL (%) and moisture content /MC (%) on system parameters - a) specific mechanical energy /SME (kJ/kg), b) on-line viscosity /η (Pa˙s), c) melt temperature /MT (ºC) and d) melt pressure /MP (bar).

3.4.2 Melt temperature and melt pressure

Lowering the moisture content increases the melt temperature and melt pressure significantly ($p < 0.05$). High moisture extrusion at a lower moisture content resulted in a higher melt temperature and higher melt pressure. This was in accordance with literature (Lin et al., 2002; Palanisamy, Franke, et al., 2019). Sorghum and pearl millet blends showed similar melt temperatures with marginal deviation, but in comparison, finger millet blend blends showed much lower melt temperatures as shown in Fig. 5.10c. Similarly, melt pressure for finger millet blends was also lower in comparison with other millet blends as shown in Fig. 5.10d. Furthermore, the range of melt pressure at wide span of incorporation and moisture content for finger millet (4.46 bar – 12.94 bar) was way lower than sorghum (6.66 bar – 35.31 bar) and pearl millet blends (5.32 bar – 22.54 bar).. The total starch content and fiber content of the three millets do not

explain the lower system values (SME, melt viscosity, temperature and pressure) observed for finger millet. The total starch content of finger millet is in between that of sorghum and pearl millet. Its total dietary fiber and insoluble dietary fiber are in fact the highest amongst the three millets. One possible explanation could have been the lower amylose starch content of finger millet (16 %) as reported in literature compared to sorghum (20 to 30 %) and pearl millet (18.3 to 24.6 %) (Deatherage et al., 1955; R. Singh & Popli, 1973; Wankhede et al., 1979). Some reports also show finger millets have a unique slimy-sticky structure when it cooked and gelatinized (Dharmaraj et al., 2014; Saha et al., 2011). . Further research work may be required to understand this type of behaviour.

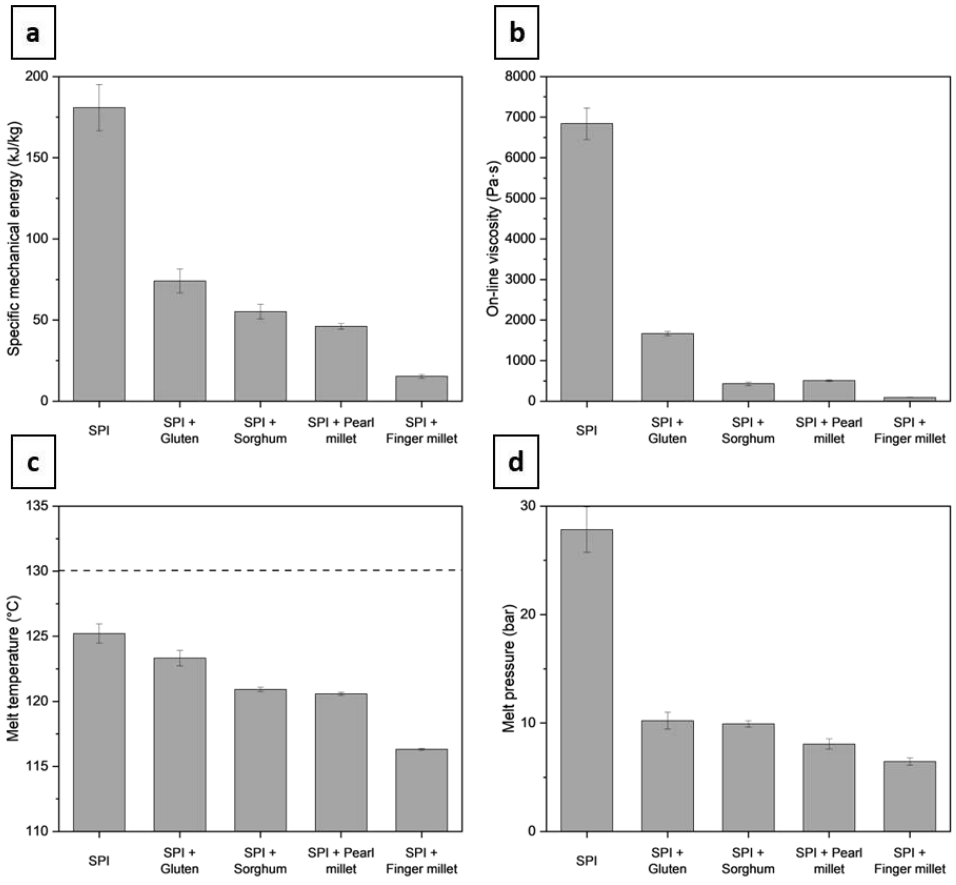

Figure 5.11 Comparison between SPI (100%), SPI + Gluten and SPI + millet blends at 30% incorporation for a) SME, b) on-line viscosity, c) melt temperature and d) melt pressure required to extrude HMMA at 65% feed moisture content.

The millet incorporation level from 10% to 30% showed a significant decrease in melt temperature and melt pressure ($p < 0.05$) for all the blends. As discussed in the SME

and viscosity section, the reason for the decrease in melt temperature and pressure remains the same because the of protein dilution factor as millet incorporation increases.

All in all, the system parameters - SME, melt viscosity, melt temperature, and pressure decreased as millet incorporation and moisture content increased. All the system parameters were positively correlated with each other. Although the water absorption capacity and water solubility of sorghum, pearl millet, and finger millet were almost the same as shown in Table 5.4, they behave differently during the high moisture extrusion process in millet-soy blends. This may be due to the nature of the carbohydrates and proteins present in the millets.

Comparative figures of system parameters were shown in Fig. 5.11. SPI 100% showed highest SME, viscosity, temperature, and pressure flowed by wheat gluten blend. The obvious reason for this was due to the higher protein concentration which ultimately leads to high protein agglomeration. Millet blends showed a significant reduction in SME and viscosity compared to SPI and SPI-gluten blend.

4 Conclusion

United Nations has identified 2023 has the International Year of Millets to focus attention on millets and increase their use as they offer opportunity to address environmental footprint of food and livelihoods in drylands. New food product development incorporating millets can help increase the use of millets in our foods. In this study we explored the suitability of millets as a blend component in high moisture meat analogues. All the three millet flours studied in this work gave good fibrous structures at incorporation levels up to 20% in blends with soy protein isolate and pearl millet even up to 30% incorporation levels. The full spectrum colour and textural behaviour of the three millet flours-SPI blends differ from each other. Sorghum blends have higher hardness and chewiness, and lower resilience, cohesiveness, and springiness. Finger millets have lower hardness and chewiness, but higher resilience, cohesiveness, and springiness. Pearl millet has an intermediate textural profile. These differences between the effect of the three millet flours on the textural profile of SPI open up opportunities to move around the textural quality in new ways for product formulators. This may lead to improved ability to meet target texture profiles. Visually, the three millets are distinct from each other in the colour space and the fiber coarseness.

This opens opportunities to develop meat analogues for different cuts of different animals. As an example, sorghum and pearl millet blend HMMA for chicken and fish analogues and finger millet with its darker, reddish pink colour and finer fibrous structure could be worked on for the back & loin cuts of mutton and beef.

Protein content and amino acid profile were also important attributes of meat analogues along with textural characteristics. The overall protein levels of the extrudates are slightly lower than that of SPI and gluten based HMMA. However, they are still within the range of protein content of real chicken. Further, the SPI-millet blends have better amino acid profile than that of gluten-based blend as they have a high essential amino acid to total amino acid ratio and high lysine content. they also attribute to both soluble and insoluble dietary fiber in the product. Additionally, for the specific case of HMMA for whole chicken meat chunks and strips, where most plant-based proteins for chicken-based products use wheat gluten in their protein blends the millets provide a better full spectrum textural profile than HMMA made from SPI alone or SPI and gluten blend. The lower hardness, chewiness, resilience and springiness compared to wheat blends are a closer texture profile to real chicken. Millets open up an opportunity to not only improve textural match for chicken analogue products but also to develop gluten-free products.

One of the key challenges for the plant-based meats is their cost compared to real meats. Millets can help optimise both ingredient cost and operating cost of extrusion. Millet flours are low-cost ingredients and may allow the meat analogue producer to reduce the cost of inputs. The millet flours also reduce the extrusion SME while improving the textural quality. The reduction in SME will result in a longer running life of the equipment and will have a positive impact on the operational cost of the process. Thus, a judicious selection of millets as secondary ingredients and their incorporation levels can play a significant role in bringing down the cost of the products and could make plant-based meat analogues more affordable. Given the sustainability benefits of millets, incorporating millets would also reduce the environmental footprint of plant-based meat analogues even further.

Chapter 6

Evaluating millet flour fractions as blend components with soy protein isolate for creating high moisture meat analogues using a twin screw extruder

This chapter has been submitted for publication as Mateen, A., & Singh, G. (2024). Evaluating millet flour fractions as blend components with soy protein isolate for creating high moisture meat analogues using a twin screw extruder. Food Hydrocolloids.

Abstract

During the high moisture extrusion of plant proteins, the interaction of protein with added starch or fibers as a secondary ingredient determines the formation of fibrous structures. In this study, finger millet was used as a model grain to develop minimally processed but compositionally and physicochemically distinct fractions to use as blend components with soy protein isolate and extruded to make high moisture meat analogues (HMMA). The effect of these fractions was studied on the instrumental texture, visual fibration, rheology and colour of HMMA. Based on the composition, the fractions were named starch rich fraction (SRF) and a fiber rich fraction (FRF). SRF had 2.2 times the amylopectin content of FRF, while FRF had 9.4 times the dietary fiber content of SRF. While all the HMMA's showed visual fibration, the degree differed, with SPI100% giving least fibers and the SRF and FRF blends giving high density of fibers. Instrumental anisotropy was maximum for SRF blends and least for SPI100%. HMMA's from FRF blends are more resilient than SPI100%, while SRF blends are less so. All other textural parameters for the blends were lower than SPI100%. Overall, when compared to SPI100% extrudates, the full spectrum textural profile of the HMMA's made from the blends was found to be closer to the band for real meat. In terms of bonding, hydrogen and disulfide bonds appeared to play a greater role in the HMMA network in the SRF blends while hydrophobic interactions played a greater role in the FRF blend extrudates. This study creates insights for the use of minimally processed fractions from whole grains to develop HMMA with diverse textures and colours similar to real meat, presenting a promising approach for producing sustainable and cost-effective meat alternatives.

Keywords: Texturization, HMMA, Fractionation, Image analysis, Rheology, Real meat

1 Introduction

While low moisture extrusion of plant proteins has been successful in minced applications such as patties and sausages, high moisture extrusion of plant proteins is being looked at for applications that involve larger pieces such as shreds, cuts & fillets (Berke, 2022; Cheftel et al., 2009). Research on high moisture meat analogue (HMMA) started in 1980s (N. Kitabatake et al., 1985; Noguchi, 1989). Single protein rich ingredients, concentrates and isolates while giving texturization (F. L. Chen et al., 2010; Ferawati et al., 2021; Kitabatake et al., 1985; Pietsch et al., 2019) are found to be too hard, chewy, rubber like and have less fibrous structure compared to the blends (Samard et al., 2019). This has led to studies on the incorporation of secondary ingredients with the primary protein contributing ingredient. A review of literature on secondary ingredients used for HMMA by Mateen & Singh (2023) included protein rich ingredients such as wheat gluten, whey protein; starch rich ingredients such as wheat starch, corn starch; fiber rich ingredients such as oat fiber, pectins (Chiang et al., 2019a; Dekkers et al., 2016; Han et al., 1989; Ramos Diaz et al., 2022; Samard et al., 2019); hydrocolloids such as xanthan gum, carrageenan, alginates (Taghian Dinani et al., 2023; F. Wang et al., 2023; J. Zhang, Liu, Jiang, Shah, et al., 2020) in the blends. In general, incorporating secondary ingredients with the primary protein ingredients improved the visual fibration and anisotropic character of HMMAs. It also results in reduction of the hardness and chewiness as measured by texture analyzer and brought them closer to values of real meat (Mateen & Singh, 2023; Samard & Ryu, 2019).

Most of the secondary ingredients used involved extensive processing in their manufacture and would also add to unfamiliar names on labels from a consumer perspective. This takes away from the proposition of a food developed from a sustainability perspective.

In this context Mateen & Singh (2023), studied the incorporation of millet flours (sorghum, pearl millet and finger millet) as secondary ingredient into soy protein isolate (SPI) to create HMMA. Millet flours improve the nutritional quality of the extrusion blend as they contribute to dietary fibers and minerals (Anitha et al., 2020; Hassan et al., 2021). Soy protein isolate and whole millet flour blends can be designed to have higher amino acid scores than soy protein alone or soy-gluten blend and in fact exceed the FAO/WHO reference pattern of amino acid taking them to within the range of real

meat protein quantitatively (Mateen & Singh, 2023). From the perspective of sustainability and climate change, they have a small environmental footprint. They can be grown in arid regions, proving livelihood opportunities due to their resilience to drought and high temperatures. Realizing their importance in contributing to Sustainable Development Goals, the United Nations declared 2023 the international year of Millets with the aim to create awareness about millets beyond their traditional geographies of drylands in Asia and Africa (D. B. Rao et al., 2022; N. D. Rao et al., 2018; J. Wang et al., 2018). Thus, addition of millets to the protein blends can complement the planetary health credentials of plant protein based meat analogues and add further dimensions of human health and societal health through livelihoods.

However, this cannot come at the cost of texture of the meat analogues. Mateen & Singh (2023) reported that incorporating millet flours into soy protein powders improved the overall texture of the HMMA and brought it much closer to real chicken meat when compared to soy protein isolate (SPI) alone or SPI-gluten blend. They also looked at full spectrum textural match which went beyond hardness and chewiness, and included other textural parameters resilience, cohesiveness, springiness and cutting strength. While hardness and chewiness can be matched by a combination of manipulating the process conditions and incorporating the secondary ingredients mentioned in the review by Mateen & Singh (2023) in the blend, the other textural properties like resilience, cohesiveness and springiness have proven to be difficult to match with real meat (Mateen et al., 2023). Therefore, it was interesting to observe that these three parameters were also found to be directionally closer to real meat with millet and SPI blends, though there was still a gap for a perfect match.

Building upon previous work, this study investigates the dry fractionation of one millet, the finger millet grain, into two distinct fractions – a fiber rich and a starch rich fraction. The impact of incorporating these two fractions in soy protein isolate as secondary blend components is evaluated. The HMMAs have been analyzed for textural, rheological and visual characteristics using instrumental and image analysis methods. Furthermore, an attempt has been made to understand these through a study of composition of the blend components and the bonds involved in the protein aggregation because of extrusion.

2 Materials and Methods

2.1 Materials

Soy protein isolate (SPI) (Solae SUPRO® 620) was procured from DuPont Shineway Luohe Food Co. Ltd., Luohe, China and Finger millet (Eleusine coracana) variety Bharathi VR 762 was procured from the Indian Institute of Millet Research (IIMR), Hyderabad, India. Harvested and sun-dried whole finger millet grains with an initial moisture content of approximately 8% were used as the raw material for fractionation and flour production. Prior to processing, the grains underwent a cleaning procedure to eliminate impurities and foreign matter. This cleaning step involved the use of a millet destoner cum aspirator (DGA S1500, Perfura Technologies Pvt. Ltd., Coimbatore, India), which effectively removed unwanted debris, ensuring grain purity.

All the chemicals and reagents were procured from Sigma-Aldrich Chemicals Pvt. Ltd., Bengaluru, India.

2.2 Fractionation, milling and blend preparation

The whole finger millet grains were dehulled using a modified laboratory vertical polisher equipped with single phase motor and a variable frequency drive (VFD) controller (Satake India Engineering Pvt. Ltd., New Delhi, India). The frequency of the motor was adjusted to 39.2 Hz to get 1800 rpm of the motor. A sample size corresponding to 200 g of whole millet was fed to the hopper situated on top and run for 6 min. The polished grains (heads) were collected in the bottom tray. Hull and brokens were collected in the side trays. The brokens polished grains which went to the side trays were recovered through a sieve process with a cutoff sieve size of 300 microns. The process conditions and weight of feed material were standardized through preliminary trials. From 200 g millet feed material, an average of 74.00 g polished head, 75.00 g broken and 46.40 g hull were obtained which accounts for 23.20 % degree of polishing, 37.00 % head yield and 74.50 % total yield calculated according to Lohani et al. (2011) and Webb et al. (1986).

The polished grains and the recovered broken grains were milled together to produce one fraction, while the hull, which was in flour form (<300 microns), was used as it after fractionation. The whole finger millet grain was separately milled to obtain whole finger millet flour and this was used as a comparator in the trials. The milling was done

using a hammer mill equipped with a 500-micron size screen (Thatha Engineering Works, Thrissur, India). These flours were packed airtight in polyethylene bags and stored in a refrigerator (4 °C) until further use.

Compositionally the flours from polished grains were found to be richer in starch while the hull flour was found to be richer in dietary fiber (data reported in section 3.1.2). Thus, the flour from the polished grain was termed as Starch Rich Flour (SRF) and the hull flour was termed as Fiber Rich Flour (FRF).

Preparation of protein blends for high moisture extrusion was done by mixing SPI with SRF, FRF and whole finger millet (WMF) flour at three different levels each (90:10, 80:20 and 70:30 ratio) (Table 6.1) using a lab scale ribbon blender (SRM, Shakti Pharmatech Pvt. Ltd., Ahmedabad, India). Thus, there were a total of nine blends and SPI 100% as a control.

2.3 Preparation of real meat

For comparing the texture profile of HMMA with real meat, fresh meat cooked according to the method described by (Isleroglu et al., 2014; Zhuang & Savage, 2008) with slight modifications. Any excess fat on the fresh meat was removed and chicken breast was split into half measuring 6 – 7 in. Lamb and beef meat (flank portion) were cut into steak sizes of similar length. Then it was cooked in a combi oven (CombiMaster Plus CMP 61, Rational AG, Landsberg am Lech, Germany) with 50% humidity at 120 °C external temperature till the internal temperature reached 75 °C. The cooked real meat was kept outside to bring it to room temperature before texture analysis. The sample preparation for texture analysis was same as mentioned in chapter 6 section 2.8.

2.4 Raw material characterization

2.4.1 Particle size distribution and bulk density

Particle size was analyzed using a sieving technique following the standard AACC method 66-20.01 (AACC, 1999). The sieving apparatus consisted of an electromagnetic sieve shaker (EMS-8, Electrolab India Pvt. Ltd., Mumbai, India) with six stacked sieves, each with progressively smaller mesh openings. The mesh sizes of the sieves used were as follows: 600 µm, 425 µm, 212 µm, 106 µm, 75 µm, and 53 µm. A starting sample weight of 150 g was utilized, and the sieves were shaken for a duration of 10

minutes. Subsequently, the various powder fractions were collected and weighed, and the percentage of material retained on each sieve was calculated.

For bulk density, 50 g of powder sample was placed in a 100 ml measuring cylinder. The cylinder was gently tapped on a laboratory bench multiple times to achieve a consistent volume. The bulk density was determined by dividing the weight of the sample by its corresponding volume and expressed the values in kg/m^3 (S. Huang et al., 2019). All the samples were analysed in triplicates.

2.4.2 Proximate composition, dietary fiber and amylose content analysis

The moisture content in the samples were assessed using a moisture analyzer (MA 50.R, Radwag, Radom, Poland) in accordance with the ISO 712:2009 method (ISO, 2009). Determination of total protein content (calculated as nitrogen × 6.25), lipid content, and ash content in SPI, whole finger millet flour, and millet fractions was conducted following standard methods (AOAC, 1990) and expressed on a dry weight basis. Ash content was determined through the gravimetric method by incinerating the samples at 550 °C in a muffle furnace. Total starch and amylose/amylopectin content were quantified using assay kits K-TSTA-100A and K-AMYL 06/18 respectively (Megazyme Ltd., Bray, Ireland). Total, soluble, and insoluble dietary fibers were analyzed through the enzymatic–gravimetric method AOAC 991.43 (AOAC, 2005) using an assay kit (K-TDFR-100A, Megazyme Ltd., Bray, Ireland). All analyses were performed in triplicate for each sample.

2.4.3 Water absorption capacity (WAC) and water solubility (WS)

This analysis was performed using the method described by Ogunwolu et al. (2009). 1 g of the raw material powder sample was mixed with 10 g of distilled water using a stirrer. The suspension was then centrifuged at 1800 × g for 20 min at 22 °C (C-24plus, Remi Electrotechnik Ltd., Vasai, India). After centrifuge, the wet pellet was weight to calculate WAC by dividing the wet pellet weight by the sample weight. The supernatant was dried overnight to calculate the WS by dividing the weight of soluble solids after drying by the sample weight.

2.4.4 Pasting properties

The pasting property of soy protein, finger millet and its fraction were analyzed as a function of temperature utilizing a starch cell attachment to the rheometer (MCR 702e,

Anton Paar GmbH, Graz, Austria) following the AACC Method 76-21 STD 2 (AACC, 1997). A homogeneous slurry from the samples was prepared with 3 g solids and 25 g water. Initially, the slurry was held for 50 °C for 50 sec, then gradually the temperature was increased from 50 °C to 95 °Cs at a heating rate of 6 °C/min. It was held at 95 °C for 5 min, then gradually the temperature was reduced from 95 °C to 50 °C at a cooling rate of 6 °C/min and held for 50 °C for 2 min. The rotational speed was 160 1/min. The instrument measures the viscosity (expressed in mPa·s) and logs five data points every two second. To ensure accuracy, duplicate measurements were conducted for each sample and results were expressed as mean values.

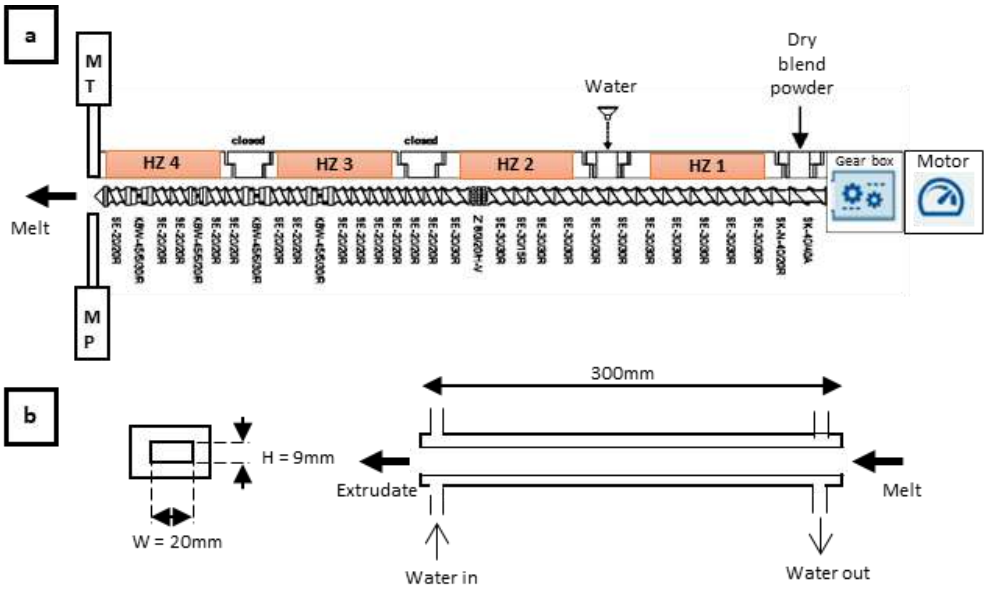

Figure 6.1 Schematic representation of (a) high moisture extrusion setup with feeding, heating zones (HZ1-HZ4) and sensors for measuring melt temperature (MT) and melt pressure (MP) and (b) long cooling die. Screw elements: SK, SKN, SE – conveying, Z – mixing and K BW – shearing elements.

2.5 High moisture extrusion

High moisture extrusion processing was done on a lab scale twin-screw extruder (TwinLab-F 20/40, Brabender GmbH & CO. KG, Duisburg, Germany) with a screw diameter of 20 mm and L/D ratio of 40. The barrel of the extruder was clamp-shell type with four heating zone (HZ1 to HZ4) powered by electrical heaters and water circulation in each zone for maintaining the set temperatures through a solenoid valve supported by a water temperature regulating cum circulator system (WTD 6es, Weinreich Industriekühlung GmbH, Lüdenscheid, Germany). The screw configuration consists of broad pitch conveying elements (SK-40/40A, SK-N-40/20R, and SE-

30/30R), narrow pitch elements (SE-20/20R), mixing element (Z-8/3/20H-V), and shear or kneading elements (KBW-45/5/30R and KBW-45/5/20R). A single screw vertical volumetric force feeder was used to feed the dry powder in the barrel at the 0 D position and water feed was at the 10 D position with a peristaltic pump (Watson-Marlow 120U/DV, Watson-Marlow Ltd., United Kingdom). Both the volumetric feeder and peristaltic pump were calibrated for each protein blend before the extrusion trial. A long cooling die, measuring 300 mm in length, 20 mm in width, and 9 mm in height, was attached to a thermostatic water circulator (Corio CD-600F, Julabo GmbH, Germany), set to maintain an inlet water temperature of 30 ºC in the cooling die with a water flow rate of 6.90 kg/hr. The schematic representation of the extruder setup, screw profile and cooling die was shown in Fig. 6.1. On attaining the steady state of the extrusion process, the extrudate samples of about 500 g were taken for further analysis.

Table 6.1 Experimental design for whole finger millet (WFM) and its fractions – polished finger millet (PFM) and hull finger millet (HFM) at barrel temperatures of 110 and 130 °C.

Run No	Primary Ingredient	Secondary ingredient	Incorporation level	Barrel temperature (°C)
1	SPI	-	100:00	110
2				130
3		WFM	90:10	110
4				130
5			80:20	110
6				130
7			70:30	110
8				130
9		PFM	90:10	110
10				130
11			80:20	110
12				130
13			70:30	110
14				130
15		HFM	90:10	110
16				130
17			80:20	110
18				130
19			70:30	110
20				130

2.6 Experimental design

From our previous experimental studies and literature, it was found that apart from moisture content, temperature plays a crucial role in texturization (Lin et al., 2002; Mateen et al., 2023). Therefore, in this study we have chosen three temperature profiles (1) 40, 60, 80, 110 ºC (from HZ1 to HZ4); (2) 40, 80, 110, 130 °C and (3) 40, 80, 120, 150 °C, but the higher temperature profile resulted in an unstable condition of extrusion because of high steam buildup. Therefore, we have collected the samples at 110 °C and 130 °C temperatures. Feed moisture content (65 %), screw speed (600 rpm), and total feed rate (4 kg/hr) were kept constant. A factorial design was used in this experiment as shown in Table 6.1.

2.7 Extruder response

The temperature thermocouple and pressure transducer were installed on-line at the end tip of the extruder screw to record the data of melt temperature (MT/ ºC) and melt pressure (MP/ bar). Load on the extruder motor in percentage was recorded to calculate specific mechanical energy (SME) using eq. (6.1) (Fang et al., 2014; Godavarti & Karwe, 1997; Osen et al., 2014). All the data of extruder response/ system parameters were recorded with a resolution of 0.1 through a user interface computer software MetaBridge (Brabender GmbH & CO. KG, Duisburg, Germany).

$$SME\ (kJ/kg) = \frac{2\pi\ x\ n\ x\ T}{MFR} \tag{6.1}$$

Where n is screw speed (rpm), T is the actual motor torque (Nm: the non-load torque was subtracted from the recorded torque values) and MFR is the mass flow rate of material (g/min).

2.8 Textural properties – TPA, cutting strength, Anisotropy and tensile strength

The textural properties of extruded samples were analyzed by using a CTX Texture Analyser (Ametek Brookfield Inc, USA) as described by Fang et al. (2014); J. Zhang et al. (2020). Extrudate samples were prepared by cutting into 20 x 20 mm cubes. Hardness, chewiness, resilience, cohesiveness, and springiness were measured as described by (Breene, 1975) using a TA3/100 AOAC standard cylindrical probe of 25.4 mm diameter with a 100 kg load cell. Measurement methods were set at 50% sample/target deformation with a 1 mm/s probe travel speed.

The cutting strength was done along and across the flow direction of extrudates by using a TA7 knife probe with a TA-CKA craft knife adapter and the setting was at 1 mm/s probe travel speed with 75% cutting of the sample's original size. The cutting strength test was done by cutting samples along and across the flow direction of extrudate to determine the anisotropic index by eq. (6.2) (Mateen et al., 2023; J. Zhang, Liu, Jiang, Faisal, et al., 2020). Tensile strength of the extrudates of size 150 mm in length and 20 mm in width was cut and pulled using a TA-DGF001 (dual grip fixture with 25 mm wide grips fitted with rubber inserts to maximize contact adhesion with sample) as described by Noguchi, (1989); Zhang et al. (2016). The measurement procedure was set at a speed of 0.5 mm s^{-1} until the extrudate was broken, and the peak tensile resistant force was recorded. All the textural measurements were done at least ten times per sample.

$$Anisotropic\ Index\ (AI) = \frac{Cutting\ strength\ along}{Cutting\ strength\ across} \tag{6.2}$$

2.9 Rheological properties

The rheological properties of extruded samples was evaluated using dynamic oscillatory measurements by a stress controlled rheometer (MCR 702e, Anton Paar GmbH, Graz, Austria). The method was based on Wang et al. (2022) with slight modifications. Before the measurements, fresh extrudates were prepared by cutting into circular shape using a circular cutting probe (diameter of 20 mm) and placed into the measuring system. The measurements were carried out using a profiled plate-plate geometry with 25 mm diameter (PPP25, Anton Paar GmbH, Graz, Austria). A constant 5 N normal force was applied to compensate small variations of the sample height of the extruded samples. Experiments were performed at 25 °C and triplicate measurement was carried out for each sample.

Amplitude test was performed within the strain range of 0.01 to 100 % at an angular frequency (ω) of 10 s^{-1}. The change of elastic modulus (G´) and viscous modulus (G´´) was recorded as a function of strain γ (%). Frequency sweep was performed in the angular frequency range of 500 to 0.1 s^{-1} with a proposed strain value by the rheometer software (RheoCompas^{TM} 1.32, Anton Paar GmbH, Graz, Austria) within the linear viscoelastic region (LVER). A power law equation eq. (6.3) was used to model G´ as a function of ω to describe the experimental data (M. A. Rao, 2007).

$$G' = K' \cdot \omega^{n'} \quad (6.3)$$

Where K′ is power law constant, n′ is frequency component and ω is angular frequency.

2.10 Macroscopic imaging and image analysis

Macroscopic images of the extruded samples were acquired using a high-resolution digital camera (Nikon D70, Nikon Co. Ltd., Thailand) within a photo box equipped with a black background and two LED light strips illuminating the sample. To reveal the internal fibrations for visual analysis, a small cut was made on the side of each sample and it was then opened.

A method of image analysis was developed using MATLAB (R2021a, MathWorks Inc., MA, USA) to quantify the visual fibrations. First, the image dimensions were set to 20 × 20 mm (height × width) make conversion between pixel and mm. Noise reduction was applied using a filter. Following this, the filtered image was converted to grayscale. The Canny edge detection algorithm was employed to identify edges within the image. These detected edges, as features, were subsequently analysed to determine parameters such as edge count, angle, and length (Fig. 6.2). The script file of matlab can be accessed from this link https://github.com/mateen-1255/Matlab-script/blob/bbe5c9303e87c288a5b7033f842b7347fec35e3c/Matlab%20Script.mlx

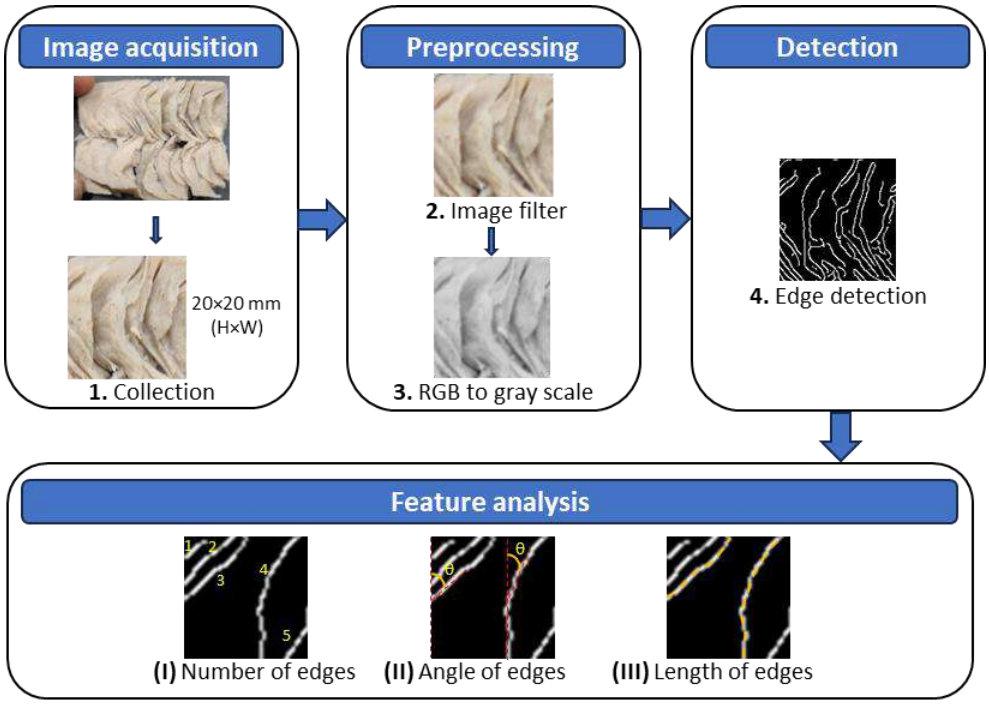

Figure 6.2 Image analysis flow for edge detection and feature analysis showing edge count, angle and path length of edges.

2.11 Colour value

The colour values of raw material, blends, and extrudate samples were measured by using a colorimeter (CR-400 chroma meter, Konica Minolta Sensing Inc., Japan). Colour was recorded according to the CIE-lab L*, a*, b* scale. L* represents brightness or lightness from 0 to 100 (black to white), a* represents green to red (positive or negative) and b* represents blue to yellow (negative or positive) (Benković et al., 2015). The total colour difference (ΔE) of the extrudates was calculated by using the following equation eq. (6.4) (Fang et al., 2014). At least five measurements were taken for each sample at randomly chosen locations.

$$\Delta E = \sqrt{(L^*_{sample} - L^*_{std})^2 + (a^*_{sample} - a^*_{std})^2 + (b^*_{sample} - b^*_{std})^2} \quad (6.4)$$

Where, L^*_{sample}, a^*_{sample}, b^*_{sample} and L^*_{std}, a^*_{std}, b^*_{std} are colour values of extrudates and raw material/protein blend respectively.

2.12 Protein solubility

Protein solubility of samples (raw and extrudates) was analysed according to the method of (F. L. Chen et al., 2011). Protein extraction was done by following buffer systems:

(1) Phosphate buffer solution (P) - 0.035mol/L pH 7.6
(2) SDS in phosphate buffer solution (P+S) – 1.5g/100ml
(3) Urea in phosphate buffer solution (P+U) – 8mol/L
(4) 2-mercaptoethanol in phosphate buffer solution (P+M) – 0.1mol/L
(5) SDS and urea in phosphate buffer solution (P+S+U)
(6) SDS and 2-mercaptoethanol in phosphate buffer solution (P+S+M)
(7) Urea and 2-mercaptoethanol in phosphate buffer solution (P+U+M)
(8) SDS, urea and 2-mercaptoethanol in phosphate buffer solution (P+S+U+M)

A sample size of 0.5 g of raw material and 1 g of extrudate (HMMA) was extracted in a centrifuge tube with 10 ml of each buffer system for 2 hours in a shaking water bath set at 40 °C. The mixture was centrifuged at 14,000 g for 10 min (C-24plus, Remi Electrotechnik Ltd., Vasai, India). The supernatant was collected to determine the soluble protein concentration by Biuret method (Plummer, 1987) at 510 nm (xMark™ Microplate Absorbance Spectrophotometer, Bio-Rad Laboratories, Inc, California,

USA) and total protein content of samples were analysed by Kjeldahl method. The protein solubility was calculated as the percentage of soluble protein in the supernatant to total protein content in the sample. Triplicate measurements were performed for each sample.

2.13 Statistical analysis

All the data were presented as mean ± SD. Analysis of variance (ANOVA) was employed to evaluate the raw material characteristics and effect of blends, incorporation level and barrel temperature on thermomechanical and extrudates properties using OriginPro software version 2023b (OriginLab Corporation, Northampton, MA, USA). Tukey test was chosen with significance of 0.05 level to identify the significant differences. A Principal Component Analysis (PCA) was carried out using the scores of all the extruded samples along with proximate composition (calculated by simple maths using raw material composition), textural properties, colour values and system parameters (SME, MT and MP) as loadings. The PCA was executed using the same software.

3 Results and Discussion

3.1 Raw material characterization

The four ingredient powders SPI, whole millet flour (WMF), starch rich flour (SRF) fraction obtained from milling dehulled grain and fiber rich flour (FRF) fraction obtained from millet hull were characterized for their particle size, bulk density, physicochemical properties and pasting properties. This was done to understand the distinctiveness of each ingredient powder, especially that of the starch rich and fiber rich fractions.

3.1.1 Particle size distribution and bulk density

Table 6.2 shows the particle size distribution and bulk density of raw material powders. As anticipated, whole finger millet flour (WMF) and its fractions (SRF and FRF) were coarser compared to SPI. More than 70% of the distribution was < 106 µm for SPI, whereas less than 20%, 40% and 46% of the distributions were < 106 µm for WMF, SRF and FRF respectively.

Bulk density was also along expected lines, with SPI being less dense than the three secondary ingredients (WMF, SRF and FRF). Among the secondary ingredients, FRF (hull fraction) displayed the lowest density (500.39 ± 16.99 kg/m^3).

Table 6.2 Particle size distribution, bulk density and physicochemical properties of SPI and finger millet flour and its fractions.

	SPI	WMF	SRF	FRF
Particle size distribution (%)				
600 > x > 425	1.51 ± 0.08^a	2.88 ± 1.65^a	0.88 ± 0.10^a	0.83 ± 0.05^a
425 > x > 212	5.02 ± 0.62^c	26.29 ± 4.20^a	17.86 ± 2.85^b	18.84 ± 1.17^b
212 > x > 106	22.90 ± 1.73^d	54.62 ± 2.73^a	42.11 ± 2.59^b	33.69 ± 1.22^c
106 > x > 75	50.42 ± 2.71^a	15.13 ± 0.82^c	35.31 ± 2.54^b	35.78 ± 1.27^b
75 > x > 53	18.88 ± 1.03^a	1.09 ± 0.89^d	3.84 ± 0.36^c	10.86 ± 0.27^b
53 > x > 0	1.27 ± 0.06^a	0.00 ± 0.00^b	0.00 ± 0.00^b	0.00 ± 0.00^b
Bulk density (kg/m^3)	323.75 ± 16.89^c	577.40 ± 20.14^a	595.93 ± 25.18^a	500.39 ± 16.99^b
Physicochemical properties				
WAC (g/g)	5.92 ± 0.18^a	2.32 ± 0.00^c	2.27 ± 0.00^c	2.97 ± 0.02^b
WS (%)	23.06 ± 0.32^a	3.66 ± 0.11^b	2.95 ± 0.08^c	3.98 ± 0.18^b
Colour value of powders				
L*	89.08 ± 0.10^a	73.93 ± 0.84^c	81.41 ± 0.22^b	63.69 ± 0.31^d
a*	2.19 ± 0.02^d	4.11 ± 0.09^b	3.28 ± 0.05^c	8.54 ± 0.12^a
b*	16.84 ± 0.42^a	9.79 ± 0.29^c	10.9 ± 0.15^b	16.92 ± 0.46^a

WAC – Water absorption capacity. WS – Water solubility. Values followed by different letters within each parameter show statistically significant differences ($p \leq 0.05$).

3.1.2 Ingredient composition

Proximate analysis of the 4 ingredients – SPI, WMF, SRF and FRF is given in Table 6.3. The FRF and SRF were found to be compositionally distinct from each other. The FRF obtained by milling of the hull had a fiber content of 26.43 ± 0.36 % db, versus the SRF obtained from milling of the polished grain which had a fiber content of 2.81 ± 0.09 % db. As expected, the WMF had an intermediate fiber content of 14.01 ± 0.35 % db. SPI had negligible fiber content (0.77 ± 0.05 % db). 85 – 90 % of the total dietary fiber in all samples were insoluble fibers.

The four ingredients also differed in starch content. SPI had negligible starch. SRF had a starch content of 82.43 ± 1.41 % db and the FRF had a starch content of 52.95 ± 2.04 % db. The starch content of WMF was 66.30 ± 1.87 % db. Further, the three flour ingredients WMF, SRF and FRF were analyzed for the amylose and amylopectin content (by subtracting from the amylose content of total starch). FRF had an amylose content of 22.48 ± 0.71 % while the SRF had an amylose content of 13.54 ± 0.15 %. The difference in amylose content between these fractions can be explained by the

spatial distribution of amylose within the grain as effected by the growth and development of grain. This pattern of amylose distribution was found generally in most of the cereal grains (Zhou et al., 2018). Though there is a difference in amylose content on starch basis, the overall level of amylose in different flour samples was similar (around 11 %) due to the higher total starch content of SRF. However, amylopectin content between the two fractions was significantly different on a flour basis with SRF having amylopectin content of ~70% and FRF ~30%.

Table 6.3 Proximate composition of SPI, WMF, SRF and FRF.

	SPI	**WMF**	**SRF**	**FRF**
Moisture content (% wb)	6.84 ± 0.22^{c}	9.19 ± 0.07^{b}	8.74 ± 0.21^{b}	10.92 ± 0.73^{a}
Protein content (% db)	96.10 ± 0.66^{a}	8.68 ± 0.16b^{bc}	9.71 ± 0.34^{b}	7.98 ± 0.35^{c}
Lipid (% db)	0.16 ± 0.02^{c}	2.21 ± 0.09^{b}	2.44 ± 0.07^{a}	2.36 ± 0.03^{ab}
Starch (% db)	0.17 ± 0.01^{d}	66.30 ± 1.87^{b}	82.43 ± 1.41^{a}	52.95 ± 2.04^{c}
Amylose (%) in starch	-	16.82 ± 0.25^{b}	13.54 ± 0.15^{c}	22.48 ± 0.71^{a}
Total dietary fiber (% db)	0.77 ± 0.05^{d}	14.01 ± 0.35^{b}	2.81 ± 0.09^{c}	26.43 ± 0.36^{a}
Soluble dietary fiber (% db)	0.19 ± 0.02^{c}	1.06 ± 0.04^{b}	0.20 ± 0.01^{c}	1.86 ± 0.08^{a}
Insoluble dietary fiber (% db)	0.58 ± 0.04^{d}	12.90 ± 0.2^{b}	2.38 ± 0.07^{c}	22.22 ± 0.28^{a}
Ash (% db)	3.52 ± 0.57^{a}	2.38 ± 0.12^{b}	1.53 ± 0.08^{c}	3.21 ± 0.13^{a}

wb – wet basis. db – dry basis. Values followed by different letters within each parameter show statistically significant differences ($p \leq 0.05$).

Ash content of the FRF at 3.21 ± 0.13 % db was more than double that of the SRF (1.53 ± 0.08% db). This is due to the distribution of higher levels of minerals in the outer layer of the grain (Tanaka et al., 1974). The difference in proteins and lipids between the two fractions were smaller. Whole millet, fiber-rich and starch-rich fractions had protein contents of 8.68, 7.98% to 9.71% db respectively. SPI had the highest protein content (96.10 ± 0.66% db) as expected of a protein isolate. Regarding lipid content, the SPI recorded the lowest value (0.16 ± 0.02% db), whereas the fiber-rich fraction contained relatively higher lipids (2.44 ± 0.07% db) compared to whole millet.

3.1.3 Physicochemical properties

The water absorption capacity (WAC) and water solubility (WS) of the ingredients are shown in Table 6.2. SPI has the highest WAC (5.92 ± 0.18 g/g) and WS (23.06 ± 0.32 %) because of higher affinity of water molecules towards protein compared to starch at room temperature. Among millet flours, FRF showed higher WAC (2.97 ± 0.02 g/g) and WS (3.98 ± 0.18 %). SRF had the least WAC (2.27 ± 0.00 g/g) and WS (2.95 ± 0.08%). The higher WAC of FRF amongst the three flours could be due to higher soluble dietary fiber content (1.86 ± 0.08 % db), as soluble fibers tend to form gel by absorbing water (Boulos et al., 2000) while its higher WS could be due to the lower starch content as starch is insoluble at room temperature.

3.1.4 Pasting properties

The results for the pasting characteristics of soy protein, whole flour and its fractions were shown in Fig. 6.3. The pasting curves were obtained by ramping the temperature to 95 °C, holding it there for seven minutes, and then cooling to 50 °C (Fig. 3). Soy proteins, while soluble at these conditions, do not build high viscosity as the temperatures are not high enough for their complete denaturation and gelation (Akinwale et al., 2017). Their pasting curve was lower than that of the millet flour and fractions and displayed a peak viscosity of 825.3 mPa·s and a final viscosity of 884.3 mPa·s.

The FRF had a pasting curve that was higher than that of SPI but was much lower than that of the whole millet flour and the starch-rich fraction. This was probably due to its lower starch and higher insoluble fiber content which resulted in a weaker gel, even though it is higher amylose. Peak and final viscosities for millet flours varied from 1320 to 2333 mPa·s and 1926 to 3266 mPa·s respectively. Pasting temperature (temperature at the onset of rise in viscosity) of WMF and its fractions (SRF and FRF) ranged from 66.7 to 71.4 °C. The pasting temperature serves as an indicator of the lowest temperature required to gelatinize the flour. The highest pasting temperature was for FRF. The high pasting temperature indicates the presence of amylose starch and fibers that are highly resistant to swelling and rupturing (Kaur & Singh, 2005). Holding strength or trough viscosity varied from 717.1 to 1618 mPa·s and SRF fractions showed highest value. Breakdown viscosity which measures the difference between magnitude of peak viscosity and trough viscosity (represents the stability of the sample against applied temperature and shear). As per breakdown viscosity values, the most stable sample was

SPI (108.1 mPa·s) followed by FRF (278.6 mPa·s). Setback viscosity measure of retrogradation tendency or syneresis of flours SRF fraction showed higher setback viscosity followed by WMF and FRF.

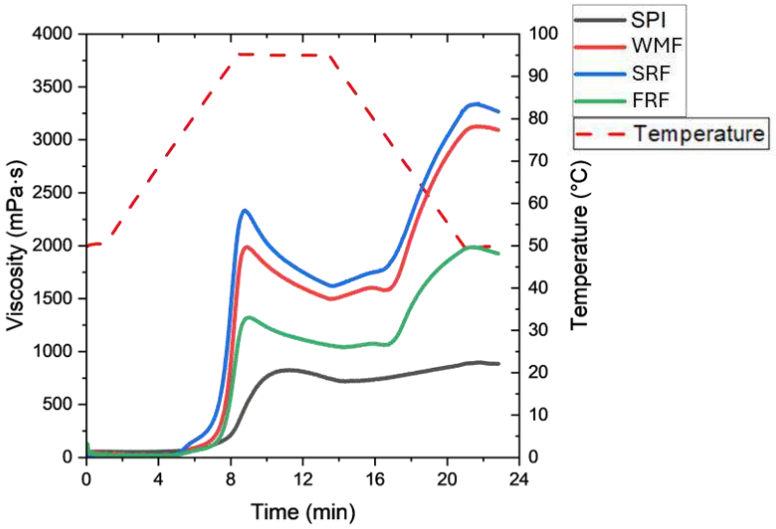

Figure 6.3 Pasting property of soy protein isolate (SPI), whole finger millet (WMF), starch rich flour (SRF) and fiber rich flour (FRF).

Thus, the above results show that the FRF and SRF fractions were compositionally very different from each other and these differences impact the physicochemical properties and pasting properties of the two fractions along expected lines.

3.1.5 Composition of the blends used in extrusion experiment

Nine blends were made by combining WMF, SRF & FRF with SPI and 100% SPI was used as a control (Table 6.1). The compositions of the blends are given in Table 6.4 and show that the biggest differentiators between the blends are protein (69.66 to 96.10%), amylopectin starch (near 0 to 21.50%) and insoluble fiber (near 0 to 7.7%). In general, it is known that proteins are key to creating networks and the hardness of the aggregates increases with protein concentration, amylopectin are water soluble and help in increasing viscosity and gel formation upon cooling and insoluble fibers while improving visual fibration, can disrupt the structures at high incorporation levels.

This study looks at how these generalizations playout when these components are a part of a complex mix such as WMF, SRF & FRF which is added to SPI and extruded under controlled high moisture conditions.

Table 6.4 Chemical composition of blends (SPI+WMF, SPI+SRF and SPI+FRF).

Compositional parameters (% db)	100 % SPI	90:20			80+20			70+30		
		SPI+: WMF	SPI+ SRF	SPI+ FRF	SPI+ WMF	SPI+ SRF	SPI+ FRF	SPI+ WMF	SPI+ SRF	SPI+ FRF
Protein	96.10	87.36	87.46	87.29	78.62	78.82	78.48	69.87	70.18	69.66
Starch	0.17	6.78	8.40	5.45	13.40	16.62	10.73	20.01	24.85	16.00
Amylose	-	1.12	1.12	1.19	2.23	2.23	2.38	3.35	3.35	3.57
Amylopectin	-	5.67	7.28	4.26	11.17	14.39	8.35	16.66	21.50	12.43
Total dietary fiber	0.77	2.09	0.97	3.34	3.42	1.18	5.90	4.74	1.38	8.47
Insoluble dietary fiber	0.58	1.81	0.76	2.74	3.04	0.94	4.91	4.28	1.12	7.07
Soluble dietary fiber	0.19	0.28	0.19	0.36	0.36	0.19	0.52	0.45	0.19	0.69
Lipid	0.16	0.37	0.39	0.38	0.57	0.62	0.60	0.78	0.84	0.82
Ash	3.52	3.41	3.32	3.49	3.29	3.12	3.46	3.18	2.92	3.43

3.2 Extruder responses: Specific mechanical energy, melt temperature and pressure

SPI 100% has high SME values and melt pressures. Incorporation of the millet fractions, both FRF & SRF result in a dramatic reduction in SME and melt pressure (Fig. 6.4a and 6.4c) with each reducing to between half to a third. Such dramatic reduction has also been reported by other researchers (Lin et al., 2002; Mateen et al., 2023).

Thus, while pasting curves ramped to 95 C show that the flours are more viscous than SPI. Under extrusion, the higher SME of 100% SPI suggests that once fully melted and denatured, with the protein chains opened and tangled, it has a much higher viscosity. However, the pasting properties, though not at extrusion temperature and pressure do serve as a good guide for predicting the order of SME of the blends with SRF showing higher SME and melt pressure compared to FRF for the corresponding processing conditions. This is probably due to the higher amylopectin content of the SRF blends, which is a more soluble starch (Green et al., 1975). Interestingly at 130 °C at 30% incorporation levels the trend reverses and FRF shows higher SME and melt pressure.

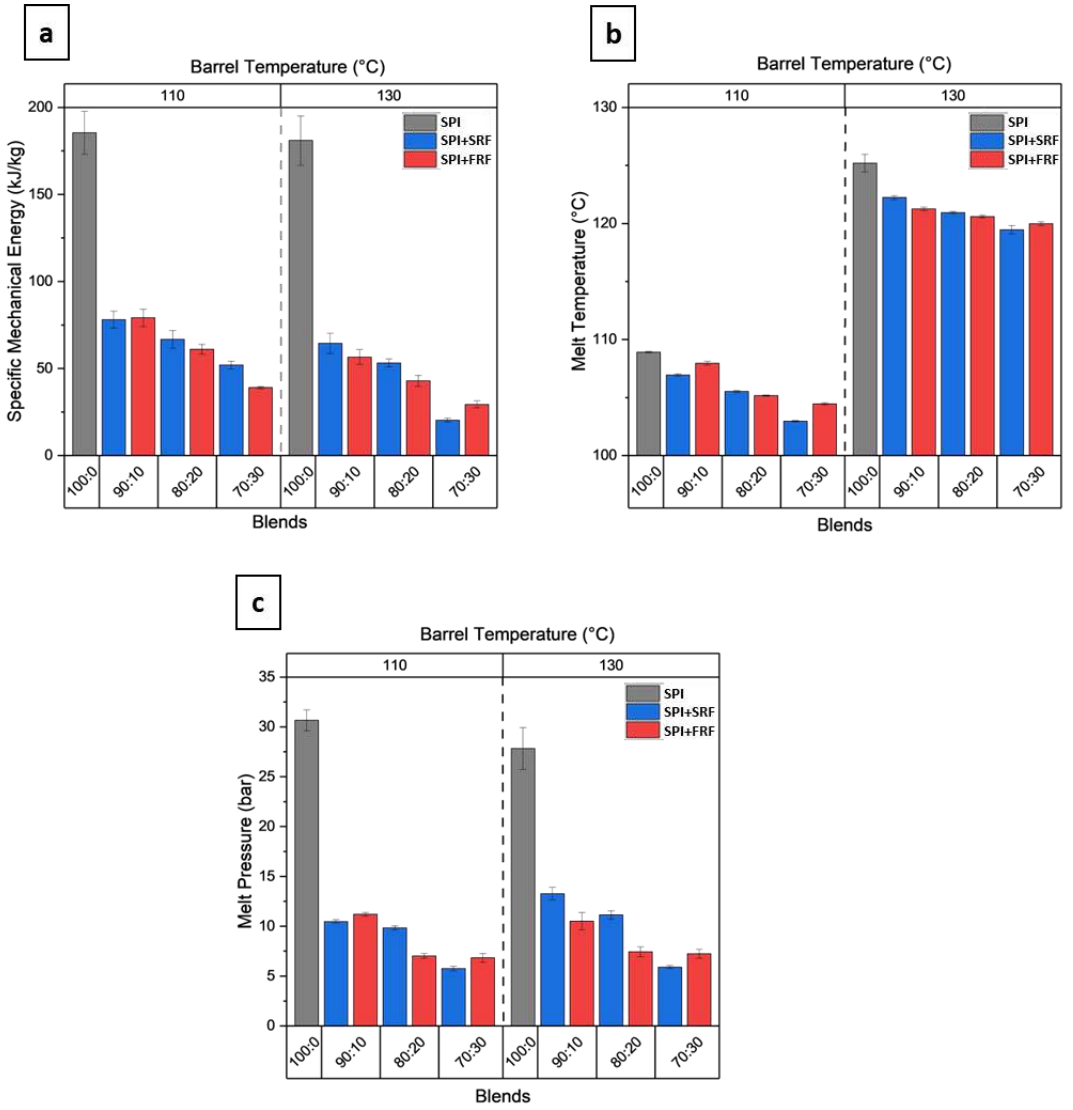

Figure 6.4 Effect of fraction blends, incorporation levels and barrel temperature on the extruder responses (a) specific mechanical energy, (b) melt temperature and (c) melt pressure.

The melt temperature (MT) follows the set barrel temperature. However, there is always a gap between set barrel temperature and melt temperature. The gap is lowest for 100% SPI and higher for the blends (Fig. 6.4b). The lower viscosity of the blend melts, as indicated by the lower SME of the blends, will lead to lower heat generation due to shear. This partially explains the gap. We had expected that the lower viscosity would also improve surface heat transfer but clearly that does not compensate for the lower shear heating. Another reason for the higher gap for the blends could be the higher endothermic enthalpy for gelatinization of starch in the millet fractions compared to that of melting of proteins (K. Li et al., 2019; S. Li et al., 2014).

3.3 Instrumental anisotropy, visual fibration and image analysis

The anisotropy in the fiber structure was studied qualitatively by visual examination of the extrudates and quantitatively using image analysis. Anisotropy was also studied by the ratio of cutting forces in longitudinal and transverse directions of the extrudates following the methods of Noguchi (1989) and Zhang et al. (2022) and referred to as anisotropic index.

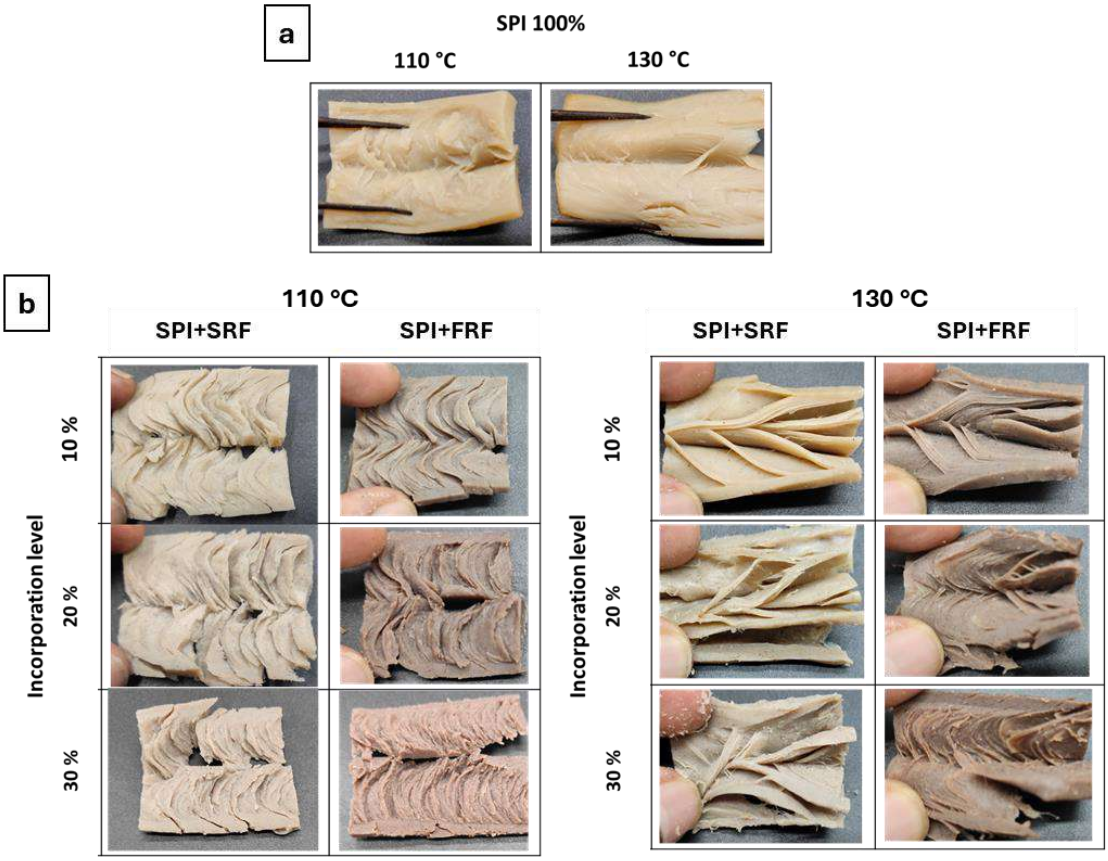

Figure 6.5 Visual images of (a) soy protein isolate (SPI) 100 %, (b) blends at 110 °C and 130 °C.

The visual images of the extrudates are presented in Fig. 6.5. All the 10 extrudates show fibers in the longitudinal direction i.e. along the direction of extrusion. However, the nature of the fibers differs in their thickness, density, length and orientation. The extrudates of SPI 100% at different temperatures showed thick fibers and low number density across a cross-section compared to the blends (Fig. 6.5a). The highly multiphasic character of the blends, due to presence of starch and fiber along with proteins, maybe contributing to the increased visual fiber structure (Dekkers, Boom, et al., 2018; Tolstoguzov, 1993). Furthermore, protein solubility analysis in different buffer systems revealed that blends containing secondary components exhibited higher

solubility in most of the solvents compared to SPI 100% HMMA (Table 6.6), indicating stronger hydrophobic interactions, hydrogen bonds, and disulfide bonds. Thus, showing a rich fibrous structure in the HMMA made from blends. SRF blends showed thicker fibers than FRF blends. As incorporation increases from 10% to 30%, the fibers seem to get thinner for both blends. Visual images of SRF blend at 130 °C showed good fibration even at 30% whereas, FRF blend showed distorted fibers at 30%. The distorted structure at higher incorporation of FRF was probably due to the higher insoluble fibers which interferes with the protein-protein interaction making it a weaker structure.

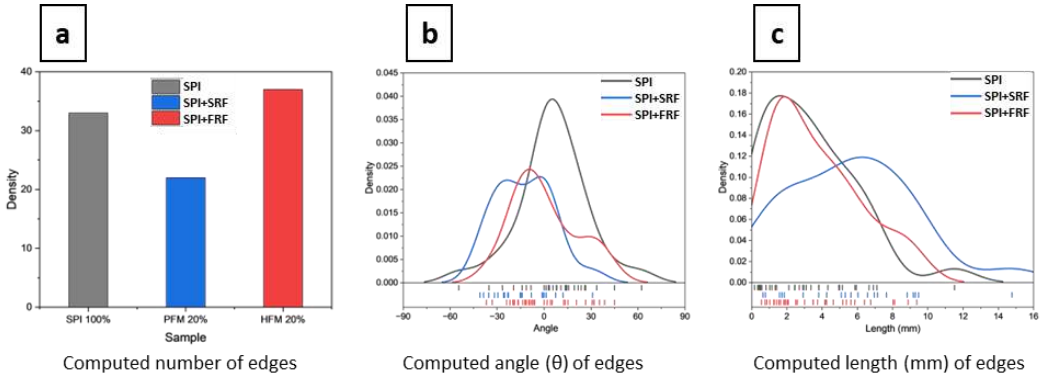

Figure 6.6 Computed visual image features (a) number of edges, (b) distribution of edge angle and (c) distribution of edge length of SPI 100% and finger millet fractions.

An image analysis method was also developed to quantify visual fibration in meat analogues. This method provides quantitative data such as number, length, and angle of fibers in terms of edges, serving as a simple and useful tool for researchers and meat analogue manufacturers. Parameters from image analysis are in line with the visual information, as expected while bringing in objectivity. As an example, the number of edges of SPI 100% is lower than of the blends (Fig. 6.6a). The 20% SRF blend had broader distribution of edge length and lowest number of edges compared to other blends at 130 °C (Fig. 6.6a). The blend extrudates at 110 °C showed a shorter fiber whereas, HMMA extruded at 130 °C showed longer fibers.

While all the extrudates showed anisotropy as characterized by presence of fibers visually and by image analysis, instrumental analysis of anisotropy revealed a slightly different story (Fig. 6.7d). SPI 100% had an anisotropic index close to 1 i.e. showing very low instrumental anisotropy. All the blends had AI more than 1. SPI 100 % showed the highest cutting strength in both directions longitudinal and transverse and both increased with increase in temperature. The cutting strength dropped in the extrudates

made from blends. Comparing only the blends with each other, though differences were small, cutting strength showed higher values for FRF blends followed by SRF and WMF blends. As incorporation increases from 10 % to 30 %, cutting strength decreased significantly ($p < 0.05$).

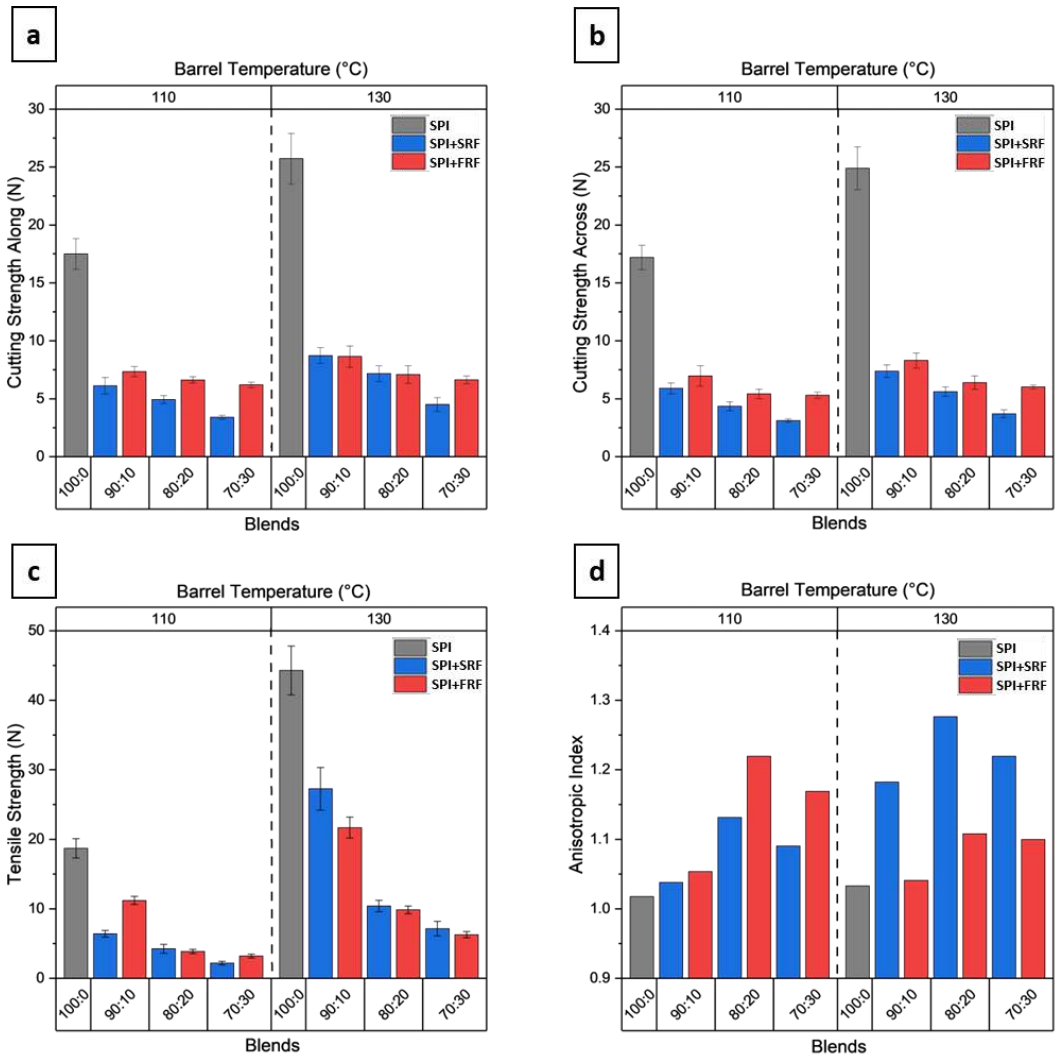

Figure 6.7 Cutting strength (a) along and (b) across the flow of extrudates, (c) Anisotropic index and (d) Tensile strength.

The instrumental measure of anisotropy as characterized by cutting strength will likely translate to an in-mouth experience of fibrous character. The results show that visual appearance of fibers may not necessarily translate to in mouth experience of fibrousness. Both visual and instrumental fibrousness should be targeted when making good HMMA's.

3.4 Textural properties

A full spectrum range of textural properties which include hardness, chewiness, cohesiveness, resilience, springiness, and tensile strength was analyzed for each extrudates. The effect of whole millet and its fractions at different incorporation levels (10, 20 and 30 %) and at different barrel temperatures (110 °C and 130 °C) on textural properties is shown in Fig. 6.8. All the independent variables had a significant effect on most of the textural properties. Incorporating the millet fractions with SPI has the most impact on hardness and chewiness. Pure SPI 100% showed hardness of 194.51 and 318.19 N at 110 C and 130 C respectively and chewiness value of 1191.41 and 1362.30 mJ at 110 and 130 °C respectively. Even at the lowest incorporation level of 10% hardness and chewiness drop down dramatically, with hardness values dropping by 50% and chewiness values by 65%. Increasing level from 10 % to 30 %, further decreases the hardness and chewiness for all the blends, but in absolute value terms this reduction is lower extent compared to the dramatic reduction between 0% and 10% incorporation. This gradual reduction with increase in incorporation level of millet fractions is expected as the secondary ingredients dilute the overall protein concentration in the matrix and protein concentration of the blend strongly correlates with these textural parameters (Mateen et al., 2023).

With respect to temperature, hardness and chewiness increases with temperature because of higher degree of protein denaturation and aggregation. Our results of temperature effect were in line with the literature (N. Kitabatake et al., 1990; Mateen et al., 2023; H. Wang, van den Berg, et al., 2022). It should be noted that the reduction is more pronounced at the higher temperature (130 °C) as 100% SPI extrudes into a very hard block at higher temperatures and the millet flours reduce hardness to half or even lesser here.

Among the blends, SRF blends showed lower hardness and chewiness compared to FRF blend over all the different incorporation levels and temperatures. The lower hardness and chewiness of the SRF blends may be due to higher starch content and lower dietary fiber content compared to FRF's (insoluble fiber content of 22.22 ± 0.28 % for FRF vs 2.38 ± 0.07 % for SRF, starch of 52.95% for FRF vs 82.43% for SRF). Rekola et al., 2023 similar observations during extrusion of pea protein and cereal brans containing wheat bran and oat bran. They observed that the extrudate with higher

insoluble dietary fiber containing wheat bran exhibited greater hardness compared to the extrudate with lower insoluble dietary fiber containing oat bran. Other studies also found similar interpretations (Ramos Diaz et al. 2022; Deng et al. 2023).

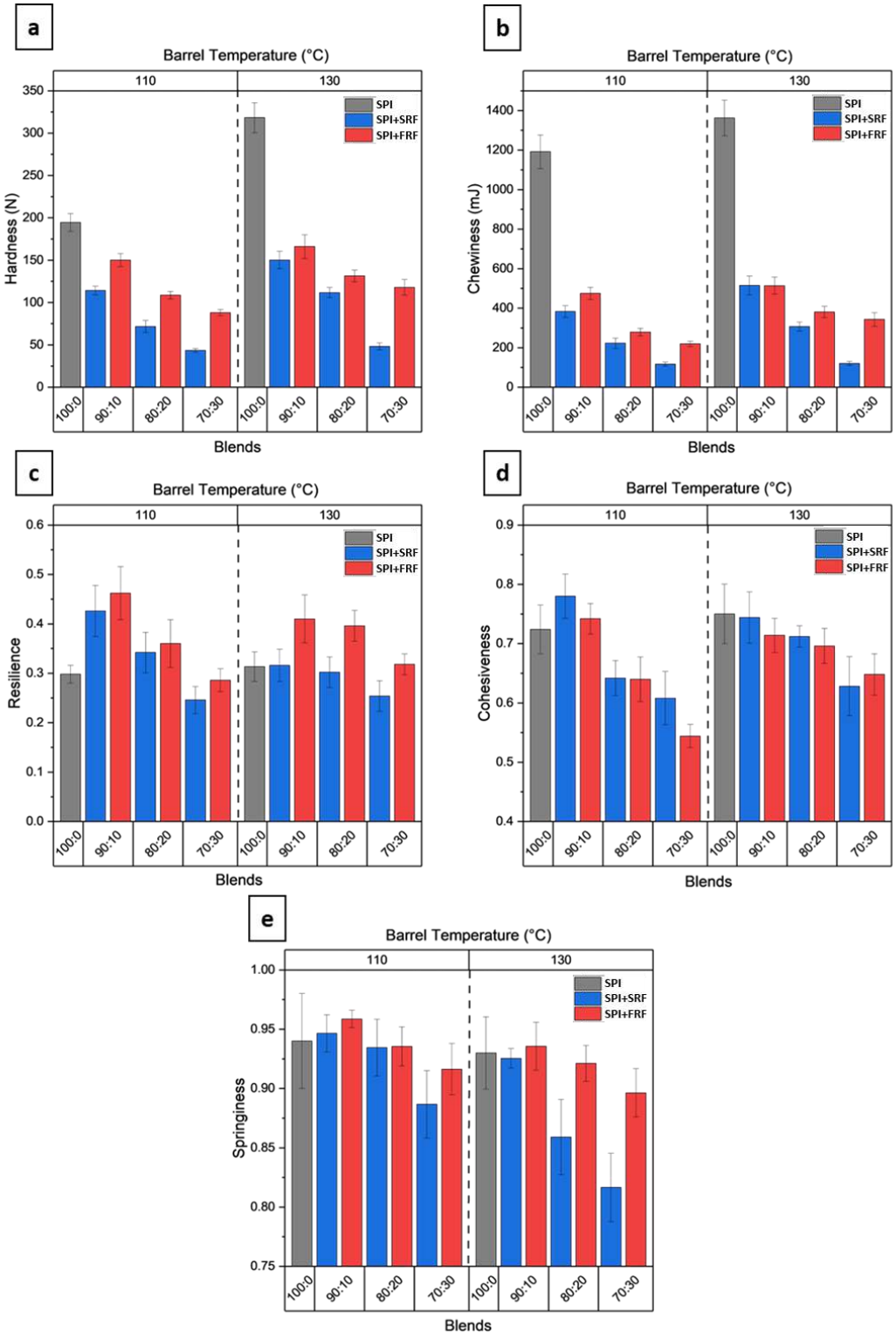

Figure 6.8 Effect of finger millet fractions at different incorporations and temperature on textural properties

The hardness and the strong gel structure of the extrudates has also been related to the ash content and divalent calcium ions in literature. Ferawati et al. (2021) showed that the extrudates made from faba bean containing higher amounts of calcium had higher hardness value than yellow pea protein when extruded at similar process conditions. Nasrollahzadeh et al. (2022) also showed the similar relationship with the calcium and the hardness of the extrudates in hemp proteins. In this study, between the SRF and FRF blends, FRF showed higher hardness, probably due to the higher ash content (3.43 % db at 30% incorporation) compared to SRF blend (2.92 % db at same incorporation) and this could also be a contributing factor. Finger millet flour is rich source of calcium with levels as high as 344 mg/100g (P. B. Devi et al. 2014) and most of the minerals are distributed in the hull which forms the FRF. This may have yielded harder extrudate.

Unlike hardness and chewiness which decreases with incorporation of the millet flours, the values of resilience for the blends were higher than that for SPI 100 %. The FRF blends showed the highest resilience followed by SRF blends and then SPI 100%. The effect of temperature and incorporation on resilience was less pronounced compared to that on hardness and chewiness. Cohesiveness did follow a pattern with values decreasing as incorporation levels increased. The drop was greater at 110 C compared to 130 C. Interestingly, cohesiveness at the 10% incorporation was either similar to SPI 100% (at 130 C) or higher (at 110C). Both SRS and FRF behaved very similarly with respect to impact on cohesiveness. Springiness values were minimally impacted by SRF at all incorporation levels and temperatures. The FRF had a stronger effect on springiness, especially at 130C where the value dropped as incorporation level increased.

Like hardness and chewiness, tensile strength also showed similar trends with respect to temperature, incorporation level and blends. However, the magnitude of differences was much larger (Fig. 6.7c). From our haptic observations it was found that the FRF blends were comparatively brittle. This observation can be correlated to the tensile strength, where the FRF blends showed lower tensile strength than polished fraction blends.

The texture profile of cooked real meat can be used as a reference to compare with HMMA made at 130 °C barrel temperature, as this process condition produced good

visual fibrations (Fig. 6.9). The texture parameters of SPI 100% are all out of range of real meat. The texture parameters of the HMMAs made with the blends start shifting towards the range of real meats. Most of the TPA parameters of beef were in the range of blend HMMA, Chicken and lamb were also in the range in hardness and chewiness and slightly lower in other parameters without significant difference ($p < 0.05$). This suggests that the HMMA made from WMF blend which was reddish-brown in colour (Fig. 6.5) and are comparable with the beef whereas, SRF blend HMMAs were whitish and brighter in colour and comparable with chicken as SRF blend HMMA showed slightly lower resilience, cohesiveness and springiness compared to other blends.

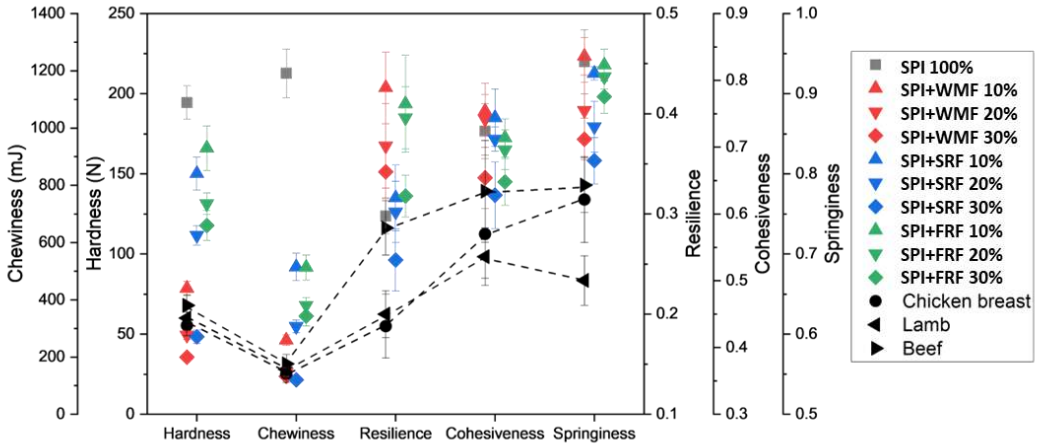

Figure 6.9 TPA profile of HMMA made from SPI 100% and blends of millet fractions (at 130 °C barrel temperature) and compared against the real meat (chicken breast, lamb and beef steak).

3.5 Rheology

3.5.1 Amplitude sweep

The rheological properties of HMMA under small amplitude sweep was shown in Fig. 6.10 where G´ and G´´ was plotted as a function of shear strain. Table 6.5 summarizes the average values of G´ and G´´ in the LVER, strain γ (%) at which the extrudates start to deform and crossover point (G´ = G´´). within the LVER, all the extrudates showed a G´ dominated over G´´, indicating an elastic (gel like) behaviour (Fischer and Windhab 2011; Lan and Lai 2023). After a critical strain value of 4 to 10 %, a nonlinear decrease and increase in the G´ and G´´ respectively, was observed in all the samples, suggesting that the structure of extrudates was irreversibly changed. A crossover of G´ and G´´ was

found with the further rise of shear strain for all the samples, indicating the sample become disintegrated and started to flow (Hong Wang et al. 2022).

All the extrudate samples had different rheological properties as effected by the blends, incorporation level and temperature. SPI 100 % had higher viscoelasticity compared to HMMA made from all the millet flour blends. Within the HMMAs made from the millet flour blends, FRF and SRF showed significantly higher averaged G´ and G´´ values than WMF blend HMMA. This suggests that these samples have more elastic property. This is also seen in the tensile strength (Fig. 6.7c). A critical shear strain corresponding to the LVER of these samples suggests that the SRF blend HMMA reached a critical strain (0.33 ± 0.00 %) earlier than FRF HMMA though it had similar G´. As barrel temperature increases from 110 °C to 130 °C, G´, G´´ and critical strain values increases. A crossover point of FRF (20 % incorporation) showed higher strain at which it disintegrates, suggesting larger LVER with less firm structure.

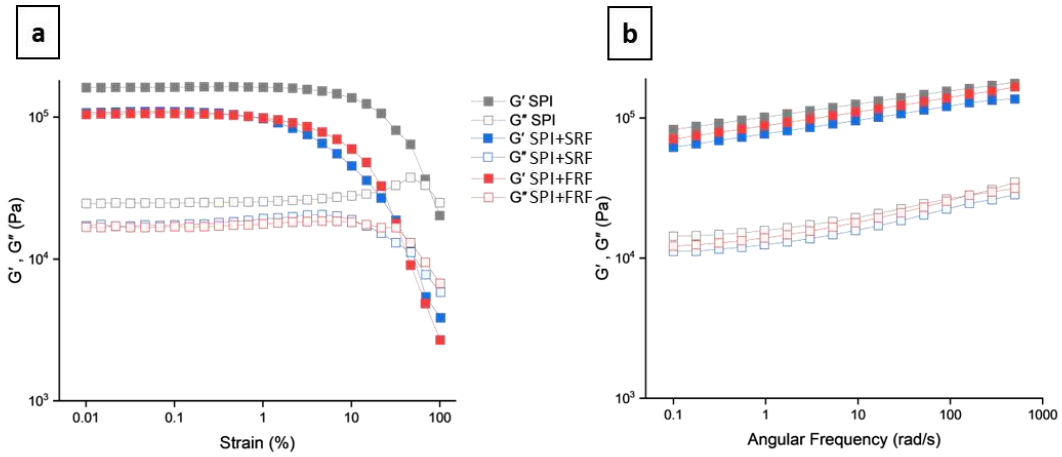

Figure 6.10 Rheological properties of HMMA tested under (a) amplitude sweep and (b) frequency sweep to understand the effect of finger millet fraction blends at 20 % incorporation and at 130 °C barrel temperature.

3.5.2 Frequency sweep

Frequency sweep results with log G´ and log G´´ were plotted against log ω as shown in Fig. 6.10b. With G´ > G´´, all the extruded samples were elastic, suggesting the typical characteristic of cross-linked networks with a gel like behaviour elucidating the distinctions in texture and structural properties. With increasing frequency, G´ and G´´ was gradually increased, which could be due to the disentangled molecular chains during the short period of oscillation (M. A. Rao 2007). The trends in the G´ and G´´

of frequency sweep as affected by the blends, incorporation and temperature were similar to the averaged G´ and G´´ modulus of amplitude sweep test.

Table 6.5 Rheological properties of HMMA samples (extruded at 20% incorporation and 130 °C barrel temperature) as determined by amplitude sweep and power law equation fit obtained from the frequency sweep.

	Amplitude test					Frequency test		
	LVER			Cross over		Power law		
	G´ ($\times 10^3$ Pa)	G´´ ($\times 10^3$ Pa)	Critical strain (%)	G´ = G´´ ($\times 10^3$ Pa)	Strain (%)	K´ ($\times 10^3$)	n´	R^2
SPI 100%	161.81 ± 1.63^{a}	25.09 ± 0.44^{a}	2.95 ± 0.02^{a}	30.36 ± 0.91^{a}	76.97 ± 0.31^{a}	101.96 ± 2.06^{a}	0.092 ± 0.003^{c}	0.998
SPI+ SRF	108.22 ± 1.01^{b}	17.36 ± 0.30^{b}	0.33 ± 0.00^{g}	10.56 ± 0.32^{c}	50.00 ± 0.27^{f}	77.22 ± 0.77^{c}	0.097 ± 0.002^{abc}	0.997
SPI+ FRF	104.82 ± 1.41^{c}	16.92 ± 0.23^{b}	0.54 ± 0.01^{e}	16.02 ± 0.16^{b}	34.04 ± 0.14^{h}	88.37 ± 2.65^{b}	0.100 ± 0.002^{ab}	0.999

LVER – Linear viscoelastic region. Values followed by different letters within each parameter show statistically significant differences ($p \leq 0.05$).

A power law model (eq. 4) was used to fit the function of log G´ and log ω and the results were shown in Table 6.5. According to Rao (2007) and Wang et al. (2022), n´ (behaviour index) is a slope of log G´ versus log ω, indicating zero for pure elastomer and positive slope for weak gels and high concentration solutions. All the values of n´ were in the range 0.09 to 0.10, implying that all the extruded samples behave like an elastomer. K´ (consistency index) was used to evaluate the viscoelastic properties. Higher K´ values was observed in SPI 100%, indicating a stronger structure than blends. FRF blend extrudate exhibited a higher K´ (88.37 ± 2.65 $\times 10^3$) than SRF extrudate (77.22 ± 0.77 $\times 10^3$), suggested that FRF has a stronger structure than SRF extrudate. Whereas K´ increases with increase in temperature. At higher temperatures, protein cross linked and created a more compact and stable structure, thus enhancing the elasticity at 130 °C. The results of effect of temperature were in accordance with the literature (Sun et al. 2022; Hong Wang et al. 2022). The rheological data was well correlated with the textural results.

3.6 Protein-protein interaction

Eight buffer solutions, described in chapter 6 section 2.12, were used for extracting proteins and the results are given in Table 6.6. Phosphate buffer (P) will extract the native state proteins, SDS (P+S) will break and extract the hydrophobically interacted proteins, urea (P+U) will break and extract hydrogen bonded and hydrophobically interacted proteins and 2-mercaptoethanol (P+M) will cleave the covalent disulfide bonds and extract the proteins. The combination buffer systems were used to understand the interaction between hydrophobic-hydrogen bonds (P+S+U), hydrophobic-disulfide bonds (P+S+M), hydrogen bonds-disulfide bonds (P+U+M) and in the isoelectric focus (P+S+U+M) (F. L. Chen et al., 2011; Liu & Hsieh, 2008). In general, and as expected, protein solubility decreases significantly ($p < 0.05$) after extrusion in all the extracting buffer systems.

The single reagent solubilization's (P+S, P+U, P+M) suggest that non-covalent bonds dominate in both raw powders and extruded HMMA's. As a result, the solubilization effect due to breaking of disulfide bonds (P+M buffer) was lower than the two non-covalent bond breaking reagents (P+S and P+U). However, when non-covalent & covalent bond breaking reagents are combined, the increase in solubility is very large. This is evidenced by the dramatic increase of solubility of P+S+M and P+U+M combinations compared to P+S+U. This suggests that the covalent disulfide linkages are harder to reach in the protein aggregates and require the non-covalent linkages to be broken for them to become accessible.

Extrudate made from the blends of SRF and FRF showed higher solubility in most of the buffers as compared to extrudate of SPI 100%. This suggests that while new linkages have been created during extrusion, these are more accessible to the reagents, compared to SPI 100%. This is probably why the solubility reduction between raw & extruded samples is lower in millet-based blends.

Q. Chen et al. (2023) found that the high moisture extrudates made from blend of pea protein isolate and amylopectin (90:10) showed significant increased protein solubility P+S and P+U compared to extrudates made from pea protein isolate alone and no difference for disulfide bonds. This suggests that the starch and fibers in the blends can form higher numbers of interactions (hydrogen bonds and hydrophobic interactions)

with the protein giving a more fibrous structure visually to the extrudates as seen in Fig. 6.5.

Table 6.6 Protein solubility of raw vs extruded samples as an effect of blends (20% incorporation and 130 °C barrel temperature).

	Native (P)	Hydrophobic (P+S)	Hydrogen bonds (P+U)	Disulfide bonds (P+M)	Hydrophobic-Hydrogen bonds (P+S+U)	Hydrophobic-Disulfide bonds (P+S+M)	Hydrogen bonds-Disulfide bonds (P+U+M)	Hydrogen bonds-Hydrophobic-Disulfide bonds (P+U+S+M)
SPI (Raw)	9.52 ± 0.31^{b}	30.28 ± 1.05^{c}	36.65 ± 1.28^{a}	27.38 ± 0.93^{a}	46.33 ± 2.18^{a}	65.22 ± 1.96^{ab}	64.66 ± 0.65^{a}	81.32 ± 3.25^{a}
SPI (HMMA)	8.61 ± 0.24^{cd}	21.01 ± 0.93^{e}	27.28 ± 1.01^{e}	18.97 ± 0.25^{fg}	38.15 ± 2.74^{cde}	46.38 ± 0.93^{f}	52.12 ± 2.08^{defg}	72.89 ± 1.46^{bc}
SPI+ SRF (Raw)	10.71 ± 0.12^{a}	35.42 ± 0.83^{ab}	35.91 ± 2.82^{a}	26.25 ± 0.63^{ab}	46.62 ± 2.18^{a}	67.93 ± 1.36^{a}	66.52 ± 1.33^{a}	78.92 ± 0.79^{ab}
SPI+ SRF (HMMA)	9.27 ± 0.11^{bc}	29.82 ± 0.69^{c}	33.60 ± 2.18^{abc}	24.74 ± 1.03^{bc}	41.07 ± 1.86^{abcde}	61.08 ± 1.22^{c}	58.18 ± 2.23^{bc}	76.88 ± 3.08^{ab}
SPI+ FRF (Raw)	10.70 ± 0.16^{a}	35.96 ± 0.84^{a}	34.50 ± 1.82^{ab}	26.13 ± 1.30^{ab}	45.80 ± 1.94^{ab}	64.91 ± 1.95^{ab}	62.18 ± 0.62^{ab}	77.03 ± 3.08^{ab}
SPI+ FRF (HMMA)	9.53 ± 0.21^{b}	33.22 ± 1.03^{b}	31.43 ± 1.30^{bcd}	22.25 ± 0.27^{d}	43.02 ± 2.01^{abcd}	52.85 ± 0.53^{e}	55.63 ± 2.33^{cde}	74.74 ± 1.49^{abc}

Values followed by different letters within each parameter show statistically significant differences ($p \leq 0.05$).

In this study there was also an increased level of disulfide bonds with the addition of SRF and FRF as secondary ingredient into SPI. This could be due to the higher level of sulphur containing amino acids in the millet (54.15 ± 0.42 mg/g protein) than SPI 100 % (19.10 ± 0.22 mg/g protein) (Mateen and Singh 2023), implying formation of greater number of disulfide bonds in the blend extrudates. SRF blend extrudate showed higher solubility in P+M as this can be correlated to comparatively higher

protein content and sulphur containing amino acids of SRF than FRF fraction (Table 6.3). FRF blend showed higher level of hydrophobic interactions and hydrophobic interaction-hydrogen bonds which would have led to highest textural values and viscoelastic properties than SRF blend extrudate.3.7 Colour values

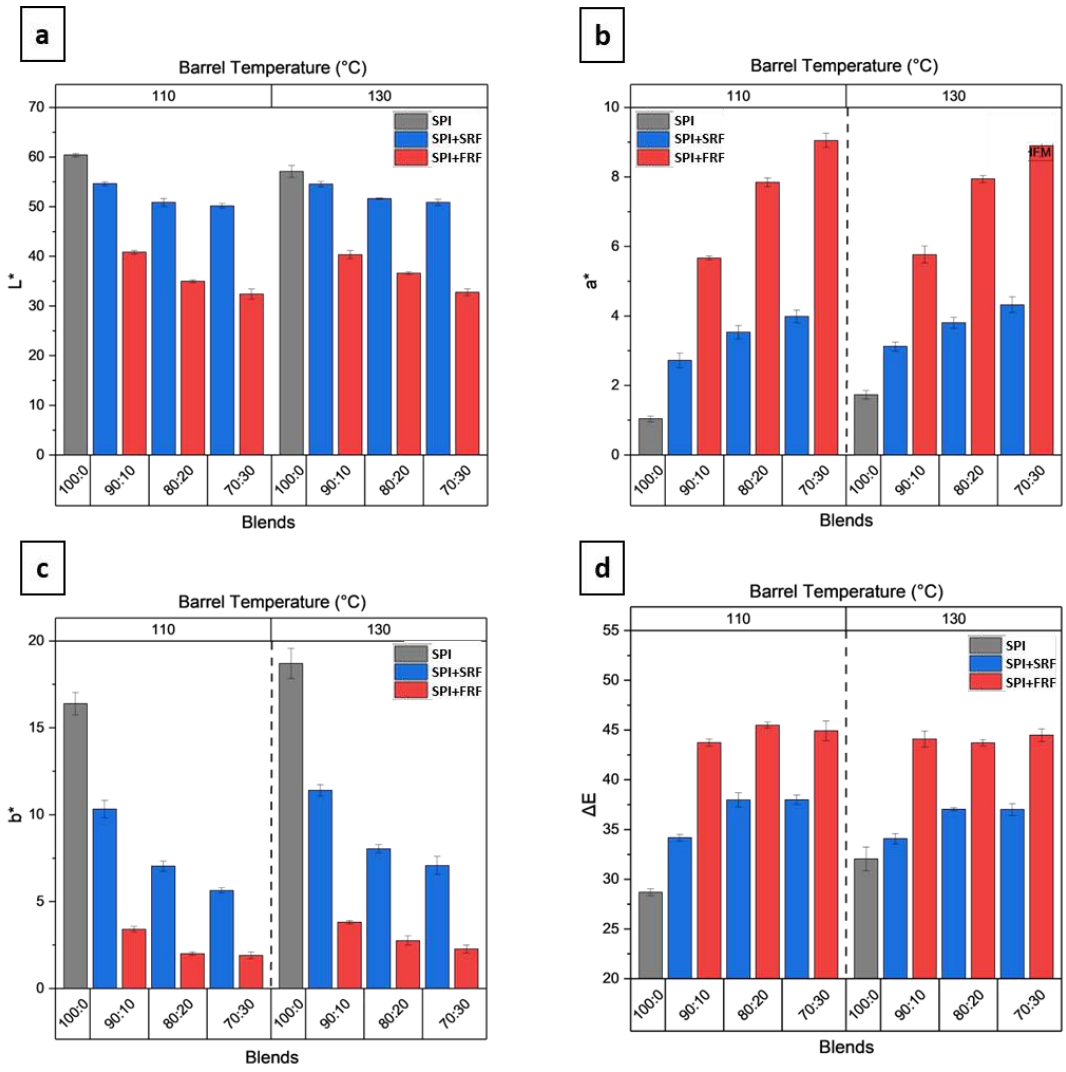

Figure 6.11 Effect of finger millet fraction blends, incorporation level and barrel temperature on colour values (a) L, (b) a*, (c) b* and (d) ΔE.*

The colour values (L* - lightness, a* - redness and b* - yellowness) of extrudates as affected by blends, incorporation level and temperature were shown in Fig. 6.11. SPI had highest L* values than blends. FRF blends were much darker in colour showing significantly ($p < 0.05$) low L*, probably because of presence of polyphenols as about 90% of polyphenols are mostly concentrated in the hull part of finger millet (Chethan and Malleshi 2007). SRF blends showed comparatively higher L* value among the blends, as it may have low polyphenols. These colour differences can also be seen in

the visual images of extrudates (Fig. 6.5). As incorporation level increases, the FRF blends showed significant ($P < 0.05$) decrease in L* whereas, there was decrease in L* of starch rich fraction blend from 10 to 20 % and no difference between 20 to 30 % incorporation level. Generally, it was believed that the higher the temperature, the darker the extrudates (Yu, Ramaswamy, and Boye 2013; Mateen, Mathpati, and Singh 2023). This was seen in case of SPI 100 % as L* decreases with increase in temperature but this was not the case with the blends, as these blends show no significant difference ($p < 0.05$).

The a* (redness) and b* (yellowness) behaves in the opposite directions as affected by the blends and incorporation level. Blends showed higher and lower values compared to SPI 100 % for a* and b* respectively. a* and b* values of SPI 100 % increases with increase in temperature. Blends showed no difference or slight increase in b* value but they are statistically not significant ($p < 0.05$). FRF blends had the highest a* value as the unextruded raw material also shown highest a* (reddish colour) (Table 6.2). Whereas SRF blends showed higher b* next to SPI 100% and FRF being least in b* value. As incorporation increases from 10 to 30 %, a* value increases significantly ($p < 0.05$) for all the blends but FRF blend's a* value increases sharply. Unlike a* value, b* value decreases with increase in incorporation level.

The total colour difference (ΔE) signifies that the difference in colour from raw material to extrudates as caused by the thermal treatment in the extruder. SPI 100% extrudates showed less colour difference compared to blends. This large colour difference in the blends may be due to the Maillard reaction and polyphenol oxidation (Amadou, Gounga, and Le 2013; Kharat et al. 2019). With increase in temperature, there was no difference in ΔE values ($p < 0.05$) implying the degree of polyphenol oxidation and Maillard reaction being the same at these temperature range in all the blends except SPI 100%. Incorporation level of FRF showed no difference whereas, SRF blends showed similar trend as a*.

All in all, HMMA made from FRF blend which looks like brown muscle can be used for mutton/lamb/beef type territory and SRF blend which resembles white muscle can be used for chicken/fish applications.

3.8 Principal component analysis (PCA)

PCA of all the ingredients, system and product parameters were done to understand the ones that contributed most into distinguishing the products (Fig. 6.12). The two principal components were able to explain 78.92% of the total variance. The SPI 100% was on the far positive side of PC1 and close to the x-axis. As the two millet fractions were incorporated into the protein, the sample scores gradually shifted towards negative PC1 in proportion to the incorporation level with 30% incorporation the most negative on PC1. The SRF blends in the negative PC2 half, and FRF blends in the positive PC2 half. Comparing the score plot with the load plot suggests that the main contributor to the clustering of the HMMA samples is the protein, fiber and starch composition with the HMMA's made using SRF blends correlated with starch content and those made using FRF blends were well correlated with the dietary fiber respectively.

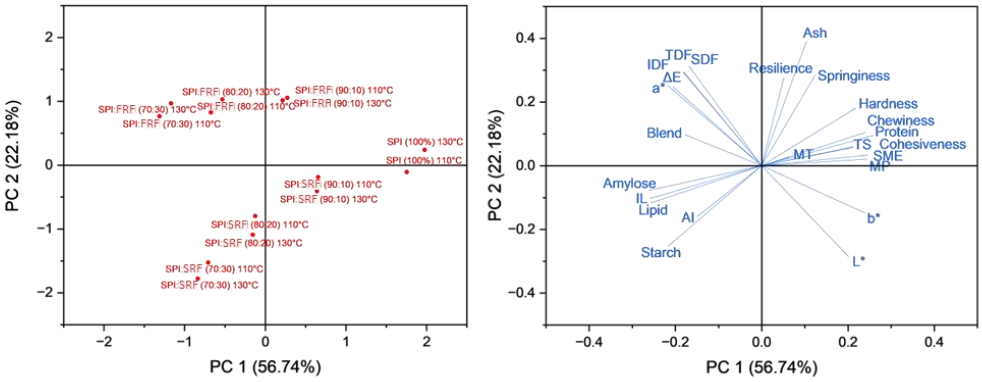

Figure 6.12 Principal component analysis (PCA) plots with all the extrudates as scores and the proximate composition, textural parameters, colour values and system parameters as loadings.

Colour of the HMMA's correlates strongly with fiber content of the feed as a* and ΔE are in same quadrant as fiber composition and L* (lightness score) is in the diagonally opposite quadrant and direction to fiber composition. Most textural properties correlate positively with protein content and negatively with SRF incorporation, while relationship with FRF is more complex. The one textural property which follows a different trend to all the other textural properties is anisotropic index which is on the opposite half of the protein composition. This suggests that SRF and FRF incorporation to protein blends is important for anisotropy.

These findings are consistent with the observed trends and explanation given for textural characteristics, visual anisotropy, colour values and system parameters involving the formation of high molecular weight aggregates through covalent, non-covalent and ionic interactions.

4 Conclusion

This study has shown that simple unit operations such as hulling and milling of millets can generate two fractions that are distinct in their composition. The difference in composition reflects in clear differences in physicochemical behaviour and pasting properties.

Further, the extrusion system properties and extruded product characteristics can be related to the compositions of the secondary ingredients. This was studied by incorporating the two fractions into blends with SPI at three different levels (10, 20 and 30%) and extruded at two temperatures (110 and 130 °C) to generate 20 different extruded samples after including the SPI 100% as controls. While all the HMMA's displayed visual texturization, the density and length of fibers increased with incorporation of the fractions. The SPI 100% HMMA's are texturally much harder, chewier, cohesive, resilient and springy compared to real meats. Incorporating the whole millet flour and fractions decreases the absolute value of most textural parameters bringing them closer to real meat. While directionally both SRF and FRF fractions behaved similarly during extrusion, there were differences in their effects. Specifically, compared to blends incorporating starch-rich SRF, the blends incorporating fiber-rich FRF resulted in the harder, chewier, more resilient, cohesive and springy. SRF blends showed higher anisotropic index compared to the FRF blend and SPI alone. As fiber content is significantly lower in SRF blends, the anisotropy could be because of a combined effect of low fiber and high starch. Rheological characterization confirmed the textural data, providing insights into viscoelasticity, deformation, and flow behaviour.

Unlike purified secondary ingredients which have simple compositions, minimally processed fractions of grains have complex compositions and the interactions of all the components with each other and the primary protein may make defining specifications for consistent product quality difficult. The results from this study suggest that it may

be potentially possible to arrive at mapping of ingredient and product characteristics for minimally processed and refined ingredients using only a few specifications.

However, much more work needs to be done before fail-safe rules can be established. Mineral composition and polyphenol composition, which have not been explored in this study, are two important parameters to understand in this context. The size distribution of starch, the different proteins in the mix and the overall amino acid composition of the proteins may also be key for establishing such relationships. Studies with pure components such as starches, fibers, metal salts and tannins in well-defined extrusion experiments will help understand these relationships.

Overall, incorporating physically processed starch rich and fiber rich fractions of finger millet represents a sustainable approach to producing high quality textured meat analogues. These low cost, natural ingredients offer a cost effective alternative to currently used ultra-processed ingredients, contributing to reduced production costs for manufacturers and promote its wider applicability in new food product development. Baking science, the understanding of wheat proteins and their interaction with each other in presence of other ingredients such as starch, water, air, sugar, fat, salt has developed over the last two decades, so much so that it even enables home bakers to make excellent products. Protein rich textured products are still in their infancy. As experimentalists play with various ingredients and the tools to understand texturization grow this science will also lead to democratization of textured protein products and inclusion of minimally processed and more sustainable ingredients in the extrusion feed blends.

Chapter 7

General discussion

7.1 Introduction

One strategy for enhancing protein intake with balanced amino acid profile from nutritional perspective to sustainability from an environmental perspective involves developing protein rich texturized products that exhibit fibrations. These products exhibit an anisotropic fibrous structure which represents an important characteristic. This thesis delves into the formation of high density fibrous structures using twin screw extrusion technology using plant based ingredients, aiming to gain a thorough understanding of process dynamics and resulting product properties. This chapter (**Chapter 7**) generate insights and findings from **Chapters 2 to 6**, providing a comprehensive overview of the composition and texture of extrudates and the innovative integration of millet flour and its fractions as secondary ingredients in the blend. The aim is to explore the implications of these studies offering a roadmap for future research and applications in the realm of protein dense product and plant based meat analogues as one of the applications.

7.2 Main findings and conclusions

Chapter 3 studies the physicochemical and nutritional characterization of different plant protein isolates. Isolates of soy, pea, chickpea, rice and wheat proteins are commonly used for making texturized plant-protein rich foods. A physicochemical analysis of these proteins shows that they differ significantly from each other. Together, water absorption capacity and water solubility of a protein are key determinants of the textural quality of their extrudates. The fibrous textures are a result of the difference in values of these properties between the key components of the blends used for extrusion. Generally, the greater the difference the more the fiber density. While the soy isolate used in this study had a water absorption capacity of more than 5 g/g protein, wheat gluten could absorb around 2 g/g. PPI, CPP and RPI had water absorption capacities in between SPI and WG. When it came to water solubility, chickpea isolate had the highest WS whereas, WG and RPI the lowest. SPI and PPI had intermediate solubilities. Thus, SPI provides the best physicochemical characteristics for high moisture extrusion. It has a high water absorption capacity and moderate solubility. It can be blended with other materials with properties very different from itself, such as wheat gluten (or millet flours which have been used in this work) to give good fibrous textures.

Another important consideration for high moisture extrusion is the least gelling concentration. Gelling plays a key role in the cooling die. SPI gelled at 12% while the gelling concentration was 14% for PPI, 16% for CPP and 20% for RPI. While WG also gelled at 12% concentration, due to its low water absorption capacity its gels released a lot of free water.

A few researchers suggest the use of oil in the blends during extrusion. While this was outside the scope of experiments in this work, if oil has to be included in the blends during extrusion, then having some emulsion capacity is important. SPI, PPI and CPP had higher emulsion capacities and would be more suitable for this compared to RPI and WG which have poor emulsion capacities.

Pasting properties of the protein powders give an indication of the melt viscosities. SPI had the highest final viscosity and RPI the least with the descending order being SPI > PPI > CPP > WG > RPI. Rheological characteristics of the powders give even a better idea of how the melts behave under extrusion conditions. Interestingly the descending order of complex viscosity for the powders is SPI > CPP > RPI > WG > PPI, which is different from the order based on the pasting curves.

There are a number of parameters that effect the textural quality of protein extrudates as described in **Chapter 4**. In this thesis we divide them into raw material parameters, system parameters, process parameters and product properties. The main raw material parameter is the protein concentration of the feed. The process parameters include feed moisture content, barrel temperature, screw speed and feed rate. The system parameters include the specific mechanical energy, melt temperature and melt pressure. The effect of protein concentration and the process parameters on the textural quality was studied for soy proteins. Protein concentration of the blend (dry basis) and moisture were found to be the most important parameter. Barrel temperature profile also had a significant impact on the texture of the extrudates. The other parameters, namely screw speed and feed rate, had smaller effects and could be used for finer modulation of texture. Apart from the figures presented in chapter 4, Fig. 7.1 shows a different way of looking into the data and understanding the impacts from the protein concentration on wet basis and process parameters on SME, L* value, hardness and chewiness values of extrudates as an example.

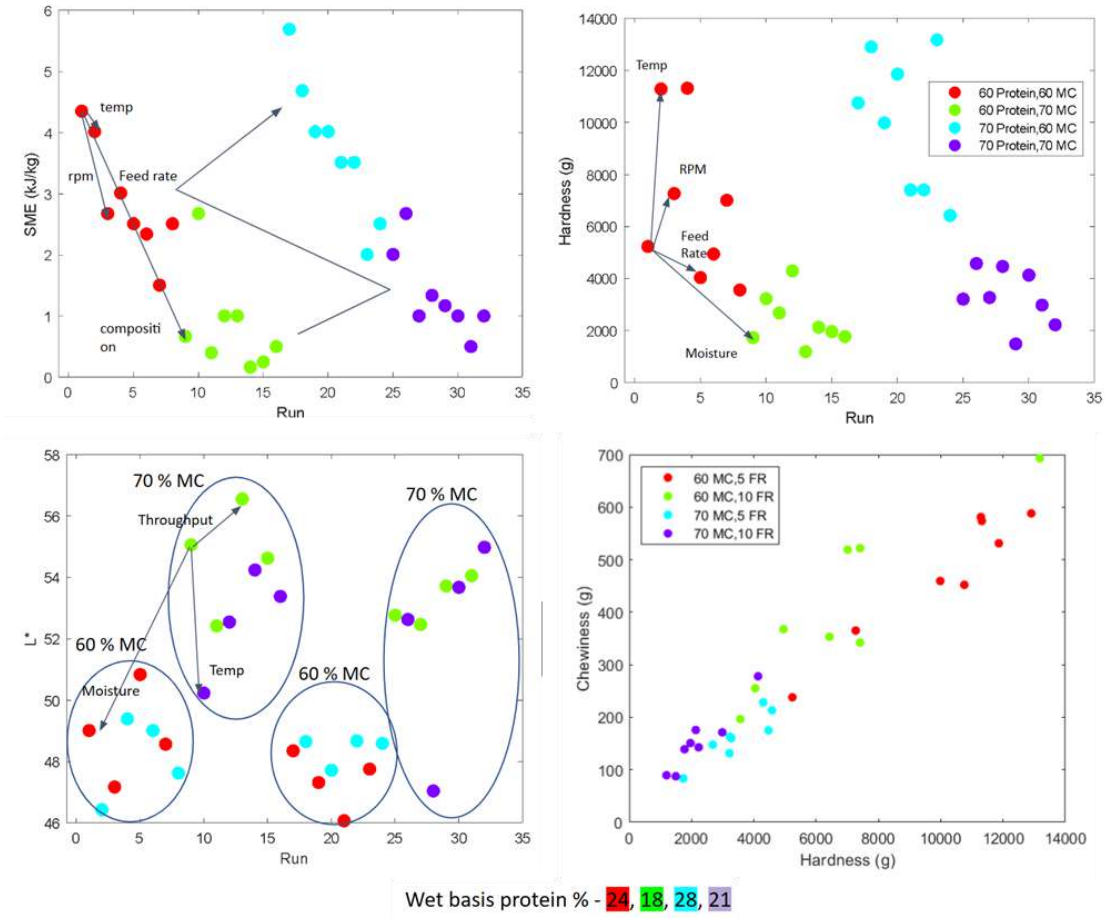

Figure 7.1 Effect of protein concentration (on wet basis) and process parameters on some system and product parameters.

Textural parameters such as hardness correlated linearly with protein concentration of wet basis. By changing protein concentration and process parameters, a wide range of hardness (11X) and chewiness (9.6X) was created. The range in values of resilience (2.2X), cohesiveness (1.4X) and springiness (1.2X) was much smaller than hardness and chewiness. Hardness and chewiness of real meat were in the range of HMMA obtained by levering process parameters. Other parameters (resilience, cohesiveness & springiness) of HMMA were out of the range obtained (higher values than real meat). A part of this gap was bridged using millet flours as blend components.

In **Chapter 5**, three types of millet - sorghum, pearl millet and finger millet flours were used as secondary components, each blended separately with soy protein isolate. The addition of millets reduced the hardness and chewiness of millets while at the same time showing improved visual fibers. This was shown from incorporation levels of millet flours up to 30%. Each millet had a slightly different effect on the texture and colour of the extrudates. Sorghum and pearl millet blends had thicker fibers and whiter

in colour while finger millet blends had finer fibers and reddish brown in colour. Comparative texture profile analysis between extrudates and real meat (chicken breast) revealed that all millet blends brought the textural values closer to those of real meat. Notably, finger millet significantly shifted the texture band towards the real meat profile. Besides providing positive changes in texture and providing a natural colour pallet, incorporation of millets also improved the amino acid profiles of the extrudates. SPI is low on sulphur containing amino acids (SAA) while millets lack lysine. Blends of SPI and millet flours at 30% showed balanced amino acid profile, good amino acid score and equivalent protein content compared to real meat, though it reduces the overall protein content marginally.

Compared to SPI and wheat gluten blends, which are the most common blends used in industry, the SPI and millet flour blends have a better amino acid score. This is because wheat gluten is low on lysine and incorporation of wheat gluten at high levels of 30% negatively impacts the amino acid scores of the extrudates significantly. Additionally, millets are gluten free and therefore the SPI and millet flour blends are suitable for a population that is gluten intolerant.

In **Chapter 6**, one of the millets, finger millet, was fractionated by separating the hull. The flour obtained from the hull and the dehulled grains were characterized. The hull flour was found to be rich in fiber and the dehulled flour was found to be low in fiber. Its starch content was much higher than the hull fraction. Therefore, the hull fraction was called fiber rich flour or FRF and the dehulled fraction was named starch rich flour or SRF. FRF had 9.4 times the fiber compared to SRF while SRF contained 1.7 times the amylopectin compared to FRF.

SPI was blended with SRF and FRF and extruded. All extrudates displayed visual fibration. However, they differed in the fiber density, that is, the number of fibers per unit cross section length. SPI100% showed the least fiber density while SRF and FRF blends showed a high density of fibers. Among the blends, SRF had the thicker and longer fibers and FRF had the thinner and shorter fibers. However visual anisotropy did not translate into cutting strength anisotropy. Cutting strength anisotropy was maximum for SRF blends and minimum for SPI100%. Extrudates from blends had a textural profile closer to real meat compared to SPI100% extrudates. SRF was closest

among different blends. Extrudates from FRF blends were more resilient than those from SPI100%; SRF blends were less resilient.

A mechanistic approach was used to understand the structure from a protein interaction in different solvents. Protein solubility in phosphate buffer showed least solubility and all extrudates showed comparatively lower protein solubility than non-extruded materials, suggesting native proteins were aggregated during the high moisture extrusion. The presence of higher hydrogen and disulfide bonds in SRF blend extrudates probably die to the higher starch/amylopectin content and resulting in a higher anisotropic index. Higher hydrophobic interactions in FRF blend extrudates was mostly due to the insoluble dietary fiber which contains hydrophobic units. Other factors for the harder structure of FRF blend extrudates could be due to the presence of Ca^{2+}in FRF.

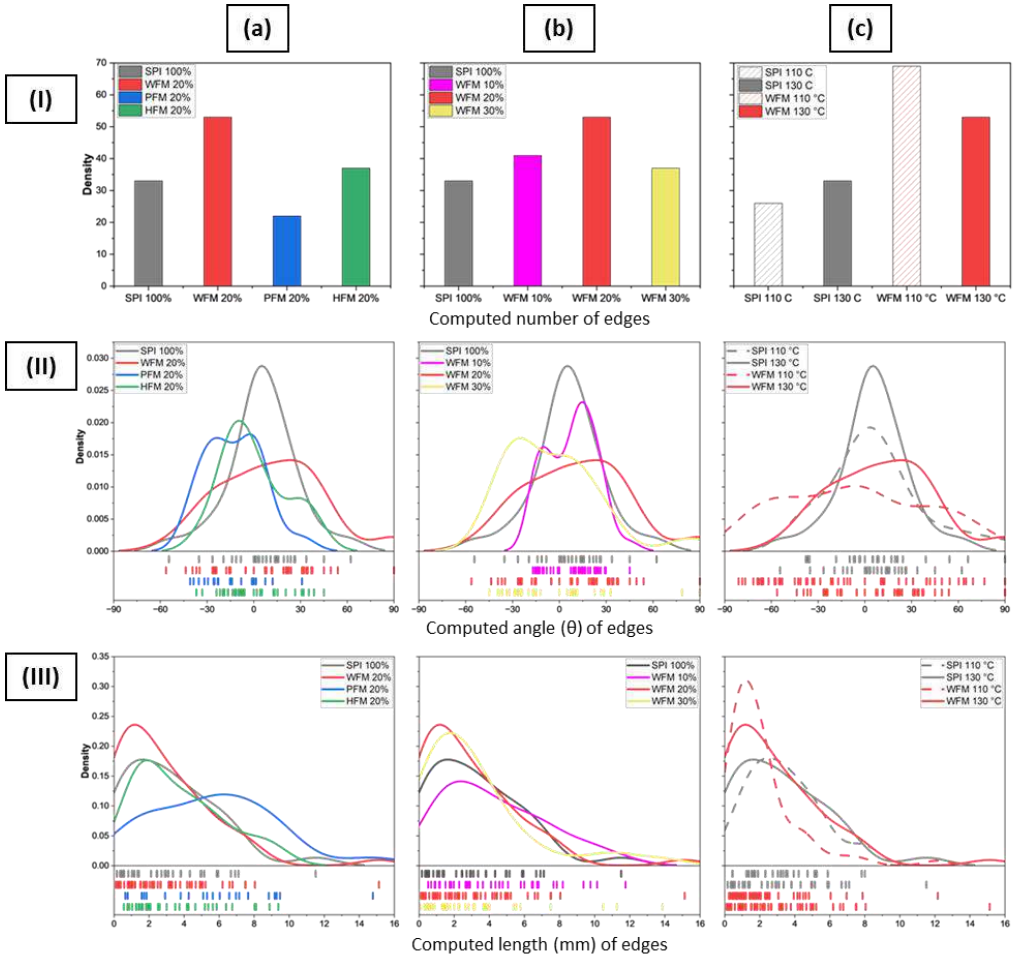

Figure 7.2 Computed visual image features (I) number of edges, (II) distribution of edge angle and (III) distribution of edge length showing for the (a) effect of blends, (b) effect of incorporation level of WFM in SPI and (c) effect of temperature (110 and 130 °C).

An image analysis method was developed to quantify the features of the fibers in the extrudates. This straightforward tool assists researchers and manufacturers in quantitatively characterizing visual fibrations. Figure 7.2 provides details of the data generated from the image analysis for whole finger millet, SRF and FRF blend extrudates, also illustrating the impact of millet incorporation levels and temperature.

7.3 Future work

While the market for textured plant proteins has grown significantly over the last decade, its future growth will depend on improving its texture and taste (GFI 2021). Anisotropic textures are expected to play a key role as they allow for a wider range of product categories including whole meat. Besides texture, these products need to deliver on nutritional parameters such as protein density, balanced amino acid profile, protein digestibility, additional nutrients such as fibers and minerals. A mass adoption of such products has a potential to lead to positive health and environmental outcomes of the global level. Hence, the scientific aim of gaining understanding in fibrous structure formation as explored in this thesis and other scientific research and publications, holds significance and may serve as the foundation for the development of the next generation of protein dense foods.

7.3.1 Protein sources and blend components

Soy and wheat gluten are the primary components in commercial meat analogue products (Wild et al. 2014; Asgar et al. 2010; GFI 2021). While this blend combination works well for minced applications, its texture is tougher for chunk applications such as soy chaap, paneer analogues, and whole meats. Further, there is an interest in improving the health and environmental credentials of the products. This has resulted developing new protein ingredients and blend components. As shown in this work, the millet-based ingredients developed, improved texture and enhanced the nutritional profile at the same time. Further, incorporation of millets contributed to an overall improved environmental profile of the soy-protein based products. We expect more research will happen in this direction to seek and develop ingredients that tick multiple boxes of nutrition, texture and environment.

A key area of future research is to work towards a clean label in protein dense foods. This thesis has explored the use of minimally processed secondary ingredients obtained

from millets. Other such ingredients need to be explored for developing blends for different use cases.

While soy, pea and wheat are the main plant proteins being used globally, there is a need to bring in other alternate proteins. A number of pulse proteins such as mung, faba, chickpea are already being used in place of soy. Proteins from waste streams such as rice and cashew are also being evaluated. Fermented proteins such as mycellial, algal and microbial are being developed for food applications. However, the physicochemical understanding of these proteins is poor compared to soy. Knowledge of their performance in texturization unit operations such as extrusion is even more limited. While there is some literature around a few of these, and even a few product launches using these, the scientific and technological knowledge is not sufficient for mainstreaming these ingredients. Research needs to be done extensively to fill this gap in the near future.

Big strides have been made in understanding the mechanical basis of texturization. This has allowed developing soy and pea based blends that texturize well. The knowledge is also helping in developing design rules for selecting secondary and tertiary components. However, the understanding is limited when it comes to texturizing proteins beyond a handful. As an example, ability to use rice protein as a primary ingredient in a blend still eludes us. Research has to be done to develop the ability to texturize the presently untexturizable proteins. Many food waste streams that are rich in proteins will then be brought into foods which will have a big positive impact on environment.

Beyond the primary and secondary ingredients, research is needed on the effect of tertiary ingredients, i.e. ingredients used at less than 5% in a blend typically, such as starches, pectins, fibers, polyphenols, Ca^{2+}. Conducting such studies can deepen our understanding of these materials.

7.3.2 Extruder and die design

The future of die design is a promising area of research, particularly in the realm of fiber development. This process typically involves phase transitions from homogeneous melts to heterogeneous bands under shear flow, which results in the formation of elongated fibers. Innovative cooling die designs could significantly enhance fiber characteristics. For instance, dies with varying height-to-width ratios, annular dies with

rotational mechanisms to introduce additional shear flow and the incorporation of a breaker plate with different sieve sizes in the cooling die could all contribute to improved longitudinal fibrations.

On the extruder side, introducing compressed gas such as air or nitrogen in the last barrel could increase porosity in the extrudates, potentially leading to better hydration and marination properties. The use oil or fat in the feed section can impede fiber formation due to its lubricating effect, which reduces shearing. To counteract this, adding melted fat or oil at the start of the cooling die through a nozzle connected to a pressured liquid pump could be beneficial. This method not only incorporates fat into the extrudates but may also create a desirable marbling effect.

7.3.3 Sensory attributes

This thesis has contributed to a better understanding of ingredients, blends and the processes involved in structure formation using twin screw extrusion technology. The fibrous products created through this technology have the potential to lay the foundation for the development of the next generation of products. However, further advancements are necessary. While product structure plays a key role, other sensory attributes, including colour, flavour, and juiciness are equally important for the development of successful new products for consumers.

This thesis delves into the inherent development of product colour and additional variations in colour can be achieved by adding external colouring agents, given that the heat treatment in the extruder naturally induces colour changes. To prevent complications in the production process, Flavors or flavour precursors are introduced into the blend during extrusion. However, Flavors can be sensitive to the elevated temperatures during processing, leading to evaporation, degradation or undesirable reactions with the matrix (proteins). Thus, stable flavours may be necessary to facilitate the development of the final flavour during the heat and shear treatment. Indian spices can be blended during the extrusion to create convenience textured products which goes well with the Indian cuisine for example, ‘hara’ (green) and ‘laal’ (red) masala textured products or ‘kababs’ which can be seasoned with coriander leaves and red chilli/paprika respectively.

Juiciness is associated with the water retention capacity in the product, playing distinct roles throughout various preparation and consumption stages. In meat, there is drip loss

during preparation, water loss during cooking/heating and water release during mastication. The moisture loss during meat cooking is from protein denaturation upon heating, altering the meat's water holding capability. Texturized products created with twin screw extrusion technology already have a preformed network, having been heated before final preparation for consumption. Consequently, the network type undergoes less change compared to meat during cooking. Juiciness during mastication is linked to how water is bound in the protein network and its release when subjected to chewing force. Water trapped in capillaries for instance is released faster than water in a protein network (Reig, Lillford, and Toldrá 2008). The moisture released during mastication not only influences juiciness but also contributes to flavour release. Flavors dissolved in water or a fat phase emulsified in water are released along with the water, facilitate a gradual release of the water phase to ensure a continued sensation of flavours during mastication. A rapid release of the water phase could lead to the perception of the product as dry and rubbery before swallowing. A systematic study of the hydration and marination processes in high moisture extruded products could enhance our understanding and lead to the development of superior quality products. Exploring cooking characteristics through various methods - such as oven baking, deep frying, and shallow frying can provide insights from a consumer's perspective on the behaviour of high moisture texturized products.

7.3.4 Nutritional value

In **Chapters 5** and **6**, fibrous structure extrudates were created using soy-millet blends and soy-millet fraction blends respectively, which are nutritionally superior compared to soy or soy-gluten blends from a balanced amino acid perspective. Beyond protein and balanced amino acids, these millets are rich in dietary fibers which promotes gut health. They also contain micronutrients for example, finger millet rich in calcium (~ 350 mg/100g), pearl millet rich in iron (~ 8 mg/100g) (Tripathi et al. 2021) which adds value to the textured products. If these products are intended to mimic real meat, it's crucial to consider the differences in nutritional value beyond just protein and essential amino acids. Meat serves as a source of heme iron and vitamin B12, with heme iron being more bioavailable compared to the nonheme iron found in plants. Individuals who rarely consume animal derived foods face a higher risk of vitamin B12 deficiency. In vegetarian diets, the need for supplements to obtain these micronutrients may arise. However, for those adopting a flexitarian or semi vegetarian diet, supplementation

becomes less of a concern as the dietary reference intake is typically met with a relatively low quantity of animal products (Food and Nutrition Board, Institute of Medicine, 2011). One can also look for ingredients which are rich in specific micronutrients which can be blended during extrusion process for example, iron rich barnyard millet (13.9 mg/100g) or adding other ingredient or fractions which is rich in natural iron.

Furthermore, it is important to consider the digestibility of proteins. The digestibility of plant proteins is commonly assessed using a protein digestibility corrected amino acid score (PDCAAS), which is determined by the ratio of the amount of limiting amino acid in 1 g of the test protein to that of the reference protein. Soy protein for instance, exhibits a PDCAAS only slightly lower (0.91) than animal derived proteins found in sources like milk and eggs. In contrast, a more substantial difference in PDCAAS is observed for various other plant proteins, including those from legumes or cereals (Hertzler et al. 2020).

It is important to highlight that a predominantly plant based diet may not necessarily exhibit inferior nutritional performance compared to current Indian diets that are rich in starch or western diets that are rich in animal products. Shifting towards a more plant based diet, for instance can contribute to increased dietary fiber intake, which tends to be low in existing diets. Additionally, micronutrients and polyphenols have the potential to enhance the nutritional content of current diets. In fact, diets stand to achieve greater balance with an increased emphasis on plant based products. However, the overall impact is contingent upon the individual consumer and their specific dietary habits. It is evident that further research is required to explore the effect of incorporating high levels of plant based products on the nutritional composition of those diets.

7.3.5 Shelf life

High moisture extruded products, containing 60-70% moisture, are perishable and must be handled with the same care as real meat. Our observations indicate that when extruded material is stored at -18°C, it maintains its physical integrity for up to 1.5 years. Nonetheless, conducting a scientific study is essential to determine these extruded product’s shelf life, examine the effects of various freezing techniques (rapid/blast or slow) and understand the freeze-thaw cycle’s influence on drip loss,

texture and the overall quality of the product. Additionally, exploring the type of packaging and barrier properties could provide significant benefits to the supply chain.

7.4 Cost analysis and scalability of high moisture texturized foods

Among all the texturization techniques for plant proteins, twin screw extrusion system proves to be the best technology for producing high moisture texturized foods at scale. For the brown field cost analysis, we made a few assumptions, such as a 500 kg/h capacity extruder, 144 production hours per week (i.e., 6 working days), and other factors based on the data available from MoFPI. The cost analysis for this business is shown in the tables below. INR currency and Indian pricing were considered for calculations.

Table 7.1 Raw materials cost (SPI and finger millet are considered).

Raw material	Blend ratio		Ingredient cost/kg	Product cost/kg
SPI		0.27	₹ 400.00	₹ 107.20
Millet	0.4	0.12	₹ 35.00	₹ 4.20
Seasonings		0.01	₹ 50.00	₹ 0.60
Water	0.6		₹ 0.04	₹ 0.02
			Total	**₹ 112.02**

Table 7.2 CapEx (capital expenditure cost), production capacity and depreciation cost.

CapEx		Production capacity		Depreciation cost	
Infrastructure	₹ 2.5 Cr	Extruder capacity (kg/h)	500	Per year	₹ 1.02 Cr
TSE* (70 dia)	₹ 2.5 Cr	No. of working days/week	6	Per hour	₹ 1,362.18
Other machines	₹ 0.1 Cr	No. of working hours/week	144	**Per kg**	**₹ 2.72**
Total	**₹ 5.1 Cr**	No. of working hours/year	7488		

* TSE – Twin screw extruder

Table 7.3 Manufacturing cost involved per kg of product and profitability

Cost involved/kg product		Profitability per kg	
Product	₹ 112.02	Manufacturing cost	123.20
Packaging	₹ 1.00	**Gross margin (60%)**	**184.80**
Utility & process	₹ 4.00	Market (Selling price)	308.00
Human resource	₹ 1.00		
Distribution	₹ 2.50		
Depreciation	₹ 2.72		
Total	**₹ 123.20**		

A 70 mm diameter twin screw extruder (TSE) barrel was considered based on volumetric and specific mechanical energy scale-up. This can deliver a throughput of 500 kg/h of product. Other CapEx and depreciation costs are shown in Table 7.2. A 20% depreciation cost was considered per annum, leading to an effective payback period of 5 years.

The OpEx cost, including depreciation for producing 1 kg of product will be INR 123.20. For profitability, a minimum gross margin of 60% was considered. Hence, the market selling price will be INR 308 (Table 7.3). When comparing the price per gram of protein, millet-based high moisture texturized protein foods have the lowest price of INR 1.18 per gram of protein, as shown in Table 7.4. Thus, the millet-based HMTP food developed in this thesis has great potential as a highly nutritious and low-cost food.

Table 7.4 Comparison of protein cost (INR/g) from different sources of protein.

Protein source	Protein content (% wb)*	Product cost/kg**	Price/g protein
Millet based HMTP	26.00	₹ 308.00	₹ 1.18
Chicken	22.30	₹ 500.00	₹ 2.24
Sheep/Lamb	20.20	₹ 1,300.00	₹ 6.44
Beef	22.50	₹ 500.00	₹ 2.22
Paneer	18.60	₹ 450.00	₹ 2.42
Tofu	15.50	₹ 380.00	₹ 2.45
Soy chaap	11.50	₹ 250.00	₹ 2.17

*Percent protein content on wet basis (fresh) was retrieved from Wood (2017). **Market prices considered for meat, dairy and traditional soy products here are as of August 22, 2024.

7.5 Concluding remarks

The primary objective of this thesis was to gain an in-depth understanding of the process, raw materials and blends involved in the formation of an anisotropic fibrous structure through high moisture extrusion using a twin screw extruder. This involved a thorough analysis of the properties of these raw materials at different stages - prior to, during and after the structure formation process. The key takeaway from the study is the significance of aligning the properties of the protein and minimally processed flours/fractions for successful structure formation to create desired textures for masses with good nutritional profile. The integration of millets into blends, represents a paradigm shift in the development of protein rich texturized products. As the demand for sustainable and affordable texturized plant based foods continues to grow, millets

stand as an ingredient and the way of minimally processed fractions as an innovative approach, offering a path to meet the expectations of texture and environmental impact.

References

References

AACC. (1997). General pasting method for wheat or rye flour or starch using the rapid visco analyser. In *American Association of Cereal Chemists International*. https://www.cerealsgrains.org/resources/Methods/Pages/76Starch.aspx

AACC. (1999). AACC Method 66-20.01. Determination of granularity of semolina and farina: Sieving method. In *AACC Approved Methods of Analysis* (11th ed.). American Association of Cereal Chemists International.

Adavalli, S. C. (2007). *Extrusion and physicochemical properties of soy-whey protein meat analog* [University of Missouri--Columbia]. https://doi.org/10.32469/10355/6272

Ahmad, R. S., Imran, A., & Hussain, M. B. (2018). Nutritional composition of meat. In *Meat Science and Nutrition*. IntechOpen. https://doi.org/10.5772/INTECHOPEN.77045

Aiking, H. (2011). Future protein supply. *Trends in Food Science & Technology*, *22*(2–3), 112–120. https://doi.org/10.1016/J.TIFS.2010.04.005

Akasha, I., Campbell, L., Lonchamp, J., & Euston, S. R. (2016). The major proteins of the seed of the fruit of the date palm (Phoenix dactylifera L.): Characterisation and emulsifying properties. *Food Chemistry*, *197*, 799–806. https://doi.org/10.1016/J.FOODCHEM.2015.11.046

Akdogan, H. (1996). Pressure, torque, and energy responses of a twin screw extruder at high moisture contents. *Food Research International*, *29*(5–6), 423–429. https://doi.org/10.1016/S0963-9969(96)00036-1

Akdogan, H. (1999). High moisture food extrusion. *International Journal of Food Science & Technology*, *34*(3), 195–207. https://doi.org/10.1046/J.1365-2621.1999.00256.X

Akdogan, H., & McHugh, T. H. (1999). Twin screw extrusion of peach puree: Rheological properties and product characteristics. *Journal of Food Processing and Preservation*, *23*(4), 285–305. https://doi.org/10.1111/J.1745-4549.1999.TB00386.X

Akinwale, T. E., Shittu, T. A., Adebowale, A. razaq A., Adewuyi, S., & Abass, A. B. (2017). Effect of soy protein isolate on the functional, pasting, and sensory acceptability of cassava starch-based custard. *Food Science & Nutrition*, *5*(6), 1163–1169. https://doi.org/10.1002/FSN3.507

Allen, A. M., & Hof, A. R. (2019). Paying the price for the meat we eat. *Environmental Science & Policy*, *97*, 90–94. https://doi.org/10.1016/J.ENVSCI.2019.04.010

Amadou, I., Gounga, M. E., & Le, G. W. (2013). Millets: Nutritional composition, some health benefits and processing - A review. *Emirates Journal of Food and Agriculture*, *25*(7), 501–508. https://doi.org/10.9755/EJFA.V25I7.12045

Anitha, S., Govindaraj, M., & Kane-Potaka, J. (2020). Balanced amino acid and higher micronutrients in millets complements legumes for improved human dietary nutrition. *Cereal Chemistry*, *97*(1), 74–84. https://doi.org/10.1002/CCHE.10227

AOAC. (1990). *Official Methods of Analysis* (15th ed.). Association of Official Analytical Chemists.

AOAC. (2005). Total, soluble, and insoluble dietary fibers in foods, Enzymatic-gravimetric method, MES-TRIS buffer. Official method 991.43 (32.1.17). In *AOAC Officila Methods of Analysis*. Association of Official Analytical Chemists International.

Aoki, K., Hara, F., Ohmichi, M., Nakatani, N., & Hosaka, H. (1989). Texturization of surimi using a twin-screw extruder. *Nippon Shokuhn Kogyo Gakkaishi*, *36*(9), 748–753. https://doi.org/10.3136/NSKKK1962.36.9_748

Arêas, J. (1992). Extrusion of food proteins. *Critical Reviews in Food Science & Nutrition*, *32*(4), 365–392. https://doi.org/10.1080/10408399209527604

Asgar, M. A., Fazilah, A., Huda, N., Bhat, R., & Karim, A. A. (2010). Nonmeat Protein Alternatives as Meat Extenders and Meat Analogs. *Comprehensive Reviews in Food Science and Food Safety*, *9*(5), 513–529. https://doi.org/10.1111/J.1541-4337.2010.00124.X

Balakrishnan, G., & Schneider, R. G. (2022). The Role of Amaranth, Quinoa, and Millets for the Development of Healthy, Sustainable Food Products—A Concise Review. *Foods 2022, Vol. 11, Page 2442*, *11*(16), 2442. https://doi.org/10.3390/FOODS11162442

Bengoechea, C., Arrachid, A., Guerrero, A., Hill, S. E., & Mitchell, J. R. (2007). Relationship between the glass transition temperature and the melt flow behavior for gluten, casein and soya. *Journal of Cereal Science*, *45*(3), 275–284. https://doi.org/10.1016/J.JCS.2006.08.011

Benković, M., Tušek, A. J., Belščak-Cvitanović, A., Lenart, A., Domian, E., Komes, D., & Bauman, I. (2015). Artificial neural network modelling of changes in physical and chemical properties of cocoa powder mixtures during agglomeration. *LWT - Food Science and Technology*, *64*(1), 140–148. https://doi.org/10.1016/j.lwt.2015.05.028

Berke, A. (2022). How should California lead on alternative meat? *A California 100 Policy Brief*, *2*. https://california100.org/app/uploads/2022/12/California100-Policy-Brief-Issue2.pdf

Berrazaga, I., Micard, V., Gueugneau, M., & Walrand, S. (2019). The role of the anabolic properties of plant- versus animal-based protein sources in supporting muscle mass maintenance: A critical review. *Nutrients 2019, Vol. 11, Page 1825*, *11*(8), 1825. https://doi.org/10.3390/NU11081825

Bhutia, D. (2014). Protein energy malnutrition in India: The plight of our under five children. *Journal of Family Medicine and Primary Care*, *3*(1), 63. https://doi.org/10.4103/2249-4863.130279

Biliaderis, C. G. (2009). Structural transitions and related physical properties of starch. In J. BeMiller & R. Whistler (Eds.), *Starch* (3rd ed., pp. 293–372). Academic Press. https://doi.org/10.1016/B978-0-12-746275-2.00008-2

BIS. (1978). *Methods of tests for edible starches and starch products, Part 2: Chemical methods*. Bureau of Indian Standards (BIS). https://www.services.bis.gov.in/php/BIS_2.0/bisconnect/standard_review/Standard_review/Isdetails?ID=MTE0NTI%3D

Björck, I., Dahlqvist, A., Noguchi, A., Asp, N. G., & Cheftel, J. C. (1983). Protein nutritional value of a biscuit processed by extrusion cooking: Effects on available lysine. *Journal of Agricultural and Food Chemistry*, *31*(3), 488–492. https://doi.org/10.1021/JF00117A006/ASSET/JF00117A006.FP.PNG_V03

Bodirsky, B. L., Dietrich, J. P., Martinelli, E., Stenstad, A., Pradhan, P., Gabrysch, S., Mishra, A., Weindl, I., le Mouël, C., Rolinski, S., Baumstark, L., Wang, X., Waid, J. L., Lotze-Campen, H., & Popp, A. (2020). The ongoing nutrition transition thwarts long-term targets for food security, public health and environmental protection. *Scientific Reports 2020 10:1*, *10*(1), 1–14. https://doi.org/10.1038/s41598-020-75213-3

Boirie, Y., Dangin, M., Gachon, P., Vasson, M. P., Maubois, J. L., & Beaufrère, B. (1997). Slow and fast dietary proteins differently modulate postprandial protein accretion. *Proceedings of the National Academy of Sciences of the United States of America*, *94*(26), 14930–14935. https://doi.org/10.1073/PNAS.94.26.14930/ASSET/BC47333F-1F1F-4A3E-BE51-444437CBFD4A/ASSETS/GRAPHIC/PQ2573359004.JPEG

Borwankar, R. P. (1992). Food texture and rheology: A tutorial review. *Journal of Food Engineering*, *16*(1–2), 1–16. https://doi.org/10.1016/0260-8774(92)90016-Y

Boulos, N. N., Greenfield, H., & Wills, R. B. H. (2000). Water holding capacity of selected soluble and insoluble dietary fibre. *International Journal of Food Properties*, *3*(2), 217–231. https://doi.org/10.1080/10942910009524629

Bounie, D., & Van Hecke, E. (1997). High moisture extrusion: optimisation of texturisation through control of rheological and textural parameters. *Smart Extrusion Workshop*, 22.

Bourne, M. C. (2002). *Food texture and viscosity : concept and measurement*. Academic Press.

Bouvier, J. M., & Campanella, O. H. (2014). Extrusion processing technology: Food and non-food biomaterials. *Extrusion Processing Technology: Food and Non-Food Biomaterials*, *9781444338119*, 1–518. https://doi.org/10.1002/9781118541685

Boye, J. I., Aksay, S., Roufik, S., Ribéreau, S., Mondor, M., Farnworth, E., & Rajamohamed, S. H. (2010). Comparison of the functional properties of pea, chickpea and lentil protein concentrates processed using ultrafiltration and

isoelectric precipitation techniques. *Food Research International*, *43*(2), 537–546. https://doi.org/10.1016/J.FOODRES.2009.07.021

Boye, J., Zare, F., & Pletch, A. (2010). Pulse proteins: Processing, characterization, functional properties and applications in food and feed. *Food Research International*, *43*(2), 414–431. https://doi.org/10.1016/J.FOODRES.2009.09.003

Bradford, M. M. (1976). A rapid and sensitive method for the quantitation of microgram quantities of protein utilizing the principle of protein-dye binding. *Analytical Biochemistry*, *72*(1–2), 248–254. https://doi.org/10.1016/0003-2697(76)90527-3

Breene, W. M. (1975). Application of texture profile analysis to instrumental food texture evaluation. *Journal of Texture Studies*, *6*(1), 53–82. https://doi.org/10.1111/J.1745-4603.1975.TB01118.X

Brishti, F. H., Chay, S. Y., Muhammad, K., Ismail-Fitry, M. R., Zarei, M., & Saari, N. (2021). Texturized mung bean protein as a sustainable food source: Effects of extrusion on its physical, textural and protein quality. *Innovative Food Science & Emerging Technologies*, *67*, 102591. https://doi.org/10.1016/J.IFSET.2020.102591

Burgess, L. D., & Stanley, D. W. (1976). A possible mechanism for thermal texturization of soybean protein. *Canadian Institute of Food Science and Technology Journal*, *9*(4), 228–231. https://doi.org/10.1016/S0315-5463(76)73681-2

Caine, W. R., Aalhus, J. L., Best, D. R., Dugan, M. E. R., & Jeremiah, L. E. (2003). Relationship of texture profile analysis and Warner-Bratzler shear force with sensory characteristics of beef rib steaks. *Meat Science*, *64*(4), 333–339. https://doi.org/10.1016/S0309-1740(02)00110-9

Camire, M. E. (1991). Protein functionality modification by extrusion cooking. *Journal of the American Oil Chemists' Society*, *68*(3), 200–205. https://doi.org/10.1007/BF02657770/METRICS

Caporgno, M. P., Böcker, L., Müssner, C., Stirnemann, E., Haberkorn, I., Adelmann, H., Handschin, S., Windhab, E. J., & Mathys, A. (2020). Extruded meat analogues based on yellow, heterotrophically cultivated Auxenochlorella protothecoides microalgae. *Innovative Food Science & Emerging Technologies*, *59*. https://doi.org/10.1016/J.IFSET.2019.102275

Catsimpolas, N., & Meyer, E. W. (1970). Gelation phenomena of soybean globulins.1. Protein-protein interactions. *Cereal Chemistry*, *47*.

Chantanuson, R., Nagamine, S., Kobayashi, T., & Nakagawa, K. (2022). Preparation of soy protein-based food gels and control of fibrous structure and rheological property by freezing. *Food Structure*, *32*, 100258. https://doi.org/10.1016/J.FOOSTR.2022.100258

Cheftel, J. C., Kitagawa, M., & Queguiner, C. (2009). New protein texturization processes by extrusion cooking at high moisture levels. *Food Reviews International*, *8*(2), 235–275. https://doi.org/10.1080/87559129209540940

Chen, F. L., Wei, Y. M., & Zhang, B. (2011). Chemical cross-linking and molecular aggregation of soybean protein during extrusion cooking at low and high moisture content. *LWT - Food Science and Technology*, *44*(4), 957–962. https://doi.org/10.1016/J.LWT.2010.12.008

Chen, F. L., Wei, Y. M., Zhang, B., & Ojokoh, A. O. (2010). System parameters and product properties response of soybean protein extruded at wide moisture range. *Journal of Food Engineering*, *96*(2), 208–213. https://doi.org/10.1016/j.jfoodeng.2009.07.014

Chen, J. sheng, Deng, Z. ying, Wu, P., Tian, J. chun, & Xie, Q. gang. (2010). Effect of gluten on pasting properties of wheat starch. *Agricultural Sciences in China*, *9*(12), 1836–1844. https://doi.org/10.1016/S1671-2927(09)60283-2

Chen, Q., Zhang, J., Liu, H., Li, T., & Wang, Q. (2023). Mechanism of high-moisture extruded protein fibrous structure formation based on the interactions among pea protein, amylopectin, and stearic acid. *Food Hydrocolloids*, *136*. https://doi.org/10.1016/J.FOODHYD.2022.108254

Chen, Q., Zhang, J., Zhang, Y., Kaplan, D. L., & Wang, Q. (2022). Protein-amylose/amylopectin molecular interactions during high-moisture extruded texturization toward plant-based meat substitutes applications. *Food Hydrocolloids*, *127*. https://doi.org/10.1016/J.FOODHYD.2022.107559

Chen, Q., Zhang, J., Zhang, Y., Meng, S., & Wang, Q. (2021). Rheological properties of pea protein isolate-amylose/amylopectin mixtures and the application in the high-moisture extruded meat substitutes. *Food Hydrocolloids*, *117*, 106732. https://doi.org/10.1016/J.FOODHYD.2021.106732

Chethan, S., & Malleshi, N. G. (2007). Finger millet polyphenols: Optimization of extraction and the effect of pH on their stability. *Food Chemistry*, *105*(2), 862–870. https://doi.org/10.1016/J.FOODCHEM.2007.02.012

Chiang, J. H., Loveday, S. M., Hardacre, A. K., & Parker, M. E. (2019a). Effects of soy protein to wheat gluten ratio on the physicochemical properties of extruded meat analogues. *Food Structure*, *19*, 100102. https://doi.org/10.1016/J.FOOSTR.2018.11.002

Chiang, J. H., Loveday, S. M., Hardacre, A. K., & Parker, M. E. (2019b). Effects of soy protein to wheat gluten ratio on the physicochemical properties of extruded meat analogues. *Food Structure*, *19*, 100102. https://doi.org/10.1016/J.FOOSTR.2018.11.002

Chove, B. E., Grandison, A. S., & Lewis, M. J. (2007). Some functional properties of fractionated soy protein isolates obtained by microfiltration. *Food Hydrocolloids*, *21*(8), 1379–1388. https://doi.org/10.1016/J.FOODHYD.2006.10.018

Clark, A. H., Kavanagh, G. M., & Ross-Murphy, S. B. (2001). Globular protein gelation—theory and experiment. *Food Hydrocolloids*, *15*(4–6), 383–400. https://doi.org/10.1016/S0268-005X(01)00042-X

Cornet, S. H. V., Snel, S. J. E., Schreuders, F. K. G., van der Sman, R. G. M., Beyrer, M., & van der Goot, A. J. (2020). Thermo-mechanical processing of plant proteins using shear cell and high-moisture extrusion cooking. In *Critical Reviews in Food Science and Nutrition*. Bellwether Publishing, Ltd. https://doi.org/10.1080/10408398.2020.1864618

Crippa, M., Solazzo, E., Guizzardi, D., Monforti-Ferrario, F., Tubiello, F. N., & Leip, A. (2021). Food systems are responsible for a third of global anthropogenic GHG emissions. *Nature Food 2021 2:3*, *2*(3), 198–209. https://doi.org/10.1038/s43016-021-00225-9

Damez, J. L., & Clerjon, S. (2008). Meat quality assessment using biophysical methods related to meat structure. *Meat Science*, *80*(1), 132–149. https://doi.org/10.1016/J.MEATSCI.2008.05.039

Damez, J. L., & Clerjon, S. (2013). Quantifying and predicting meat and meat products quality attributes using electromagnetic waves: An overview. *Meat Science*, *95*(4), 879–896. https://doi.org/10.1016/J.MEATSCI.2013.04.037

Damodaran, S. (1997). Food proteins and their applications. In *Food Proteins and their Applications*. CRC Press. https://doi.org/10.1201/9780203755617

Dangin, M., Guillet, C., Garcia-Rodenas, C., Gachon, P., Bouteloup-Demange, C., Reiffers-Magnani, K., Fauquant, J., Ballèvre, O., & Beaufrère, B. (2003). The rate of protein digestion affects protein gain differently during aging in humans. *Journal of Physiology*, *549*(2), 635–644. https://doi.org/10.1113/JPHYSIOL.2002.036897

Dankar, I., Haddarah, A., Omar, F. E. L., Sepulcre, F., & Pujolà, M. (2018). 3D printing technology: The new era for food customization and elaboration. *Trends in Food Science & Technology*, *75*, 231–242. https://doi.org/10.1016/J.TIFS.2018.03.018

Davies, J., & Lightowler, H. (1998). Plant-based alternatives to meat. *Nutrition & Food Science*, *98*(2), 90–94. https://doi.org/10.1108/00346659810201050/FULL/XML

Day, L. (2013). Proteins from land plants – Potential resources for human nutrition and food security. *Trends in Food Science & Technology*, *32*(1), 25–42. https://doi.org/10.1016/J.TIFS.2013.05.005

de Angelis, D., Kaleda, A., Pasqualone, A., Vaikma, H., Tamm, M., Tammik, M. L., Squeo, G., & Summo, C. (2020). Physicochemical and sensorial evaluation of meat analogues produced from dry-fractionated pea and oat proteins. *Foods*, *9*(12). https://doi.org/10.3390/foods9121754

Deatherage, W. L., MacMaster, M. M., & Rist, C. E. (1955). A partial survey of amylose content in starch from domestic and foreign varieties of corn, wheat and sorghum and from some other starch-bearing plants. *American Association of Cereal Chemists, 13*, 31–42.

Dekkers, B. L., Boom, R. M., & van der Goot, A. J. (2018). Structuring processes for meat analogues. In *Trends in Food Science and Technology* (Vol. 81, pp. 25–36). Elsevier Ltd. https://doi.org/10.1016/j.tifs.2018.08.011

Dekkers, B. L., Hamoen, R., Boom, R. M., & van der Goot, A. J. (2018). Understanding fiber formation in a concentrated soy protein isolate - Pectin blend. *Journal of Food Engineering*, *222*, 84–92. https://doi.org/10.1016/J.JFOODENG.2017.11.014

Dekkers, B. L., Nikiforidis, C. V., & van der Goot, A. J. (2016). Shear-induced fibrous structure formation from a pectin/SPI blend. *Innovative Food Science and Emerging Technologies*, *36*, 193–200. https://doi.org/10.1016/j.ifset.2016.07.003

Deng, Q., Wang, Z., Fu, L., He, Z., Zeng, M., Qin, F., & Chen, J. (2023). High-moisture extrusion of soy protein: Effects of insoluble dietary fiber on anisotropic extrudates. *Food Hydrocolloids*, *141*, 108688. https://doi.org/10.1016/J.FOODHYD.2023.108688

Devi, P. B., Vijayabharathi, R., Sathyabama, S., Malleshi, N. G., & Priyadarisini, V. B. (2014). Health benefits of finger millet (Eleusine coracana L.) polyphenols and dietary fiber: A review. *Journal of Food Science and Technology*, *51*(6), 1021–1040. https://doi.org/10.1007/S13197-011-0584-9/METRICS

Devi, S., Varkey, A., Dharmar, M., Holt, R. R., Allen, L. H., Sheshshayee, M. S., Preston, T., Keen, C. L., & Kurpad, A. V. (2020). Amino acid digestibility of extruded chickpea and yellow pea protein is high and comparable in moderately stunted south Indian children with use of a dual stable isotope tracer method. *The Journal of Nutrition*, *150*(5), 1178–1185. https://doi.org/10.1093/JN/NXAA004

Dharmaraj, U., Ravi, R., & Malleshi, N. G. (2014). Cooking characteristics and sensory qualities of decorticated finger millet (Eleusine coracana). *Journal of Culinary Science & Technology*, *12*(3), 215–228. https://doi.org/10.1080/15428052.2014.880100

EAT-Lancet. (2019). *EAT-Lancet commission summary report - Healthy diet from sustainable food systems*. https://eatforum.org/content/uploads/2019/07/EAT-Lancet_Commission_Summary_Report.pdf

Emery, P. W. (2013). Amino acids: Chemistry and classification. *Encyclopedia of Human Nutrition*, *1–4*, 64–71. https://doi.org/10.1016/B978-0-12-375083-9.00009-X

Emin, M. A., Quevedo, M., Wilhelm, M., & Karbstein, H. P. (2017). Analysis of the reaction behavior of highly concentrated plant proteins in extrusion-like conditions. *Innovative Food Science and Emerging Technologies*, *44*, 15–20. https://doi.org/10.1016/j.ifset.2017.09.013

Engelen, M. P. K. J., Rutten, E. P. A., De Castro, C. L. N., Wouters, E. F. M., Schols, A. M. W. J., & Deutz, N. E. P. (2007). Supplementation of soy protein with branched-chain amino acids alters protein metabolism in healthy elderly and even more in patients with chronic obstructive pulmonary disease. *The American Journal of Clinical Nutrition*, *85*(2), 431–439. https://doi.org/10.1093/AJCN/85.2.431

Faisal, S., Zhang, J., Meng, S., Shi, A., Liu, L., Wang, Q., Maleki, S. J., & Adhikari, B. (2022). Effect of high-moisture extrusion and addition of Transglutaminase on major peanut allergens content extracted by three step sequential method. *Food Chemistry*, 132569. https://doi.org/10.1016/J.FOODCHEM.2022.132569

Fang, Y., Zhang, B., & Wei, Y. (2014). Effects of the specific mechanical energy on the physicochemical properties of texturized soy protein during high-moisture extrusion cooking. *Journal of Food Engineering*, *121*(1), 32–38. https://doi.org/10.1016/J.JFOODENG.2013.08.002

Fang, Y., Zhang, B., Wei, Y., & Li, S. (2013). Effects of specific mechanical energy on soy protein aggregation during extrusion process studied by size exclusion chromatography coupled with multi-angle laser light scattering. *Journal of Food Engineering*, *115*(2), 220–225. https://doi.org/10.1016/J.JFOODENG.2012.10.017

FAO. (1995). Chemical composition and nutritive value. In *Sorghum and millets in human nutrition*. Food and Agriculture Organization of the United Nations. https://www.fao.org/3/t0818e/T0818E00.htm#Contents

FAOSTAT. (2021). *Production/yield quantities of millet in world*. Food and Agriculture Organization of the United Nations (FAO). https://www.fao.org/faostat/en/#data/QCL/visualize

FAO/WHO. (2013). Dietary protein quality evaluation in human health. In *Report of an FAO expert consultation*. Food and Agriculture Organization of the United Nations.

Farchi, S., De Sario, M., Lapucci, E., Davoli, M., & Michelozzi, P. (2017). Meat consumption reduction in Italian regions: Health co-benefits and decreases in GHG emissions. *PLOS ONE*, *12*(8), e0182960. https://doi.org/10.1371/JOURNAL.PONE.0182960

Ferawati, F., Zahari, I., Barman, M., Hefni, M., Ahlström, C., Witthöft, C., & Östbring, K. (2021). High-moisture meat analogues produced from yellow pea and faba bean protein isolates/concentrate: Effect of raw material composition and extrusion parameters on texture properties. *Foods 2021, Vol. 10, Page 843*, *10*(4), 843. https://doi.org/10.3390/FOODS10040843

Fischer, P., & Windhab, E. J. (2011). Rheology of food materials. *Current Opinion in Colloid & Interface Science*, *16*(1), 36–40. https://doi.org/10.1016/J.COCIS.2010.07.003

Friedman, H. H., Whitney, J. E., & Szczesniak, A. S. (1963). The texturometer - A new instrument for objective texture measurement. *Journal of Food Science*, *28*(4), 390–396. https://doi.org/10.1111/J.1365-2621.1963.TB00216.X

Ganjyal, G. M. (2020). Extrusion cooking cereal grain processing. In *Extrusion Cooking*. http://www.sciencedirect.com:5070/book/9780128153604/extrusion-cooking

Garí, J. A. (2002). Review of the African millet diversity. *International Workshop on Fonio, Food Security and Livelihood among the Rural Poor in West Africa.* http://www.ipgri.org

GFI. (2021). *Database of solutions for the alternative protein industry (2021)*. Good Food Institute. https://gfi.org/solutions/

Gibson, D. L., & Dwivedi, B. K. (1970). Production of meat substitutes from spent brewers' yeast and soy protein. *Canadian Institute of Food Technology Journal*, *3*(3), 113–115. https://doi.org/10.1016/S0008-3860(70)74291-8

Gilani, G. S., Cockell, K. A., & Sepehr, E. (2005). Effects of antinutritional factors on protein digestibility and amino acid availability in foods. *Journal of AOAC INTERNATIONAL*, *88*(3), 967–987. https://doi.org/10.1093/JAOAC/88.3.967

Giles, H. F., Mount, E. M., & Wagner, J. R. (2005). Extrusion: The definitive processing guide and handbook. In *Extrusion*. William Andrew. http://www.sciencedirect.com:5070/book/9780815514732/extrusion

Godavarti, S., & Karwe, ; M V. (1997). Determination of specific mechanical energy distribution on a twin-screw extruder. *Journal of Agricultural Engineering Research*, *67*, 277–287.

Gomez-Zavaglia, A., Mejuto, J. C., & Simal-Gandara, J. (2020). Mitigation of emerging implications of climate change on food production systems. *Food Research International*, *134*, 109256. https://doi.org/10.1016/J.FOODRES.2020.109256

González, N., Marquès, M., Nadal, M., & Domingo, J. L. (2020). Meat consumption: Which are the current global risks? A review of recent (2010–2020) evidences. *Food Research International*, *137*, 109341. https://doi.org/10.1016/J.FOODRES.2020.109341

González-García, S., Esteve-Llorens, X., Moreira, M. T., & Feijoo, G. (2018). Carbon footprint and nutritional quality of different human dietary choices. *Science of The Total Environment*, *644*, 77–94. https://doi.org/10.1016/J.SCITOTENV.2018.06.339

Gorissen, S. H. M., Horstman, A. M. H., Franssen, R., Crombag, J. J. R., Langer, H., Bierau, J., Respondek, F., & van Loon, L. J. C. (2016). Ingestion of wheat protein increases in vivo muscle protein synthesis rates in healthy older men in a randomized trial. *The Journal of Nutrition*, *146*(9), 1651–1659. https://doi.org/10.3945/JN.116.231340

Grabowska, K. J., Tekidou, S., Boom, R. M., & van der Goot, A. J. (2014). Shear structuring as a new method to make anisotropic structures from soy–gluten blends. *Food Research International*, *64*, 743–751. https://doi.org/10.1016/J.FOODRES.2014.08.010

Grabowska, K. J., Zhu, S., Dekkers, B. L., De Ruijter, N. C. A., Gieteling, J., & Van Der Goot, A. J. (2016). Shear-induced structuring as a tool to make anisotropic

materials using soy protein concentrate. *Journal of Food Engineering*, *188*, 77–86. https://doi.org/10.1016/J.JFOODENG.2016.05.010

Grahl, S., Palanisamy, M., Strack, M., Meier-Dinkel, L., Toepfl, S., & Mörlein, D. (2018). Towards more sustainable meat alternatives: How technical parameters affect the sensory properties of extrusion products derived from soy and algae. *Journal of Cleaner Production*, *198*, 962–971. https://doi.org/10.1016/J.JCLEPRO.2018.07.041

Green, M. M., Blankenhorn, G., & Hart, H. (1975). Which starch fraction is water-soluble, amylose or amylopectin? *Journal of Chemical Education*, *52*(11), 729–730. https://doi.org/10.1021/ED052P729

Grunert, K. G., Bredahl, L., & Brunsø, K. (2004). Consumer perception of meat quality and implications for product development in the meat sector—a review. *Meat Science*, *66*(2), 259–272. https://doi.org/10.1016/S0309-1740(03)00130-X

Guo, J., Usman, M., Swanson, G., Fang, B., Rao, J., Chen, B., & Xu, M. (2024). Influence of germination and pulse type on texture of high moisture meat analogs. *Food Hydrocolloids*, *146*, 109207. https://doi.org/10.1016/J.FOODHYD.2023.109207

Guo, W., & Greaser, M. L. (2022). Muscle structure, proteins, and meat quality. In *New Aspects of Meat Quality: From Genes to Ethics* (2nd ed., pp. 15–37). Woodhead Publishing. https://doi.org/10.1016/B978-0-323-85879-3.00026-X

Guo, Z., Teng, F., Huang, Z., Lv, B., Lv, X., Babich, O., Yu, W., Li, Y., Wang, Z., & Jiang, L. (2020). Effects of material characteristics on the structural characteristics and flavor substances retention of meat analogs. *Food Hydrocolloids*, *105*, 105752. https://doi.org/10.1016/J.FOODHYD.2020.105752

Guy, R. (2001). Extrusion cooking : technologies and applications. *Woodhead Publishing*.

Guyony, V., Fayolle, F., & Jury, V. (2023). High moisture extrusion of vegetable proteins for making fibrous meat analogs: A review. *Food Reviews International*, *39*(7), 4262–4287. https://doi.org/10.1080/87559129.2021.2023816

Hager, D. F. (1984). Effects of Extrusion upon Soy Concentrate Solubility. *Journal of Agricultural and Food Chemistry*, *32*(2), 293–296. https://doi.org/10.1021/JF00122A029/ASSET/JF00122A029.FP.PNG_V03

Han, O., Park, Y.-H., Lee, S.-H., Lee, H.-Y., & Min, B.-L. (1989). The texturization properties of textured extrudate made by a mixture of rice flour and isolated soybean protein. *Korean Journal of Food Science and Technology*, *21*(6), 780–787. https://koreascience.kr/article/JAKO198903041951713.page

Hassan, Z. M., Sebola, N. A., & Mabelebele, M. (2021). The nutritional use of millet grain for food and feed: a review. *Agriculture and Food Security*, *10*(1), 1–14. https://doi.org/10.1186/S40066-020-00282-6/TABLES/7

Hayashi, N., Hayakawa, I., & Fujio, Y. (1991). Texture evaluation of dehulled whole soybean extrudate treated with a twin-screw extruder. *Journal of Food Science and Technology-Mysore*, *38*(9), 842–849. https://doi.org/10.3136/NSKKK1962.38.842

Hayashi, N., Hayakawa, I., & Fujio, Y. (1992). Hydration of heat-treated soy protein isolate and its effect on the molten flow properties at an elevated temperature. *International Journal of Food Science & Technology*, *27*(5), 565–571. https://doi.org/10.1111/J.1365-2621.1992.TB01223.X

Hertzler, S. R., Lieblein-Boff, J. C., Weiler, M., & Allgeier, C. (2020). Plant proteins: Assessing their nutritional quality and effects on health and physical function. *Nutrients*, *12*(12), 3704. https://doi.org/10.3390/NU12123704

Holman, B. W. B., & Hopkins, D. L. (2021). The use of conventional laboratory-based methods to predict consumer acceptance of beef and sheep meat: A review. *Meat Science*, *181*, 108586. https://doi.org/10.1016/J.MEATSCI.2021.108586

Hou, H. L., Zhang, G. P., Xin, C., & Zhao, Y. Q. (2020). Numerical simulation and process optimization of internal thread cold extrusion process. *Materials 2020, Vol. 13, Page 3960*, *13*(18). https://doi.org/10.3390/MA13183960

Hua, X. Y., Long, Y., Ong, D. S. M., Theng, A. H. P., Shi, J. K., Osen, R., Wu, M., & Chiang, J. H. (2023). Mathematical optimisation of extruded mixed plant protein-based meat analogues based on amino acid compositions. *Current Research in Food Science*, *7*, 100648. https://doi.org/10.1016/J.CRFS.2023.100648

Huang, S., Martinez, M. M., & Bohrer, B. M. (2019). The compositional and functional attributes of commercial flours from tropical fruits (Breadfruit and Banana). *Foods*, *8*(11), 586. https://doi.org/10.3390/FOODS8110586

Huang, Z., Liu, Y., An, H., Kovacs, Z., Abddollahi, M., Sun, Z., Zhang, G., & Li, C. (2024). Utilizing Haematococcus pluvialis to simulate animal meat color in high-moisture meat analogues: Texture quality and color stability. *Food Research International*, *175*, 113685. https://doi.org/10.1016/J.FOODRES.2023.113685

Hughes, G. J., Ryan, D. J., Mukherjea, R., & Schasteen, C. S. (2011). Protein digestibility-corrected amino acid scores (PDCAAS) for soy protein isolates and concentrate: criteria for evaluation. *Journal of Agricultural and Food Chemistry*, *59*(23), 12707–12712. https://doi.org/10.1021/JF203220V

Ilo, S., & Berghofer, E. (2003). Kinetics of lysine and other amino acids loss during extrusion cooking of maize grits. *Journal of Food Science*, *68*(2), 496–502. https://doi.org/10.1111/J.1365-2621.2003.TB05701.X

Immonen, M., Chandrakusuma, A., Sibakov, J., Poikelispää, M., & Sontag-Strohm, T. (2021). Texturization of a blend of pea and destarched oat protein using high-moisture extrusion. *Foods 2021, Vol. 10, Page 1517*, *10*(7), 1517. https://doi.org/10.3390/FOODS10071517

Isleroglu, H., Kemerli, T., & Kaymak-Ertekin, F. (2014). Effect of steam-assisted hybrid cooking on textural quality characteristics, cooking loss, and free moisture

content of beef. *International Journal of Food Properties*, *18*(2), 403–414. https://doi.org/10.1080/10942912.2013.833219

ISO. (2009). *Cereals and cereal products - Determination of moisture content - Reference method (ISO Standard No 712:2009)*. https://www.iso.org/standard/44807.html

Jeon, Y. H., Gu, B. J., & Ryu, G. H. (2023). Investigating the potential of full-fat soy as an alternative ingredient in the manufacture of low- and high-moisture meat analogs. *Foods*, *12*(5), 1011. https://doi.org/10.3390/FOODS12051011

Jeunink, J., & Cheftel, J. C. (1979). Chemical and physicochemical changes in field bean and soybean proteins texturized by extrusion. *Journal of Food Science*, *44*(5), 1322–1325. https://doi.org/10.1111/J.1365-2621.1979.TB06430.X

Kaleda, A., Talvistu, K., Vaikma, H., Tammik, M. L., Rosenvald, S., & Vilu, R. (2021). Physicochemical, textural, and sensorial properties of fibrous meat analogs from oat-pea protein blends extruded at different moistures, temperatures, and screw speeds. *Future Foods*, *4*, 100092. https://doi.org/10.1016/J.FUFO.2021.100092

Kantanen, K., Oksanen, A., Edelmann, M., Suhonen, H., Sontag-Strohm, T., Piironen, V., Diaz, J. M. R., & Jouppila, K. (2022). Physical properties of extrudates with fibrous structures made of faba bean protein ingredients using high moisture extrusion. *Foods 2022, Vol. 11, Page 1280*, *11*(9), 1280. https://doi.org/10.3390/FOODS11091280

Kaunisto, E., Wassén, S., & Stading, M. (2024). A thermodynamical finite element model of the fibre formation process during extrusion of high-moisture meat analogues. *Journal of Food Engineering*, *362*, 111760. https://doi.org/10.1016/J.JFOODENG.2023.111760

Kaur, M., & Singh, N. (2005). Studies on functional, thermal and pasting properties of flours from different chickpea (Cicer arietinum L.) cultivars. *Food Chemistry*, *91*(3), 403–411. https://doi.org/10.1016/J.FOODCHEM.2004.06.015

Kelley, J. J., & Pressey, R. (1966). Studies with soybean protein and fiber formation. *Cereal Chemistry*, *43*, 195–206. https://www.cerealsgrains.org/publications/cc/backissues/1966/Documents/CC1966a18.html

Kendler, C., Duchardt, A., Karbstein, H. P., & Emin, M. A. (2021). Effect of oil content and oil addition point on the extrusion processing of wheat gluten-based meat analogues. *Foods 2021, Vol. 10, Page 697*, *10*(4), 697. https://doi.org/10.3390/FOODS10040697

Ketnawa, S., Chaijan, M., Grossmann, L., & Rawdkuen, S. (2024). High-moisture soy protein-mushroom-based meat analogue: physicochemical, structural properties and its application. *International Journal of Food Science & Technology*, *59*(1), 596–614. https://doi.org/10.1111/IJFS.16595

Khalid, E. K., Babiker, E. E., & EL Tinay, A. H. (2003). Solubility and functional properties of sesame seed proteins as influenced by pH and/or salt concentration.

Food Chemistry, *82*(3), 361–366. https://doi.org/10.1016/S0308-8146(02)00555-1

Kharat, S., Medina-Meza, I. G., Kowalski, R. J., Hosamani, A., Ramachandra, C. T., Hiregoudar, S., & Ganjyal, G. M. (2019). Extrusion processing characteristics of whole grain flours of select major millets (foxtail, finger, and pearl). *Food and Bioproducts Processing*, *114*, 60–71. https://doi.org/10.1016/J.FBP.2018.07.002

Kheya, S. A., Talukder, S. K., Datta, P., Yeasmin, S., Rashid, M. H., Hasan, A. K., Anwar, M. P., Islam, A. K. M. A., & Islam, A. K. M. M. (2023). Millets: The future crops for the tropics - Status, challenges and future prospects. *Heliyon*, *9*(11), e22123. https://doi.org/10.1016/J.HELIYON.2023.E22123

Kim, T., Riaz, M. N., Awika, J., & Teferra, T. F. (2021). The effect of cooling and rehydration methods in high moisture meat analogs with pulse proteins-peas, lentils, and faba beans. *Journal of Food Science*, *86*(4), 1322–1334. https://doi.org/10.1111/1750-3841.15660

Kinsella, J. E., & Whitehead, D. M. (1989). Proteins in whey: Chemical, physical, and functional properties. *Advances in Food and Nutrition Research*, *33*(C), 343–438. https://doi.org/10.1016/S1043-4526(08)60130-8

Kitabatake, N. A., Shimizu, Y. U., & Doi, E. T. (1988). Continuous production of fish meat sol using a twin-screw extruder. *Journal of Food Science*, *53*(2), 344–348. https://doi.org/10.1111/J.1365-2621.1988.TB07702.X

Kitabatake, N., Megard, D., & Cheftel, J. C. (1985). Continuous gel formation by HTST extrusion-cooking: Soy proteins. *Journal of Food Science*, *50*(5), 1260–1265. https://doi.org/10.1111/J.1365-2621.1985.TB10457.X

Kitabatake, N., Tahara, M., & Dol, E. (1990). Thermal Denaturation of Soybean Protein at Low Water Contents. *Agricultural and Biological Chemistry*, *54*(9), 2205–2212. https://doi.org/10.1080/00021369.1990.10870318

Klont, R. E., Brocks, L., & Eikelenboom, G. (1998). Muscle fibre type and meat quality. *Meat Science*, *49*(SUPPL. 1), S219–S229. https://doi.org/10.1016/S0309-1740(98)90050-X

Krintiras, G. A., Gadea Diaz, J., Van Der Goot, A. J., Stankiewicz, A. I., & Stefanidis, G. D. (2016). On the use of the Couette Cell technology for large scale production of textured soy-based meat replacers. *Journal of Food Engineering*, *169*, 205–213. https://doi.org/10.1016/J.JFOODENG.2015.08.021

Krintiras, G. A., Göbel, J., Bouwman, W. G., Jan Van Der Goot, A., & Stefanidis, G. D. (2014). On characterization of anisotropic plant protein structures. *Food & Function*, *5*(12), 3233–3240. https://doi.org/10.1039/C4FO00537F

Krintiras, G. A., Göbel, J., Van Der Goot, A. J., & Stefanidis, G. D. (2015). Production of structured soy-based meat analogues using simple shear and heat in a Couette Cell. *Journal of Food Engineering*, *160*, 34–41. https://doi.org/10.1016/J.JFOODENG.2015.02.015

Kumar, P., Chatli, M. K., Mehta, N., Singh, P., Malav, O. P., & Verma, A. K. (2016). Meat analogues: Health promising sustainable meat substitutes. *Critical Reviews in Food Science and Nutrition*, *57*(5), 923–932. https://doi.org/10.1080/10408398.2014.939739

Kumar, P., Sharma, N., Ahmed, M. A., Verma, A. K., Umaraw, P., Mehta, N., Abubakar, A. A., Hayat, M. N., Kaka, U., Lee, S. J., & Sazili, A. Q. (2022). Technological interventions in improving the functionality of proteins during processing of meat analogs. *Frontiers in Nutrition*, *9*, 3133. https://doi.org/10.3389/FNUT.2022.1044024/BIBTEX

Lan, Y. C., & Lai, L. S. (2023). Pasting and rheological properties of water caltrop starch as affected by the addition of konjac glucomannan, guar gum and xanthan gum. *Food Hydrocolloids*, *136*, 108245. https://doi.org/10.1016/J.FOODHYD.2022.108245

Le Gall, M., Quillien, L., Sève, B., Guéguen, J., & Lallès, J. P. (2007). Weaned piglets display low gastrointestinal digestion of pea (Pisum sativum L.) lectin and pea albumin 2. *Journal of Animal Science*, *85*(11), 2972–2981. https://doi.org/10.2527/JAS.2006-795

Lee, J. S., Choi, I., & Han, J. (2022). Construction of rice protein-based meat analogues by extruding process: Effect of substitution of soy protein with rice protein on dynamic energy, appearance, physicochemical, and textural properties of meat analogues. *Food Research International*, *161*. https://doi.org/10.1016/J.FOODRES.2022.111840

Lee, J. S., Kim, S., Jeong, Y. J., Choi, I., & Han, J. (2023). Impact of interactions between soy and pea proteins on quality characteristics of high-moisture meat analogues prepared via extrusion cooking process. *Food Hydrocolloids*, *139*, 108567. https://doi.org/10.1016/J.FOODHYD.2023.108567

Li, K., Liu, J. Y., Bai, Y. H., Zhao, Y. Y., Zhang, Y. Y., Li, J. G., Zhang, H., & Zhao, D. B. (2019). Effect of bamboo shoot dietary fiber on gel quality, thermal stability and secondary structure changes of pork salt-soluble proteins. *CyTA - Journal of Food*, *17*(1), 706–715. https://doi.org/10.1080/19476337.2019.1641161

Li, M., & Lee, T. C. (1996). Effect of extrusion temperature on solubility and molecular weight distribution of wheat flour proteins. *Journal of Agricultural and Food Chemistry*, *44*(3), 763–768. https://doi.org/10.1021/JF950582H

Li, S., Wei, Y., Fang, Y., Zhang, W., & Zhang, B. (2014). DSC study on the thermal properties of soybean protein isolates/corn starch mixture. *Journal of Thermal Analysis and Calorimetry*, *115*(2), 1633–1638. https://doi.org/10.1007/S10973-013-3433-4/METRICS

Lin, S., Huff, H. E., & Hsieh, F. (2000). Texture and chemical characteristics of soy protein meat analog extruded at high moisture. *Journal of Food Science*, *65*(2), 264–269. https://doi.org/10.1111/J.1365-2621.2000.TB15991.X

Lin, S., Huff, H. E., & Hsieh, F. (2002). Extrusion process parameters sensory characteristics, and structural properties of a high moisture soy protein meat analog. *Journal of Food Science*, *67*(3), 1066–1072. https://doi.org/10.1111/J.1365-2621.2002.TB09454.X

Listrat, A., Lebret, B., Louveau, I., Astruc, T., Bonnet, M., Lefaucheur, L., Picard, B., & Bugeon, J. (2016). How muscle structure and composition influence meat and flesh quality. *Scientific World Journal*, *2016*. https://doi.org/10.1155/2016/3182746

Liu, K. S., & Hsieh, F. H. (2007). Protein–protein interactions in Moisture-Extruded Meat Analogs and Heat-Induced Soy Protein Gels. *Journal of the American Oil Chemists' Society*, *84*(8), 741–748. https://doi.org/10.1007/S11746-007-1095-8

Liu, K. S., & Hsieh, F. H. (2008). Protein–Protein Interactions during High-Moisture Extrusion for Fibrous Meat Analogues and Comparison of Protein Solubility Methods Using Different Solvent Systems. *Journal of Agricultural and Food Chemistry*, *56*(8), 2681–2687. https://doi.org/10.1021/JF073343Q

Liu, Y., Li, X., Chen, Z., Yu, J., Wang, F., & Wang, J. (2014). Characterization of structural and functional properties of fish protein hydrolysates from surimi processing by-products. *Food Chemistry*, *151*, 459–465. https://doi.org/10.1016/J.FOODCHEM.2013.11.089

Lohani, U. C., Pandey, J. P., & Shahi, N. C. (2011). Effect of degree of polishing on milling characteristics and proximate compositions of barnyard millet (Echinochloa frumentacea). *Food and Bioprocess Technology 2011 5:3*, *5*(3), 1113–1119. https://doi.org/10.1007/S11947-011-0518-6

Longvah, T., Ananthan, R., Bhaskarachary, K., & Venkaiah, K. (2017). *Indian food composition tables* (T. Longvah, Ed.). National Institute of Nutrition, ICMR.

Lopes da Silva, J. A., & Rao, M. A. (2007). Rheological behavior of food gels. In *Rheology of Fluid and Semisolid Foods* (pp. 339–401). Springer. https://doi.org/10.1007/978-0-387-70930-7_6/COVER

Lyu, X., Ying, D., Zhang, P., & Fang, Z. (2023). Effect of whole tomato powder or tomato peel powder incorporation on the color, nutritional, and textural properties of extruded high moisture meat analogues. *Food and Bioprocess Technology*, *17*(1), 231–244. https://doi.org/10.1007/S11947-023-03133-X/TABLES/4

Ma, K. K., Greis, M., Lu, J., Nolden, A. A., McClements, D. J., & Kinchla, A. J. (2022). Functional performance of plant proteins. *Foods*, *11*(4), 594. https://doi.org/10.3390/FOODS11040594

Majzoobi, M., & Abedi, E. (2014). Effects of pH changes on functional properties of native and acetylated wheat gluten. *International Food Research Journal*, *21*(3), 1183.

Makeri, M. U., Mohamed, S. A., Karim, R., Ramakrishnan, Y., & Muhammad, K. (2017). Fractionation, physicochemical, and structural characterization of winged bean seed protein fractions with reference to soybean. *International Journal of*

Food Properties, *20*, 2220–2236. https://doi.org/10.1080/10942912.2017.1369101

Malav, O. P., Talukder, S., Gokulakrishnan, P., & Chand, S. (2015). Meat analog: A review. *Critical Reviews in Food Science and Nutrition*, *55*(9), 1241–1245. https://doi.org/10.1080/10408398.2012.689381

Malhotra, A., & Coupland, J. N. (2004). The effect of surfactants on the solubility, zeta potential, and viscosity of soy protein isolates. *Food Hydrocolloids*, *18*(1), 101–108. https://doi.org/10.1016/S0268-005X(03)00047-X

Maningat, C. C., Jeradechachai, T., & Buttshaw, M. R. (2022). Textured wheat and pea proteins for meat alternative applications. *Cereal Chemistry*, *99*(1), 37–66. https://doi.org/10.1002/CCHE.10503

Marinangeli, C. P. F., & House, J. D. (2017). Potential impact of the digestible indispensable amino acid score as a measure of protein quality on dietary regulations and health. *Nutrition Reviews*, *75*(8), 658–667. https://doi.org/10.1093/NUTRIT/NUX025

Mateen, A., Mathpati, M., & Singh, G. (2023). A study on high moisture extrusion for making whole cut meat analogue: Characterization of system, process and product parameters. *Innovative Food Science & Emerging Technologies*, *85*. https://doi.org/10.1016/J.IFSET.2023.103315

Mateen, A., & Singh, G. (2023). Evaluating the potential of millets as blend components with soy protein isolate in a high moisture extrusion system for improved texture, structure, and colour properties of meat analogues. *Food Research International*, *173*, 113395. https://doi.org/10.1016/J.FOODRES.2023.113395

Mathanker, S. K., Weckler, P. R., & Bowser, T. J. (2013). X-Ray Applications in Food and Agriculture: A Review. *Transactions of the ASABE*, *56*(3), 1227–1239. https://doi.org/10.13031/TRANS.56.9785

Mathevon, E., Mioche, L., Brown, W. E., & Culioli, J. (1995). Texture analysis of beef cooked at various temperature by mechanical measurements, sensory assessment and electromyography. *Journal of Texture Studies*, *26*(2), 175–192. https://doi.org/10.1111/J.1745-4603.1995.TB00792.X

Mathmann, K., Kuhn, M., & Briesen, H. (2014). Application of micro-computed tomography in food and beverage technology using the examples of textured vegetable protein and filtration steps in the brewing process. *5th Conference on Industrial Computed Tomography (ICT)*. https://www.ndt.net/search/docs.php3?id=15720

Mattice, K. D., & Marangoni, A. G. (2020). Comparing methods to produce fibrous material from zein. *Food Research International*, *128*, 108804. https://doi.org/10.1016/J.FOODRES.2019.108804

Maung, T. T., Gu, B. Y., & Ryu, G. H. (2021). Influence of extrusion process parameters on specific mechanical energy and physical properties of high-

moisture meat analog. *International Journal of Food Engineering*, *17*(2), 149–157. https://doi.org/10.1515/IJFE-2020-0042

Maurice, T. J., & Stanley, D. W. (1978). Texture-structure relationships in texturized soy protein IV. Influence of process variables on extrusion texturization. *Canadian Institute of Food Science and Technology Journal*, *11*(1), 1–6. https://doi.org/10.1016/S0315-5463(78)73151-2

McClements, D. J., & Grossmann, L. (2022). Next-generation plant-based foods: Design, production, and properties. In *Next-Generation Plant-based Foods: Design, Production, and Properties*. Springer International Publishing. https://doi.org/10.1007/978-3-030-96764-2/COVER

McMindes, M. K., Mueller, I., Orcutt, M. W., Altemueller, P. A., & Godinez Eduardo. (2014). *Protein composition and its use in restructured meat and food products* (Patent 8,685,485). U.S. Patent and Trademark Office. https://patents.google.com/patent/US8685485B2/en

Megard, D., Kitabatake, N., & Cheftel, J. C. (1985). Continuous restructuring of mechanically deboned chicken meat by HTST extrusion-cooking. *Journal of Food Science*, *50*(5), 1364–1369. https://doi.org/10.1111/J.1365-2621.1985.TB10478.X

Mengerink, Y., Kutlán, D., Tóth, F., Csámpai, A., & Molnár-Perl, I. (2002). Advances in the evaluation of the stability and characteristics of the amino acid and amine derivatives obtained with the o-phthaldialdehyde/3-mercaptopropionic acid and o-phthaldialdehyde/N-acetyl-L-cysteine reagents. High-performance liquid chromatography-mass spectrometry study. *Journal of Chromatography. A*, *949*(1–2), 99–124. https://doi.org/10.1016/S0021-9673(01)01282-1

Meuser, F., van Lengerich, B., & Reimers, H. (1984). Extrusion cooking of starches, comparison of experimental results derived from laboratory and scale extruders by means of system analysis. *Starch - Stärke*, *36*(6), 194–199. https://doi.org/10.1002/STAR.19840360603

Miedzianka, J., Walkowiak, K., Zielińska-Dawidziak, M., Zambrowicz, A., Wolny, S., & Kita, A. (2023). The functional and physicochemical properties of rice protein concentrate subjected to acetylation. *Molecules*, *28*(2), 770. https://doi.org/10.3390/MOLECULES28020770/S1

Mitchell, J. R., & Areas, J. A. G. (1992). Structural changes in biopolymers during extrusion. In J. L. Kokini, C. Ho, & M. V. Karwe (Eds.), *Food extrusion science and technology* (pp. 345–360). Marcel Dekker Inc.

Moisio, T., Forssell, P., Partanen, R., Damerau, A., & Hill, S. E. (2015). Reorganisation of starch, proteins and lipids in extrusion of oats. *Journal of Cereal Science*, *64*, 48–55. https://doi.org/10.1016/J.JCS.2015.04.001

Mościcki, L. (2011). Extrusion-cooking techniques: Applications, theory and sustainability. *Extrusion-Cooking Techniques: Applications, Theory and Sustainability*. https://doi.org/10.1002/9783527634088

Moure, A., Domínguez, H., Zúiga, M. E., Soto, C., & Chamy, R. (2002). Characterisation of protein concentrates from pressed cakes of Guevina avellana (Chilean hazelnut). *Food Chemistry*, *78*(2), 179–186. https://doi.org/10.1016/S0308-8146(01)00397-1

Murray, B. S. (2007). Stabilization of bubbles and foams. *Current Opinion in Colloid & Interface Science*, *12*(4–5), 232–241. https://doi.org/10.1016/J.COCIS.2007.07.009

Nakai, S. (1983). Structure-function relationships of food proteins with an emphasis on the importance of protein hydrophobicity. *Journal of Agricultural and Food Chemistry*, *31*(4), 676–683. https://doi.org/10.1021/JF00118A001/ASSET/JF00118A001.FP.PNG_V03

Nakai, Shuryo., & Modler, H. W. (H. W. (1996). *Food proteins : properties and characterization*. VCH. https://www.wiley.com/en-us/Food+Proteins%3A+Properties+and+Characterization-p-9780471186144

Nasrollahzadeh, F., Alexi, N., Skov, K. B., Roman, L., Sfyra, K., & Martinez, M. M. (2024). Texture profiling of muscle meat benchmarks and plant-based analogues: An instrumental and sensory design approach with focus on correlations. *Food Hydrocolloids*, 109829. https://doi.org/10.1016/J.FOODHYD.2024.109829

Nasrollahzadeh, F., Roman, L., Skov, K., Jakobsen, L. M. A., Trinh, B. M., Tsochatzis, E. D., Mekonnen, T., Corredig, M., Dutcher, J. R., & Martinez, M. M. (2023). A comparative investigation of seed storage protein fractions: The synergistic impact of molecular properties and composition on anisotropic structuring. *Food Hydrocolloids*, *137*. https://doi.org/10.1016/J.FOODHYD.2022.108400

Nasrollahzadeh, F., Roman, L., Swaraj, V. J. S., Ragavan, K. V., Vidal, N. P., Dutcher, J. R., & Martinez, M. M. (2022). Hemp (Cannabis sativa L.) protein concentrates from wet and dry industrial fractionation: Molecular properties, nutritional composition, and anisotropic structuring. *Food Hydrocolloids*, *131*, 107755. https://doi.org/10.1016/J.FOODHYD.2022.107755

Nieuwland, M., Geerdink, P., Brier, P., Van Den Eijnden, P., Henket, J. T. M. M., Langelaan, M. L. P., Stroeks, N., Van Deventer, H. C., & Martin, A. H. (2014). Reprint of "Food-grade electrospinning of proteins." *Innovative Food Science & Emerging Technologies*, *24*, 138–144. https://doi.org/10.1016/J.IFSET.2014.07.006

Nijdam, D., Rood, T., & Westhoek, H. (2012). The price of protein: Review of land use and carbon footprints from life cycle assessments of animal food products and their substitutes. *Food Policy*, *37*(6), 760–770. https://doi.org/10.1016/J.FOODPOL.2012.08.002

Nikmaram, N., Leong, S. Y., Koubaa, M., Zhu, Z., Barba, F. J., Greiner, R., Oey, I., & Roohinejad, S. (2017). Effect of extrusion on the anti-nutritional factors of food products: An overview. *Food Control*, *79*, 62–73. https://doi.org/10.1016/J.FOODCONT.2017.03.027

NIN. (2011). *Dietary guidelines for Indian - A manual*. https://www.nin.res.in/downloads/DietaryGuidelinesforNINwebsite.pdf

Noguchi, A. (1989). Extrusion cooking of high moisture protein foods. *American Association of Cereal Chemists, Inc.*, 343–370.

Noguchi, A. (1990). Extrusion cooking of high moisture protein foods. In C. L. , P. Mercier & J. M. Harper (Eds.), *Extrusion Cooking* (pp. 343–369). Minnesota: AACC.

Norton, L. E., Layman, D. K., Bunpo, P., Anthony, T. G., Brana, D. V., & Garlick, P. J. (2009). The leucine content of a complete meal directs peak activation but not duration of skeletal muscle protein synthesis and mammalian target of rapamycin signaling in rats. *The Journal of Nutrition*, *139*(6), 1103–1109. https://doi.org/10.3945/JN.108.103853

Ogunwolu, S. O., Henshaw, F. O., Mock, H. P., Santros, A., & Awonorin, S. O. (2009). Functional properties of protein concentrates and isolates produced from cashew (Anacardium occidentale L.) nut. *Food Chemistry*, *115*(3), 852–858. https://doi.org/10.1016/J.FOODCHEM.2009.01.011

O'Kane, F. E., Happe, R. P., Vereijken, J. M., Gruppen, H., & Van Boekel, M. A. J. S. (2004). Heat-induced gelation of pea legumin: Comparison with soybean glycinin. *Journal of Agricultural and Food Chemistry*, *52*(16), 5071–5078. https://doi.org/10.1021/JF035215H

Onwulata, C. I., Tunick, M. H., & Thomas-Gahring, A. E. (2014). Pasting and extrusion properties of mixed carbohydrate and whey protein isolate matrices. *Journal of Food Processing and Preservation*, *38*(4), 1577–1591. https://doi.org/10.1111/JFPP.12118

Ortega, D. L., Sun, J., & Lin, W. (2022). Identity labels as an instrument to reduce meat demand and encourage consumption of plant based and cultured meat alternatives in China. *Food Policy*, *111*, 102307. https://doi.org/10.1016/J.FOODPOL.2022.102307

Osen, R., Toelstede, S., Eisner, P., & Schweiggert-Weisz, U. (2015). Effect of high moisture extrusion cooking on protein–protein interactions of pea (Pisum sativum L.) protein isolates. *International Journal of Food Science & Technology*, *50*(6), 1390–1396. https://doi.org/10.1111/IJFS.12783

Osen, R., Toelstede, S., Wild, F., Eisner, P., & Schweiggert-Weisz, U. (2014). High moisture extrusion cooking of pea protein isolates: Raw material characteristics, extruder responses, and texture properties. *Journal of Food Engineering*, *127*, 67–74. https://doi.org/10.1016/j.jfoodeng.2013.11.023

Ozturk, O. K., & Hamaker, B. R. (2023). Texturization of plant protein-based meat alternatives: Processing, base proteins, and other constructional ingredients. *Future Foods*, *8*, 100248. https://doi.org/10.1016/J.FUFO.2023.100248

Palanisamy, M., Franke, K., Berger, R. G., Heinz, V., & Töpfl, S. (2019). High moisture extrusion of lupin protein: influence of extrusion parameters on extruder responses

and product properties. *Journal of the Science of Food and Agriculture*, *99*(5), 2175–2185. https://doi.org/10.1002/jsfa.9410

Palanisamy, M., Töpfl, S., Aganovic, K., & Berger, R. G. (2018). Influence of iota carrageenan addition on the properties of soya protein meat analogues. *LWT*, *87*, 546–552. https://doi.org/10.1016/J.LWT.2017.09.029

Palanisamy, M., Töpfl, S., Berger, R. G., & Hertel, C. (2019). Physico-chemical and nutritional properties of meat analogues based on Spirulina/lupin protein mixtures. *European Food Research and Technology 2019 245:9*, *245*(9), 1889–1898. https://doi.org/10.1007/S00217-019-03298-W

Park, J. H., Chatpaisarn, A., & Ryu, G. H. (2017). Effects of gluten and moisture contents on texturization of extruded soy protein isolate. *Journal of the Korean Society of Food Science and Nutrition*, *46*(4), 473–480. https://doi.org/10.3746/JKFN.2017.46.4.473

Pearson, A. M., & Young, R. B. (1989). Composition and Structure. *Muscle and Meat Biochemistry*, 1–33. https://doi.org/10.1016/B978-0-12-548055-0.50005-2

Peng, J., Zhu, K. X., Guo, X. N., & Zhou, H. M. (2021). The impact of phosphates on the fibrous structure formation of textured wheat gluten. *Food Hydrocolloids*, *119*. https://doi.org/10.1016/J.FOODHYD.2021.106844

Petruccelli, S., & Añón, M. C. (1995). Thermal Aggregation of Soy Protein Isolates. *Journal of Agricultural and Food Chemistry*, *43*(12), 3035–3041. https://doi.org/10.1021/JF00060A009/ASSET/JF00060A009.FP.PNG_V03

Phillips, S. M. (2017). Current concepts and unresolved questions in dietary protein requirements and supplements in adults. *Frontiers in Nutrition*, *4*, 253663. https://doi.org/10.3389/FNUT.2017.00013/BIBTEX

Pietsch, V. L., Bühler, J. M., Karbstein, H. P., & Emin, M. A. (2019). High moisture extrusion of soy protein concentrate: Influence of thermomechanical treatment on protein-protein interactions and rheological properties. *Journal of Food Engineering*, *251*, 11–18. https://doi.org/10.1016/j.jfoodeng.2019.01.001

Pietsch, V. L., Emin, M. A., & Schuchmann, H. P. (2017a). Process conditions influencing wheat gluten polymerization during high moisture extrusion of meat analog products. *Journal of Food Engineering*, *198*, 28–35. https://doi.org/10.1016/J.JFOODENG.2016.10.027

Pietsch, V. L., Emin, M. A., & Schuchmann, H. P. (2017b). Process conditions influencing wheat gluten polymerization during high moisture extrusion of meat analog products. *Journal of Food Engineering*, *198*, 28–35. https://doi.org/10.1016/J.JFOODENG.2016.10.027

Pietsch, V. L., Soergel, F., & Giannini, M. (2021). *Combining extrusion, electron microscopy and rheology to study the product characteristics of meat analog products*. https://assets.thermofisher.com/TFS-Assets/MSD/Reference-Materials/WP04-combining-extrusion-electron-microscopy-rheology-meat-analog.pdf

Pietsch, V. L., Werner, R., Karbstein, H. P., & Emin, M. A. (2019). High moisture extrusion of wheat gluten: Relationship between process parameters, protein polymerization, and final product characteristics. *Journal of Food Engineering, 259*, 3–11. https://doi.org/10.1016/J.JFOODENG.2019.04.006

Plummer, D. T. (1987). *An introduction to practical biochemistry* (3rd ed.). McGraw-Hill.

Pöri, P., Nisov, A., & Nordlund, E. (2022). Enzymatic modification of oat protein concentrate with trans- and protein-glutaminase for increased fibrous structure formation during high-moisture extrusion processing. *LWT, 156*, 113035. https://doi.org/10.1016/J.LWT.2021.113035

Prasert, W., Pantoa, T., Chitisankul, W. T., & Pengpinij, W. (2022). Effects of Sacha inchi (Plukenetia volubilis L.) oil and extrusion process conditions on physicochemical properties of fortified omega-3 fibrous high moisture meat analogs. *Journal of Food Processing and Preservation*, *46*(12), e17227. https://doi.org/10.1111/JFPP.17227

Prudêncio-Ferreira, S. H., & Arêas, J. G. (1993). Protein-protein interactions in the extrusion of soya at various temperatures and moisture contents. *Journal of Food Science*, *58*(2), 378–381. https://doi.org/10.1111/J.1365-2621.1993.TB04279.X

Raigar, R. K., Dalbhagat, C. G., & Mishra, H. N. (2020). Effect of pilot scale roasting on color and textural attributes of soybean kernels. *Journal of Food Processing and Preservation*, *44*(11), e14883. https://doi.org/10.1111/JFPP.14883

Ramos Diaz, J. M., Kantanen, K., Edelmann, J. M., Suhonen, H., Sontag-Strohm, T., Jouppila, K., & Piironen, V. (2022). Fibrous meat analogues containing oat fiber concentrate and pea protein isolate: Mechanical and physicochemical characterization. *Innovative Food Science & Emerging Technologies*, *77*. https://doi.org/10.1016/J.IFSET.2022.102954

Rampal, P. (2018). An analysis of protein consumption in India through plant and animal sources. *Food and Nutrition Bulletin*, *39*(4), 564–580. https://doi.org/10.1177/0379572118810104

Ranasinghesagara, J., Hsieh, F. H., Huff, H., & Yao, G. (2009). Laser scanning system for real-time mapping of fiber formations in meat analogues. *Journal of Food Science, 74*(2), E39–E45. https://doi.org/10.1111/J.1750-3841.2008.01032.X

Ranasinghesagara, J., Hsieh, F. H., & Yao, G. (2005). An image processing method for quantifying fiber formation in meat analogs under high moisture extrusion. *Journal of Food Science, 70*(8), e450–e454. https://doi.org/10.1111/J.1365-2621.2005.TB11513.X

Ranasinghesagara, J., Hsieh, F., & Yao, G. (2006). A photon migration method for characterizing fiber formation in meat analogs. *Journal of Food Science*, *71*(5), E227–E231. https://doi.org/10.1111/J.1750-3841.2006.00038.X

Ranganathan, J., Vennard, D., Waite, R., Lipinski, B., Searchinger, T., & Dumas, P. (2016). *Shifting diets for a sustainable food future: Creating a sustainable food future*. https://www.wri.org/research/shifting-diets-sustainable-food-future

Rani, M., Siddiqi, R. A., Sharma, R., Gill, B. S., & Sogi, D. S. (2023). Functional and structural properties of gliadin as influenced by pH, extraction protocols, and wheat cultivars. *International Journal of Biological Macromolecules*, *234*, 123484. https://doi.org/10.1016/J.IJBIOMAC.2023.123484

Rao, D. B., Bhandari, R., & Tonapi, A. V. (2022). *A White Paper on Millets*. https://www.nutrihubiimr.com/white-paper

Rao, M. A. (2007). Flow and functional models for rheological properties of fluid foods. *Food Engineering Series*, 27–58. https://doi.org/10.1007/978-0-387-70930-7_2/COVER

Rao, N. D., Min, J., DeFries, R., Ghosh-Jerath, S., Valin, H., & Fanzo, J. (2018). Healthy, affordable and climate-friendly diets in India. *Global Environmental Change*, *49*, 154–165. https://doi.org/10.1016/J.GLOENVCHA.2018.02.013

Rehrah, D., Ahmedna, M., Goktepe, I., & Yu, J. (2009). Extrusion parameters and consumer acceptability of a peanut-based meat analogue. *International Journal of Food Science & Technology*, *44*(10), 2075–2084. https://doi.org/10.1111/J.1365-2621.2009.02035.X

Reig, M., Lillford, P. J., & Toldrá, F. (2008). Structured meat products. *Food Materials Science: Principles and Practice*, 501–523. https://doi.org/10.1007/978-0-387-71947-4_21/COVER

Rekola, S. M., Kårlund, A., Mikkonen, S., Kolehmainen, M., Pomponio, L., & Sozer, N. (2023). Structure, texture and protein digestibility of high moisture extruded meat alternatives enriched with cereal brans. *Applied Food Research*, *3*(1), 100262. https://doi.org/10.1016/J.AFRES.2023.100262

Renkema, J. M. S. (2004). Relations between rheological properties and network structure of soy protein gels. *Food Hydrocolloids*, *18*(1), 39–47. https://doi.org/10.1016/S0268-005X(03)00040-7

Renkema, J. M. S., & Van Vliet, T. (2002). Heat-induced gel formation by soy proteins at neutral pH. *Journal of Agricultural and Food Chemistry*, *50*(6), 1569–1573. https://doi.org/10.1021/JF010763L

Riaz, M. N. (2000). Extruders in food applications. In *Extruders in Food Applications*. CRC Press. https://doi.org/10.1201/9781482278859

Riazi, F., Tehrani, M. M., Lammers, V., Heinz, V., & Savadkoohi, S. (2023). Unexpected morphological modifications in high moisture extruded pea-flaxseed proteins: Part I, topological and conformational characteristics, textural attributes, and viscoelastic phenomena. *Food Hydrocolloids*, *136*, 108304. https://doi.org/10.1016/J.FOODHYD.2022.108304

Richter, J. K., Montero, M. L., Ikuse, M., Wagner, C. E., Ross, C. F., Saunders, S. R., & Ganjyal, G. M. (2024). The interaction between wheat and pea protein influences the final chemical and sensory characteristics of extruded high moisture meat analogs. *Journal of Food Science*, *89*(1), 104–120. https://doi.org/10.1111/1750-3841.16815

Ruiz De Huidobro, F., Miguel, E., Blázquez, B., & Onega, E. (2005). A comparison between two methods (Warner–Bratzler and texture profile analysis) for testing either raw meat or cooked meat. *Meat Science*, *69*(3), 527–536. https://doi.org/10.1016/J.MEATSCI.2004.09.008

Ryu, G.-H. (2020). Extrusion cooking of high-moisture meat analogues. *Extrusion Cooking*, 205–224. https://doi.org/10.1016/B978-0-12-815360-4.00007-9

Ryu, K. K., Kang, Y. K., Jeong, E. W., Baek, Y., Lee, K. Y., & Lee, H. G. (2023). Applications of various natural pigments to a plant-based meat analog. *LWT*, *174*, 114431. https://doi.org/10.1016/J.LWT.2023.114431

Sabaté, J., Sranacharoenpong, K., Harwatt, H., Wien, M., & Soret, S. (2015). The environmental cost of protein food choices. *Public Health Nutrition*, *18*(11), 2067–2073. https://doi.org/10.1017/S1368980014002377

Sadler, M. J. (2004). Meat alternatives — market developments and health benefits. *Trends in Food Science & Technology*, *15*(5), 250–260. https://doi.org/10.1016/J.TIFS.2003.09.003

Saha, S., Gupta, A., Singh, S. R. K., Bharti, N., Singh, K. P., Mahajan, V., & Gupta, H. S. (2011). Compositional and varietal influence of finger millet flour on rheological properties of dough and quality of biscuit. *LWT - Food Science and Technology*, *44*(3), 616–621. https://doi.org/10.1016/J.LWT.2010.08.009

Saldanha do Carmo, C., Knutsen, S. H., Malizia, G., Dessev, T., Geny, A., Zobel, H., Myhrer, K. S., Varela, P., & Sahlstrøm, S. (2021). Meat analogues from a faba bean concentrate can be generated by high moisture extrusion. *Future Foods*, *3*, 100014. https://doi.org/10.1016/J.FUFO.2021.100014

Samard, S., Gu, B. Y., & Ryu, G. H. (2019). Effects of extrusion types, screw speed and addition of wheat gluten on physicochemical characteristics and cooking stability of meat analogues. *Journal of the Science of Food and Agriculture*, *99*(11), 4922–4931. https://doi.org/10.1002/JSFA.9722

Samard, S., & Ryu, G. H. (2019). A comparison of physicochemical characteristics, texture, and structure of meat analogue and meats. *Journal of the Science of Food and Agriculture*, *99*(6), 2708–2715. https://doi.org/10.1002/JSFA.9438

Sandoval Murillo, J. L., Osen, R., Hiermaier, S., & Ganzenmüller, G. (2019). Towards understanding the mechanism of fibrous texture formation during high-moisture extrusion of meat substitutes. *Journal of Food Engineering*, *242*, 8–20. https://doi.org/10.1016/j.jfoodeng.2018.08.009

Sathe, S. K., & Salunkhe, D. K. (1981). Functional properties of the great northern bean (Phaseolus vulgaris L.) proteins: Emulsion, foaming, viscosity, and gelation

properties. *Journal of Food Science*, *46*(1), 71–81. https://doi.org/10.1111/J.1365-2621.1981.TB14533.X

Saunders, J., Izydorczyk, M., Levin, D. B., Saunders, J., Izydorczyk, M., & Levin, D. B. (2011). Limitations and Challenges for Wheat-Based Bioethanol Production. *Economic Effects of Biofuel Production*. https://doi.org/10.5772/20258

Scarborough, P., Appleby, P. N., Mizdrak, A., Briggs, A. D. M., Travis, R. C., Bradbury, K. E., & Key, T. J. (2014). Dietary greenhouse gas emissions of meat-eaters, fish-eaters, vegetarians and vegans in the UK. *Climatic Change*, *125*(2), 179–192. https://doi.org/10.1007/S10584-014-1169-1/TABLES/4

Schaafsma, G. (2000). The protein digestibility–corrected amino acid score. *The Journal of Nutrition*, *130*(7), 1865S-1867S. https://doi.org/10.1093/JN/130.7.1865S

Schlemmer, U., Frølich, W., Prieto, R. M., & Grases, F. (2009). Phytate in foods and significance for humans: Food sources, intake, processing, bioavailability, protective role and analysis. *Molecular Nutrition & Food Research*, *53*(S2), S330–S375. https://doi.org/10.1002/MNFR.200900099

Schmid, E. M., Farahnaky, A., Adhikari, B., & Torley, P. J. (2022). High moisture extrusion cooking of meat analogs: A review of mechanisms of protein texturization. *Comprehensive Reviews in Food Science and Food Safety*, *21*(6), 4573–4609. https://doi.org/10.1111/1541-4337.13030

Schösler, H., Boer, J. de, & Boersema, J. J. (2012). Can we cut out the meat of the dish? Constructing consumer-oriented pathways towards meat substitution. *Appetite*, *58*(1), 39–47. https://doi.org/10.1016/J.APPET.2011.09.009

Schreuders, F. K. G., Dekkers, B. L., Bodnár, I., Erni, P., Boom, R. M., & van der Goot, A. J. (2019). Comparing structuring potential of pea and soy protein with gluten for meat analogue preparation. *Journal of Food Engineering*, *261*, 32–39. https://doi.org/10.1016/j.jfoodeng.2019.04.022

Schreuders, F. K. G., Schlangen, M., Bodnár, I., Erni, P., Boom, R. M., & van der Goot, A. J. (2022). Structure formation and non-linear rheology of blends of plant proteins with pectin and cellulose. *Food Hydrocolloids*, *124*, 107327. https://doi.org/10.1016/J.FOODHYD.2021.107327

Schreuders, F. K. G., Schlangen, M., Kyriakopoulou, K., Boom, R. M., & van der Goot, A. J. (2021). Texture methods for evaluating meat and meat analogue structures: A review. *Food Control*, *127*, 108103. https://doi.org/10.1016/J.FOODCONT.2021.108103

Schuchmann, H. P. (2008). Extrusion for the design of food structures. *Chemie Ingenieur Technik*, *80*(8), 1097–1106. https://doi.org/10.1002/CITE.200800065

Seetapan, N., Raksa, P., Limparyoon, N., Srirajan, S., Makmoon, T., Israkarn, K., Gamonpilas, C., Methacanon, P., & Fuongfuchat, A. (2023a). High moisture extrusion of meat analogues using mung bean (Vigna radiata L.) protein and flour blends: investigations on morphology, texture and rheology. *International Journal*

of Food Science & Technology, *58*(4), 1922–1930. https://doi.org/10.1111/IJFS.16334

Seetapan, N., Raksa, P., Limparyoon, N., Srirajan, S., Makmoon, T., Israkarn, K., Gamonpilas, C., Methacanon, P., & Fuongfuchat, A. (2023b). High moisture extrusion of meat analogues using mung bean (Vigna radiata L.) protein and flour blends: investigations on morphology, texture and rheology. *International Journal of Food Science & Technology*, *58*(4), 1922–1930. https://doi.org/10.1111/IJFS.16334

Sha, L., & Xiong, Y. L. (2020). Plant protein-based alternatives of reconstructed meat: Science, technology, and challenges. *Trends in Food Science & Technology*, *102*, 51–61. https://doi.org/10.1016/J.TIFS.2020.05.022

Sheard, P. R., Fellows, A., Ledward, D. A., & Mitchell, J. R. (1986). Macromolecular changes associated with the heat treatment of soya isolate. *International Journal of Food Science & Technology*, *21*(1), 55–60. https://doi.org/10.1111/J.1365-2621.1986.TB01929.X

Sheethal, H. V., Baruah, C., Subhash, K., Ananthan, R., & Longvah, T. (2022). Insights of Nutritional and Anti-nutritional Retention in Traditionally Processed Millets. *Frontiers in Sustainable Food Systems*, *5*, 735356. https://doi.org/10.3389/FSUFS.2021.735356/BIBTEX

Shevkani, K., Singh, N., Kaur, A., & Rana, J. C. (2015). Structural and functional characterization of kidney bean and field pea protein isolates: A comparative study. *Food Hydrocolloids*, *43*, 679–689. https://doi.org/10.1016/J.FOODHYD.2014.07.024

Shobana, S., Sreerama, Y. N., & Malleshi, N. G. (2009). Composition and enzyme inhibitory properties of finger millet (Eleusine coracana L.) seed coat phenolics: Mode of inhibition of α-glucosidase and pancreatic amylase. *Food Chemistry*, *115*(4), 1268–1273. https://doi.org/10.1016/J.FOODCHEM.2009.01.042

Sim, S. Y. J., Srv, A., Chiang, J. H., & Henry, C. J. (2021). Plant proteins for future foods: A roadmap. *Foods*, *10*(8), 1967. https://doi.org/10.3390/FOODS10081967

Simonsky, R. W., & Stanley, D. W. (1982). Texture-structure relationships in textured soy protein. V. Influence of pH and protein acylation on extrusion texturization. *Canadian Institute of Food Science and Technology Journal*, *15*(4), 294–301. https://doi.org/10.1016/S0315-5463(82)72615-X

Singh, P., Arora, A., Strand, T. A., Leffler, D. A., Catassi, C., Green, P. H., Kelly, C. P., Ahuja, V., & Makharia, G. K. (2018). Global prevalence of celiac disease: Systematic review and meta-analysis. *Clinical Gastroenterology and Hepatology*, *16*(6), 823–836. https://doi.org/10.1016/J.CGH.2017.06.037

Singh, R., & Popli, S. (1973). Amylose content and amylolytic studies on high yielding varieties of bajra (Pennisetum typhoides). *Journal of Food Science and Technology*.

Singh, R., Sá, A. G. A., Sharma, S., Nadimi, M., Paliwal, J., House, J. D., & Koksel, F. (2023). Effects of feed moisture content on the physical and nutritional quality attributes of sunflower meal-based high-moisture meat analogues. *Food and Bioprocess Technology*, *1*, 1–17. https://doi.org/10.1007/S11947-023-03225-8/TABLES/6

Smetana, S., Pernutz, C., Toepfl, S., Heinz, V., & Van Campenhout, L. (2019). High-moisture extrusion with insect and soy protein concentrates: cutting properties of meat analogues under insect content and barrel temperature variations. *Journal of Insects as Food and Feed*, *5*(1), 29–34. https://doi.org/10.3920/JIFF2017.0066

Smetana, S., Ristic, D., Pleissner, D., Tuomisto, H. L., Parniakov, O., & Heinz, V. (2023). Meat substitutes: Resource demands and environmental footprints. *Resources, Conservation and Recycling*, *190*, 106831. https://doi.org/10.1016/J.RESCONREC.2022.106831

Son, Y. (2007). Determination of shear viscosity and shear rate from pressure drop and flow rate relationship in a rectangular channel. *Polymer*, *48*(2), 632–637. https://doi.org/10.1016/J.POLYMER.2006.11.048

Sorba, A., & Sopade, P. A. (2013). Changes in rapid visco-analysis (RVA) viscosity reveal starch digestion behaviours. *Starch - Stärke*, *65*(5–6), 437–442. https://doi.org/10.1002/STAR.201200176

Soto-Madrid, D., Pérez, N., Gutiérrez-Cutiño, M., Matiacevich, S., & Zúñiga, R. N. (2022). Structural and physicochemical characterization of extracted proteins fractions from chickpea (Cicer arietinum L.) as a potential food Ingredient to replace ovalbumin in foams and emulsions. *Polymers*, *15*(1), 110. https://doi.org/10.3390/POLYM15010110

Stanley, D. W., Cumming, D. B., & deMan, J. M. (1972). Texture — structure relationships in texturized soy protein 1. Textural properties and ultrastructure of rehydrated spun soy fibers. *Canadian Institute of Food Science and Technology Journal*, *5*(3), 118–123. https://doi.org/10.1016/S0315-5463(72)74105-X

Suman, S. P., & Joseph, P. (2013). Myoglobin chemistry and meat color. *Annual Review of Food Science and Technology*, *4*(1), 79–99. https://doi.org/10.1146/ANNUREV-FOOD-030212-182623

Sun, D., Wu, M., Zhou, C., & Wang, B. (2022). Transformation of high moisture extrusion on pea protein isolate in melting zone during: From the aspects of the rheological property, physicochemical attributes and modification mechanism. *Food Hydrocolloids*, *133*, 108016. https://doi.org/10.1016/J.FOODHYD.2022.108016

Suri, S. (2020, October 16). *India's protein deficiency and the need to address the problem*. Observer Research Foundation. https://www.orfonline.org/expert-speak/indias-protein-deficiency-and-the-need-to-address-the-problem

Suryawan, A., Orellana, R. A., Fiorotto, M. L., & Davis, T. A. (2011). Leucine acts as a nutrient signal to stimulate protein synthesis in neonatal pigs,. *Journal of Animal Science*, *89*(7), 2004–2016. https://doi.org/10.2527/JAS.2010-3400

Tabilo-Munizaga, G., & Barbosa-Cánovas, G. V. (2005). Rheology for the food industry. *Journal of Food Engineering*, *67*(1–2), 147–156. https://doi.org/10.1016/J.JFOODENG.2004.05.062

Taghian Dinani, S., Broekema, N. L., Boom, R., & van der Goot, A. J. (2023). Investigation potential of hydrocolloids in meat analogue preparation. *Food Hydrocolloids*, *135*, 108199. https://doi.org/10.1016/J.FOODHYD.2022.108199

Tan, S. H., Mailer, R. J., Blanchard, C. L., & Agboola, S. O. (2011). Canola proteins for human consumption: Extraction, profile, and functional properties. *Journal of Food Science*, *76*(1), R16–R28. https://doi.org/10.1111/J.1750-3841.2010.01930.X

Tanaka, K., Yoshida, T., & Kasai, Z. (1974). Distribution of mineral elements in the outer layer of rice and wheat grains, using electron microprobe X-Ray analysis. *Soil Science and Plant Nutrition*, *20*(1), 87–91. https://doi.org/10.1080/00380768.1974.10433231

Tang, J. E., Moore, D. R., Kujbida, G. W., Tarnopolsky, M. A., & Phillips, S. M. (2009). Ingestion of whey hydrolysate, casein, or soy protein isolate: Effects on mixed muscle protein synthesis at rest and following resistance exercise in young men. *Journal of Applied Physiology*, *107*(3), 987–992. https://doi.org/10.1152/JAPPLPHYSIOL.00076.2009/ASSET/IMAGES/LARGE/ZDG0090987010005.JPEG

Tang, X., Shen, Y., Zhang, Y., Schilling, M. W., & Li, Y. (2021). Parallel comparison of functional and physicochemical properties of common pulse proteins. *LWT*, *146*, 111594. https://doi.org/10.1016/J.LWT.2021.111594

Temba, M. C., Njobeh, P. B., Adebo, O. A., Olugbile, A. O., & Kayitesi, E. (2016). The role of compositing cereals with legumes to alleviate protein energy malnutrition in Africa. *International Journal of Food Science & Technology*, *51*(3), 543–554. https://doi.org/10.1111/IJFS.13035

Thiébaud, M., Dumay, E., & Cheftel, J. C. (1996). Influence of process variables on the characteristics of a high moisture fish soy protein mix texturized by extrusion cooking. *LWT - Food Science and Technology*, *29*(5–6), 526–535. https://doi.org/10.1006/FSTL.1996.0080

Tiefenbacher, K. F. (2019). New products require new thinking—Ideas and examples. In K. F. Tiefenbacher (Ed.), *The technology of wafers and waffles II - Recipes, product development and know-how* (pp. 131–220). Academic Press. https://doi.org/10.1016/B978-0-12-809437-2.00008-3

Tilman, D., & Clark, M. (2014). Global diets link environmental sustainability and human health. *Nature 2014 515:7528*, *515*(7528), 518–522. https://doi.org/10.1038/nature13959

Toews, R., & Wang, N. (2013). Physicochemical and functional properties of protein concentrates from pulses. *Food Research International*, *52*(2), 445–451. https://doi.org/10.1016/J.FOODRES.2012.12.009

Tolstoguzov, V. B. (1988). Creation of fibrous structures by spinneretless spinning. In *Food Structure* (pp. 181–196). Woodhead Publishing. https://doi.org/10.1533/9781845698348.181

Tolstoguzov, V. B. (1993). Thermoplastic extrusion—the mechanism of the formation of extrudate structure and properties. *Journal of the American Oil Chemists' Society*, *70*(4), 417–424. https://doi.org/10.1007/BF02552717

Tolstoguzov, V. B., Grinberg, V. Y., & Gurov, A. N. (1985). Some physicochemical approaches to the problem of protein texturization. *Journal of Agricultural and Food Chemistry*, *33*(2), 151–159. https://doi.org/10.1021/JF00062A001/ASSET/JF00062A001.FP.PNG_V03

Toribio-Mateas, M. A., Bester, A., & Klimenko, N. (2021). Impact of plant-based meat alternatives on the gut microbiota of consumers: A real-world study. *Foods*, *10*(9), 2040. https://doi.org/10.3390/FOODS10092040/S1

Tripathi, M. K., Mohapatra, D., Jadam, R. S., Pandey, S., Singsh, V., Kumar, V., & Kumar, A. (2021). Nutritional Composition of Millets. *Millets and Millet Technology*, 101–119. https://doi.org/10.1007/978-981-16-0676-2_5/COVER

United Nations. (2022). *World Population Prospects 2022: Summary of Results. UN DESA/POP/2022/TR/NO. 3*.

Usman, M., Swanson, G., Chen, B., & Xu, M. (2023). Sensory profile of pulse-based high moisture meat analogs: A study on the complex effect of germination and extrusion processing. *Food Chemistry*, *426*, 136585. https://doi.org/10.1016/J.FOODCHEM.2023.136585

Utsumi, S., & Kinsella, J. E. (1985). Forces involved in soy protein gelation: effects of various reagents on the formation, hardness and solubility of heat-induced gels made from 7S, 11S, and soy isolate. *Journal of Food Science*, *50*(5), 1278–1282. https://doi.org/10.1111/J.1365-2621.1985.TB10461.X

van Dijk, M., Morley, T., Rau, M. L., & Saghai, Y. (2021). A meta-analysis of projected global food demand and population at risk of hunger for the period 2010–2050. *Nature Food 2021 2:7*, *2*(7), 494–501. https://doi.org/10.1038/s43016-021-00322-9

Vatansever, S., Tulbek, M. C., & Riaz, M. N. (2020). Low- and high-moisture extrusion of pulse proteins as plant-based meat ingredients: A review. *Cereal Foods World*, *65*(4). https://doi.org/10.1094/CFW-65-4-0038

Vermeulen, S. J., Campbell, B. M., & Ingram, J. S. I. (2012). Climate change and food systems. *Annual Review of Environment and Resources* , *37*, 195–222. https://doi.org/10.1146/ANNUREV-ENVIRON-020411-130608

Wang, F., Gao, Y., Gu, X., Luan, B., Zhu, Y., Huang, Y., & Zhu, X. (2023). High-moisture extrusion cooking on soybean-wheat protein mixtures: Effect of sodium alginate/xanthan gum/maltodextrin on promoting a fibrous structure. *Frontiers in Nutrition*, *9*, 3260. https://doi.org/10.3389/FNUT.2022.1077601

Wang, H., Fu, Y., Zhao, Q., Hou, D., Yang, X., Bai, S., Diao, X., Xue, Y., & Shen, Q. (2022). Effect of Different Processing Methods on the Millet Polyphenols and Their Anti-diabetic Potential. *Frontiers in Nutrition*, *9*, 101. https://doi.org/10.3389/FNUT.2022.780499/BIBTEX

Wang, H., van den Berg, F. W. J., Zhang, W., Czaja, T. P., Zhang, L., Jespersen, B. M., & Lametsch, R. (2022). Differences in physicochemical properties of high-moisture extrudates prepared from soy and pea protein isolates. *Food Hydrocolloids*, *128*, 107540. https://doi.org/10.1016/J.FOODHYD.2022.107540

Wang, J., Vanga, S. K., Saxena, R., Orsat, V., & Raghavan, V. (2018). Effect of Climate Change on the Yield of Cereal Crops: A Review. *Climate 2018, Vol. 6, Page 41*, *6*(2), 41. https://doi.org/10.3390/CLI6020041

Wang, K., Li, C., Wang, B., Yang, W., Luo, S., Zhao, Y., Jiang, S., Mu, D., & Zheng, Z. (2017). Formation of macromolecules in wheat gluten/starch mixtures during twin-screw extrusion: effect of different additives. *Journal of the Science of Food and Agriculture*, *97*(15), 5131–5138. https://doi.org/10.1002/JSFA.8392

Wang, T., Yue, M., Xu, P., Wang, R., & Chen, Z. (2018). Toward water-solvation of rice proteins via backbone hybridization by casein. *Food Chemistry*, *258*, 278–283. https://doi.org/10.1016/J.FOODCHEM.2018.03.084

Wankhede, D. B., Shehnaz, A., & Raghavendra Rao, M. R. (1979). Preparation and physicochemical properties of starches and their fractions from finger millet (Eleusine coracana) and foxtail millet (Setaria italica). *Starch - Stärke*, *31*(5), 153–159. https://doi.org/10.1002/STAR.19790310505

Webb, B. D., Pomeranz, Y., Afework, S., Lai, F. S., & Bollich, C. N. (1986). Rice grain hardness and its relationship to some milling, cooking, and processing characteristics. *Cereal Chemistry*, *63*(1), 27–30.

Webb, D., Dogan, H., Li, Y., & Alavi, S. (2023). Physico-chemical properties and texturization of pea, wheat and soy proteins using extrusion and their application in plant-based meat. *Foods*, *12*(8), 1586. https://doi.org/10.3390/FOODS12081586

Wee, M. S. M., Goh, A. T., Stieger, M., & Forde, C. G. (2018). Correlation of instrumental texture properties from textural profile analysis (TPA) with eating behaviours and macronutrient composition for a wide range of solid foods. *Food & Function*, *9*(10), 5301–5312. https://doi.org/10.1039/C8FO00791H

Wild, F., Czerny, M., Janssen, A. M., Kole, A. P. W., Zunabovic, M., & Domig, K. J. (2014). The evolution of a plant-based alternative to meat. From niche markets to widely accepted meat alternatives. *Agro Food Industry Hi-Tech*, *25*(1), 45–49.

Withana-Gamage, T. S., Wanasundara, J. P., Pietrasik, Z., & Shand, P. J. (2011). Physicochemical, thermal and functional characterisation of protein isolates from Kabuli and Desi chickpea (Cicer arietinum L.): a comparative study with soy (Glycine max) and pea (Pisum sativum L.). *Journal of the Science of Food and Agriculture*, *91*(6), 1022–1031. https://doi.org/10.1002/JSFA.4277

Wittek, P., Ellwanger, F., Karbstein, H. P., & Emin, M. A. (2021). Morphology development and flow characteristics during high moisture extrusion of a plant-based meat analogue. *Foods*, *10*(8), 1753. https://doi.org/10.3390/FOODS10081753

Wittek, P., Karbstein, H. P., & Emin, M. A. (2021). Blending proteins in high moisture extrusion to design meat analogues: Rheological properties, morphology development and product properties. *Foods 2021, Vol. 10, Page 1509*, *10*(7), 1509. https://doi.org/10.3390/FOODS10071509

Wittek, P., Zeiler, N., Karbstein, H. P., & Emin, M. A. (2021). High Moisture Extrusion of Soy Protein: Investigations on the Formation of Anisotropic Product Structure. *Foods 2021, Vol. 10, Page 102*, *10*(1), 102. https://doi.org/10.3390/FOODS10010102

Wood, J. D. (2017). Meat composition and nutritional value. In F. Toldra´ (Ed.), *Lawrie's Meat Science* (8th ed., pp. 635–659). Woodhead Publishing. https://doi.org/10.1016/B978-0-08-100694-8.00020-0

Wu, F., Meng, Y., Yang, N., Tao, H., & Xu, X. (2015). Effects of mung bean starch on quality of rice noodles made by direct dry flour extrusion. *LWT - Food Science and Technology*, *63*(2), 1199–1205. https://doi.org/10.1016/J.LWT.2015.04.063

Wu, G. (2016). Dietary protein intake and human health. *Food & Function*, *7*(3), 1251–1265. https://doi.org/10.1039/C5FO01530H

Wu, M., Sun, Y., Bi, C. H., Ji, F., Li, B. R., & Xing, J. J. (2018). Effects of extrusion conditions on the physicochemical properties of soy protein/gluten composite. *International Journal of Agricultural and Biological Engineering*, *11*(4), 230–237. https://doi.org/10.25165/IJABE.V11I4.4162

Xia, S., Shen, S., Ma, C., Li, K., Xue, C., Jiang, X., & Xue, Y. (2023a). High-moisture extrusion of yeast-pea protein: Effects of different formulations on the fibrous structure formation. *Food Research International*, *163*, 112132. https://doi.org/10.1016/J.FOODRES.2022.112132

Xia, S., Shen, S., Song, J., Li, K., Qin, X., Jiang, X., Xue, C., & Xue, Y. (2023b). Physicochemical and structural properties of meat analogues from yeast and soy protein prepared via high-moisture extrusion. *Food Chemistry*, *402*, 134265. https://doi.org/10.1016/J.FOODCHEM.2022.134265

Xia, S., Song, J., Li, K., Hao, T., Ma, C., Shen, S., Jiang, X., Xue, C., & Xue, Y. (2023c). Yeast protein-based meat analogues: Konjac glucomannan induces the fibrous structure formation by modifying protein structure. *Food Hydrocolloids*, *142*, 108798. https://doi.org/10.1016/J.FOODHYD.2023.108798

Xia, S., Song, J., Ma, C., Hao, T., Hou, Y., Shen, S., Li, K., Ma, L., Xue, Y., Xue, C., & Jiang, X. (2023d). Effects of moisture content and processing temperature on the strength and orientation regulation of fibrous structures in meat analogues. *Food Hydrocolloids*, *145*, 109113. https://doi.org/10.1016/J.FOODHYD.2023.109113

Xia, S., Xue, Y., Xue, C., Jiang, X., & Li, J. (2022). Structural and rheological properties of meat analogues from Haematococcus pluvialis residue-pea protein by high moisture extrusion. *LWT*, *154*, 112756. https://doi.org/10.1016/J.LWT.2021.112756

Xiong, Y. L. (2017). Structure-function relationships of muscle proteins. In S. Damodaran (Ed.), *Food Proteins and their Applications* (pp. 341–392). CRC Press. https://doi.org/10.1201/9780203755617-12

Xiong, Y. L. (2023). Meat and meat alternatives: where is the gap in scientific knowledge and technology? *Italian Journal of Animal Science*, *22*(1), 482–496. https://doi.org/10.1080/1828051X.2023.2211988

Yada, R. Y. (2018). Proteins in food processing. In *Proteins in Food Processing, Second Edition*. Woodhead Publishing. https://doi.org/10.1016/B978-0-08-100722-8.00007-3

Yang, F., Zhang, M., & Bhandari, B. (2017). Recent development in 3D food printing. *Critical Reviews in Food Science and Nutrition*, *57*(14), 3145–3153. https://doi.org/10.1080/10408398.2015.1094732

Yang, L., Ying, Z., Li, H., Li, J., Zhang, T., Song, Y., & Liu, X. (2023). Extrusion production of textured soybean protein: The effect of energy input on structure and volatile beany flavor substances. *Food Chemistry*, *405*, 134728. https://doi.org/10.1016/J.FOODCHEM.2022.134728

Yang, Y., Churchward-Venne, T. A., Burd, N. A., Breen, L., Tarnopolsky, M. A., & Phillips, S. M. (2012). Myofibrillar protein synthesis following ingestion of soy protein isolate at rest and after resistance exercise in elderly men. *Nutrition and Metabolism*, *9*(1), 1–9. https://doi.org/10.1186/1743-7075-9-57/FIGURES/5

Yao, G., Liu, K. S., & Hsieh, F. (2004). A new method for characterizing fiber formation in meat analogs during high-moisture extrusion. *Journal of Food Science*, *69*(7), 303–307. https://doi.org/10.1111/J.1365-2621.2004.TB13634.X

Yeater, M., Casco, G., Miller, R. K., & Alvarado, C. Z. (2017). Comparative evaluation of texture wheat ingredients and soy proteins in the quality and acceptability of emulsified chicken nuggets. *Poultry Science*, *96*(12), 4430–4438. https://doi.org/10.3382/PS/PEX250

Yu, L., Ramaswamy, H. S., & Boye, J. (2013). Protein rich extruded products prepared from soy protein isolate-corn flour blends. *LWT - Food Science and Technology*, *50*(1), 279–289. https://doi.org/10.1016/J.LWT.2012.05.012

Zahari, I., Ferawati, F., Helstad, A., Ahlström, C., Östbring, K., Rayner, M., & Purhagen, J. K. (2020). Development of high-moisture meat analogues with hemp

and soy protein using extrusion cooking. *Foods 2020, Vol. 9, Page 772*, *9*(6), 772. https://doi.org/10.3390/FOODS9060772

Zahari, I., Ferawati, F., Purhagen, J. K., Rayner, M., Ahlström, C., Helstad, A., & Östbring, K. (2021). Development and characterization of extrudates based on rapeseed and pea protein blends using high-moisture extrusion cooking. *Foods*, *10*(10). https://doi.org/10.3390/FOODS10102397

Zahari, I., Östbring, K., Purhagen, J. K., & Rayner, M. (2022). Plant-based meat analogues from alternative protein: A systematic literature review. *Foods*, *11*(18). https://doi.org/10.3390/FOODS11182870

Zahari, I., Purhagen, J. K., Rayner, M., Ahlström, C., Helstad, A., Landers, M., Müller, J., Eriksson, J., & Östbring, K. (2023). Extrusion of high-moisture meat analogues from hempseed protein concentrate and oat fibre residue. *Journal of Food Engineering*, *354*, 111567. https://doi.org/10.1016/J.JFOODENG.2023.111567

Zahari, I., Rinaldi, S., Ahlstrom, C., Östbring, K., Rayner, M., & Purhagen, J. (2023). High moisture meat analogues from hemp – The effect of co-extrusion with wheat gluten and chickpea proteins on the textural properties and sensorial attributes. *LWT*, *189*, 115494. https://doi.org/10.1016/J.LWT.2023.115494

Zeng, Y., Chen, E., Zhang, X., Li, D., Wang, Q., Sun, Y., Hussain, A., Zeng, Y., Chen, E., Zhang, X., Li, D., Wang, Q., & Sun, Y. (2022). Nutritional value and physicochemical characteristics of alternative protein for meat and dairy—A Review. *Foods 2022, Vol. 11, Page 3326*, *11*(21), 3326. https://doi.org/10.3390/FOODS11213326

Zhang, C., Wu, X., Chen, J., & Zhou, J. (2024). Novel fungal alternative proteins from Penicillium limosum for enhancing structural and functional properties of plant-based meat analogues. *Food Chemistry*, *444*, 138627. https://doi.org/10.1016/J.FOODCHEM.2024.138627

Zhang, J., Chen, Q., Kaplan, D. L., & Wang, Q. (2022). High-moisture extruded protein fiber formation toward plant-based meat substitutes applications: Science, technology, and prospect. *Trends in Food Science & Technology*, *128*, 202–216. https://doi.org/10.1016/J.TIFS.2022.08.008

Zhang, J., Chen, Q., Liu, L., Zhang, Y., He, N., & Wang, Q. (2021). High-moisture extrusion process of transglutaminase-modified peanut protein: Effect of transglutaminase on the mechanics of the process forming a fibrous structure. *Food Hydrocolloids*, *112*, 106346. https://doi.org/10.1016/J.FOODHYD.2020.106346

Zhang, J., Liu, L., Jiang, Y., Faisal, S., & Wang, Q. (2020). A new insight into the high-moisture extrusion process of peanut protein: From the aspect of the orders and amount of energy input. *Journal of Food Engineering*, *264*, 109668. https://doi.org/10.1016/J.JFOODENG.2019.07.015

Zhang, J., Liu, L., Jiang, Y., Faisal, S., Wei, L., Cao, C., Yan, W., & Wang, Q. (2019). Converting peanut protein biomass waste into “double Green” meat substitutes

using a high-moisture extrusion process: A multiscale method to explore a process for forming a meat-like fibrous structure. *Journal of Agricultural and Food Chemistry*, *67*(38), 10713–10725. https://doi.org/10.1021/ACS.JAFC.9B02711/SUPPL_FILE/JF9B02711_SI_001.PDF

Zhang, J., Liu, L., Jiang, Y., Shah, F., Xu, Y., & Wang, Q. (2020). High-moisture extrusion of peanut protein-/carrageenan/sodium alginate/wheat starch mixtures: Effect of different exogenous polysaccharides on the process forming a fibrous structure. *Food Hydrocolloids*, *99*. https://doi.org/10.1016/J.FOODHYD.2019.105311

Zhang, J., Liu, L., Liu, H., Yoon, A., Rizvi, S. S. H., & Wang, Q. (2019). Changes in conformation and quality of vegetable protein during texturization process by extrusion. In *Critical Reviews in Food Science and Nutrition* (Vol. 59, Issue 20, pp. 3267–3280). Taylor and Francis Inc. https://doi.org/10.1080/10408398.2018.1487383

ZHANG, J., MENG, Z., CHENG, Q., LI, Q., ZHANG, Y., LIU, L., SHI, A., & WANG, Q. (2022). Plant-based meat substitutes by high-moisture extrusion: Visualizing the whole process in data systematically from raw material to the products. *Journal of Integrative Agriculture*, *21*(8), 2435–2444. https://doi.org/10.1016/S2095-3119(21)63892-3

Zhang, T., Dou, W., Zhang, X., Zhao, Y., Zhang, Y., Jiang, L., & Sui, X. (2021). The development history and recent updates on soy protein-based meat alternatives. *Trends in Food Science & Technology*, *109*, 702–710. https://doi.org/10.1016/J.TIFS.2021.01.060

Zhang, T., Yu, S., Pan, Y., Li, H., Liu, X., & Cao, J. (2023). Properties of texturized protein and performance of different protein sources in the extrusion process: A review. *Food Research International*, *174*, 113588. https://doi.org/10.1016/J.FOODRES.2023.113588

Zhang, W., Li, S., Zhang, B., Drago, S. R., & Zhang, J. (2016). Relationships between the gelatinization of starches and the textural properties of extruded texturized soybean protein-starch systems. *Journal of Food Engineering*, *174*, 29–36. https://doi.org/10.1016/J.JFOODENG.2015.11.011

Zhang, X., Zhao, Y., Zhang, T., Zhang, Y., Jiang, L., & Sui, X. (2022). High moisture extrusion of soy protein and wheat gluten blend: An underlying mechanism for the formation of fibrous structures. *LWT*, *163*, 113561. https://doi.org/10.1016/J.LWT.2022.113561

Zhang, Y., Huang, X., Zeng, X., Li, L., & Jiang, Y. (2023). Preparation, functional properties, and nutritional evaluation of chickpea protein concentrate. *Cereal Chemistry*, *100*(2), 310–320. https://doi.org/10.1002/CCHE.10608

Zhang, Y., & Ryu, G. H. (2023a). Effects of process variables on the physicochemical, textural, and structural properties of an isolated pea protein-based high-moisture

meat analog. *Foods 2023, Vol. 12, Page 4413*, *12*(24), 4413. https://doi.org/10.3390/FOODS12244413

Zhang, Y., & Ryu, G.-H. (2023b). Effects of pea protein content and extrusion types on physicochemical properties and texture characteristic of meat analogs. *JSFA Reports*, *3*(1), 30–40. https://doi.org/10.1002/JSF2.97

Zhao, H., Shen, C., Wu, Z., Zhang, Z., & Xu, C. (2020). Comparison of wheat, soybean, rice, and pea protein properties for effective applications in food products. *Journal of Food Biochemistry*, *44*(4), e13157. https://doi.org/10.1111/JFBC.13157

Zhao, Y., Sui, W., Zhang, J., Liu, R., Wu, T., Xu, J., & Zhang, M. (2024). Intervening effect of polysaccharides on structured soy-based meat analogues by high-moisture extrusion. *Food and Bioprocess Technology*. https://doi.org/10.21203/RS.3.RS-3703308/V1

Zhou, Q., Li, X., Yang, J., Zhou, L., Cai, J., Wang, X., Dai, T., Cao, W., & Jiang, D. (2018). Spatial distribution patterns of protein and starch in wheat grain affect baking quality of bread and biscuit. *Journal of Cereal Science*, *79*, 362–369. https://doi.org/10.1016/J.JCS.2017.07.017

Zhuang, H., & Savage, E. M. (2008). Validation of a combi oven cooking method for preparation of chicken breast meat for quality assessment. *Journal of Food Science*, *73*(8). https://doi.org/10.1111/J.1750-3841.2008.00931.X

Žilić, S., Barać, M., Pešić, M., Dodig, D., & Ignjatović-Micić, D. (2011). Characterization of proteins from grain of different bread and durum wheat genotypes. *International Journal of Molecular Sciences*, *12*(9), 5878–5894. https://doi.org/10.3390/IJMS12095878

Zink, J. I., Zeneli, L., & Windhab, E. J. (2023). Micro-foaming of plant protein based meat analogues for tailored textural properties. *Current Research in Food Science*, *7*, 100580. https://doi.org/10.1016/J.CRFS.2023.100580